GUI for the analysis of complexity and entropy in physiological signals

A primer on Complexity and Entropy

David Mayor and Duncan Banks

2022

David Mayor is a visiting Fellow at the University of Hertfordshire (UK).

He may be contacted at: davidmayor@welwynacupuncture.co.uk

http://electroacupuncture.qeeg.co.uk/

Duncan Banks is a Senior Lecturer at the Open University (UK) and Professor of Physiology at Busitema University (Uganda).

He may be contacted at: duncan.banks@open.ac.uk

DEDICATION

To all the researchers who have made this possible

(around 20,100 at the last count[1]),

to our long-suffering wives, and to our grandchildren.

[1] This represents the number of individuals whose papers on complexity and/or entropy measures were indexed in PubMed on August 27, 2020. Given that numbers of publications on these topics have greatly increased since then [see Footnote 6], author numbers will also be much larger now.

PREFACE

This 'Primer' is intended as an introductory guide to the measures implemented in the second version of the CEPS pipeline. It is not intended to be exhaustive but should give enough background information for the reader to be able to use the pipeline without too much difficulty. It was written so that we could better understand the pipeline measures and use them without making too many horrible mistakes. However, as clinicians and not computer or complexity scientists, we cannot guarantee that the Primer – like the pipeline – is free from errors. Both should be used 'at your own risk'. If you want more than the bare bones, technical details are included in the Appendix to the main text, and there are enough references to keep you reading for a very long time.

If you do find any major errors or omissions, feel free to write to us about them, although we cannot guarantee that we will be alive to answer.

David Mayor

davidmayor@welwynacupuncture.co.uk

Duncan Banks

duncan.banks@open.ac.uk

7 December 2022

CONTENTS

COMPLEXITY AND ENTROPY

"Fluctuations are not an accidental aspect of life: they are at the core of its functioning"

(Jeffery *et al.* 2019)

"Great care must be taken in concluding that properties true for one dimension or entropy formula are true for another, intuitively related, formula" (Pincus 1991)[2]

"It is a challenging task to choose an entropy measure that adequately quantifies the target dynamical process and to provide a correct estimate of this measure from real-life time series" (Xiong *et al.* 2017)

"One key lesson of nonlinear dynamics is that no single analytic technique in itself is sufficient to characterize a system in its entirety. A battery of tests best suffices"

(Webber & Zbilut 1994)

SOME BASIC DEFINITIONS

Chaos

A dynamic system exhibits deterministic chaotic behaviour when even very small differences in initial conditions result in unpredictable – and sometimes large – differences in output (Gleick 1987, p. 8).

Complexity

In physiology, complexity refers to the irregularity or unpredictability of a dynamic process and is quite different from 'variability' (Lipsitz 1995). The greater the complexity, the greater the range of possible adaptive responses (Lipsitz 2002).[3]

Entropy

In general terms, entropy – as introduced by Claude Shannon in his seminal 1948 paper on the mathematics of communication (Shannon 1948) – is a measure of the information or average inherent uncertainty in a given string of data. Shannon drew an explicit comparison between this formulation of entropy and the Boltzmann entropy of statistical thermodynamics.

[2] Indeed, in some circumstances, different entropies may change in opposite directions: Shannon entropy and Approximate entropy in anaesthesia, for instance (Bruhn *et al.* 2001).

[3] Some researchers would not accept this description of complexity. Hsu *et al.* (2017), for example, state that 'complexity is different from irregularity'.

Fractality

Fractal patterns in shapes and data series exhibit both 'self-similarity' (i.e. exhibiting a similar pattern at different scales in space or time, with that pattern still visible as you zoom in or out) and 'long memory' (i.e. with slowly decaying statistical dependence between points that are far apart in space or time). One example of a fractal shape would be the British coastline (Mandelbrot 1967), while the Fibonacci numbers form a data series with fractal (self-similarity) properties.[4]

Nonlinearity

Nonlinearity can be defined as characterising a system whose output is not simply definable or predictable from knowing its input – in other words, its components interact non-additively (Campbell 1987).

Stationarity

Data may be stationary or nonstationary. The mean, variance (or standard deviation) and autocorrelation5 structure of a strongly stationary process do not change over time, as in 'white noise'. In weak-sense stationarity, however, while the mean and autocovariance of the data do not vary, the variance merely remains finite. Neither electroencephalography (EEG) nor electrocardiography (ECG) RR interval (Rri) data, for example, are consistently weak-sense stationary (Ignaccolo *et al*. 2010; Magagnin *et al*. 2011).

Living organisms are complex, containing many interdependent constituents that interact nonlinearly and at different scales, from chromosomes to limbs (Baranger 2000). These interactions are not completely predictable, but nor are they completely random. They may be somewhere in between, in the realm of unpredictability and deterministic chaos. Quantifying complexity thus uses nonlinear and probabilistic methods of analysis rather than traditional, linear approaches based on calculus or simple causality.

[4] As a geeky teenager in the 1960s, I (DM) subscribed to the *Fibonacci Quarterly* journal. Fractals have been a topic in that journal since 1993, whiles papers mentioning Fibonacci numbers have appeared in the journals *Chaos* and *Fractals* since they were first published (1991 and 1993, respectively), in *the Journal of Nonlinear Science* since 1992 (journal first published in 1991), in the *Journal of Complexity* since 1985 (its first year of publication), in *Complexity* in 1996 (also the journal's first year of publication), in *Nonlinear Dynamics* since 2003 (first published in 1990) and in *Entropy* since 2013 (first published in 1996).

[5] Autocorrelation quantifies the degree of similarity between a given time series and a lagged version of itself over successive time intervals, using Pearson's correlation coefficient *R*, so results may be between -1 and +1.

Many such methods have been applied to physiological signals (see, for example, Henriques *et al.* 2020, or Mayor *et al.* 2021). They include measures of dimension, such as the fractal or correlation dimensions, the related methods of the Hurst exponent and detrended fluctuation analysis, and measures of chaos or unpredictability, such as the maximal Lyapunov or Hurst exponents, and a mushrooming number of entropies, derived from information theory, that in some way quantify the amount of information needed to predict future states (Lipsitz 1995). Complexity may be low in both highly regular and very random processes, but conditional entropies (such as Approximate entropy or Sample entropy) will be low in the former and higher in the latter (Yentes *et al*. 2013).

Many studies suggest that – at many scales – complexity, nonlinearity and entropy may be greater in health and youth than in ill-health and older age (Bodduluri *et al*. 2018; Brindle *et al*. 2016; Byun *et al*. 2019; Chiang *et al*. 2016; Costa *et al*. 2005a; Cuesta *et al*. 2007; Eroğlu *et al*. 2020; Goldberger *et al*. 2002; Pincus *et al.* 1991b; Pregowska *et al*. 2019; West 2006, p. 283; Zadeh *et al*. 2016), although not all research converges to the same or even the opposite conclusion (Faes *et al*. 2019b; Fernández *et al*. 2013; Jin *et al.* 2017; Long *et al*. 2018; Melis *et al*. 2019; Xiong *et al*. 2017). In a sense, quantifying complexity, nonlinearity and entropy can thus be seen as ways of at least partially and asymptotically fulfilling the ancient dream of measuring the force of life itself.

Chaos, complexity, nonlinearity and entropy are all fascinating topics, but to actually make use of them is difficult if you are not familiar with programming languages and coding. A number of complexity and entropy measures require selection of appropriate values for embedding dimension and lag, and this can pose significant problems. Perhaps for these reasons, relatively few clinical studies take advantage of the wealth of research findings in these areas.[6] I hope that CEPS, and this accompanying nontechnical Primer, will enable medical researchers and others to make better use of the constructs involved in these rapidly evolving fields in their own work.

[6] For example, of 34,647 studies located in PubMed with the search term 'entropy', only 508 (< 1.5%) were listed as clinical studies; while of 1,734,525 returns for 'complexity', only 22,768 (< 1.4%) were clinical studies, and for 'chaos' only 65 of 13,493 returns (< 0.5%) were clinical studies [Figures retrieved July 27, 2020]. By 7 December 2022, numbers of clinical studies had increased by 15.0%, 12,4% and 30.8%, respectively. Strikingly, over the same 27-month period numbers of all studies on entropy had increased by 43.3%, those on complexity by only 16.7%,

The most commonly used measures – and some less commonly used – are described briefly here in a way that will enable clinicians to use them appropriately, but without having to take in too much technical detail. Those with names in bold are – or will be – implemented in CEPS. More detailed information is provided in the **Appendix**, including on Data requirements, Parameter settings and Expected or Reported values. These details – which are briefly summarised in the CEPS Manual -have been obtained from published studies when these are available, but in most cases have not been based on a process of systematic review. They should thus be considered as examples and guidelines to be explored in practice, not as set rules to be followed blindly (Henriques *et al*. 2020).

As Peng Li, an experienced entropy researcher, and his colleagues have written, using fixed input parameters may not work well all the time, but using different combinations quickly becomes cumbersome. Studies that explore how to define parameters often propose approaches based on retrospectively 'maximising … pre-hypothesised group differences, [although] it is not necessarily … always true that those hypothesized group differences exist' (Shi *et al*. 2017). Researchers are encouraged to make their own considered decisions when using these measures and their parameters. To assist in deciding which measures may be appropriate to use in different situations, a summary of data requirements and susceptibilities is provided in Mayor *et al*. 2021 (Table 8).

Because values of complexity and entropy measures will vary depending on parameters used and data analysed, and because such values are often not reported in studies whose aim is to *compare* measures for efficiency, sensitivity to differences, robustness to noise and so forth (Cuesta-Frau & Vargas 2019), a useful task for future researchers will be to provide at least ball-park figures for expected values. Again, we hope that CEPS will facilitate this.

COMPLEXITY MEASURES

Dimensions & Exponents

"One of the main objectives for measuring fractality is to distinguish reliably between fractal (healthy) and non-fractal (unhealthy) patterns for diagnostic purposes"

(Stadnitski 2012)

The 'fractal dimension' of a data series which exhibits patterns of 'self-similarity' and 'long memory' is a ratio measure of the pattern's complexity and of how detail in the pattern changes with the scale at which it is measured (Mandelbrot 1967). Subtypes of fractal dimension include **Higuchi's fractal dimension** (FD_H) (Higuchi 1988)[7] and **Correlation dimension** (D_2) (Grassberger & Procaccia 1983b).

Another measure of long-range memory or dependence of a time series, somewhat akin to autocorrelation for linear data, is the **Hurst exponent** (H) (Hurst 1965). For time series, Fractal dimension (FD) ≈ 2 – *H* (Henriques *et al.* 2020). A related method is **Detrended Fluctuation Analysis** (DFA) (Peng *et al.* 1994), where the resulting scaling exponent, α, is a generalised version of H. Another, but quite different, measure that results in a scaling exponent α is the **Allan Factor** (AF) (Allan 1966). The measure is described in relatively simple terms by Abney *et al.* (2014).

A different approach is to use the **Largest Lyapunov exponent** (LLE) to estimate the amount of chaos (sensitivity to initial conditions) and predictability in a system (Rosenstein *et al.* 1993). The Lyapunov exponents quantify divergence between recurrent trajectories in 'state space' or 'phase space' (see below). The periodic nature of such trajectories can be visualised using recurrence plots (Eckmann *et al.* 1986, 1987). **Recurrence Quantification Analysis** (RQA) is a powerful tool that enables estimation of the LLE as well as other aspects of the periodic but irregular cyclical processes found everywhere in nature, particularly in human and animal physiology.

[7] Other methods of computing FD include Katz's and Petrosian's and 'box counting' (see Gómez *et al.* 2009 for a comparison).

The **Poincaré plot** (PP) is another, but simpler, phase space method of analysing the short- and longer-term properties of dynamic systems (Woo *et al.* 1992**)**. There are now also several additional measures based on the PP but providing more information on temporal variation, such as multiscale PP (Henriques *et al.* 2016), the **Extended Poincaré plot** (EPP) (Satti *et al.* 2019), the **Complex Correlation Measure** (CCM) (Karmakar *et al.* 2009) and **Phase entropy** (PhEn) (Rohila & Sharma 2019).

A final complexity measure introduced here is **Lempel-Ziv complexity** (LZC) (Lempel & Ziv 1976). As with many complexity measures, interpretability can be an issue. It has been suggested that LZC from quasi-periodic physiological signals could be interpreted as a 'harmonic variability index' (Aboy *et al.* 2006). Its advantages over some other measures include that it is very simple to compute, it does not require long data segments to be calculated, and no parameters need to be specified for its estimation (Gutiérrez-de Pablo *et al.* 2020). **Multiscale Lempel-Ziv complexity** (mLZC) has also been developed (Ibáñez-Molina *et al.* 2015).[8]

SYMBOLIC DYNAMICS

The methods of **Symbolic dynamics** (SymDyn) are introduced here, although distinct from both complexity and entropy measures as such. The term 'symbolic dynamics' was first used by Morse and Hedlund in 1938 (Morse & Hedlund 1938), appearing in PubMed only in 1989 and then in studies on physiological time series such as HRV from 1995 (Voss *et al*. 1995), particularly by Alberto Porta and his associates for short-term HRV of 300 beats or so. A useful overview is provided by Henriques *et al.* (2020). The basic principle is that data with many values is transformed into much simpler strings of far fewer symbols. The dynamics of the symbol strings are then analysed, rather than those of the original data.

[8] An alternative method of multiscale LZC based on Costa's **Multiscale Entropy** approach has also been proposed, but is as yet less frequently used than mLZC (Chipperfield *et al.* 2019).

ENTROPY MEASURES – *A very brief taxonomy, and a little history*

"It is not meaningful to report an entropy value for a pathological group without reporting the 'healthy' entropy value" (Yentes *et al.* 2013)

"Multiple entropy analyses should be performed to assess HRV in order for objective results and caution should be paid when drawing conclusions based on observations from a single measure" (Shi *et al.* 2017)

Shannon entropy (SE), a measure of the information or average inherent uncertainty in a given string of data, was introduced by Claude Shannon in his seminal 1948 paper on the mathematics of communication (Shannon 1948), with higher values indicating greater uncertainty. He drew an explicit comparison between this formulation of entropy and the Boltzmann entropy of statistical thermodynamics. It is appropriate for discrete data (**Differential entropy**, DiffEn, was proposed as the equivalent measure of complexity for continuous random variables).

Related entropies are **Rényi entropy** (RE) (Rényi 1961) and **Tsallis entropy** (TE), both generalised but different versions of SE (Tsallis 1988), as well as Min-entropy (M-E) and Max-entropy, themselves both members of the Rényi entropy family. Tsallis introduced a positive 'entropic index' q of 'non-extensivity' into his equation for entropy (Bhagat *et al.* 2009). For $q = 1$, this then becomes the equation for Shannon entropy, and as $q \rightarrow \infty$, that for min-entropy.

In 2002, Bandt and Pompe introduced **Permutation entropy** (PE), derived from SE but based on an ordinal pattern probability distribution (Zunino *et al.* 2017) and more robust to noise. In their original paper, they demonstrated a similarity between PE and the Lyapunov exponent. Since then, a number of related entropies have been developed, including **Amplitude-aware Permutation entropy** (AAPE) (Azami & Escudero 2016b), **Improved Multiscale Permutation entropy** (ImPE) (Azami & Escudero 2016a), Permutation min-entropy (PM-E), **Multiscale Permutation min-entropy (**mPM-E) (Zunino *et al.* 2015) and others. As yet, these are not widely used in clinical studies.

As early as 1959, Kolmogorov and Sinai published papers on 'metric entropy', later known as Kolmogorov or Kolmogorov-Sinai entropy (KSE) (Sinai 2009). This provides an

estimate of 'information loss rate' (Ono 2018) and can be related to SE (Finn *et al.* 2003), PE (Bandt & Shiha 2007; Amigó *et al.* 2005; Keller & Sinn 2010), ApEn (Pincus *et al.* 1991b) and to the Lyapunov exponents (Pesin 1977; Kamizawa *et al.* 2014). However, KSE is difficult to estimate accurately for 'real-world' time series of finite length (Costa *et al.* 2002), is not suited to nonstationary data (Faure & Lesne 2014) and is badly compromised by noise (Pincus 1995). As a result, in recent years it has been less used than other forms of entropy; it is not implemented in CEPS.

Conditional entropy (CE) was introduced by Shannon (1948), but little used for physiological time series until an Italian group published their algorithm for **Corrected conditional entropy** (CCE) in 1998 (Porta *et al.* 1998). CE is related to other entropy measures for *pairs* of variables, such as Relative entropy (or Kullback–Leibler divergence) (Kullback & Leibler 1951; Cover & Thomas 1991), or Joint entropy and Mutual information, which are both beyond the scope of this Primer and CEPS.

Approximate entropy (ApEn), originally derived from KSE (Pincus 1991), but less susceptible to noise (Pincus 1991b) is a form of CE, but far more frequently used than either KSE or CE in clinical research. ApEn quantifies regularity rather than complexity, evaluating the appearance of repetitive patterns (Escudero *et al.* 2006). Lower values of ApEn indicate more regular signals (Li *et al.* 2008a).

Sample entropy (SampEn) is a related measure, also derived from KSE but without the bias in ApEn that results from including self–comparisons. Furthermore, SampEn is faster to compute than ApEn and less dependent on record length (Richman & Moorman 2000). Together, 'ApEn and SampEn are arguably the two families of statistics most extensively used in the non-linear biosignal processing realm' (Cuesta-Frau *et al.* 2018a).

For very short data series, two simple measure based on SampEn, the **Coefficient of Sample entropy** (CoSEn) and **Quadratic Sample entropy** (QSE), were proposed by the originators of SampEn (Lake & Moorman 2011; Lake 2011), but have not, so far, proved very popular.

Neither ApEn or SampEn, despite acting as measures of predictability, can be interpreted as implying any intrinsic physiological complexity (Takahashi *et al*. 2009), and

both are highly sensitive to the parameters used in their calculation (Chen *et al.* 2009). A more accurate measure of complexity, less dependent on data length and more robust to noise, is **Fuzzy entropy** (FE), based on fuzzy set theory (Chen *et al.* 2007). Because of its advantages over ApEn and SampEn, its use has increased rapidly, and FE has been dubbed a 'second-generation' conditional entropy (Cuesta-Frau *et al.* 2017), SE, RE and TE being 'first-generation' metrics, as are ApEn and SampEn. The latter two have even been dubbed 'primitive measures' (Udhayakumar *et al.* 2016b).

To take into account the complex fluctuations over multiple time scales inherent in a hierarchy of interacting healthy regulatory mechanisms, a 'multiscale' version of SampEn was introduced as **Multiscale entropy** (mSE) by Costa *et al.* (2002, 2005b). Other multiscale entropies have followed, including of FE and the versions of PE mentioned above. Several are implemented in CEPS, including **Refined composite multiscale Sample entropy based on standard deviation** (RcmSEσ) and **Refined composite multiscale Fuzzy entropy based on standard deviation** (RcmSEσ), as well as two measures suited to short data – CmSE and MmSE (Wu *et al*. 2013).

A further measure, the **Complexity index** (CI) was derived from mSE as the area under the mSE curve plotted against time scale factor (τ), bearing in mind the slope of the curve (Costa *et al.* 2008). The CI has also been used with MPM-E (Martínez-Rodrigo *et al.* 2019), and in principle can be estimated for any multiscale method.

There are many other types of entropy, such as **Distribution entropy** (DE) (Li *et al.* 2015a), introduced to overcome some of the shortcomings of ApEn and SampEn for short data segments), **Bubble entropy** (BE) (Manis *et al.* 2017), Compression entropy, related to LZC (Ziv & Lempel 1977; Baumert *et al.* 2004), **Phase entropy** (PhEn) (Rohila & Sharma 2019) and **Diffusion entropy** (DnEn) (Grigolini *et al.* 2001), with derivative measures such as Balanced estimation of diffusion entropy (BEDE) (Qi & Yang 2011), Correlation-dependent BEDE (cBEDE) (Pan *et al.* 2014) and Factorial moment based diffusion entropy (FMDE) (Yang *et al.* 2017). In addition, there are cross-entropies and other multivariate entropies for exploring multi-channel data, but these are not considered further here.

The above are all primarily applied to time series data. Time-frequency or frequency domain measures include **Spectral entropy** (SpEn), originally derived as Shannon entropy

of the power spectral density (PSD) of the data (Inouye *et al.* 1991), which is a linear measure (Li *et al.* 2008b) used mostly to describe the irregularity of the signal spectrum in EEG analysis. More recently, other spectral entropies based on RE and TE have been proposed (Bruña *et al.* 2010). **Differential entropy** of various types (DiffEn) is also primarily a time-frequency measure. 'State' and 'Response' entropies, derived from Spectral entropy, are used predominantly in EEG studies of anaesthesia (Bein 2006), but as proprietary measures associated with specific equipment (the Datex-Ohmeda Entropy™ Module), they are not considered further here.

Broadly, entropy methods fall into two classes, those based on SE that denote *amount* or frequency of information (such as Distribution entropy and the variants of PE) and those that assess conditional probabilities or *rate* of information production, sometimes known now as 'conditional' entropies (e.g. ApEn, SampEn, mSE and FE) (Azami & Escudero 2018). The variants of PE are also described as 'ordinal' (based on relative frequencies of ordinal or symbolic patterns resulting from sorting sub-sequences) and the conditional entropies as relying more on sub-pattern 'amplitude' information, respectively (Cuesta-Frau 2019b). Compared to FD_H or a conditional entropy like ApEn, entropies such as SE may be relatively insensitive to signal bandwidth and high-frequency components of a signal such as EEG (Ferenets *et al.* 2006). They may thus be complementary in their application.

Dispersion entropy (DE) is a method capable of detecting simultaneous frequency and amplitude changes. It is faster than PE and SampEn and relatively insensitive to noise (Rostaghi & Azami 2016), and outperformed SampEn, PE and FE in a further study by its originators (Azami *et al.* 2016a). Like DE, **Slope entropy** (SlopeEn) (Cuesta-Frau 2019b) and **Amplitude-aware PE** (AAPE) (Azami & Escudero 2016b) compensate for the shortcomings of the individual ordinal and conditional types of entropy by combining aspects of both. In CEPS we have implemented SlopeEn and **Refined Composite Multiscale Dispersion entropy** (RcmDE), a version of DE (Azami *et al.* 2017b). Another strategy would be to use both ordinal- and amplitude- based entropies in the same study (Cuesta-Frau *et al.* 2018a).

Measures of stationarity and nonlinearity

Some measures of complexity and entropy require weak-sense stationarity of data. Simple methods of assessing stationarity are included in the CEPS pipeline, including two 'reverse-arrangement' tests and a 'moving window' test. 'Detrending' may improve stationarity for some data but will not be necessary for others.

For linear data, using nonlinear measures of complexity or entropy may not be productive. It is therefore advisable to check data for nonlinearity in some way beforehand, although no one method will be capable of assessing all types of non-linearity (Faes *et al.* 2019a).

Embedding, dimension and time delay

In chaos theory, a sequential one-dimensional series of data points – as in a time series – can be displayed or 'embedded' as m-dimensional patterns in a higher dimensional 'phase space' in which all possible states of a system are represented as points. Starting from a particular initial condition, the system evolves over time, with these points moving in trajectories or orbits through the phase space. A cluttered 1-dimensional time series in which patterns are not at all obvious may unfold as a set of clean orbits in an embedding space with appropriate choices of 'embedding dimension' m and 'time delay' τ ('*tau*') (Borg 2001).

Nonlinear time-series analysis methods thus often involve delay-coordinate embedding, a well-established means of reconstructing the hidden dynamics of the system that generated the time series (Takens 1981). If the embedding is correct, then certain properties of the original system, its 'dynamic invariants', are preserved in the embedded (reconstruction) space. As a result, many conclusions drawn from the reconstruction-space dynamics are also true of the real, underlying dynamics (adapted from Iwanski & Bradley 1998). However, it can be challenging to determine the most appropriate values for these parameters for a given dataset.

M is often estimated using the **False Nearest Neighbours** (FNN) method of Kennel *et al.* (1992). Although frequently used, there are some reservations in the literature on the original method (Fredkin & Rice 1995; Hegger & Kantz 1999), and a number of variants have

been suggested (Chelidze 2017). One of these is the **Averaged False Neighbours** (AFN) method[9] (Cao 1997).

Time delay τ is often estimated using the **Auto-Mutual Information** (AMI) method of Fraser & Swinney (1986). However, other more recent methods may generate more accurate parameters, and which methods to use may depend what sort of system is being studied (Deshmukh *et al.* 2020; Myers & Khasawneh 2020).

Time delay τ has to be estimated first, and then the embedding dimension m (Cao 1997). The delay τ is always an integral multiple of the data sampling period, so requires knowledge of sampling frequency (Iwanski & Bradley 1998). Of course, values of m will not be identical for different complexity measures, even if estimated for the same data, and because complexity and entropy measures will vary with τ and m, comparing results from different studies is not necessarily straightforward.

[9] Cao did not use this name for his method initially, but in a later paper (Cao & Soofi 1999).

ACKNOWLEDGEMENTS

To the various researchers who supported this project by providing words of encouragement, code for the different measures implemented in CEPS, or verifying results using our pipeline: Pedro Bernaola-Galván, Paolo Castiglioni, David Cornforth, Garland Culbreth, David Cuesta-Frau, Javier Escudero, Luis Estrada, Nelson Fernández, Carlos Gershenson, Jean-Marc Girault, Paolo Grigolini, Chang Francis Hsu, Anne Humeau-Heurtier, Zhiqiang Huo Antonio Ibáñez-Molina, Aleksandar Kalauzi, Chandan Karmakar, Ieva Kizlaitienė, Frank Lad, Peng Li, Alireza Mani, George Manis, Petros Maragos, Diego Mateos, Esther Meerwijk, Mirjana Platiša, Pasquale Nardone, Ashish Rohila, Giuseppe Sanfilippo, Guillermo Santamaría Bonfil, Carlos Sevcik, Gintautas Tamulevičius, João Paulo Teixeira, Gwendolyn van der Linden, Chang Yan and Luciano Zunino. And to those in our families who may justifiably feel that they have not been given enough attention during the project's development.

ABOUT THE AUTHORS

David Mayor was an acupuncture practitioner from 1982 until the Coronavirus crisis forced his early retirement in 2020. He has been actively involved in acupuncture research since 1996, has been an honorary member of the UK Acupuncture Association of Chartered Physiotherapists (AACP) since his presentation at their 2001 conference of theoretical research on the possible effects of electroacupuncture and transcutaneous electrical nerve stimulation (TENS) on the EEG, is a Fellow of the British Acupuncture Council and also a visiting Fellow at the University of Hertfordshire. He has written and edited a number of acupuncture textbooks. Information about his collaborative research activities can be found at http://electroacupuncture.qeeg.co.uk.

Duncan Banks studied human physiology at Leeds University and then for a PhD at Sheffield University where his projects involved the effect of anaesthetic agents on the central nervous system. Then followed a series of post-doctoral positions at Medical Schools in Birmingham and Bristol where he researched the pathways in the brain that control blood pressure, respiration and head and neck pain. His first lecturing appointment was with Guy's and St. Thomas' Hospital Medical School in Central London followed by a part time appointment as Professor of Oral Biology at the National University Singapore. His latest position is as a Senior Lecturer in Biomedical Sciences at the Open University, UK. He also holds an honorary position of Professor of Physiology at Busitema University Medical School, Uganda. His notable achievements include involvement in the first operations on deep brain stimulation in humans to treat Parkinson's disease, the first wearable devices for monitoring the elderly and infirm, development of surgical robots and the first ECG watch. He is currently investigating a variety of medical innovations and the management of Big Data sets, particularly physiological signals.

Abbreviations

α (alpha)	Scaling or fractal exponent; co-recurrence; threshold (in SymDyn); see too 'q'
α1, α2	Short- and long-term exponents
δ or Δ (delta)	Difference; also Scaling exponent (in DnEn), Threshold (in SlopeEn); Quantization factor (in GEDEM)
γ (gamma)	Vertical increments threshold (in SlopeEn)
μ (mu)	Mean
π (pi)	Archimedes' constant, ~3.14159
σ (sigma)	Standard deviation (SD)
τ (tau)	Time delay or scale factor; threshold or window length (in SymDyn)
ζ (zeta)	Bin number or quantisation level (in SymDyn)
!	Factorial (i.e. n ! = 1 x 2 x 3 x … n)
*	Product (a * b = a x b)
$\in$ [5, 25]	In the range between 5 and 25
0V	No variation (in SymDyn)
1V	One variation (in SymDyn)
2LV	Two like variations (in SymDyn)
2UV	Two unlike variations (in SymDyn)
2V	Two variations (in SymDyn)
%DET	Determinism (in RQA)
%REC	Recurrence Rate (in RQA)
A	Adjusting coefficient (in AAPE); Autopoiesis (as in ESCHA)
AAPE	Amplitude-aware Permutation Entropy
AE	Average Entropy
AF	Allan Factor
AFN	Averaged False Neighbours
AI	Area Index (HRA)
AMI	Auto-Mutual Information
ApEn	Approximate Entropy
ASI	Asymmetric Spread Index
AttnEn	Attention Entropy
AvgApEn	ApEn Profile based on averaged ApEn values
AvgSampEn	SampEn Profile based on averaged SampEn values
BE	Bubble Entropy
BEDE	Balanced Estimation of Diffusion Entropy
cBEDE	Correlation-dependent BEDE
c.	circa
c	Number of classes to be mapped (in RCmDE)
C	Complexity (as in ESCHA)
CAFE	Centred and averaged Fuzzy Entropy
cApEn	Corrected ApEn
cBEDE	Correlation-dependent balanced estimation of diffusion entropy (DE)
CCE	Corrected Conditional Entropy
CCM	Complex Correlation Measure
CE	Conditional Entropy

CEP	Complexity-Entropy Plane
CEPS	Complexity and Entropy for Physiological Signals
CI	Complexity Index
C_{JS}	Jensen-Shannon Complexity
CmSE	Composite mSE (multiscale Sample Entropy)
CoSEn	Coefficient of Sample Entropy
CoSiEn	Cosine Similarity Entropy
CPEI	Composite_Permutation Entropy_Index
d	Order, Embedding (or Permutation) dimension (in ImPE); Time delay (in FE and RCmDE)
D_2	Correlation Dimension
DE	Dispersion Entropy (may also refer to Diffusion Entropy)
DET	A symmetry descriptor
DFA	Detrended Fluctuation Analysis
DiffEn	Differential Entropy
DistEn	Distribution Entropy
DIV	A symmetry descriptor, the inverse of L_{max}
D_l	Local Dimension
DnEn or DE	Diffusion Entropy
DP	A symmetry descriptor
DPE	Delayed Permutation Entropy
e	Euler's number or Napier's constant, ~ 2.71828
E	Emergence (as in ESCHA)
ECG	Electrocardiography or electrocardiogram
EoD_m	Entropy of Difference of order m
EEG	Electroencephalography or electroencephalogram
EI	Ehlers' index (HRA)
EMG	Electromyography or electromyogram
EMGdi	Diaphragmatic EMG
ENT	SE of line length distribution (in RQA)
EoE	Entropy of Entropy
ePDF	Empirical Probability Density Function (in DistEn)
EPP	Extended Poincaré Plot
ESCHA	Emergence, self-organisation, complexity, homoeostasis and autopoiesis
Ex	Extropy (as in SEx, Shannon Extropy)
f	Frequency (as in $1/f^{\alpha}$ noise)
fApEn	Fuzzy ApEn
FD	Fractal Dimension
FD_Amp	Amplitude Fractal Dimension
FD_B	Box-counting Fractal Dimension (also FD_Box, as in FD_Box_Moisy)
FD_C	Corrected Fractal Dimension
FD_Dist	Distance Fractal Dimension
FD_H	Higuchi's Fractal Dimension
FD_K	Katz Fractal Dimension
FD_LRI	Fractal dimension based on linear regression intersection
FD_M	Mandelbrot's Fractal Dimension
FD_P	Petrosian Fractal Dimension

FD_PRI	Fractal dimension based on polynomial regression intersection
FD_S	Sevcik Fractal Dimension
FD_Sign	Sign Fractal Dimension
FD_V	Variance Fractal Dimension
FE	Fuzzy Entropy
FFT	Fast Fourier Transform
FMDE	Factorial Moment Based Diffusion Entropy (DE)
fMRI	Functional Magnetic Resonance Imaging
FNN	False Nearest Neighbours
FP	Fuzzy Power
fSampEn	Fixed SampEn, or Fuzzy SampEn
GEDEM	Gait Evaluation Differential Entropy Method
GDistEn	Gridded Distribution Entropy
GI	Guzik's index (HRA)
GPP	Generalised Poincare plot
H	Hurst Exponent
H	Homoeostasis (as in ESCHA)
HR	Heart Rate
HRA	Heart Rate Asymmetry
HRV	Heart Rate Variability
ImAAPE	Improved multiscale AAPE
ImPE	Improved Multiscale Permutation Entropy
IncrEn	Increment Entropy
k	Lag; word length (in SymDyn); coarse-graining (in PhEn)
k_{max}	Maximum value of *k*
K	Adjusting coefficient (in DPE)
K_2	Correlation entropy (RE with $q = 2$)
knn	K-nearest-neighbour (model-free approach in CE)
KSE	Kolmogorov-Sinai Entropy
l	Time delay (in AAPE)
L	Word sequence (or pattern) length (in SymDyn), or L_{max}
LAM	Laminarity (in RQA)
LDA	Linear Discriminant Analysis
LLE	Largest Lyapunov Exponent
L_{max}	Length of longest (diagonal) line segment (in RQA)
L_{mean}	Average length of diagonal lines (in RQA)
ln	Logarithm
log	Logarithm
LSampEn	Local SampEn
LZC	Lempel-Ziv Complexity
m; *m*	Multiscale; or Embedding Dimension, Pattern length; or (Polynomial) Order
M	Bin number (in DistEn)
MAD	Mean (or Median) Absolute Deviation
mAAPE	Multiscale AAPE
MESA	Maximum entropy spectral analysis
mf	Membership function (in FE)
mFD_M	multiscale Fractal Dimension, according to Maragos

mFmDFA	Multifractal Multiscale Detrended Fluctuation Analysis
MI	Maximum number of trajectory iterations
mLZC	Multiscale Lempel-Ziv Complexity
MMG	Mechanomyography
MmSE	Modified multiscale Sample Entropy
mPE	Multiscale Permutation Entropy
mPM-E	Multiscale Permutation Min-Entropy
mPhEn	Multiscale Phase Entropy
mSE	Multiscale Entropy
mSEμ	mSE computed for mean coarse-graining
mSEσ	mSE computed for standard deviation coarse-graining
$mSE\sigma^2$	mSE computed for variance coarse-graining
mSE_{MAD}	mSE computed for mean absolute deviation coarse-graining
mSlope	Multiscale Slope
n	Number (e.g. of data points); Order (in PE) or Fuzzy power (in FE)
N	Number (e.g. of study participants, or of forbidden words (in SymDyn)
N 02	Percentage of words consisting only of symbols 0 and 2 (in SymDyn)
NLD	Fractal dimension based on Normalised Length Density
PD_2	Pointwise Correlation Dimension
PDF	Probability Density Function (in SpEn)
PE	Permutation Entropy
PhEn	Phase Entropy
PI	Percentage Index, or Porta's index (HRA)
PJSC	Permutation_Jensen-Shannon_Complexity
PLZC	Permutation Lempel-Ziv Complexity
PM_E	Permutation Min-Entropy
PP	Poincaré Plot
PPG	Photoplethysmography
PPi	Pulse-to-Pulse interval
PSD	Power Spectral Density
q	Entropic index, order or exponent, sometimes 'α' (in RE and TE)
QSE	Quadratic Sample Entropy
r	Pearson's correlation coefficient; Tolerance (similarity threshold)
RATIO	%DET/%REC (in RQA)
RCmDE	Refined Composite Multiscale Dispersion Entropy
RCmFEσ	Refined Composite Multiscale Fuzzy Entropy based on Standard Deviation
RCmSEσ	Refined Composite Multiscale Sample Entropy based on Standard Deviation
RE	Rényi Entropy
RPE	Rényi Permutation Entropy
rf	Ratio Factor (in FNN estimation of m)
RPDE	Recurrence Period Density Entropy
RQA	Recurrence Quantification Analysis
RR	Recurrence rate, an RQA measure
RRi	RR Interval
RSE	Rényi Spectral Entropy
s	Second(s)
s_1	Number of 'slices' (i.e. bins) (in AE and EoE)

S	Scale factor (in RCmFEσ)
SampEn	Sample Entropy
SD	Symmetry Descriptor (also Standard Deviation)
SD1	Standard Deviation along the minor axis of the PP
SD2	Standard Deviation along the major axis of the PP
SE	Shannon Entropy
SEx	Shannon Extropy
SI	Slope index (HRA), or Superinformation ('randomness of randomness')
SlopeEn	Slope Entropy
smSE	Short time mSE
SP	Symmetry plot
SpEn	Spectral Entropy
SRQA	Symmetrical Recurrence Quantification Analysis (also SQA)
SSE	Shannon Spectral Entropy
SymDyn	Symbolic Dynamics
T-E	Tone_Entropy
TE	Tsallis Entropy
TPE	Tsallis Permutation Entropy
Θ	Inverse of persistence
TREND	Measure of stationarity (in RQA)
TSE	Tsallis Spectral Entropy
TT	Trapping time (in RQA)
VM	Volatility Method
Vmax	Length of longest vertical line (in RQA)
w	Window length (in mLZC)
WE	Wavelet Entropy
WmSE	Windowed-MSE
x_{max}	Maximum value of x
x_{min}	Minimum value of x

APPENDIX. Further information on measures implemented in CEPS

Linear measures

A number of parameter-free linear measures of complexity and variability exist and should not be ignored, as they provide different insights into the behaviour of data that may be useful in addition to those from nonlinear measures. In the time domain, Hjorth Complexity, or 'Complexity of the first order' (Hjorth 1973), for example, quantifies deviation of a signal's shape from a simple sine wave, with values further from unity (1) indicating greater complexity (Hjorth 1970). For variability, it may be instructive to compare results from more exotic nonlinear measures with those from simple measures like standard deviation or variance, or RMSSD, the root-mean-square of successive differences between peaks or zero-line crossings in periodically or irregularly repeating data such as the heart beat or respiration. Other time-domain measures include 'Jitter' and 'Shimmer' (Teixeira *et al*. 2013). These linear measures are not described further in this Appendix.

Nonlinear measures

Nonlinearity (VM)[10]

In CEPS we have implemented a relatively fast and simple approach, developed to assess nonlinearity in heart rate variability (HRV) data by Pedro Bernaola-Galván and colleagues at the University of Málaga, (Bernaola-Galván *et al.* 2017). Their method examines autocorrelations in the magnitude series (or 'volatility') of the original time series and the deviations of these from the same functions for a sample of linear Gaussian noise (i.e. surrogate data). If $\{y_i\}$ represents the original time series, then its volatility ($|x_i|$) is defined as the absolute (unsigned) values of the series increments: $|x_i| = |y_{i+1} - y_i|$. The nonlinearity measure that results, ΔC, is the sum of squares of the deviations (δC) between the autocorrelation functions $C_{|x|}$ and $C_{|\text{noise}|}$. We are calling this the 'volatility method' (VM) of assessing nonlinearity.

We have used the VM in our own research (Mayor *et al.* 2019). Pedro Bernaola-Galván's MATLAB code for the VM is used and made available in CEPS, with permission.

[10] This section was written in consultation with Pedro Bernaola-Galván.

The test returns three values for lags ('distances') from 1 to 20. The first value (v1) is the measure of nonlinearity itself, ΔC; the second value (v2) is the statistical *p*-value for v1; the third value (v3) is the mean of ΔC for the surrogate ensemble at each lag, i.e. the expected value of ΔC in the absence of nonlinearity. Signals are considered to be significantly nonlinear when $p < 0.05$.

Data requirements

For accurate results, data should exhibit approximate weak-sense stationarity (Bernaola-Galván *et al.* 2017). As yet, there has been no systematic study of the effects of noise or data length on this measure. Sampling frequency will be more of an issue in RRi data during exercise than at rest. Preliminary tests have been carried out on EEG data, and here sampling frequency will become more critical in calculating ΔC. Further work is required to determine whether EEG data should be coarse-grained before analysis, and whether it is appropriate to analyse bandpass-filtered or full-range EEG.

Parameter setting

This measure is parameter-free.

Reported values – some examples

ECG RR: ΔC c. 0 to 0.18 (*N*=10, 10-min data, Bernaola-Galván *et al.* 2017)
ECG RR: median ΔC (IQR): 2.02 (0.40 – 5.84); 36% nonlinear: 13.32 (5.44 – 8.62); 64% linear: 1.88 (0.16 – 0.72) (*N*=66, 1989 x 5-min data, Mayor *et al.* 2019)
PPG peak-peak: median ΔC (IQR): 2.01 (0.46 – 6.08); 36% nonlinear: 13.90 (5.50 – 8.56); 64% linear: 1.83 (0.17 – 0.780) (*N*=66, 1991 x 5-min data, Mayor *et al.* 2019)

Embedding, dimension and time delay

Auto-Mutual Information (AMI)[11]

AMI is used to estimate time delay τ (*tau*) when working with complexity measures such as D_2 or LLE. The parameter τ has to be estimated first, and then the embedding dimension *m* (Cao 1997). The delay τ is always an integral multiple of the data sampling period, so requires knowledge of sampling frequency (Iwanski & Bradley 1998). *Tau* is

[11] In some papers this is termed 'average mutual information' rather than 'auto-mutual information'.

estimated from the first minimum in the mutual information plot (Fraser & Swinney 1986). However, this will not always reveal such a minimum unequivocally (Myers & Khasawneh 2020), and 'whether the first, local minimum, or the global minimum best determine the optimal delay is still a point open to discussion' (Jevtic *et al.* 2011).

Data requirements

Stationarity of data is required (Iwanski & Bradley 1998). AMI is relatively immune to oversampling but can be affected by data smoothing (Deshmukh *et al.* 2020) and its more subtle minima are not robust to noise (Moore *et al.* 2020). AMI is not appropriate for coarse-grained data as used in computing MSRE (Gow *et al.* 2015).

Parameter setting

Bin size B

One method of selecting B is to set it as the smallest whole number $\geq \sqrt{(n/8)}$, where n is the number of data points in the series (Moore *et al.* 2020). Thus, for a 5-minute RRi time series, B would be 7, but for an EEG epoch of some 2,000 data pints, B would be 16.

Max time delay τ_{max}

Given the result below, a reasonable starting point for RRi data might be to set $\tau_{max} = 20$.

Expected values – some examples

ECG: first minimum of the AMI occurred for $\tau = 18$ in one study (Moore *et al.* 2020).

For linear time series data, the first zero of the autocorrelation function can be used instead of AMI but is not so accurate for nonlinear data (Fraser & Swinney 1986). Other methods include taking τ as ≈ 25% of the pseudo cycle of the signal in phase space (Destexhe *et al.* 1988). In one study of D_2 in the EEG, results were similar whether this method was used or the autocorrelation method (Hornero *et al.* 1999).

The *rate* of decrease in AMI can itself be used as a measure of regularity, with results similar to those of ApEn in EEG data (e.g. lower in those with Alzheimer's disease than age-matched controls) (Abásolo *et al.* 2007).

False Nearest Neighbours (FNN)

Embedding dimension *m* is often estimated using FNN (Kennel *et al.* 1992). The percentage of FNN is plotted against *m*, and the first minimum or plateau in the resulting graph provides the estimate for *m*. However, this graphical method does not always give clear results, and requires an additional parameter, *rf*, the ratio factor, or ratio of the distance of iteration to that of the nearest neighbour. If *rf* exceeds a given threshold, a point is marked as a false neighbour (Hegger *et al.* 2000, 2007).

Data requirements

Noisy data (i.e. with a low signal-to-noise ratio) may result in very low τ and hence inappropriate values for *m* (Lim & Puthusserypady 2005). Data should thus be checked for noise before applying FNN methods (Aittokallio *et al.* 1999). FNN is not appropriate for coarse-grained data as used in computing MSRE (Gow *et al.* 2015).

Parameter setting

Embedding dimension m

Using the original FNN method, *m* should be plotted from 1 to 10 (Kennel *et al*. 1992). However, for smaller datasets, selecting high values of *m* is likely to give poor results (Krakovská *et al.* 2015).

Time delay τ

$\tau = 1$ (Kennel *et al*. 1992)

Ratio factor rf

rf = 2 (Hegger *et al.* 2007); *rf* = 10 (Hegger *et al.* 2000)

Reported values and the use of plots

A good variety of FNN plots can be found by searching online for images of 'fnn "embedding dimension" plots'. A simple example is shown in Acharya *et al.* 2011.

Averaged False Neighbours (AFN)

AFN is another method of estimating embedding dimension *m*. It is claimed to be more widely useful than FNN in that it (1) does not contain any subjective parameters except for τ; (2) does not strongly depend on how many data points are available; (3) can clearly distinguish deterministic from stochastic signals; (4) works well for time series from high-dimensional attractors; and (5) is computationally efficient (Cao 1997). Cao's method has been used, for instance, to show that the embedding dimension *m* of the EEG varies considerably during epileptic seizures but is relatively stable at other times (Yuan *et al.* 2008).

Data requirements

Noise may affect results, as for FNN (Krakovská *et al.* 2015).

Parameter setting

Embedding dimension m

m can be plotted from 1 to 10, as for FNN (Cao 1997). Again, high values of *m* may not provide good results for small datasets (Krakovská *et al.* 2015).

Time delay τ

τ = 1 to >10 (Cao 1997)

Reported values and the use of plots

Some AFN plots can be found by searching online for images of "afn "embedding dimension" plots". A simple example with $m_{max} = 8$ is shown in Krakovská *et al.* (2015).

COMPLEXITY MEASURES

Fractal dimension – an informal review

In 1967, Benoit Mandelbrot used the term 'fractional dimension' to describe the dimension of heterogeneous 'self-similar' curves, such as those of the British coastline, where each portion can be considered a reduced-scale image of the whole (Mandelbrot 1967). He later amended this to 'fractal dimension' (FD) (Mandelbrot 1982), and there are now many studies on FD,[12] and many methods of estimating it. In principle, FD, sometimes also known as the Hausdorff dimension, quantifies the roughness or smoothness of time series or spatial data in the limit as the observational scale becomes infinitesimally fine (Gneiting *et al*. 2012). It is for this reason that FD can only be *estimated* for real-world (rather than infinitesimal) data: 'the Fractal Dimension of natural phenomena is only measurable using statistical approaches' (Ezeiza *et al*. 2013). Furthermore, like Hausdorff's original 'gebrochene Dimension' (Hausdorff 2019), later reinvented by Richardson (Fuss 2013), FD can take values that are not just whole numbers. In fact, every set with a non-integer dimension is a fractal (Raghavendra & Dutt 2010).

The earliest method for estimating FD that is applicable to time-series data was probably the 'box counting' method (FD-B). Here, the time series graph is initially covered by a single box, which is then in turn divided into four quadrants, and the number of cells required to cover the curve is counted. Each subsequent quadrant is divided into four sub-quadrants, until the box width equals the resolution of the data, keeping track of the number of quadrants required to cover the graph at each step. The box-counting FD is based on this procedure. If the number of boxes required at width or scale ε is $N(\varepsilon)$, then FD-B is the slope of the least squares regression line of best fit of log $N(\varepsilon)$ against log ε (Gneiting *et al*. 2012). An early proponent of the FD-B method was Kenneth Falconer (Falconer 1985; Dubuc 1988). A Google Scholar search returned more hits for FD-B (1770) than for any other FD method – although there were only 212 hits in SCOPUS (the first dating from 1991).

[12] More than 36,000 studies were located in SCOPUS using the search term "fractal dimension", or around 2,800 if the search was limited to medicine or neuroscience subject areas (3 April 2022). Comparable results for "entropy" were nearly 290,000 and 15,360. There thus appear to be relatively more FD than entropy studies in medical/neuroscience research (18.2%) than in research generally (12.4%).

After FD-B, the most commonly used FD estimators are Higuchi FD (FD_H) (Higuchi 1988), with 453 hits in SCOPUS from 1996 (1480 in Google Scholar), Katz FD (FD_K) (Katz 1988), with 79 hits from 2004 (394 in Google Scholar), and Petrosian FD (FD-P) (Petrosian 1995), although with only 23 hits, from 2011 (267 in Google Scholar). More recent FD measures are Sevcik FD (FD_S) (Sevcik 1998), with 14 hits from 2014, and two other measures proposed by Paolo Castiglioni: Mandelbrot FD (FD_M), sometimes known as Castiglioni FD, and 'corrected' Mandelbrot FD (FD-C) (Castiglioni 2010), the latter with only 2 hits since 2015 in SCOPUS (13 in Google Scholar). When searches were restricted to medical or neuroscience studies, these numbers were much reduced, but the same three FD methods were still top of the list. Many studies use FDs – usually these three methods – as features for machine or deep learning, but unhelpfully only compare classification results for the different algorithms used, not for the different input features (e.g., Boostani *et al*. 2009; Dhanka *et al*. 2020; Humairani *et al*. 2021; Moctezuma & Molinas 2020; further references below).

CEPS originally only included Higuchi FD (FD_H), for which setting a parameter is required. The parameter-free methods mentioned above have now been added to enable comparison between them. 'A careful selection of FD algorithm is required for specific applications' (Esteller *et al*. 2001a). Indeed, some authors recommend using a combination of FD and other nonlinear methods (Kesić *et al*. 2016). In general, FD may decrease with ageing and disease, suggesting a new definition of disease as a loss of complexity, rather than the loss of regularity (West 2010).

More generally, FD can be considered as the first (D_0) in a set of 'generalised fractal dimensions', the second (D_1) being the 'information dimension', including measures such as Shannon entropy, and the third the correlation dimension (D_2), with further generalised dimensions being associated with correlation integrals in phase-space. Such generalised FDs may also be multiscale/multivariate (Alberti *et al*. 2020).

A very useful, if somewhat technical, review of different types of fractal dimension has been provided by Witold Kinsner (2008), in which he classified them as either based on morphology (e.g. Length, Self-similarity, Hausdorff/covering, Minkowski-Bouligand, Mass or Gyration dimensions), entropy (e.g. Information or Correlation dimensions, Rényi

Dimension or Mandelbrot Singularity Spectra), or Transform FDs (e.g. Spectral, Variance or Lyapunov dimensions). Most of the FDs he covers are not included in this informal review, but hopefully the last two will be, at some point in the future.

Paolo Castiglioni kindly provided codes for FD_C and FD_M; Carlos Sevcik provided code for FD_S.

Fractal dimension – measure by measure

Higuchi's Fractal Dimension (FD_H)

FD_H of a shape or time series is always between 1.0 (for the equivalent of a simple curve) and 2.0 (for white noise, or for a curve that covers a complete surface or fills a complete space), with the fractional part of its value providing a measure of the complexity of the series. FD_H is simple and quick to calculate, as it does not require reconstruction of the time series dynamic in embedded space like D_2 or the LLE (Ahmadlou *et al.* 2011). However, it does depend on choosing a parameter, k_{max}, where k represents the data point interval (Müller *et al.* 2017) or 'degree of time stretch' (Kalauzi *et al.* 2009). Relative values of FD_H in a particular experimental context are thus likely to be more meaningful than trying to compare values in different studies.

One way of selecting k_{max} is to plot FD_H against values of k from 1 to m, where m does not exceed half the number of data points in your sample (Gomolka *et al.* 2018), and then select the value of k_{max} for which FD_H plateaus or 'saturates' (Klonowski *et al.* 2004).

Data requirements

Higuchi originally published his method as appropriate for irregular and discrete time series (Higuchi 1988; Gómez *et al.* 2009), but it has been used for continuous data in many studies as well.

This method is relatively insensitive to noise and data length but is faster for longer samples (Esteller *et al.* 2001a), and not suitable for very short epochs of < 100 samples (Kalauzi *et al.* 2009; cf. Accardo *et al.* 1997). In some EEG research, it was found to be robust to nonstationarity provided bandpass frequencies were carefully chosen (Salazar-Varas & Vazquez 2019) or if short time series were used and the data demonstrated at least weak-sense stationarity (Gómez *et al.* 2009). However, other EEG researchers state that stationarity of data is a prerequisite (Sabeti *et al.* 2009), or that the measure is indeed sensitive to noise (Accardo *et al.* 1997; Khoa *et al.* 2012).

The FD_H method has been used with both global and sub-band EEG data (Ahmadlou *et al.* 2011; Lebiecka *et al.* 2018) but is affected by the filter parameters used (Anier *et al.* 2004). In general, FD_H has been characterised as 'an accurate numerical measure no matter what the nature (stationary, nonstationary, deterministic or stochastic) of the analysed signal' (Kesić & Spasić 2016).

Parameter setting

Because of the dependence of FD_H on k_{max}, this parameter should be selected consistently for all the data in a study: If using the plateau method to assess k_{max}, for a subset of the data, the resulting value should be retained for the remainder of the analysis. Some authors select k_{max} to give the greatest significant difference between groups (Gomolka *et al.* 2018). However it is used, values of k_{max} in the EEG literature vary considerably. One researcher, for example, chooses a k_{max} about 40 (Antonio Ibañez-Molina, Personal communication, November 15, 2020).

Reported values – some examples

$1 < FD\_H < 2$, with higher values indicating 'healthier' fractal dimension in most cases – but not all (Wajnsztejn *et al.* 2016).
If $FD\_H > 2$, you may require a longer data sample.
ECG: in normal breathing 1.1, in apnoea/hypopnea 1.5 ($N = 39$, Acharya *et al*. 2011).

The use of plots

Illustrations of plots of FD_H against k_{max} can be found in the literature (Antonio *et al.* 2016; Garner *et al.* 2018; Gomes *et al.*2017; Gomolka *et al.* 2018; Müller *et al.* 2017; Smits *et al.* 2016; Spasić *et al.* 2005; Wajnsztejn *et al.* 2016). A Table of values of FD_H against k_{max} is provided in Alves *et al*. (2019).

Fractal Dimension Box-counting (FD_B or FD_Box)

The Box-counting FD (or 'box dimension') is usually applied to objects of 2 or more dimensions but can also be used for 1-dimensional data segments (Moisy 2008, 2022).

FD_B has been used in a number of studies on electromyography and muscle fatigue, reviewed by Rampichini *et al*. (2020). It has also been used in a study of simultaneous EEG and facial muscle electromyography (EMG), where it was greater in the EEG at rest than when listening to music (particularly rock music), whereas in the EMG it was lower at rest and higher when listening to any type of music (relaxing, pop or rock) (Soundirarajan *et al*.

2021). FD-B has also been used in analysis of foetal ECG patterns (Hopkins *et al*. 2006), where it differentiated better between groups with normal and adverse birth/neonatal outcomes than FD_S, but not so well as a method developed by one of the authors, the 'dimension of zero set' (Hopkins *et al*. 2006).

A variant of FD-B called the 'morphological covering method', using changes (erosions, dilations) in the radius of disc-shaped covers at multiple scales rather than boxes, was developed in the 1960s for image analysis, and then applied by Maragos and Sun (1993) to time series signals. However, it does not appear to have been much used for physiological data, although a multiscale version has been proposed for automatic speech recognition (Maragos & Potamianos 1999) and has also been used for fractal analysis of musical instrument signals (Zlatintsi & Maragos 2013). Recently, the method has also been used in a machine learning EEG study on music-induced emotion recognition (Avramidis *et al*. 2021), performing better than FD_H in differentiating arousal states – although values of the two FD measures in the different states were not provided, as is frustratingly common for machine learning studies.

Another 'covering' method but using lines rather than boxes or other 2-dimensional covers, is the 'FD of the zero set' (Henderson *et al*. 2000; Henderson 2004), the zero set being the set of zero crossings of a suitably selected straight line. This method, FD-Z, has been used in studies of foetal ECG (Hopkins *et al*. 2006) and the ECG in dementia (Goh 2005). In the former, it outperformed both FD-B and FD_S, and in the latter study it outperformed FD_K, FD-P and FD_S. Values were higher in healthy individuals than in those with dementia. The method may be less sensitive to artefacts than conventional EEG spectral analysis (Henderson *et al*. 2006).

A multiresolution FD_B (FD_MB) was proposed for discrete time signals by Raghavendra and Dutt in 2010. Other multiresolution box-counting methods also exist, but Raghavendra and Dutt found that theirs provided a more accurate estimate of FD for four standard functions than both FD_H and FD_S, with FD_K being less accurate and FD_S showing saturation for both small and large FD, i.e., between 1.0 and 1.2, and between 1.8 and 2.0. Computation times for FD_K and FD_MBC were lower than that for FD_H or FD_S. Waveform amplitude had greater effect on FD_K than on FD_H or FD_S. Both FD_H and

FD_S increased with sampling frequency, whereas FD_K decreased, as it did with sample length; FD_H and FD_MBC did not change with sample length unless it was very short (Raghavendra & Dutt 2010).

Katz Fractal Dimension (FD_K) and its variants

Michael Katz created FD_K by extending Mandelbrot's definition of the fractal dimension or 'convolutedness' of a curve to waveforms, or monovariate time series (Castiglioni 2014a). In his original paper (1988), Katz defined FD_K as log(n) / (log(n) + log(d/L)), where n + 1 is the number of waveform points in the xy plane, d is the planar extent (diameter) of the waveform, and L is its total length. With this formulation, he showed that FD_K ranges from 1.0 (for a straight line) to approximately 1.15 for random-walk waveforms, approaching 1.5 for the most convoluted waveforms.

FD_K has been criticised as not measuring the FD of waveforms (Sevcik 1998), and as containing an error in its definition of distance that results in it tending to underestimate the true FD of a system (Castiglioni 2010, 2014a; Esteller *et al* 2001a).

FD_K was found in one EEG sub-band study to detect Alzheimer's disease (AD) more effectively than FD_H, with decreased fractality of the brain dynamics in the β band of those with AD (Ahmadlou *et al*. 2011). In contrast, the same group found that FD_K did not show significant differences between the EEG of those with major depressive disorder (MDD) and those without, whereas FD_H was greater in the high frequency sub-bands (β and γ) in those with MDD (Ahmadlou *et al*. 2012). Both FD_K and FD_H were able to discriminate between the EEG of MDD patients and healthy controls in a different study (as was LZC) (Akar *et al*. 2015).

In a machine learning EEG study on encephalopathy (Jacob & Gopakumar 2018), FD_K was better able to differentiate between those with the condition and healthy individuals than FD_H. Results were provided for the two methods for the EEG sub-bands (delta to beta), indicating clearly that there was little agreement between them except in the alpha band, where FD was greater for both measures in healthy individuals than in those with encephalopathy. FD_K was found more useful that both FD_H and FD_S in an EEG

study on handgrip force, increasing linearly with force. During the movement and holding periods but remaining low during a preparation period (Liu *et al*. 2005).

Another group also found FD_K provided the most repeatable and discriminative results between preictal and ictal EEG, although most accurate estimates of the FD were found with FD_H (Esteller *et al*. 2001a). Others too have noted that although FD_K may discriminate between sleep stages, its values are not accurate and should be interpreted with caution (Raghavendra & Dutt 2009). Similarly, in a machine learning EEG study on drowsiness (Pavithra *et al*. 2014), while FD_K, FD_H and FD-P were all greater when alert than when drowsy, and although FD_K was computationally fast, FD_H yielded more accurate and consistent results.

FD_K was found to be less useful than FD_H and FD_S for sleep spindle detection in an EEG machine learning EEG study (Hekmatmanesh *et al*. 2017). It was also found less useful than FD_H for classification in a machine learning EEG study comparing 10 schizophrenic patients with healthy individuals (Katebi & Sabeti 2012),

Using FD_H, significant differences were found in the EEG over the sensorimotor cortex (electrodes C3, Cz, C4) between advanced music students and non-musicians exposed to audiovisual stimulation (music accompanied by a video of a human figure walking at the same rhythm). Significant differences were not found with either FD-P or FD_K (Hadjidimitriou *et al*. 2010).

In one EEG epilepsy study (Esteller *et al*. 2001a), for short data (250 samples), FD_K was found less computationally demanding than FD_H or FD-P, but this was reversed for longer data (4000 or 8000 samples).

In a machine learning EMG study of FD-B, FD_H, FD_K and FD_S as features, FD_K performed best using several different kernel machines. In contrast, the other FD measures did not all perform well with every classifier tested. Computation times also varied with different FD-classifier combinations, indicating that both FD method and the classifier to be used need to be considered carefully (Lima *et al*. 2016); with more complex classifiers, the same researchers found that FD methods performed better (Coelho & Lima 2014). FD_K has been used in a number of studies on electromyography and muscle fatigue, reviewed by

Rampichini *et al*. (2020). FD_K, along with FD_S and Variance FD (see below) has also been used in analysis of lung sounds (Gnitecki & Moussavi 2005).

Data requirements

The dynamic range of FD_K was enhanced in the presence of noise in one EEG epilepsy study, although the authors also claimed it was relatively insensitive to noise (Esteller *et al*. 2001a).

The authors of one EEG study of imagined motor tasks found that classification was generally (but not always) most accurate when using 2-second windows (rather than 1- or 1.5-second windows), with data sampled at 250 Hz (Salazar-Varas & Vazquez 2019).

According to the authors of one HRV study (Garner *et al*. 2018), results for short data (e.g., 1000 data points) may be erroneous, with FD_K > 2.0. Cubic spline interpolation of the data, increasing length in steps up to 15,000 samples, reduced FD_K, but also reduced the significance of differences in FD_K between young obese and non-obese participants (both N = 43). Greatest differences were found for 2,000 samples (2 Hz interpolation), but at all interpolation steps FD_K was greater in those of normal weight.

On the other hand, other authors have reported that FD_K becomes less efficient than FD_H as data length increases (Esteller *et al*. 2001a). Some reviewers concluded that for short recording lengths, and/or when estimating changes in FD is more important than its exact quantification, FD_K may be more appropriate to use than FD_H (Lau *et al*. 2021). In any case, compared to FD_H, FD_K is strongly influenced by amplitude, duration and units of measure (frequency, sampling frequency) of the waveform (Raghavendra & Dutt 2009). In Castiglioni's strongly worded critique, this renders it 'practically useless for any real biomedical application' (Castiglioni 2010).

Reported values – some examples

In one EEG epilepsy study (Esteller *et al*. 2001a), estimated FD was between 1 and 1.2 for window lengths greater than 750 points, and between 1 and 1.3 for window lengths lower than 250 points. The curve that was closest to the ideal straight line with slope = 1 was obtained for a window size of 250 points.

Castiglioni's corrections to FD_K: FD_M (Mandelbrot's FD) and FD_C (corrected FD)

Paolo Castiglioni, in a much-cited paper critiquing Katz's original method of calculating FD_K (Castiglioni 2010), proposed two corrected versions. In the first of these, which he called Mandelbrot's FD (here FD_M), he changed the definition of distance used and by so doing rendered the algorithm faster. He found that FD_M, correctly estimates the true FD of what are called 'Weierstrass cosine functions'[13] when FD <1.5, but that it tends to progressively overestimate FD for FD >1.5 and as data length increases. In a second, 'corrected' version (FD-C), FD is estimated as an average over consecutive, overlapping windows; for the Weierstrass cosine functions, FD_C is closer to the 'true' FD value than FD_M, even for as few as 10 data points, increasing linearly with data length, so that the overestimate that occurs with FD_M is no longer found. Castiglioni concluded that 'FD_C might become particularly useful for those biomedical applications where only small sets of consecutive data (between 10 and 100 samples) are available.' (Castiglioni 2010).

Castiglioni and colleagues went on to compare results using both FD_C and FD_H in a follow-up paper on blood pressure using very short samples (segments of 18 data points) in two individuals (2011). FD_H underestimated the theoretical value of FD for fractional Brownian motion when > 1.8 (i.e., showed negative bias), whereas bias was less for FD_C for all values of FD. FD_C for both mean arterial pressure and heart rate was lower at night-time than during the day. This finding was followed up by a 24-hour ambulatory study (N = 47), in which FD_C of systolic blood pressure at night showed an increasing trend very close to significant (p = 0.06), whereas diastolic blood pressure and heart rate both decreased (although not significantly) (Faini *et al*. 2014).

Two sleep studies followed in 2014. In one (N = 2), *bivariate* FD_C was analysed for heart rate and respiratory signals, considered together in 2-dimensional space, for 15-second windows with 10-second overlap. Whereas monovariate FD_C based on respiration decreased with sleep depth, bivariate FD_C increased with depth of sleep (without rapid eye movements, or non-REM), with intermediate values during dreaming (REM sleep) (Castiglioni *et al*. 2014b). In the second sleep study, FD_C of ECG RR intervals was found to

[13] These are examples of functions that are continuous, but nowhere differentiable (Fuss 2013)

be greater during obstructive sleep apnoea than during 'mixed' apnoea (Castiglioni *et al*. 2014c).

The same year, a further paper appeared (Castiglioni *et al*. 2014a), with FD_C now termed FD_{MC}. The authors noted that whereas FD_C for EMG and mechanomyogram (MMG) signals did not vary substantially following exercise, FD_K, FD_M and a further measure, corrected FD_K, all did, suggesting that FD_C might provide a different, and more reliable, estimator of 'convolutedness' than the others.[14]

At the University of the Basque Country in Spain, Castiglioni fractal dimension (FD-C) has been used in deep learning speech analysis classification (Ezeiza *et al*. 2013), in particular for detection of Alzheimer's disease (López-de-Ipiña *et al*. 2015, 2018), and in machine learning analysis of mild cognitive impairment (López-de-Ipiña *et al*. 2015b). It has also been used for characterisation of essential tremor by the same research group (López-de-Ipiña *et al*. 2018b), and in aquaculture, where it outperformed FD_H and FD_K in the detection of contaminated water from fish behaviour (Eguiraun *et al*. 2014; Martinez 2015[15]). The Basque researchers sometimes call FD_C the 'Castiglioni-Katz FD' (Eguiraun *et al*. 2014).

In Vilnius (Lithuania), FD_C has been used for speech emotion classification (Tamulevičius *et al*. 2019). FD_C and FD_M were used in a machine learning EMG study, but neither performed as well as FD_K, although FD_C produced better results than FD_M (Coelho & Lima 2014).

FD_M is called the 'Castiglioni FD' by Kizlaitienė in her Master's thesis (2021). In turn she critiqued Castiglioni's approach as having its own weaknesses, and proposed her own new amendments, which she called Amplitude FD (here, FD_Amp), Distance FD (FD_Dist), Sign FD (FD_Sign), Linear Regression Intersection FD (FD_LRI) and Poli Intersection FD (Polynomial Regression Intersection FD, FD_PRI), although acknowledging that Sign FD might not be reliable as a measure.

[14] Convolutedness is defined following Mandelbrot, who suggested that the FD of a winding river could be calculated using the formula FD = log *(L)*/log(*d*), where *L* is the length of the river and *d* is the direct distance between its source and mouth. If the latter is fixed, then the river becomes more convoluted as the river becomes longer.

[15] Eguiraun and Martinez are, in fact, the same person.

Other variants on FD-K – Line length (L), or normalised length density' (NLD)

'Line length' (FD-L) is another, somewhat simpler variant of FD-K, proposed by Esteller *et al*. (2001b, 2003) on the basis of a prior US patent by Olsen *et al*. (1994). Esteller and her colleagues observed that the logarithm functions in equations for FD-K could be dropped without affecting its ability to detect seizures from the EEG. The resulting measure is also more computationally efficient than FD-K (Esteller *et al*. 2001b), and proportional to variations in both signal amplitude and frequency. It is responsive to changes in EEG in response to electrical stimulation of the brain, as reflected in pre-/post-stimulation ratios of the measure: FD_L dimensional complexity decreased after stimulation (Esteller *et al*. 2004).

Very simply, the total line length of a curve, *L*, such as a 2-second EEG epoch, is given by the sum of the absolute distances between successive data points $x(1)$ to $x(k)$:

$$L = \frac{1}{N}\sum_{k=1}^{N-1} abs\left[x(k-1) - x(k)\right],$$

where *N* is the total number of points in the epoch.[16] Values can be averaged over a number of EEG channels (Esteller *et al*. 2004). FD_L has also been used by a Belgian group for automatic burst detection in the EEG of premature babies, taking the median rather than average values over all channels recorded (nine in this case) (Koolen *et al*. 2013).

FD_L was also computed for EEG sub-bands in a machine learning study on epileptic signal classification. FD-L, as expected, was greater in the higher-frequency sub-bands (Guo *et al*. 2010).[17] FD_L varies diurnally, with location-specific characteristics that appear to be specific to the individual (Duckrow & Tcheng 2007). Because of such variations, FD_L is often used in combination with other features in machine or deep learning EEG studies on epilepsy, rather than simply analysing feature values or thresholds (Boonyakitanont *et al*. 2020).

[16] This formulation is very similar to that of NLD (Kalauzi et al. 2009).
[17] A graph of FD-L against frequency of a synthetic sinewave signal is shown in Duckrow and Tcheng (2007).

In one review of machine and deep learning EEG studies, FD_L was found to be a useful feature for epileptic seizure detection, although not one of the top performers (Boonyakitanont *et al*. 2020). The authors of another such review recommended that FD_L should be in any list of features suitable for EEG seizure detection because it provides some measure of signal complexity (Siddiqui *et al*. 2020).

Another FD estimator for 1-dimensional signals is the 'normalised length density' (NLD) method, more accurate than FD-H for very short epochs ($N < 100$ or even < 30 samples), although there is a trade-off in that accuracy is lower for such short signals. Very simply, NLD is the signal length divided by the number of samples, and normalised for average signal amplitude (Kalauzi *et al*. 2009):

$$NLD = \frac{1}{N}\sum_{i=2}^{N}\left|y_n(i) - y_n(i-1)\right|$$

.

Here $y_n(i)$ represents the ith signal *after amplitude normalisation*. Apart from the normalisation step, NLD thus appears to be identical to the earlier FD-L, described above (Esteller *et al*. 2004), although its creators took the additional step of calculating NLD for a set of Weierstrass functions (for which FD values are known from theory), rather than regarding it as a raw complexity measure (Aleksandar Kalauzi, Personal communication, 22 April 2022). Kalauzi *et al*. had earlier (2005) proposed another simple algorithm for estimating FD, which they called the 'consecutive differences' method. They found the NLD approach provided more accurate values for FD when $N < 30$, although results using the two methods were similar for longer samples ($30 \leq N \leq 100$) (Kalauzi *et al*. 2009).

NLD has been used in classifying EEG changes associated with the emotions elicited by watching various music video clips (Kroupi *et al*. 2011), and also automatic EEG classification of the perception of unpleasant odours, although it was not particularly useful for this task (and even less so for classification using ECG and HRV rather than EEG data) (Kroupi *et al*. 2016). NLD has also been used in the analysis of non-language sounds (animal or machine sounds, music, etc.); interestingly, NLD and FD_H were significantly correlated in this particular study (Burns & Rajan 2019), as they were in the original EEG study by Kalauzi *et al*. (2009).

Petrosian_Fractal Dimenson (FD_P)

FD-P was introduced by Petrosian In a 1995 study on preictal EEG. FD-P has also been used alongside FD-H in a recent machine learning sparse EEG study on epilepsy. No numerical results were provided (Moctezuma & Molinas 2020).

In another machine learning EEG study, comparing 10 schizophrenic patients with healthy individuals (Katebi & Sabeti 2012), FD-P differentiated poorly between them compared to FD-K and FD-H. Mean values of FD-H were consistently higher in the healthy individuals for a number of electrodes, but this was not the case for either FD-K or FD-P. In an EEG study on driver drowsiness ($N = 10$), mean FD-P was consistently higher at all EEG electrodes when alert than when drowsy, whereas for FD-H the opposite was true at prefrontal electrodes Fp1 and Fp2. Mean values of FD-H were between about 1.65 and 1.80, and of FD-P between about 1.025 and 1.031. Overall classification accuracy was greater for FD-H (Mardi *et al*. 2011).

ECG FD-P was also a key feature in an automated (machine learning) feature fusion study on sleep classification in which over 100 EEG, EMG, ECG and EOG features were used in total. No other FD measures were included except for Esteller's 'line length' variant of FD-K, titled 'mean curve length' in the study (Yan *et al*. 2019). In another elaborate deep learning EEG study on epilepsy classification using 11 features, seven of them FD measures, FD-P was the fastest to compute, followed by FD-S and then the 'morphological covering method'. FD-MB was the slowest; otherwise, as usual in such studies, results for individual features were not reported (Malekzadeh *et al*. 2021).

Using FD-H, significant differences were found in the EEG over the sensorimotor cortex (electrodes C3, Cz, C4) between advanced music students and non-musicians exposed to audiovisual stimulation (music accompanied by a video of a human figure walking at the same rhythm). Significant differences were not found with either FD-P or FD-K (Hadjidimitriou *et al*. 2010).

FD-P was used as a feature in studying Parkinsonian gait and was found to be reduced compared to gait in healthy individuals; numerical results were not provided in this deep learning (multilayer perceptron) study (Sarbaz *et al*. 2012).

Binarisation and data requirements

In his 1995 paper on preictal EEG, Petrosian binarised the data using five different methods:

(a) average method: sample assigned to value of 1 if it was above the signal average value, and 0 otherwise;
(b) modified zone method: sample assigned to be 1 if it was outside the range defined by the average ± standard deviation, and 0 otherwise;
(c) 'differential' method: sample given value 1 if the difference between two consecutive samples is positive, and 0 if it is negative;
(d) 'zone differential' method: consecutive samples with positive or negative 'differentials' given value 1 if the 'local extremum' exceeded standard deviation value, and 0 otherwise;
(e) 'modified zone differential' method: as (d), but with an *a priori* chosen boundary value Δ instead of the standard deviation value.

Petrosian noted that FD-P decreased preictally and increased during seizure if binarisation methods (a) and (b) were selected (see below, under Data requirements), but that the opposite trend was found for methods (c) to (e). Clearly, methods have to be chosen with care. Methods (c) and (d) have both been criticised as potentially ambiguous for some data (Goh *et al*. 2005). Few studies appear to use method (e).

No window length effect was observed in the range of 150 to 2000 points in one EEG epilepsy study (Esteller *et al*. 2001a).

Sevcik_Fractal Dimension (FD_S)

Carlos Sevcik proposed the FD that now bears his name in 1998, as a fast alternative to FD-K suitable for waveform analysis. It provides an asymptotic approximation to the Hausdorff dimension, applied to waveforms linearly transformed into (i.e., embedded in) a unit square (Sevcik 1998). Values converge rapidly to a steady state as data length increases; FD-S is thus useful for relatively short data ('even when a few points are considered').

In one EEG machine learning study (Schneider *et al*. 2009), although FD-H was better able to differentiate between those with and without epilepsy, results with FD-S were not far behind (and those with FD-K the least useful). Given that FD-S (and FD-K) are less

computationally demanding than FD-H, the authors of the study suggested that it might be preferable to use them rather than FD-H in some circumstances.

FD-S was found more useful than FD-K in a machine learning study of EEG sleep spindle detection (Hekmatmanesh et cl. 2017), and more useful than FD-B, FD-K and FD-H for machine learning classification of normal and heart murmur sounds (50 cases of each) (Komalasari *et al*. 2020). As so often in machine learning studies, comparative FD values were not provided, although box plots of results were included in the latter study, as they were in a machine learning study on classification of communication signal modulation types using FD-S as well as FD-B, FD-H, FD-P and FD-S. FD-S performed best, with the greatest computational efficiency; in contrast, FD-H was very slow indeed (Shi 2018).

Other measures of fractal dimension

Other FD methods suited to time-series data include a parametric *k*-nearest neighbour algorithm (Polychronaki *et al*. 2010) and methods based on FD-H such as FD 'tortuosity' and 'residuals' (Finotello *et al*. 2015).

Another such measure is a Canadian 'variance FD' (FD_V) based on the Hurst exponent, first used for image analysis (Zhang *et al*. 1989), and then for Brownian motion (Zhang *et al*. 1990). It has been used, for example, in the analysis of heart and lung sounds (e.g., Carvalho *et al*. 2005; Gnitecki & Moussavi 2005), and in analysis of the endocardial electrogram, for which it was less useful as a classifier than FD-B or FD-S (Novák *et al*. 2009). It has also been used, alongside DFA, in the analysis of EEG drowsiness patterns (Tantisatirapong *et al*. 2010). Multiscale DF-V was also used in classification of epileptic EEG signals, performing (in order) better than FD-S, FD-H, FD-K and FD-B, which performed least well (Rahmawati *et al*. 2021). In another EEG study, FD_V was increased at 12 electrodes located over the sensorimotor cortex during a motor imagery task (Phothisonothai *et al*. 2009). Multiscale FD_V has also been used for analysis of gait following stroke (with higher FD_V in the affected leg) (Ren *et al*. 2018).

Witold Kinsner included FD_V in his technical paper on a unified approach to fractal dimensions (2008). An improved version of FD_V was published by Ghanbari and Kinsner

in 2018, using 'polyscale' (rather than multiscale) analysis, with all scales used simultaneously (see too Ghanbari 2021). Values of FD_V are – as for any FD in principle – between 1 and 2.

Another FD covered by Kinsner and his students (Ghanbari 2021; Marcynuk 2014) is 'Spectral FD'. Unlike other FDs, which are for self-similar signals, Spectral FD is applicable to the broader set of self-affine time series (Marcynuk 2014). If β [beta] is the 'spectral exponent', then the spectral FD, D_β can be defined by:

$$D_\beta = 1 + \frac{3 - \beta}{2}$$

.

The 'size measure relationship' (SMR) method and an unnamed method were developed by Paramanathan and Uthayakumar (2008a, 2008b). The first of these was also used in a study on the non-linear analysis of (Tamil) speech (Rani *et al*. 2016) but does not appear to have been used otherwise. The SMR method is claimed to be more accurate and less computationally burdensome than both FD-H and FD-K (particularly for longer data segments, such as 8000 samples), and does not require calculation of k_{max} (unlike FD-H). The other (unnamed) method was again faster than both HF-D and HF-K, but not as fast as the SMR method; values of k_{min} and k_{max} are selected automatically by the algorithm used.

Some of these FD measures were used in our analysis of the effects of paced breathing in our CEPS 2 study (Mayor et al. 2023), where they are presented in a Table.

Allan Factor (AF)

AF analysis (Allan 1966) examines temporal correlations in spike trains or similar discrete data (Kello *et al.* 2013) and so 'is akin to spectral analysis for a point process' (Kello *et al.* 2017). It estimates the scaling of event clustering across multiple temporal scales (Abney *et al.* 2014) and is derived as the variance of the signal divided by twice the mean, with Allan variance – as opposed to ordinary variance – defined in terms of the variability of data point counts in successive windows of identical length T, i.e. in terms of the first derivative of the signal (Fadel *et al.* 2004a; Engin 2007).

An AF curve can be created by plotting AF against window size T on a log-log scale, resulting in a straight line with positive slope α, sometimes considered a 'fractal coefficient' or 'fractal exponent' (Lamanna *et al.* 2012). If $\alpha \sim 1$, the data will exhibit 1/*f* fluctuations, more influenced by past fluctuations at longer time scales; if $\alpha \ll 1$, fluctuations will be more random (Abney *et al.* 2014). For a data block of length T_{max}, T is progressively increased from a single bin minimum to a maximum of $T_{max}/6$, so that ≥ 6 non-overlapping windows are used for each measure of AF.[18] The increase in variance relative to the mean occurs because longer windows are more likely to reveal rarer clusters of events (Fadel *et al.* 2004a).

Data requirements

AF has been used with RRi data of 2,048 data points, sampled at 128 or 250 Hz, and is useful for data with 'linear non-stationarities' (Engin 2007). Samples of just less than 2,000 data points have been used in respiration research (Fadel *et al.* 2004a), of around 6,000 points for muscle sympathetic nerve activity (Fadel *et al.* 2004b). and of some 33,000 data points in one study of music, speech and animal vocalization. Some authors suggest that the AF fractal exponent α becomes less reliable for samples of less than 5,000 or even 10,000 data points (Lamanna *et al.* 2012). However, downsampling from 44.1 kHz to 11 kHz did not appreciably affect values in one study (Kello *et al.* 2017). AF cannot be used to estimate fluctuations in signal *amplitude* (Fadel *et al.* 2004b).

Parameter setting

In one study of very lengthy neonatal RRi data (several days), the AF was evaluated at five time scales, from 5 to 25 s long (Doyle *et al.* 2010). In another, of infant limb movements and vocalisations, again of many days duration, recordings were converted into a binary time series of behaviour onsets ('1'), other time points with no such onsets being coded as '0'. Time windows T varied as powers of t, i.e. $T = 2^t$, with t ranging from 4 to 12, so from approximately 16 s to 68 min (Abney *et al.* 2014).

Reported values – some examples

AF > 1 indicates that a sequence is less ordered than a homogeneous Poisson point (i.e. random) process, while AF < 1 occurs for sequences which are more ordered (Engin 2007), approaching zero for increasing window size in periodic signals. For an uncorrelated random process, AF = 1 for all window sizes (Fadel *et al.* 2004a). For a fractal process, AF increases as a power of the window size T and may reach values ≥

[18] Others have suggested that useful values for the window or counting time T typically range from 50% of the minimum inter-event interval to approximately $T_{max}/10$ (Lowen *et al.* 1997).

1 (Fadel *et al.* 2004a). AF for RRi and sympathetic nerve activity data may be > 1 in some individuals and < 1 in others (Fadel *et al.* 2004b).

The use of plots

Example of log/log AF plots are shown by Lowen *et al.* (1997), Fadel *et al.* (2004a, 2004b) and Lamanna *et al.* (2012).

Correlation Dimension (D_2)

"The brain shows deterministic chaos with a correlation dimension of D_2=6, the smooth muscles D_2=3" (Başar & Güntekin 2007)

Correlation dimension (D_2), like the Largest Lyapunov exponent (LLE) (see below), is a measure derived from chaos theory, in which nonlinear dissipative dynamical systems do not approach stationary or periodic states asymptotically, but – with appropriate values of their parameters – tend instead towards 'strange attractors', fractal shapes (Mandelbrot 1983, p. 197) in which motion is chaotic, i.e. unpredictable over long times and not periodic, as well as being extremely sensitive to initial conditions. D_2 was introduced in 1983 as the 'correlation exponent', a measure of strange attractors to help distinguish between deterministic chaos and random noise. Its value is close to that of other measures used in chaos theory, such as the Hausdorff and information dimensions, and it is related theoretically to the Lyapunov exponents (Grassberger & Procaccia 1983a). It is sometimes stated that D_2 signifies the number of independent variables required to describe a dynamic system (Nayak *et al.* 2018), but this is not accepted by all authorities (Pincus & Goldberger 1994). A proprietary measure, the 'pointwise correlation dimension' (PD_2), faster to compute than D_2 and better suited to nonstationary data, was introduced in 1991 (Skinner *et al.* 1991).

Data requirements

D_2 is always an approximation and would require very long data samples for accurate estimation. However, 'reasonable' results (i.e. accurate to within ± 5%) may require 'only a few thousand points' (Grassberger & Procaccia 1983a); it is thus not really suited to short RRi datasets, for instance,[19] but could be used in analysing longer or

[19] The proprietary 'point-D_2' algorithm proposed by Skinner *et al.* is, however, reportedly accurate for even as few as 1,500 data points, unlike the Grassberger-Procaccia algorithm (Skinner *et al.* 2001).

even 24-hour ECG recordings: 10,000 beats were used by Lerma *et al.* (2015). Similarly, for EEG data, 10,000 to 15,000 data points would be required (Ahmadlou *et al.* 2011). It has thus been used for both discrete and continuous data. Downsampling (e.g. by 50%) may increase D_2 but without affecting its stability and usefulness (Fang *et al.* 2002).

Because long data samples are need for reasonable results, D_2 also requires data that is reasonably stationary and noise-free (Grassberger & Procaccia 1983b; Accardo *et al.* 1997); EEG data with a high sampling rate has been both segmented and normalised (to zero mean and SD of one) in some studies (Ehlers *et al.* 1998). D_2 has been computed for EEG and MEG (magnetoencephalography) data in filtered bands, but the effect of such filtering was not known at the time (van Cappellen van Walsum *et al.* 2003). However, EMG D_2 may be affected when bandpass and notch filters are used (Aschero & Gizdulich 2010), and D_2 was more robust at low frequencies when low-pass filtering was applied to voice recordings (MacCallum 2011); as another example, D_2 in nystagmus increased as filter cut-off frequency decreased (Shelhamer 1997).

Parameter setting

Embedding dimension m[20]

EEG data: 9 (Lee *et al.* 2008), 13 (Jeong *et al.* 2001), 16 (Wang *et al.* 2010)

RRi data: 7 (Nayak *et al.* 2018), 20 (Lerma *et al.* 2015; Melillo *et al.* 2011).

As for LLE (below), *m* is often estimated using the method of Kennel *et al.* (1992) (see above).

Time delay τ

EEG data: 1 (Ahmadi & Amirfattahi 2010), 3 (Wang *et al.* 2010), 4 (Lee *et al.* 2008); ECG RRi data: τ = 10 RR intervals (Tarvainen *et al.* 2019); 5 (Lerma *et al.* 2015).

As for LLE, τ is often estimated using the method of Fraser & Swinney (1986) (see above).

Reported values – some examples

EEG c. 6 (Başar & Güntekin 2007); c 1.75 to 2.2 in *gamma* band, 1.87 to 2.34 in *delta* band, in schizophrenics (Lee *et al.* 2008); 4.64 in healthy individuals vs 3.88 in epileptic patients (Hornero *et al.* 1999); c. 7.5 prior to total sleep deprivation, c. 7.3 after total sleep deprivation (Jeong *et al.* 2001); D_2 is higher at all EEG electrodes when eyes are open than when they are closed (Stam *et al.* 1996).

[20] See above for a brief discussion of phase space and *m*.

Whole ECG data: normal breathing 2.7, apnoea 3.8, hypopnea 4.6 (*N* = 39, Acharya *et al*. 2011); 3.5 to 5.2 for 6 x 10^4 data points (Babloyantz & Destexhe 1988);

RRi data: ~4.9 (Babloyantz & Destexhe 1988); ~3.6 in normal sinus rhythm, less in cardiac pathology (*N* = 300, Acharya *et al.* 2004); 11.0 (in women) vs 10.6 (in men), lower in cardiac pathology (*N* = 100, Lerma *et al.* 2015); ~1.3 in static exercise, 0.4 in dynamic exercise (*N* = 23, Weippert *et al.* 2013)

EMG c. 3 (Başar & Güntekin 2007)

The use of plots

Plots of D_2 against *m* can be found in Stam *et al.* (1995), Hornero *et al.* (1999), Bogaert *et al.* (2001), Kannathal *et al.* (2004), Mekler (2008) and Nurujjaman *et al.* (2009). Carvajal *et al.* (2005) include plots of D_2 against *m* and against τ.

Hurst Exponent (H)

The Hurst exponent (H) (Hurst 1965) is a long-established measure of the long-term 'memory' or dependence of a time series, somewhat akin to autocorrelation. It has been described as a measure of the smoothness of a fractal time series (Kannathal *et al.* 2004). For 1-dimensional (i.e. series) data, H = 2 – FD (Schepers *et al.* 1992), and H ≈ DFA α (Bryce & Sprague 2012). Unlike other nonlinear complexity measures such as D_2, LLE and RQA, computing H does not require state space reconstruction (Henriques *et al.* 2020), so no parameters are needed.

Data requirements

Stationarity is required (unless estimating H from DFA) (Henriques *et al.* 2020), although in one functional magnetic resonance imaging (fMRI) study (i.e. of sparse data), both H and FD_H were more robust to artefact noise than DFA, for example (Rubin *et al.* 2013). H has been used for short series (~500 data points) in limb movement studies (Crevecoeur *et al.* 2110; Warlop *et al.* 2017), and for 15,000 RR interval samples in HRV research (Żebrowski *et al.* 2015), as well as in EEG research using 5,000 samples (Paul *et al.* 2019) or even 50,000 samples – for a 'dynamical' analysis of H over time (Rahmani *et al.* 2018). Downsampling may affect results (Makarava *et al.* 2014), but has been used in EEG studies, where H has also sometimes been computed in different frequency bands (Gupta *et al.* 2018; Racz *et al.* 2018; Amezquita-Sancheza *et al.* 2019). Alternatives to H have been suggested for shorter data samples (~100 data points) (Qi & Yang 2011).

Parameter setting

No parameters are required.

Expected values – some examples

0 < H < 1; values of H > 1 indicate nonstationarity or unsuccessful detrendng (Bryce & Sprague 2012)
0 < H < 0.5: time series has long-range anti-correlations
H = 0.5 there is no correlation in the time series (Brownian motion)
0.5 < H < 1: time series has long-range correlations
H = 1: the time series is precisely self-similar (Henriques *et al.* 2020).

ECG: in normal breathing 0.6, in apnoea/hypopnea 0.2 (N = 39, Acharya *et al*. 2011).

EEG: In one study, H was ≈0.47 in men with eyes open, ≈0.41 with eyes closed, 0.29-0.34 in epileptics when free of seizures, and ≈0.19 during seizures (Nurujjaman *et al.* 2009).

Detrended Fluctuation Analysis (DFA)

DFA quantifies short- and long-term fractal-like correlations in a time series, i.e. at different scales. The output, scaling exponent α, is the slope of a line fitting the plot of the logarithm of the 'fluctuation function' $F(n)$ against the logarithm of n, where n is the number of points in a box or segment the size of the window of observation. The scaling exponent α is inversely related to the 'roughness' of the data (Peng *et al.* 1995) and is similar to H (Henriques *et al.* 2020); indeed, for stationary time series, H and α coincide (Bernaola-Galván *et al.* 2017). In some situations, α may even be directly related to fractal dimension D, with $D = 2 - \alpha/2$ (Kotimäki *et al.* 2013). In HRV analysis, α is considered in two ranges: the short-term exponent $\alpha 1$ is computed over shorter segments (e.g. 4-16 beats), and the long-term exponent $\alpha 2$ over longer segments (e.g. 16 to 64 beats) (Peng *et al.* 1995), with a 'crossover' between them (**Figure 1**). Other ranges have also been used.

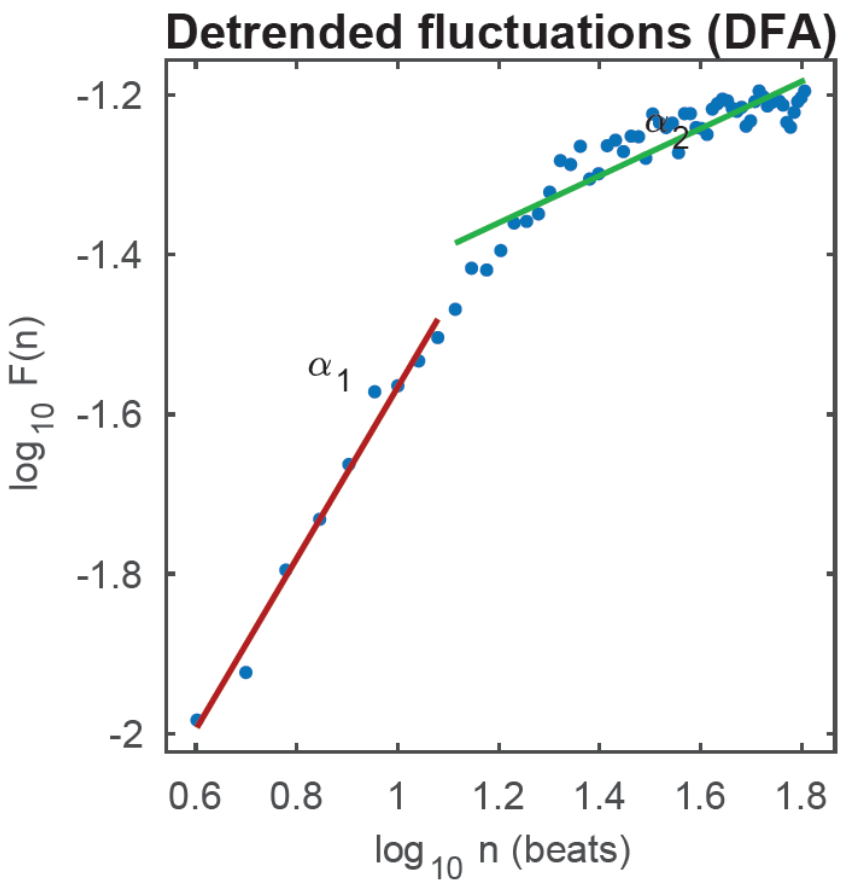

Figure 1. Example of short-term exponent α1 and long-term exponent α2 for RRi data (output from Kubios HRV).

Although most researchers consider DFA to be a nonlinear method, some see α1 as in itself a linear measure (Bernaola-Galván *et al.* 2017), and DFA has been criticised for other reasons as well (Bryce & Sprague 2012).

Data requirements

DFA requires a non-periodical, discrete time series as an input (Terrier 2019). It is thus frequently used with RRi and stride data. However, DFA has also been used in many EEG studies, in both full-band and band-filtered data (Stam & de Bruin 2004). Although bandpass filtering may affect DFA results, inducing a spurious crossover in the DFA graph at a position related to the filter cut-off frequencies (Valencia *et al.* 2008), or emphasising short-range correlations with overestimation of α1 (Meisel *et al.* 2017), wavelet-based filtering will have less of an effect, for example on respiratory (breath-to-breath interval) or ECG RRi data (Busha 2010). Downsampling may reduce DFA α (Rhea *et al.* 2015).

DFA may be less robust to EEG artefact noise than H (Rubin *et al.* 2013) or SampEn (Cirugeda-Roldán *et al.* 2012), and in RRi data may be sensitive to ectopic beats

(Henriques *et al.* 2020). In EEG studies, sample length may be ~1,000 or ~5,000 data points (Abásolo *et al.* 2008; Meisel *et al.* 2017); in HRV studies, ~300.

It is generally considered that stationarity is not required when using DFA, but this may not in fact always be the case (Bryce & Sprague 2012).

Parameter setting

Box (window) size n

n should not exceed one-tenth of the signal length (Hu *et al.* 2001), and is > 1 (Paolo Castiglioni, Personal communication, October 12, 2020). Thus, in one EEG study with 1,280 data points per 5-s epoch, DFA was computed for values of n between 3 and 128 (Abásolo *et al.* 2008). In HRV and related studies, a short-term range $10 < n < 40$ and a long-term range $70 < n < 200$ have been used (Penzel *et al.* 2003; Dehkordi *et al.* 2016), as well as the ranges of 4-16 beats and 16 to 64 beats originally used by Peng *et al.* (1995). A single range or two ranges of window size may be used in CEPS; the former will result in a single value of α, whereas the latter will provide information on both short-term and long-term exponents.

Polynomial order m

DFA is conventionally plotted linearly, i.e. with Polynomial order (m) = 1, but greater values of m are possible, resulting in a generalised measure, 'DFAm' (Höll *et al.* 2016).

Expected values of α, α1 and α2 – some examples

< 0.5 indicates anti-correlation (Pu *et al.* 2016) or 'anti-persistence' (Terrier 2019)[21]
≈ 0.5 indicates uncorrelated randomness (white noise);
≈ 1.0 indicates long-range correlation (1/f-noise)
≈ 1.5 indicates random-walk or Brown noise (Henriques *et al.* 2020).

ECG RRi data: ~0.8 in normal sinus rhythm, less in most cardiac pathologies (N = 300, Acharya *et al.* 2004; cf. Fiskum *et al.* 2018). In adult trauma patients, those requiring life-saving interventions, both the mean of α1 and median of α2 were *higher* than in those who did not (1.24 vs 1.12 and 1.09 vs 1.00, respectively) (Kumar *et al.* 2019).

In one EEG study, two scaling regions were found, one for small window sizes (< 0.04 s) with scaling exponent α1 > 1.7, the second corresponding to larger window sizes (0.08 to 0.43 s), with exponent α2 between 0.59 and 1.07; for a window size of 10 to 25 data points (from around 0.04 to 0.10 s), a narrow band showed the bend or 'kink' between the two regions. These scaling properties were found in all channels for all participants, both healthy and with Alzheimer's disease (Abásolo *et al.* 2008). In another study, long-term paraplegics showed greater α1 than able-bodied controls when supine, and greater α2 than controls when seated (Castiglioni *et al.* 2019b).

[21] This interpretation has been questioned when DFA is used with *stationary* data (Carpena *et al.* 2017).

The use of plots

A plot of DFA against scale is shown in Struzik *et al.* (2004).

Multifractal Multiscale Detrended Fluctuation Analysis (mFmDFA)

mFmDFA was introduced by Gierałtowski *et al.* (2012) and has been used with beat-t-beat blood pressure (BP), RRi, pulse-to-pulse interval (PPi) and EEG data by Castiglioni and colleagues in Milan (Castiglioni *et al.* 2017; Castiglioni & Faini 2019). As for DFA itself, for RRi data mFmDFA α at shorter scales ($n < 16$) may depend more on the linear components of HRV dynamics (in able-bodied, supine individuals), whereas differences at larger scales ($n > 16$) in the same individuals when seated may depend more on nonlinear components (Castiglioni *et al.* 2019).

Data requirements

Consider the requirements mentioned above for DFA. Although mFmDFA is generally used for long datasets, such as two-hour recordings for RRi and BP data (Castiglioni *et al.* 2017) or more than 200,000 data points in one EEG application (Castiglioni & Faini 2019), with a suggested minimum of 15,000 data points in RRi research (Gierałtowski *et al.* (2012), the 'Fast DFA' algorithm (Castiglioni & Faini 2019) may also be appropriate for short data.

Low-amplitude (10%) noise may not markedly affect mFmDFA, whereas 20% noise may do so; nonstationarity is not an issue (Gierałtowski *et al.* 2012).

Parameter setting

Box (window) size or scale n

Again, consider the examples above for DFA. In their 2012 study, Gierałtowski *et al.* (2012 set a scale range of 10 to $N/50$ (N being the number of data points); a range of between 16 and $N/7$ data points has also been used (Castiglioni *et al.* 2017).

Multifractal parameter q

$-5 \leq q \leq +5$, step interval 0.5, with $q = 0.0001$ instead of $= 0$ (Castiglioni *et al.* 2017).

For q = 2, the multifractal method coincides with the traditional 'monofractal' DFA (Kantelhardt 2002).[22]

Polynomial order m

m may be 1 or 2 when using the 'Fast DFA' algorithm (higher values are possible but will decrease the speed of the algorithm (Castiglioni & Faini 2019). For short recordings, *m* = 1 should suffice (Castiglioni *et al.* 2019).

Expected values of $\alpha(q,n)$, $\alpha 1$ and $\alpha 2$ – some examples

Output $\alpha(q,n)$ will depend on q and n, but also on m, resulting in different values of $\alpha(q,n)$ for DFA_1 (i.e. $m = 1$) and DFA_2 ($m = 2$). Furthermore, for RRi or similar data, it is possible to compute $\alpha_m(q,n)$ for both the series of absolute increment magnitudes, $|\Delta RRi_i|$ (as in VM, above), and as $\alpha_s(q,n)$ for the series of increment *signs*, or $\Delta RRi_i/|\Delta RRi_i|$ when $|\Delta RRi_i| > 0$, and 0 when $|\Delta RRi_i| = 0$. In their study on RRi in spinal cord injury, Castiglioni *et al.* (2019) found differences between groups in $\alpha_s(q,n)$ but not $\alpha_m(q,n)$ or traditional HRV indices.

The use of plots

Log-log plots of 'variability function' $F_q(n)$ against n for RRi series are shown in Castiglioni *et al.* (2019b), and of $\alpha(q,n)$ against log n in Castiglioni *et al.* (2017).

To create plots, the local slopes $\alpha(q,n)$ can be calculated as a continuous function of n (using the first derivative) or as the slope of a regression line, for instance between 4-16 beats and between 16-64 beats in order to calculate short- and long-term coefficients (Paolo Castiglioni, Personal communication, October 12, 2020).

Largest Lyapunov Exponent (LLE)

Trajectories or orbits in phase space (see above) form an 'attractor' that is reconstructed from the original data series and may converge or diverge. The mean exponential rate of divergence of two initially close orbits is the Lyapunov exponent, LE, sometimes considered a measure of dependency on initial conditions (Kannathal *et al.* 2004) but also quantifying predictability; theoretically, the LE is difficult to estimate for finite time series (Henriques *et al.* 2020).

[22] In this case, the code used in CEPS provides the fluctuation (variability) function $F_q(n)$ for all scales between the minimum n=4 and the maximum n=N/4, somewhat as in Peng's original proposal (Paolo Castiglioni, Personal communication, October 12, 2020).

For LE < 0, the trajectory will converge asymptotically to a stable fixed point or stable periodic orbit, whereas for LE = 0, the system will be in some sort of steady state mode (e.g. periodic or quasiperiodic). For LE > 0, the trajectory will be unstable and chaotic, and nearby points, no matter how close initially, will diverge to any arbitrary separation. All regions in the phase space will eventually be visited (Elert 1998-2016). As LE increases, chaos also increases and predictability decreases. Thus, computation of only the largest Lyapunov exponent (LLE) is sufficient to assess a system as chaotic (Henriques *et al.* 2020). LLE represents divergence of the system (Zbilut *et al.* 2002).

Data requirements

The LLE may be used with short and noisy datasets (Henriques *et al.* 2020), with 50 data points suggested as a minimum (Mehdizadeh & Sanjari 2017), although some authorities state that even longer data samples are required than for D_2 (Eckmann & Ruelle 1992), with ~16,000 points used in one EEG study, albeit with a faster algorithm than that implemented in CEPS (Röschke *et al.* 1995). Certainly, data length can affect results (Wolf & Bessoir 1991), as can noise (Mehdizadeh and Sanjari 2017), although others have suggested that the LLE may in fact be more resilient to noise than the fractal dimension (Wolf & Bessoir 1991). Values will also depend on data length and resolution (Röschke *et al.* 1995), and stability of the embedding dimension *m* may require a minimum of 200-300 points (Smith Hussain *et al.* 2020). In one early HRV study, 500, 625 and 750 data points (beats) produced similar results for LLE (Hagerman *et al.* 1996).

Data should be stationary, so detrending may be appropriate (Tewatia *et al.* 2011). The LLE method has been used with both global and sub-band EEG data (Adeli *et al.* 2008), although filtering may affect values of *m*, τ and LLE itself (Mehdizadeh & Sanjari 2017; Raffalt *et al.* 2020).

Parameter setting

Embedding dimension m

Select the smallest embedding dimension that yields convergence of the results; $m = 10$ has been suggested for physiological data (Mestivier *et al.* 1998; cf. Röschke *et al.* 1995) and is most commonly used in gait studies (Mehdizadeh 2018), but smaller (Humeau *et al.* 2005; Gnitecki *et al.* 2008; Raffalt *et al.* 2019) and much higher values have also been used (Tewatia *et al.* 2011). Methods also exist for calculating *m* (Kennel *et al.* 1992) (see FNN and AFN, above).

Time delay τ ('tau')

τ between sample points in the original data is used to reconstruct the trajectories of the attractor in phase space. Values vary between studies: τ of 20-40 were used in one study on breath sounds, for instance (Gnitecki *et al* 2008), of 13 in a study of laser Doppler flowmetry (Humeau *et al.* 2005) and of 6–30 data points in studies on gait, τ =10 occurring most commonly (Mehdizadeh 2018). The AMI method can be used to estimate τ.

Mean period

The mean period (reciprocal of mean frequency of power spectrum, obtained by Rosenstein *et al.* from the fast Fourier transform, FFT) is required in some algorithms for LLE. It is approximately equal to the lag when the autocorrelation function of the time series reduces to (1 – 1/*e*) x its initial value, where *e* is Euler's number (Rosenstein *et al.* 1993).[23]

Maximum number of trajectory iterations, MI

MI of 300 was used in one classic EEG study (Röschke *et al*. 1995). At least 50 consecutive cycles are needed to estimate the LLE reliably (Mehdizadeh & Sanjari 2017), so this is taken as the default value for MI in CEPS. These numbers can provide a starting point for experimenting to determine the maximum number of iterations in your data.

It will probably be more useful to set *m* and τ using a group average state space reconstruction method rather than setting them individually, as found in gait studies, where LLE is frequently used (Raffalt *et al.* 2018a).

Expected values – some examples

To be useful, LLE must be > 0, but values will vary depending on methods used; comparisons are therefore most likely to be meaningful within studies or where data is of similar length and resolution (Humeau *et al.* 2005; Mehdizadeh 2018; Raffalt *et al.* 2019; Smith Hussain *et al.* 2020).

When used in gait studies, a larger LLE is usually associated with poorer balance (Caronni *et al.* 2020), in contrast to the many aspects of physiology where increasing complexity suggests a healthier state.

Similarly, in sleep apnoea, ECG LLE was lower during normal breathing (0.04) than in apnoea (0.06) or hypopnea (0.05) (*N* = 39, Acharya *et al*. 2011);

RRi data: LLE ~0.5 in normal sinus rhythm and may be larger or smaller in cardiac pathologies (*N* = 300, Acharya *et al.* 2004).

[23] However, if the autocorrelation function descends very slowly with increasing lag, this may not be practicable to compute (Liao & Jan 2014).

The use of plots

Plotting LLE against m, τ, mean period or MI is advisable before selecting parameters for a research project.

Recurrence Quantification Analysis (RQA)

"Implementation of RQA is far simpler than its actual interpretation"

(von Borell *et al*. 2007)

While the LLE quantifies divergence between trajectories in phase space, RQA quantifies the periodic nature of those trajectories in a 'recurrence plot' of the data[24] (Marwan *et al.* 2002; Zbilut *et al.* 2002). There is a natural linkage between fractals and recurrence (Webber 2012). The following measures are often computed:

1. %REC* Percentage of plot filled with recurrent points, or Recurrence rate, related to D_2 (Iwanski & Bradley 2004)

2. %DET * Percentage of recurrent points forming diagonal lines with a minimum of two adjacent points, or Determinism (increases with predictability)

3. ENT* Shannon entropy of the line length distribution[25]

4. Lmax* Length of longest (diagonal) line segment in plot; shorter Lmax indicate chaotic behaviour, longer Lmax periodicity (Iwanski & Bradley 2004); 1/Lmax ≈ LLE (Eckmann *et al.* 1987; Trulla *et al.* 1996)

5. TREND* A measure of how the plot becomes paler away from the central diagonal, or how stationary a system is over the course of measurements (von Borell *et al.* 2007)

6. LAM* Ratio in the plot between recurrence points forming vertical structures and the entire set of recurrence points, or Laminarity

[24] Images of such plots can be viewed on many internet webpages. A particularly informative source is that by Marwan *et al.* (*Recurrence Plots and Cross Recurrence Plots*. www.recurrence-plot.tk) [Retrieved August 4, 2020].

[25] Not to be confused with the SE of the original data series!

7. RATIO %DET/%REC

8. TT* Average length of vertical lines, or Trapping time – how long the system can stay in a particular state (Nayak *et al.* 2018)

9. Vmax Length of longest vertical line

10. Lmean Average length of diagonal lines

(* Output measures available from CEPS are asterisked in this list.)

Measures of complexity based on vertical structures in recurrence plots permit detection of transitions between periodic and chaotic states, as well as 'laminar' chaos-chaos transitions (Marwan *et al.* 2002). Other measures can also be derived in RQA but are not considered here. Some Iranian studies use linear discriminant analysis (LDA) – a method available in MATLAB – to reduce the number of RQA features and improve classification accuracy in HRV or EEG research (Mohebbi *et al.* 2011; Mehrnam *et al.* 2017).

Data requirements

RQA may be used with short (n = 30) and nonstationary or nonchaotic datasets,[26] as well as noisy ones (with a threshold adjustment) (von Borell *et al.* 2007; Chen *et al.* 2012; Webber 2012). RQA becomes computationally expensive for long data series (Chen & Yang 2012).

RQA has been used for band-filtered EEG data (Niknazar *et al.* 2013; Murugappan *et al.* 2020), as well as in HRV studies. Different filter types will affect RQA results from EEG data in different ways (Sharanya *et al.* 2014), and sampling rate or downsampling will also affect results (García-González *et al.* 2009; Rhea *et al.* 2011).

Parameter setting

Embedding dimension m

m = 10 was recommended by Zbilut *et al.* (2002), except for very noisy data (see too the discussion of m under LLE, above), and is standard in the Kubios HRV software package (Tarvainen *et al.* 2019); in HRV studies, m is usually somewhat < 20 (Mestivier *et al.* 1997); values of 3, 6, 9 and 12 were tested by Marwan *et al.* (2002), and 4, 6, 8 and 16 for inter-breath interval data by Terrill *et al.* (2009).

[26] RQA may thus be more generally applicable than LLE on its own.

For EEG, m = 3 has been used (Shabani *et al.* 2016). Theoretically, for some low-dimensional systems, calculation of m may not be required (Cao 1997; Thiel *et al.* 2004), and differences between some RQA measures for different conditions may be relatively independent of m (Terrill *et al.* 2009). There is a useful discussion of m in RQA by Malik (Malik 2020).

Time delay τ ('tau')

Time delay τ is not critical; oversampling is reasonable, provided more noise is not introduced (Zbilut *et al.* 2002). However, Eckmann *et al.* (1987) recommended that τ should not be too small, although τ = 1 has been used (Schinkel *et al.* 2008) and is appropriate for RRi or inter-breath interval data (Terrill *et al.* 2009; Melillo *et al.* 2011).

For EEG data, τ = 4 has been used (Shabani *et al.* 2016).

Threshold r[27]

Kubios HRV software uses $\sqrt{m}$*SDNN as a default setting (Tarvainen *et al.* 2019), based on prior research (Dabiré *et al.* 1998; Melillo *et al.* 2011); others have used r = 5, for example (Giuliani *et al.* 1998), or much higher values (77 – 170) (Marwan *et al.* 2002). A number of strategies exist for selecting r, such as at a fixed percentage of recurrence point density. This percentage could be, for example, 1% (Marwan *et al.* 2007) or 5% (Malik 2020). In CEPS, r is pre-selected as the square root of m rather than a fixed percentage of the maximal plot distance or plot density, but this can be amended manually. If r is too small, too few recurrence points will result to reveal anything about the underlying recurrence structure (Henriques *et al.* 2020).

Minimum line length (L_{min})

L_{min}, is usually set at 2 (Webber & Zbilut 1994), but in EEG studies L_{min} = 10 (Shabani *et al.* 2016) or even L_{min} = 20 have been used (Becker *et al.* 2010).

Expected values – some examples

In an HRV study on sleep apnoea (N = 58), %REC was c 38-45, and ENT (SE) c. 3.2-3.6 (Trimer *et al.* 2014), In another HRV study (N = 108), on diabetic autonomic dysfunction, L_{max} was 55 ± 21 in the diabetic participants, but 37 ± 14 in the healthy (Mestivier *et al.* 1997). In an HRV study on ventricular tachyarrhythmias (VT, N = 17), both L_{max} and V_{max} were higher shortly before onset of VT than at control times, particularly with higher values of m and r, when mean V_{max} could be as great as 520, and L_{max} 350 (Marwan *et al.* 2002). In a smaller HRV study with healthy participants only, %REC was between 122 (before exercise) and 460 (after), corresponding results for %DET, L_{max} and ENT being 96 & 99, 26 & 43, 3 & 3.6 (Figueiredo *et al.* 2018). ENT may decrease with increasing noise as well as increasing signal regularity (Rhea *et al.* 2011).

[27] In some academic papers, 'ε' is used rather than r.

The use of plots

Recurrence plots are less easy to interpret than the measures computed from them. However, it may be useful to investigate how these measures change depending on the four parameters used in creating the plots before fully analysing a particular dataset. The FNN or AFN methods may also be used to estimate m, and the AMI method to estimate τ.

Recurrence Period Density Entropy (RPDE)

RPDE is a relatively new member of the family of RQA measures. In PubMed, for instance, 453 RQA studies have been indexed since 1997, but only nine on RPDE, the earliest being published in 2011.[28]

RPDE quantifies the periodicity, repetitiveness or extent of recurrences of a signal in phase space (Green 2012; Supriya *et al*. 2020) and is related to both the Kolmogorov-Sinai entropy and the Pesin fractal dimension of the set of recurrence times (Kraemer *et al*. 2018; Marwan *et al*. 2015). The measure – also known as 'recurrence time entropy' (Marwan *et al*. 2015) – was introduced by Max Little and colleagues at Oxford University as a method for online acoustic speech pathology screening (Little *et al*. 2006, 2007). It has therefore been used mostly in research on speech and respiration, especially in the diagnosis of Parkinson's disease using machine learning (e.g., Boruah *et al*. 2020). Airflow pattern complexity (RPDE) was reduced in cases of severe chronic obstructive pulmonary disease (COPD) (Dames *et al*. 2014) and was also found to be a possible early indicator of asbestosis, in both smokers and non-smokers (Sá *et al*. 2019).

There are fewer studies on the ECG or EEG, for example,[29] although RPDE has been used in a number of machine learning EEG studies (e.g., Bahari *et al*. 2013).

In their 2007 paper, Little *et al*. normalised RPDE between 0 (its value for a perfectly periodic signal) and its maximum (the value for white noise), simply by dividing RPDE by

[28] PubMed searches, 30 March 2022.
[29] There are currently (30 March 2022) around 380 entries for RPDE in Google Scholar. Of these, around 330 include the word 'voice' (320 'vocal', 110 'breath', 90 'respiration'), and around 150 include 'Parkinson's'. Eighty studies include the term 'EEG' (40 'MRI') and 50 'ECG' (65 'heart rate').

the latter. Most authors have followed this procedure since (e.g., Marwan *et al*. 2014, 2015; Mukherjee *et al*. 2015; Arunachalam *et al*. 2017). Mukherjee *et al*. (2015) found the normalised RPDE from ECG signals was higher in healthy individuals than in those with congestive heart failure and were able to define the threshold between them. They suggested that as this result is based on phase space dynamics rather than the signal itself, these results are likely to be more robust than those based on MSE, for example.

In ECG analysis, RPDE has been found useful in documenting clear transitions from normal rhythmic to abnormal rhythmic behaviour in long duration recordings (Nair & Kiasaleh 2014). And in a study of 5-minute HRV recordings in healthy individuals as well as others with end stage renal disease, RPDE was found to decrease significantly when moving from a supine to a standing position, with significant changes (decreases or increases) in a number of other RQA measures (Calderón-Juárez *et al*. 2022).

RPDE based on single-channel EEG has been used in the classification of schizophrenia, being higher in schizophrenics than normal controls, with the proviso, however, that the phase space embedding. Involved may amplify noise in the signal, particularly for non-stationary data (Green 2012).

There thus appear to be contradictory opinions on the usefulness of RPDE. Furthermore, there are also a number of studies in which RPDE was perhaps not as informative as other, more standard RQA measures (e.g., Paoletti *et al*. 2014; Rolink *et al*. 2015; Akbarian & Erfanian 2018; Ledesma-Ramírez *et al*. 2019; Soloviev *et al*. 2020; Tavasoli *et al*. 2021).

RPDE has also been used in climate analysis (Marwan *et al* 2021), as well as in financial forecasting (Soloviev *et al*. 2020).

Data requirements

RPDE does not require data to be linear or normally distributed (Nair & Kiasaleh 2014; Supriya *et al*. 2020).

Parameter settings

Values of *m*, the embedding dimension, should be tested between 3 and 10 (Kraemer *et al*. 2018). but can also be selected using the FNN method (Mukherjee *et al*. 2015).

Embedding delay τ can be selected using the AMI method (Mukherjee *et al*. 2015).

Reported values – some examples

Nair and Kiasaleh (2014) used RPDE in the analysis of ECG data, with values in the 0.45 to 0.75 range indicating chaotic behaviour. Values outside this range they considered as noise-like behaviour (if > 0.75) or (if < 0.45) as rhythmic.

The use of plots
Little *et al*. (2006) include a plot of DFA α against RPDE that clearly differentiates between normal and pathological speech.

Symmetrical Recurrence Quantification Analysis (SRQA, or SQA)

'Symmetrical Recurrence Quantification Analysis' (SRQA) is an extension of the RQA method proposed by Jean-Marc Girault specifically to detect chaos–chaos or chaos–periodic, symmetry-breaking or symmetry-increasing bifurcations in data (Girault 2015; Abdennaji *et al*. 2021). As yet, the method, which combines recurrence (in phase space) and symmetry (in time series), does not appear to have been used by other researchers.

In phase space, four kinds of 'isometry' are necessary to describe the possible symmetries present in a time series: translation T, (vertical) reflection R, inversion I and Glide reflection G. The same isometries are used in centred and averaged fuzzy entropy (CAFE) (Girault & Humeau-Heurtier 2018). SRQA output is in the form of a Symmetry plot (SP) and Symmetry descriptors (SDs).

Girault (2015) describes a number of simple SDs, based on RQA, but defined in terms of chaotic rather than recurrent properties:

DP, quantifying the number of pairs of recurring 2-tuples (ordered pairs) that are symmetric

DET, quantifying the percentage of points that formed diagonal or 'anti-diagonal' segments in relation to the total number of recurrence points

DIV (the inverse of L_{max}, the maximum length of diagonals in the plot), quantifying divergence between symmetric trajectories in phase space and approximately equivalent to the largest Lyapunov exponent, LLE (rate of separation of close trajectories). If it is not possible to measure L_{max}, no values of *DIV* result.

Other SDs based on RQA are also possible, as well as cross symmetrical recurrence plots. In a further paper (Abdennaji *et al*. 2021), Girault and colleagues used *RR* (recurrence rate), *ENTR* (entropy), *LAM* (laminarity), L_{max}, *L* (meanline), *TT* (trapping time) and *TREND*, for example.

The SRQA measures

Two sets of functions are provided, for the symmetry plot itself, using the four different symmetries Translation (T), Rotation (R), Inversion (I) and Glide (G), and for the three output measures defined by Girault and derived from the plot, as mentioned above.

Data requirements

Normalisation or binarisation of the data may be required, as in Abdnnaji *et al* 2021.

Parameter settings

m: pattern size or length (embedding dimension in RQA)

r: similarity criterion, or tolerance (threshold in RQA) – between 0.1 * SD and 0.25 * SD (but see under 'The use of plots', below).

Centring or non-centring (of the pattern).

Reported values – some examples

Values of the Symmetry descriptors (SDs) DP, DET, DIV (and LLE) shown in plots by Girault (2015) are between 0 and 1.

The use of plots

Girault (2015) includes plots of Symmetry descriptors (SDs) DP, DET, DIV and LLE derived from the logistic map for different values of r, from 3.5 to 4.0, as well as of the SDs from the cubic map for r between 0.5 and 3.0, and between 2.2 and 3.0.

Another RQA variant is the 'fuzzy recurrence' method proposed by Pham (Pham 2016, 2018, 2022), for which MATLB code is available (Pham n.d.).

The Poincaré plot (PP) and Extended Poincaré plot (EPP)[30]

"The Poincaré plot, also named return map, is the simplest technique to describe the nonlinear dynamics of a biosignal such as heart rate" (Karmakar *et al.* 2015)

The Poincaré plot is a scatter plot of the correlations between two immediately consecutive points in a time series, with the original time series along the x-axis and lagged points along the y-axis (with lag $k = 1$). SD1 and SD2, the standard deviations along the minor and major axes of the plot (orthogonal axes rotated through 45°), provide measures of the short-term and long-term recurrence in the data (see **Figure 2**). Above the major axis (or 'line of identity'), there is an increase or acceleration between each point and the next, whereas below the line of identity, there is a decrease or deceleration.

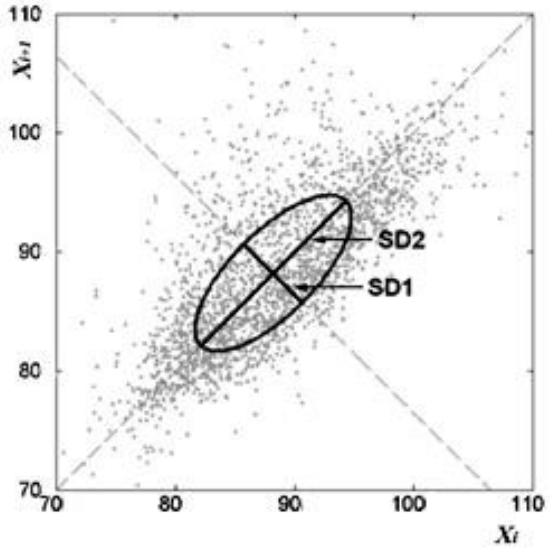

Figure 2. Poincare plot, showing SD1 and SD2.

The ratio of the number of points above the line of identity to the total number of points in the plot provides a measure of 'heart rate asymmetry' (HRA) (Porta *et al.* 2008). Various alternative measures of HRA exist, including one based on a ratio of the Shannon

[30] This section was written in consultation with Alireza Mani.

entropies of the accelerations and of the complete time series. Values of this version of HRA > 0.5 indicate sympathetic influence, those < 0.5 reflect parasympathetic influence and deceleration. (Jelinek *et al.* 2011b; Rohila & Sharma 2020).

In effect, the Poincaré plot is a simplified recurrence plot, and is sometimes known as a 'return map'. It is not always considered a nonlinear method, as SD1 is identical to the linear time domain measure RMSSD and SD2 is also linear (Brennan *et al.* 2001; Ciccone *et al.* 2017).

Poincaré plots have been used frequently in HRV studies (Henriques *et al.* 2020), less often in EEG research, and only occasionally in studies on blood pressure variability (Blanc *et al.* 1999), temperature or respiration (Satti *et al.* 2019; Bottaro *et al.* 2020).

In CEPS, an extended version of the Poincaré plot is implemented in which the lag *k* can take any discrete value, not just 1, so that longer-term correlations in physiological time series can be detected; the plots themselves are not visualised (Satti *et al.* 2019). Such lagged (extended) Poincaré plots incorporate autocovariance information and can indicate nonlinear time series properties that might be masked by the strong correlation between successive beats if only 1-lagged plots are used (Thakre & Smith 2006).

Data requirements

Poincaré plots have been used with both discrete (e.g. RRi) and continuous (e.g. EEG) data, with noisy (Bolaños *et al.* 2016) and missing (Kim *et al.* 2011) data, with nonlinear and even 'grossly' nonstationary data (Blanc *et al.* 1999; Lund *et al.* 2003). However, for continuous data, sampling rate may need to be considered (Hayashi *et al.* 2015), and band-filtering will also affect results (Bolaños *et al.* 2016).

Data sequences (RRi) from 50 to 50,000 were used in one study; SD1 and SD2 increased with RRi data length, while SD1/SD2 decreased (Thakre & Smith 2006).

Parameter setting

Lag k

In the EPP method, k =1 returns the conventional plot. Values of k from 1 to 20 were used in the study by Satti *et al.* (2019), and from 1 to 10 by Thakre and Smith in their different lagged plot method (2006).

Expected values – some examples (from Thakre & Smith 2006)

r (Pearson's correlation coefficient between X_n and X_{n+k} for *k* from 1 to k_{max})
SD1 0.0222 to 0.0253 (increasing with increasing data length *N*)
SD2 0.0531 to 0.1522 (increasing with increasing data length *N*)
SD1/SD2 0.4013 to 0.1962 (decreasing with increasing data length *N*)

All three measures showed a curvilinear and increasing relationship in healthy individuals when plotted against *k* from 1 to 10 that became more linear in those with congestive heart failure (Thakre & Smith 2006). However, in another study, while SD1 and SD1/SD2 increased with *k*, SD2 decreased (Shi *et al.* 2009).

The use of plots

Plots of *r*, SD1 and SD2 against *k* are shown in Satti *et al.* (2019). Plotting SD2 against lag *k* for our own RRi research data showed alternate increases and decreases with each lag for some recordings but not for others, suggesting inherent oscillations in the former.

Heart rate asymmetry

"The accelerations and decelerations of heart rate are well-defined physiological processes, even though the specific mechanisms that govern them are very complex … The widespread belief that it is the parasympathetic branch of the autonomic system which is responsible for decelerations and the sympathetic branch which is responsible for accelerations is only a first approximation and in reality, these processes are much more complex"

(Mieszkowski *et al*. 2016)

'Heart rate asymmetry' (HRA) is a flourishing area of research, and HRA has been found even in neonates (Czippelova *et al*. 2014). It is usually considered in terms of unevenness in the distribution of points above and below the line of identity in the Poincaré plot, which indicates *instantaneous* changes in the beat-to-beat heart rate (Karmakar *et al*. 2009a).

Heart rate may accelerate or decelerate, and HRV has been found to differ in phases of acceleration and deceleration. As described below, there are a number of measures of heart *rate* asymmetry (HRA), such as Porta's, Guzik's, the Slope and Area indices, but until

recently none could estimate such asymmetries in heart rate *variability*. An Asymmetric Spread Index (ASI), based on the Poincaré plot, was created to remedy this shortcoming.

Three frequently used measures of HRA were developed first[31]: Ehlers' index (EI) (Ehlers *et al*. 1998), Guzik's index (GI) (Guzik *et al*. 2006; Piskorski & Guzik 2007a) and Porta's index (PI) (Porta *et al*. 2006).[32] Karmakar *et al*. went on to develop a Slope index (SI) (Karmakar *et al*. 2012) and an Area index (Yan *et al*. 2017). They also proposed redefinitions of EI, GI and PI to represent increasing *patterns* of increase or decrease in HR, not just instantaneous changes (Karmakar *et al*. 2009).[33] More recently, Rohila and Sharma (2020) published their Asymmetric spread index (ASI). Another approach has been to use coarse graining (i.e., multi-scaling) of the data prior to using asymmetry indices (Chladekova *et al*. 2012; Czippelova *et al*. 2015; Goshvarpour *et al*. 2021). A multiscale asymmetric DFA approach is also possible (e.g., Mieszkowski *et al*. 2016; Alvarez-Ramirez *et al*. 2017; Piskorski *et al*. 2018).

Ehlers' index (EI)

EI was initially proposed as a measure of 'slope asymmetry' to quantify nonlinear structure in EEG data, estimated by the skewness of differences between successive samples (without reference to Poincaré plots):

$$\frac{\sum (x_i - x_{i-1})^3}{\left(\sum (x_i - x_{i-1})^2 \right)^{3/2}}.$$

EI does not have a pre-defined range, but a significant distance from 0 indicates asymmetry (Chladekova *et al*. 2012). In the EEG, EI (slope asymmetry) is mostly positive, and was greatly reduced compared to placebo during mild alcohol intoxication (Ehlers *et al*.

[31] A further method, 'sample asymmetry analysis' (SAA), was developed by Lake and Moorman's group in 2003. In a study of neonatal sepsis, they noted marked asymmetry of the frequency histograms of RR intervals, with large deviations to the right of the distribution median, the consequence of long RR intervals during HR decelerations, and only small deviations to the left, the consequence of fewer and smaller HR accelerations (Kovatchev et al. 2003). Although there are more hits in Google Scholar for SAA (128) than the methods covered here, it appears to have remained popular almost exclusively in the fields of neonatology and severe infection monitoring.

[32] In Google Scholar on 25 April 2022, there were around 35 hits for EI, 40 for GI and 52 for PI when searching for the name as a phrase. For AI (AND the phrase "Poincaré plot") there were around 21 hits, and for SI (AND "Poincaré plot"), 36 hits. There was only one result for the ASI.

[33] Guzik's group have called this approach the 'Karmakar index' (Graff et al. 2013).

1998). In itself, in contrast to the HRA indices developed later, it is a linear measure, although used to quantify nonlinearity.

A redefined version, calculating EI along the minor axis of the Poincaré plot rather than the actual time series signal, has also been proposed (Karmakar *et al*. 2009b).

Guzik's index (GI)

The standard descriptors of the Poincaré plot are SD1 and SD2, where SD1 is the dispersion of the points in the plot perpendicular to the line of identity (LI, where $y = x$) and SD2 is the dispersion along this line. SD1 is interpreted as the instantaneous beat-to-beat variability of the RR intervals, so a measure of short-term HRV, while SD2 is related to long-term HRV. For RR interval data, both are measured in units of time, e.g., ms (Guzik *et al*. 2006).

GI is based solely on SD1. If D_i is the distance from point P_i to the LI, then:

$$GI = \frac{\sum_{i=1}^{l} D_i}{\sum_{i=1}^{m} D_i} \times 100$$

where l is the number of points above LI and m the total number of points in the plot other than those on the LI itself.

D_i is calculated using:

$$D_i = \frac{|RR_{i+1} - RR_i|}{\sqrt{2}}$$

SD1 itself can be decomposed into two parts, $SD1_{up}$ (SD1 for the number of points above the line of identity) and $SD1_{down}$ (for the number of points below the line). In their 2006 paper, Guzik *et al*. derived two further variables, C_{up} (or C_d, for HR decelerations) and C_{down} (or C_a, for HR accelerations), describing the relative contributions of $SD1_{up}$ and $SD1_{down}$, respectively, to SD1:

$$C_{up} = \frac{SD1_{up}^2}{SD1^2}, \quad C_{down} = \frac{SD1_{down}^2}{SD1^2}$$

In a subsequent paper, they noted that HRA causes contributions from heart rate decelerations to contribute more to short-term variability than accelerations, but that for long-term variability (substituting SD2 for SD1 in the above equations), the relation is reversed, suggesting that some compensatory mechanism might be in play (Piskorski & Guzik 2012). They also introduced a number of subsidiary descriptors: $SD1_a$, $SD1_d$ (and correspondingly for $SD2$), $SDNN_a$ and $SDNN_b$. For 24-hour recordings, 'jumping' (disjoint) 300-second windows can provide mean values of these measures (Piskorski *et al*. 2019).

The same asymmetry measures were applied to systolic blood pressure (SBP) data: in healthy supine individuals, although increases were significantly fewer than reductions, their contribution to short-term blood pressure variability was significantly larger. HRA and SBP asymmetry were independent, and the latter showed no difference between women and men (Guzik *et al*. 2010a). Guzik *et al*. (2014) demonstrated that stroke volume (SV), cardiac output (CO) and systemic vascular resistance (SVR) have asymmetrical properties as well.

Other researchers have noted that GI asymmetry may be significant for congestive heart failure (CHF), but not for atrial fibrillation or in healthy individuals (Alvarez-Ramirez *et al*. 2017), or that both GI and PI may be raised prior to surgery for coronary artery bypass graft in those liable to develop atrial fibrillation after their surgery (Ranuzzi *et al*. 2017). C_{up} is reduced in heart failure compared to healthy individuals, especially at Poincaré plot lag ('order') range 2-5 (Platiša *et al*. 2020). Furthermore, GI asymmetry decreased with atropine infusion and increased with scopolamine administration, indicating that parasympathetic blockade reduces the prevalence of asymmetries (Karmakar *et al*. 2012b). A similar result was found using the redefined version of GI proposed by Karmakar *et al*. (Karmamakr *et al*. 2010). Thus, higher values of GI may indicate important deviations of the normal functioning of the vagal tone to regulate the heart rhythm (Alvarez-Ramirez *et al*. 2017). In a different study, significantly increased GI (i.e., a shift from acceleration to deceleration) following attendance on a yoga course was interpreted as indicating an increase in vagal tone (Frank *et al*. 2020). In another such study, whereas GI increased during yoga (compared to metronome-paced breathing), it did so more clearly at higher scales (greater lags) than in the conventional Poincaré plot (i.e., with lag = 1) (Goshvarpour *et al*. 2021). In contrast to the yoga studies, but as might be expected, GI (and, to a lesser extent, PI) were *decreased* in

children suffering from attention deficit/hyperactivity disorder (ADHD) at rest and in response to physiological stress (orthostasis), compared to in age-matched controls (Tonhajzerová *et al*. 2014). The same group found that resting heart rate time GI, PI and EI were significantly reduced in adolescent girls with major depression, although without significant differences in response to orthostasis (Tonhajzerová *et al*. 2012).

Guzik *et al*. have also explored what they call heart rate 'microstructure' (Guzik & Piskorski 2020), simply by counting the number of HR acceleration and deceleration runs, the total number of beats in runs of specific lengths, and then dividing by the total number of normal RR intervals. They also defined (Shannon) entropic measures to summarise the distribution of deceleration and acceleration runs separately and observed that the acceleration-related part of entropy is greater than that of decelerations (Piskorski & Guzik 2011a). In patients who had suffered an acute myocardial infarction, for example, fewer deceleration 'runs' (consecutive RR decreases) over 2 to 10 cycles during 24-hour ECG recordings indicated an increased risk of mortality (Guzik *et al*. 2011a).[34] Fewer acceleration runs also occurred, but without the same prognostic value (Guzik & Piskorski 2020). Reduced numbers of deceleration runs may also be associated with greater risk of cardiac arrhythmia in COPD (for which cardiovascular disease is the most common comorbid condition) (Kong *et al*. 2020). Guzik and colleagues also noted that an *increased* number of both longer deceleration and acceleration runs are more common in those with severe obstructive sleep apnoea (Guzik *et al*. 2013b; cf. Jiang *et al*. 2017), and an increased number of deceleration runs was also found in pre-term infants at risk of sepsis (Billois *et al*. 2021). In longstanding type 1 diabetes, both $SD1_{up}$ and $SD1_{down}$ were reduced, whereas the number of changes was not (Guzik *et al*. 2010b). On a more everyday level, the ratio of decelerations to accelerations was found higher in late adolescence when supine than when seated, with fewer 2-beat runs but more and longer monotonic runs (4-9 beats), suggesting simultaneous vagal withdrawal and sympathetic activation with the minimal orthostatic stress induced by

[34] Deceleration runs and 'Deceleration capacity' (DC) (Bauer et al. 2006; Nasario-Junior et al. 2014) are probably regulated by similar physiological processes (Guzik et al. 2012). DC may be enhanced more than 'acceleraton capacity' (AC) by slow (0.1 Hz) breathing (Wang et al. 2015). The relationship between C_{up} and DC is explained in the online supplementary material to Platiša et al. 2019b.

sitting (Wierzba *et al*. 2019). Guzik *et al*. (2013a) observed that HRA may be found even in 1-minute ECG recordings.

Guzik's group also noted that positive emotions may result in more decelerations in short-term variability (C_{up}) compared to negative emotions, and that C_{up} correlates with subjective ratings of affect (Kaczmarek *et al*. 2019). GI, PI, SI and the GI subsidiary descriptors introduced by Piskorski and Guzik (2012) have thus been used in studies on classification of emotional responses (Moharreri *et al*. 2018, 2019). Karmakar *et al*. (2014a) noted that GI was significantly lower in those who were depressed than in the non-depressed – particularly for women (the difference was not significant in men). In contrast, both EI and PI were significantly *greater* in women with depression than those without, the difference again not being significant in men. They concluded that the three different methods may provide partially independent information and that their simultaneous quantification might be useful for a more comprehensive analysis of asymmetry, with the EI result, for instance, indicating a 'shift towards sympathetic predominance' in depression.

Parvaneh *et al*. (2015) found that GI and SI reduced significantly with increasing levels of driving stress (low-moderate-high), whereas although PI was lower at moderate than at low stress levels, it increased again when stress level was high.[35] Other researchers, using GI with 25 HRV measures in a machine learning study on stressful motor tasks, found that GI and associated HRA measures were the most revealing features used for stress detection in the hand (but not the knee) task (Karthikeyan *et al*. 2022). Other researchers have observed significant reductions in GI and EI with stressful tasks (Stroop and arithmetic tests), but lower PI only in response to the arithmetic test (Visnovcova *et al*. 2014).

In a further study, using the ordinal pattern approach originated by Bandt and Pompe in their 2002 development of permutation entropy, Guzik and colleagues interpreted 'zigzag'-like patterns as related to vagal modulation, more consistent acceleration and deceleration runs as related to sympathetic influences (Graff *et al*. 2013).[36]

[35] The same group of researchers noted that GI, PI and SI behave differently during exposure to coloured light (red, green, blue, yellow), with PI lower for blue and yellow, GI lower for red and green, and SI reduced only during exposure to blue. They speculated that this reduction might be linked to lower parasympathetic activity (Parvaneh et al. 2017).

[36] Another variant of GI, the 'SKG' index, was proposed by Kramarić et al. in 2019 as a marker of neonatal stress but does not appear to have been used as yet by other researchers.

GI may range from 0 to 100 (Chladekova *et al*. 2012).

Porta's index (PI)

PI is simply the number of points below the LI (*b*), divided by the total number of points in the Poincaré plot (*m*) (excepting those located on the LI itself) x 100:

$$PI = (b/m) * 100.$$

PI ≠ 50% indicates asymmetry, or 'time irreversibility'. PI may range from 0 to 100% (Chladekova *et al*. 2012). Thus, while GI compares the *magnitude* of acceleration and decelerations, PI compares the *number* of increments and decrements in the RR time-series (Karmakar *et al*. 2014b). If PI is significantly less than 50%, this indicates the presence of bradycardic runs (with heart period lengthening) (Porta *et al*. 2006a) and given that an increase in HR is linked with increased sympathetic activity, if PI is significantly greater than 50%, this suggests a shift of sympatho-vagal balance toward sympathetic dominance (Czippelova *et al*. 2015; Jelinek *et al*. 2011; Karmakar *et al*. 2014b), and/or vagal withdrawal (Porta *et al*. 2008). It is thus not surprising that PI decreases with sleep stage (depth), being greatest during REM sleep (Yan *et al*. 2021a).

PI was found to increase significantly during controlled breathing at 10 or 15 breaths per minute, compared to spontaneous breathing, but without any particular relationship to respiratory asymmetry (expiration/inspiration ratio, I/E), indicating that respiratory asymmetry is only one of several factors contributing to HRA (De Maria *et al*. 2020, 2021). Others have noted that PI and GI increased only in the seated position, but not when supine, and that the I/E ratio may have effects on PI (and GI), both indices being larger with 1:1 ratio breathing than with 'physiological' 1:2 breathing (Wang *et al*. 2013) or 2:1 breathing, indicating that the I/E ratio should be considered in HRA analysis, though not necessarily in HRV analysis (Klintworth *et al*. 2012). In another study, the increase in GI and PI with paced 'resonance' breathing was associated with decreased HRV complexity and considered 'a dynamical signature of disrupted physiologic control systems' (Iardukhina *et al*. 2019). Wang *et al*. (2013), comparing the effects of breathing at 6 and 15 breaths per minute (but with the same I/E ratio), also noted that GI and PI increased more when breathing at the

lower rate, with durations of RR interval (RRi) increases being less than those of RRi decreases only during the slow breathing (Wang *et al*. 2014).

Foetal PI was found to increase significantly after 35 weeks gestation compared to before 32 weeks (the corresponding increase in GI was not significant) (Karmakar *et al*. 2014b, 2015b). In a rather different study, a decrease in PI (rather than GI, SI or AI) was associated with increased levels of serum fibrinogen and carbohydrate antigen 19-9 (CA199) In newly diagnosed gastric cancer patients (Shi *et al*. 2019). PI was also found to decrease during brief regular treadmill walking as against resting in a seated position; in contrast, GI, SI and AI remained unchanged. However, following data detrending, only GI remained unchanged. The authors of this study (some of whom had developed both AI and SI in the first place) concluded that GI may not be sensitive to short-term HRA, but that SI and AI may capture both short- and long-term HRA features (Wang *et al*. 2018).

Slope index (SI)

The slope S_i of each point P_i in the Poincaré plot (i.e., y/x) is RR_{i+1}/RR_i, and the slope of each point relative to the line of identity (RS_i) is then given by:

$$RS_i = S_{LI} - S_i.$$

The SI is defined as the sum of the relative slopes of points above the LI divided by the sum of the relative slopes of all points in the Poincaré plot, other than those located on the LI:

$$SI = \frac{\sum_{i=1}^{l} |R\theta_i|}{\sum_{i=1}^{m} |R\theta_i|} \times 100 \quad ,$$

where l is the number of points above the LI and m the number of all points in the plot except those on the LI (Karmakar *et al*. 2012a; Yan *et al*. 2017). Because pre-processing RR interval data may change the locations of points in the Poincaré plot relative to its global coordinates, and so the value of SI, Karmakar's group have suggested that care be taken when selecting and reporting the particular reference point (coordinates origin) used, particularly for short-term data. Different strategies may be appropriate in different situations (Yan *et al*. 2019).

Karmakar *et al*. (2015a) found that SI was better than GI and PI for discriminating between healthy individuals and patients with cardiac dysfunctions.

Area index (AI)

The AI is defined as the sum of the areas of the sectors corresponding to the points that are located above the line of identity (LI), divided by the sum of the areas of the sectors corresponding to all the points in the Poincaré plot (other than those that located exactly on the LI). If S_i is the sector area corresponding to point P_i l the number of points above the LI, b the number of points below the LI, and m the number of points not on the LI, then $m = l + b$ (Yan *et al*. 2017), and:

$$AI = \frac{\sum_{i=1}^{l} |S_i|}{\sum_{i=1}^{m} |S_i|} \times 100$$

.

AI was found to decrease following percutaneous coronary intervention (PCI, or angioplasty plus stenting) in both male and female patients with coronary artery disease. A similar – though less significant - pattern of change was found with PI, while GI and SI could either increase or decrease in men and tended to increase rather than decrease in women following the intervention. The authors concluded that 'AI should be considered as a potential reference indicator for monitoring the recovery of cardiovascular system function in patients after PCI (Yan *et al*. 2021b). As with SI, data pre-processing may affect results, but Karmakar's group have stated that AI (rather than SI) metrics should be the first choice in general, as in many situations they showed relatively stable performance (Yan *et al*. 2019).

Asymmetric Spread Index (ASI)

Any point P_i in the Poincaré plot can be defined in terms of Cartesian or polar coordinates. Using the latter, if its distance from the origin of the X_i and X_{i+1} axes (CEPS Primer Figure 2), or 'polar axis', is d_i, and the slope of the point relative to the origin (its 'angular coordinate' or phase angle) is θ_i, then ai, the 'arc length' of the point (its distance from the diagonal line of identity in the plot along an arc centred on the origin) = θ_i x d_i. The ASI is then defined as the standard deviation of arc length corresponding to the points

above the line of identity (LI) in the plot, divided by twice the standard deviation of the arc length corresponding to all points in the plot (excluding those on the line of identity itself).

Mathematically, ASI is defined as:

$$ASI = \sqrt{\frac{\sum_{j=1}^{m} \frac{(a_j - \bar{a})^2}{m}}{2 \times \sum_{k=1}^{m+n} \frac{(a_k - \bar{a})^2}{m+n}}},$$

where m is the number of points above LI (starting from $j = 1$), n is the number of points below LI (starting from $k = 1$), and

$$\bar{a} = \frac{\sum_{j=1}^{m} a_j}{m}.$$

A greater spread of scatter points in the plot indicates an increased variability, while closely bunched points indicate less variability.

The ASI was found to be greater in real than in synthetic HRV data, and to increase during *taiji* practice. The ASI was also better able to discriminate between normal sinus arrhythmia and congestive heart failure or acute myocardial infarction than standard measures of HRA (Rohila & Sharma 2020a). As yet, other authors do not appear to have used this measure.

Data requirements

ASI has been used on data with from 500 to 10,000 samples (data points) (Rohila & Sharma 2020).

Parameter settings

No parameters ae required for the ASI.

Reported values – some examples

For ECG inter-beat interval time series data, ASI > 50 is claimed by its originators to indicate variability due to parasympathetic tone over sympathetic tone, whereas ASI < 50 suggests dominance of variability due to sympathetic tone over parasympathetic tone. ASI ≈ 50 then indicates a balanced response of both sympathetic and parasympathetic tone.

The use of plots
No plots have been published that make use of the ASI.

Generalised Poincare plot (GPP)

HRA analysis based on GPP is more challenging to understand than the EPP and the HRA measures described so far. so should only be undertaken after reading the original papers by its developers, in particular Mirjana Platiša and Aleksandar Kalauzi. The method is based on quantification of Pearson correlation coefficients $r(j, k)$ between symmetrical ($j = k$) and asymmetrical summed j previous and k following RR intervals up to the 100th 'order' ($j,k \leq 100$), or, in other words, $r(RRn\text{-}j,RRn+k)$ (Platiša *et al*. 2019a). A normalised index of asymmetry (NAI) results, negative if the summed preceding RR intervals are shorter and those following are longer. Given that parasympathetic control mechanisms are faster than sympathetic ones, one possible hypothesis is that maxima of $r(j, k)$ for short-term correlations ($j, k = 1$) might indicate a tendency to parasympathetic modulation, longer-term correlations ($j, k \approx 10$) possibly predominant sympathetic control (Platiša *et al*. 2016).

The Complex Correlation Measure (CCM)

A further Poincaré plot descriptor that does take multiple lags into account and so provides information on the temporal dynamics of the plot is the 'Complex Correlation Measure' (CCM)[37] introduced by Karmakar *et al.* (2009a).

The CCM is based on moving windows of three consecutive points in the plot (Jelinek *et al.* 2013). The measure conveys information about four different lag correlations of the signal and can be expressed as a function of autocorrelation at different lags (Karmakar *et al.* 2009b). The original formulation by Kharmakar *et al.* is:

[37] Sometimes referred to as a 'Complex Correlation Index'.

$$CCM = \frac{1}{C_n(N-2)} \sum_{i=1}^{n-2} \|A(i)\|$$

where $C_n = \pi * SD1 * SD2$, or the area of the fitted ellipse over the Poincaré plot (Karmakar *et al.* 2012).

An alternative algorithm was proposed by Zhang *et al.* (2015):

$$\mathrm{CCM}(m) = \frac{\mathrm{SD}_1}{\mathrm{SD}_2 * (N-2)} \sum_{i=1}^{N-m-1} \|A(i)\|$$

In both algorithms, A (*i*) represents the area of the *i* th triangle created by the three consecutive points in the plot:

$$A(i) = \frac{1}{2} \begin{vmatrix} x_i & x_{i+m} & 1 \\ x_{i+1} & x_{i+m+1} & 1 \\ x_{i+2} & x_{i+m+2} & 1 \end{vmatrix}$$

Five PP patterns were correctly differentiated for RRi data using CCM in the study by Zhang *et al.* (2015): 'Comet' (sinus rhythm), 'Torpedo' (sinus rhythm), 'Fan' (atrial fibrillation or multifocal atrial tachycardia), 'double sided lobe' (DSL) (sinus rhythm with atrial premature beats) and 'triple sided lobe' (TSL) (sinus rhythm with ventricular premature beats). CCM may reveal more about physiological status than comparing conventional static PPs (Abubaker *et al.* 2013; Karmakar *et al.* 2015), as the latter may look almost identical even though their temporal structures are very different (Jelinek *et al.* 2011a). It has been suggested that the CCM may be more sensitive to parasympathetic nervous system activity than SD1 and SD2 (Jelinek *et al.* 2011a), and the CCM may even differentiate better between in- and ex-vivo HRV than conventional PP (Janoušek *et al.* 2013).

Data requirements

Long-term recordings were used in one study of CCM for RRi data (Karmakar *et al.* 2009b), with 4,000 RR intervals subdivided into 20 windows with 200 RR intervals in

each window (Karmakar *et al.* 2009a); 2-min (c. 120 data point) and 1,000 data point recordings have also been used (Jelinek *et al.* 2011a, 2013).

Parameter setting

Lag m

Values of *m* between 1 and 100 were used in Karmakar *et al.* (2009), between 1 and 8 in in Karmakar *et al.* (2015) and from 1 to 70 in González *et al.* (2018)

Expected values – some examples

RRi CCM was found to be lower in depressed patients than in health controls (0.29 ± 0.12 vs 0.36 ± 0.14) (Jelinek *et al.* 2011a).

The use of plots

Plots of CCM, SD1 and SD2 against *m* from 1 to 100 are shown in Karmakar *et al.* (2009a), and – with SD1/DSD2 as well – against *m* from 1 to 8 in Karmakar *et al.* (2015). Plots of CCM, SD1, SD2, SD1/SD2 and the SD1-SD2 ellipse area against *m* from 1 to 70 in González *et al.* (2018), illustrating the advantages of CCM over the more traditional PP measures. Interesting plots of both CCM and its accuracy against lag are shown in Cerrada *et al.* (2020).

Lempel-Ziv Complexity (LZC)

Lempel-Ziv complexity (LZC) considers the ordering of variations in a signal, not only their relative frequency (as analysed by SE (Jernajczyk *et al.* 2006). There are several variants of LZC. In their 1976 paper, its originators discussed how, even though an absolute measure for complexity may be nonexistent, it is possible to evaluate the complexity of a finite binary sequence by counting the number of different sub-strings (or sub-words) encountered when a binary sequence is viewed as a stream (from left to right). A complexity counter *c(n)* is increased by one unit every time a new subsequence of consecutive characters is encountered (Aboy *et al.* 2006). The resulting sequence decomposition can be into a shorter 'primitive' or a longer 'exhaustive' production process; for the algorithm to be implemented in CEPS, by Quang Thai, exhaustive complexity can be considered as a lower limit of 'LZ76' complexity, the primitive complexity an upper limit (Thai 2020); both need to be considered (Lempel & Ziv 1976).

Multiscale Lempel-Ziv Complexity (mLZC)

Several multiscale versions of LZC also exist (Ibáñez-Molina *et al.* 2015; He *et al.* 2018; Chipperfield *et al.* 2019). There are similarities between the method originated by Ibáñez-Molina *et al.* and the mSE approach of Costa *et al.*, but while scaling in mSE is used to explore temporal dependencies in the signal (the approach also taken by Chipperfield *et al.*), in Ibáñez-Molina's version of mLZC the window scaling aims to capture different oscillatory properties and was created for use with EEG data (Ibáñez-Molina *et al.* 2015).

Classical LZC when used with EEG data neglects rapid components of the signals (Ibáñez-Molina *et al.* 2018). This is not the case for mLZC, which may therefore be more capable of differentiating between eyes open and eyes closed conditions (Ibáñez-Molina *et al.* 2015), between depressive individuals and healthy controls (Kalev *et al.* 2015), and between non-ictal and ictal periods in epilepsy (Artan 2016).

Data requirements

LZC can be used with both discrete (e.g. HRV) and continuous (e.g. EEG) data, but a process of 'symbolisation', particularly of the latter, is required before the method can be used, as computing LZC requires binary data. A common strategy that is robust to outliers is to partition the original data into binary sequences using the median amplitude (for EEG data) as a threshold: '0' if the original data point was less than the median, '1' if greater (Aboy *et al.* 2006; Simons & Abásolo 2017; Gutiérrez-de Pablo *et al.* 2020). This method has also been used with local field potential sub-band data in the brain (Zhu *et al.* 2020) and in the EEG frequency bands (Liu *et al.* 2016).

Another approach to partitioning that may improve results is based on *k*-means clustering (Zhou *et al.* 2011). Three- and four-symbol conversions are also possible (Abásolo *et al.* 2006; Kamath 2013),[38] and 'distance-based' LZC for signal pairs (e.g. from different EEG electrodes) has also been used (Simons & Abásolo 2017).

Data needs to be in binary form, but not necessarily stationary (Simons & Abásolo 2017). LZC is not completely accurate for real-world, finite data (Estevez-Rams *et al.* 2013), but is quite robust to noise (Fernández *et al.* 2013), although perhaps less so than SampEn (Escudero *et al.* 2015a). Thus, some authors have suggested that for EEG data, samples should be at least 40 if not 60 s long (20,000-30,000 data points in their study) (Cerquera *et al.* 2018). Others have recommended 1,000 or preferably 10,000

[38] Whatever the method, the process of partitioning or symbolising data may itself affect results without shedding light on the underlying properties that are 'really' embedded in the data (Wang & Schonfeld 2009), so should not be undertaken blindly.

points for accuracy of results (Rivolta *et al.* 2014), and LZC has been considered as suitable for short EEG datasets (Fernández *et al.* 2013).

Similarly, in RRi data, some authors have stated that short sequences of 50 points may provide accurate values in the presence of noise (Balasubramanian *et al.* 2015), or even 10 points in clean data (Balasubramanian & Nagaraj 2016). However, in one study of diaphragm muscle contraction, LZC for samples of 400-600 points was less stable than for longer samples (Torres *et al.* 2008).

In any case, because computing LZC entails scanning from left to right, LZC will increase with data length – linearly if the data is stationary (Rapp *et al.* 2005). Therefore, either samples of equal length must be compared, or the data must be normalised against its upper bound (Lempel & Ziv 1976; Zhang *et al.* 2009).

LZC of EEG data increases with spectral (e.g. noise) bandwidth (Aboy *et al.* 2006; Ferenets *et al.* 2006).

As for simple LZC, mLZC is reasonably robust to noise and is appropriate for short datasets (Ibáñez-Molina *et al.* 2015). It works well with time series having a 1/*f* structure but may be less appropriate for data without that structure, which could result in similar values of mLZC at different scales (Antonio Ibáñez-Molina, Personal communication, November 15, 2020). Given that HRV demonstrates 1/*f* scaling (Kobayashi & Musha 1982), mLZC may be useful for this data as well as for EEG. Indeed, mLZC may be used with data of structure $1/f^{\alpha}$ ($\alpha \neq 1$), with better differentiation between results likely for greater values of α (Antonio Ibáñez-Molina, Personal communication, November 20, 2020).

Parameter setting

LZC is parameter-free. However, some authors state that using only a binary conversion may reveal underlying dynamics less effectively than four- or even eight-symbol conversion. The optimum number (bin size) may vary from application to application, suggesting that a range of numbers should be tested (Balasubramanian & Nagaraj 2016). Quantising/partitioning at between 20 and 60 symbols gave particularly useful results in one study of diaphragm muscle contraction in dogs (Torres *et al.* 2008). However, others have cautioned that using more than two levels of quantisation may require unrealistically long data (Rivolta *et al.* 2014), and one research group found that while EEG signal complexity changes may be evaluated with only 2 quantification levels, amplitude variations can be evaluated with a high number of levels (200) (Sarlabous *et al.* 2009).

Window length w

For mLZC, scale or length w is required as a parameter. Only odd-numbered lengths should be selected (as many scales as you want). This parameter does not represent 'scale' itself, but a vector with the number of points used to obtain the binarisation. For EEG data, dividing the sampling rate by the frequency of interest provides the

number of points needed to obtain a binary sequence that approximately captures the activity at that frequency. This number should be an odd number, excluding '1'. You can use as many scales as you want (Antonio Ibáñez-Molina, Personal communications, September 7 and November 15, 2020).

Expected values – some examples

Spatial patterns of LZC in the EEG may differ between those at risk of dementia and those who are not, even years before it manifests clinically (Gutiérrez-de Pablo *et al.* 2020).

mLZC results are likely to be higher at smaller values of w (with more random binary sequences than at larger values); furthermore, binary sequences capturing slower rhythms tend to be more regular than those that capture fast rhythms in the data (Antonio Ibáñez-Molina, Personal communication, November 15, 2020). Results for $w = 1$ should be discarded.

The use of plots

Plots of LZC against series length are included in Estevez-Rams *et al* (2014) and Rivolta *et al.* (2014), in the latter accompanied by interesting scatter plots of SampEn against LZC. Multiscale LZC is plotted against window length in Ibáñez-Molina *et al.* (2015).

Permutation Lempel-Ziv Complexity (PLZC)

There are now many variants of LZC, including distance based LZC (Simons & Abásolo 2017), hierarchical LZC (Han *et al*. 2020), joint or conditional LZC (Zozor *et al*. 2005), and even multiscale dispersion LZC (Mao *et al*. 2020). One such variant is Permutation Lempel-Ziv Complexity (PLZC), in which the quantisation of data required by the LZC algorithm is performed using PE.

Permutation Lempel-Ziv Complexity (PLZC) was developed by a group from Yanshan University in China. In their first published study, they found that PLZC outperformed LZC based on four standard methods of coarse-graining the data (mean, median, mid-point and *k*-means), providing better differentiation of EEG signals recorded in different anaesthesia and epileptic states. PLZC was also more robust to noise (Bai *et al*. 2015a). In their second paper, written in collaboration with researchers from New Zealand (Bai *et al*. 2015b), PLZC was found to correlate closely with GABAergic anaesthetic drug

effect, outperforming LZC, the composite PE index, PE itself and some other standard indices of the depth of anaesthesia.

Confusingly, an Argentinian group have termed their own mix of LZC and PE 'Lempel-Ziv permutation complexity', or LZPC (Zozor *et al*. 2014), but PLZC – described as a 'standardised' version of the Zozor method in one paper (Tosun *et al*. 2019) – appears more frequently in citations. Bai *et al.* did not in fact refer to the earlier paper in their 2015 papers, nor in their 2019 review of nonlinear neural dynamics (Bai *et al*. 2019), so the exact relationship between PLZC and LZPC remains unclear.

PLZC has been used in the analysis of stock market dynamics (Li & Wang 2017; Wang 2021), and of sleep stage EEG (Mateos *et al*. 2021), with one study finding that whereas LZC merely reflected spectral changes in EEG activity, both PE and PLZC reflected genuine changes in the nonlinear dynamics of the EEG (Tosun *et al*. 2019). More generally, PLZC was one of several features found to be useful for quantifying levels of consciousness using a machine learning method ('support vector machine', SVM) (Liang *et al*. 2020). In another SVM study, mean multiscale PLZC results were significantly lower in regions where seizure-related ('focal') signal changes were detected than in non-focal regions, being lower for periodic than for noisy signals (Borowska 2021). These findings were significant only at scales of 2 or above, so would not have been detected using PLZC without multiscaling. In an EEG study on monkeys, however, both PE and PLZC *without* multi-scaling were shown to increase complexity with conscious awareness, and also (in frontal and fronto-parietal areas) with ketamine-induced 'dissociative' anaesthesia, often accompanied in humans by hallucinations and dream-like, immersive experiences. Other anaesthetics, such as propofol and medetomidine, reduced PLZC over the whole brain. Fisher Information, a local quantifier, was inversely related to PE and PLZC, which are global quantifiers (Fuentes *et al*. 2021).

A number of complexity measures were introduced in 2015, such as SQA (Girault 2015). Of these, PLZC seems to be the most used.

Parameter settings for PLZC

Values of *m* between 3 and 5 were tested in the study by Borowska (2021). Bai *et al*. (2015b) found that *m* = 4 and *tau* = 2 were found to perform best in distinguishing states of anaesthesia from ranges of 3 – 7 (*m*) and 1 to 3 (*tau*), respectively.

Larger values of *m* become computationally costly, and also necessitate longer data: for *m* = 7, for example, 7! (or 5040) types of symbols will be required to calculate PLZC, and data segments will need to be > 7! * 7! * 7! in length.

The Complexity-Entropy Plane (CEP) and Jensen-Shannon complexity (C_{JS})

"… there is also a natural limit in the amount of information that can be conveyed by a single metric. A natural evolution is then to consider multiple (complementary) metrics at the same time and represent them as points in a plane (or a space)"

(Zanin & Olivares 2021)

Measures of statistical or structural complexity (the intricacy of the dynamic patterns that may emerge from a system which in itself appears much simpler than its dynamics [Martin *et al*. 2006]) complement those of entropy, unpredictability or randomness. It thus makes sense to plot complexity against entropy in the 'Complexity-Entropy Plane' (CEP) (Crutchfield & Young 1989), without prescribing how one depends on the other, and so in a parameter-free way. Indeed, 'there is a large range of possible complexity-entropy behaviors. Specifically, there is not a universal complexity-entropy curve, there is not a general complexity-entropy transition, nor is it [the] case that complexity-entropy diagrams for different systems are even qualitatively similar' (Feldman *et al*. 2008). Such scatter plots have been used, for example, in the analysis of MRI brain images (Young *et al*. 2008), EEG in tonic-clonic epilepsy (Rosso *et al*. 2005), solar wind magnetic field fluctuations (Weygand & Kivelson 2019) and turbulence (Weck *et al*. 2015), or legal language (Friedrich 2021). In more general terms, a particular variant of the CEP was introduced to reveal subtle differences between stochastic noise and deterministic chaos (Rosso *et al*. 2007).

In their seminal paper, Rosso *et al*. extended the CEP to create the 'Complexity-Entropy Causality Plane' (CECP), using (normalised) Jensen-Shannon complexity (C_{JS}) as the measure of complexity (rather than LZC, for example) and (normalised) PE as the measure

of entropy (rather than conventional Shannon entropy). CECP plots usually include crescent-shaped curves that indicate the maximum and minimum possible C_{JS} for a given PE, with stochastic processes tended toward C_{min} and chaotic processes toward C_{max} (as seen in a useful review by Lorimer 2020, p. 211). CECP plots have been used in the study of geomagnetic auroral currents [Osmane *et al*. 2019], for differentiating song types (Ribeiro *et al*. 2012), for gearbox fault detection (Radhakrishnan & Kamarthi 2016) and to remove redundant data for smart sensing applications (Nascimento *et al*. 2021), among other applications.

The CECP is insensitive to external noise, non-stationarity, and trends (Radhakrishnan & Kamarthi 2016). In several studies by Rosso and his colleagues, CECP is referred to instead as CCEP (e.g., Borges *et al*. 2019).

Other variants of the CEP are also possible, such as the multiscale LZC and dispersion entropy plane, applied in the analysis of heart rate time series by Mao *et al*. (2020), in which they showed that ageing and disease correspond to the loss of complexity. Another variant is the PLZC-PE plane proposed by Mateos *et al*. (2017), in which the complexity-entropy coordinates for noisy data appear in alignment, whereas chaotic sequences have a lower complexity and appear below this 'noise-line'. Another study by the same group noted that EEG complexity in the PLZC-PE plane was greater in healthy individuals than in those with some pathology such as epilepsy (Diaz *et al*. 2017). The same authors (Mateos *et al*. 2017) suggested that Rényi or Tsallis entropy could be used in the CECP, an approach taken by a number of authors, including Mao *et al*. (2018), who also used power spectral entropy in place of PE in their analysis of EEG and ECG sleep data, and by Dai *et al*. (2019) in their 'generalised entropy plane'. Another approach has been to use multiscale weighted versions of both JSC and PE in the CEP (Greco *et al*. 2021). A useful review and critique of CECP and some of its variants, such as the Fisher-entropy plane and multi-scale planes (Zunino *et al*. 2012), is provided by Zanin and Olivares (2021).

The measure

A useful illustration of the CECP is provided by Zanin and Olivares (2021, Figure 2), showing relative positions of chaotic and nonlinear stochastic systems

(nearer to the curve of greatest complexity), coloured (and white) noise and regular oscillations (nearer to the curve of least complexity).

Data requirements

5,000 data points were used in one study on time series data by Rosso and colleagues (Borges *et al*. 2019).

Parameter settings

These will vary depending on the entropy measure used. CECP plots often display results for a range of parameters.

Plots are central to presenting CECP results. A number of studies show not only the CECP plane itself, but also (multiscale) plots of entropies against each other, the effects of noise or entropy parameters, or even 3-dimensional plots. For Rényi complexity-entropy curves, plots of the complexity/entropy derivative (dC_α/dH_α) against the Rényi parameter α for different values of the embedding dimension are another possibility (Jauregui *et al*. 2018). Clustering of results can also be informative in CE(C)P (e.g., Friedrich 2021). Mateos *et al*. (2021), for example, show some interesting differences in sleep stage EEG using a variety of planes (C-E, Fisher Information – Shannon entropy, LZC – Shannon entropy).

In CEPS 2, Permutation_Jensen-ShannonComplexity (PJSC) has been implemented.

C0 Complexity

Etymologically, the term complexity comes from the Latin *plexus*, meaning 'interwoven', or in other words difficult to separate (Gershenson & Fernández 2012). There are indeed several possible strands of complexity definitions.

Algorithmic or Kolmogorov complexity (KC), for example (sometimes termed Solomonoff-Kolmogorov-Chaitin complexity after those who contributed most to its development), can be considered as the quantity of information in any mathematical object, such as a string of symbols (Kolmogorov 1965). More formally, $K(x)$, the Kolmogorov complexity of x, is defined as the length of the shortest computer program (in binary) that generates x (Li & Vitányi 1990).

D'Alessandro and Politi (1990), critiquing KC and LZC as merely 'reproposing the concept of entropy', developed a first order topological complexity, C1, corresponding to the growth rate of the number of admissible words in an infinite symbol sequence (the size of its 'vocabulary'), and a second order complexity C2, measuring the growth rate of the number of irreducible forbidden words in the sequence (the size of its underlying 'grammar'). C1 represents the randomness of the sequence, while C2 is correlated with fractal dimension and the Lyapunov exponents. Their definition of C2 was amended by Xu *et al*. (1994), who later found that their redefined measure was able to distinguish between those with and without schizophrenia: in the former, C2 with eyes open was lower than with eyes closed, but for the non-schizophrenics C2 was greater with open eyes (Tong *et al*. 1996).

C0 Complexity was first proposed for EEG analysis by the same group (Chen *et al*. 1998) to overcome problems caused by the coarse-graining information loss inherent in methods such as KC, C1 or C2. For C0, the FFT is used to calculate the amplitude spectrum of the original time series, components greater than the mean for the whole are retained, and then an inverse FFT used to create a new time series for the retained components (the 'regular component' of the original series). The difference between the original and the new time series is the 'disorder component', with C0 being the ratio of area of the disorder component to that of the original time series (Chen *et al*. 2000). The same research group then modified C0, giving it a more rigorous mathematical foundation and using the power rather than the amplitude spectrum. They observed that C0 was high when resting with

eyes open was high, low during deep sleep, and between the two when resting with eyes closed or during light sleep (at all channels other than O1). C0 is always a real number between 0 and 1: for periodic time series, it approaches 0 as data length increases; for a random time series with zero mean, it approaches 1 (Shen *et al*. 2005).

EEG C0 has been used in epilepsy research and was found to decrease preictally (Zhou *et al*. 2008). In this study, using C0 based on the power rather than amplitude spectrum did not appear to offer particular advantages.

C0 has also been used, for example, in studies on hypothermia recovery (in rats) (Lu *et al*. 2008), ataxia (in mice) (Yu *et al*. 2019), depression (Shi *et al*. 2020), magnetic stimulation of acupuncture points, which reduced C0 (Geng *et al*. 2017), detection of very weak signals in the presence of noise (Hu *et al.* 2021), and degradation of roller bearings (Li *et al*. 2017). In the latter study, computation time was considerably lower for C0 than for measures such as LZC, ApEn and SampEn. C0 has also been adapted for measuring the complexity of two-dimensional patterns (Cao *et al*. 2007). It appears that few, if any, studies on C0 complexity have been conducted outside China.

Data requirements

Zhou *et al*. found that C0 did not precisely reflect dynamic changes in EEG complexity during
ictal events when using 1000 data points, that C0 fluctuated greatly when using 200 data points, and that using sliding windows of 600 points was a reasonable compromise, with a 200-point step (400-point overlap). Filtering the data affected its amplitude, but C0 only slightly, although reducing the effect of noise on C0 (Zhou *et al*. 2008). Other researchers have found that C0 can provide robust results with short signals and so is suitable for use with nonstationary data (Cai & Sun 2009).

Parameter settings

Whereas most C0 studies appear to follow the algorithm proposed by Chen *et al*., defining the regular and disorder components of a time series with respect to the mean of the amplitude (or power) spectrum for the whole, at least one study (Li *et al*. 2017) appears to have varied this threshold *r*, from 1 to 10.

Reported values – some examples

The use of plots

Li *et al*. (2017) plotted C0 against the threshold separating the regular and disorder components of a signal, against signal to noise ratio (in decibels, dB) for different values of the threshold, and against number of data points, comparing results with those for LZC, ApEn and SampEn. Data length had most effect on ApEn, less on SampEn and least on LZC and C0 (for more than around 400 data points).

Complexity Estimate (CE)

'Complexity invariance' uses information about complexity differences between two time series as a correction factor for existing distance measures such as Euclidean distance. The method was introduced by Batista *et al*., first in 2011 and then more widely in 2014 in order to improve classification and clustering accuracy. It is based on a very simple time series 'complexity estimate' (CE), defined as the square root of the sum of the squares of differences between each data point and the next data point:

$$CE(Q) = \sqrt{\sum_{i=1}^{n-1}(q_i - q_{i+1})^2}$$

.

Its originators suggest that CE 'works so well because it is a good estimate of the intrinsic dimensionality of the time series' (i.e., of the number of variables needed in a minimal representation of the data), not of the number of variables that happened to be used to record the time series (its recorded dimensionality). The higher the intrinsic dimensionality, the higher is the CE.

CE has been used in a number of studies on the application of complexity-invariant distance to a wide range of data, from air pollution (Amato *et al*. 2020) to particle accelerator physics (Arpaia *et al*. 2020). However, it has rarely been used on medical data (e.g., He *et al*. 2020), and only one study was located on applying CE to physiological data such as the EEG (Kimiskidis *et al*. 2015). In that study, CE was used alongside other complexity and entropy measures to differentiate between states of high and low cortical excitability prior to

transcranial magnetic stimulation (TMS), i.e., more likely to experience an abnormal (epileptic) or normal (non-epileptic) response to the stimulation.

Data requirements

CE is not greatly affected by downsampling (Batista *et al*. 2014).

Emergence, self-organisation,complexity, homoeostasis & autopoiesis (ESCHA)

The three meta-measures emergence, self-organisation and complexity – along with homoeostasis and its extension as autopoiesis, or a system's capacity to maintain its unity and identity (Fernández *et al*. 2010) – are based on information theory. They have been used together as general descriptors of dynamical systems, particularly by Nelson Fernández (Colombia), Carlos Gershenson (Mexico) and Guillermo Santamaría-Bonfil (Mexico) (Santamaría-Bonfil *et al*. 2017). The terms are not new and have been defined differently in different disciplines (Prokopenko *et al*. 2009; Gershenson & Fernández 2012). Their precise mathematical formulation by Santamaría-Bonfil *et al*. (2017), for both discrete and continuous data, although no doubt liable to further evolution, makes them useful in the framework of CEPS. However, although there is a large literature on ESC, with many fascinating byways and ramifications (e.g., Abrahão & Zenil 2021; Gershenson 2012; Heylighen *et al*. 2006; Signorelli & Meling 2021), to our knowledge researchers have so far made little use of these particular formulations to date in physiology or medicine.

In general, self-organisation, emergence and unpredictability (uncertainty, entropy) are characteristic of complex systems (Tang *et al*. 2021), and of their chaotic behaviour in particular (Pourafzal & Fereidunian 2020).

Information can be seen as a quantifiable pattern (Gershenson & Fernández 2012), and pattern formation can be described as information self-organizing (Gershenson 2012). Self-organising systems are thus those that produce a global pattern from the interactions of their components, with high organisation (order) characterised by low information and low organisation (chaos) characterized by high information (Gershenson & Fernández 2012). Self-organisation is strongly dependent on the observer: the same system can be considered

as self-organising or self-disorganising, depending on the scale and on the partition of the state space (Gershenson & Heylighen 2003).

If self-organisation (*S*) represents how much order there is in a system – i.e., a reduction of entropy (Gershenson & Heylighen 2003) – then emergence (*E*) indicates how much variety there is within it (Gershenson & Fernández 2012). *S* can be quantified as the difference between input and output information ($S = I_{in} - I_{out}$), E as their ratio ($E = I_{out}/I_{in}$). The system's complexity *C*, the amount of information needed to describe a process, a system, or an object (Prokopenko *et al*. 2009), can then be defined by the equation $C = 4 * E * S$ (Santamaría-Bonfil *et al*. 2017), or alternatively as the product of the system's information (disorder) and disequilibrium *E* (Martin *et al*. 2006; López-Ruiz *et al*. 1995).[39] More generally, *C* can be defined as the balance between change (chaos) and stability (order) (Fernández *et al*. 2014). Thus, *C* is maximal when the system tends to high S or high E (i.e., discernible patterns with some noise or high noise with some discernible patterns) (Ponce-Flores *et al*. 2020).

In a simplified version of the measures (focusing on the information produced by a system), emergence can be interpreted as the opposite of self-organisation, while complexity represents their balance. Intuitively, emergence refers to properties of a higher scale that are not present at the lower scale. If the dynamics of a system are considered as a process, then emergence can be defined as the novel information produced by that process which was not present beforehand (Gershenson & Fernández 2012).

Homoeostasis (*H*) can be seen as a measure of the stability or adaptability of the system, strongly related to its robustness, but also to sensitivity to initial conditions. If *d* is 'normalised Hamming distance', then $d(I_{in}, I_{out})$ can be used as a measure of how much information change results from a process, and *H* can be defined as its opposite: $H = 1 - d(I_{in}, I_{out})$. Both *S* and *C* are measured in bits, while *H* and *E* are unitless (Gershenson & Fernández 2012).

Autopoiesis, the ability of a system to self-produce, and perhaps the most salient characteristic of living systems [Gershenson 2012], is defined as the ratio between the

[39] In their 2012 paper, Gershenson and Fernández defined *C* as simply the product of E and S, but by 2014 had changed this to $4 * E * S$, 4 being a normalisation constant (Fernández et al. 2014).

complexity of a system and the complexity of its 'environment' (Fernández *et al*. 2014), in particular those environmental factors known to influence the system itself (Guillermo Santamaría-Bonfil. Personal communication, 25 March 2022). Where the exact factors are not known, the complexities of a selection of possible factors, or their aggregate (e.g., average), could be used in the ratio. It might also be possible to compare the complexity of a single system variable and those of all the other, related system variables. In such situations, data normalisation would be a sensible strategy (Fernández *et al*. 2017).

The ESCHA measures

Two sets of functions are provided, for discrete and continuous data. The former are based on the discrete Shannon entropy, the latter on differential entropy (Santamaría-Bonfil *et al*. 2017).

Data requirements

Discrete data will consist of a number of real values, whereas continuous data will contain values of a probability distribution function, or PDF (Santamaría-Bonfil *et al*. 2017). When considering autopoiesis, data should be normalised.

Parameter settings

For continuous (PDF) data, the minimum and maximum values will be required, as well as 'distSampleSize', an integer value that corresponds to an approximate sample size (Santamaría-Bonfil *et al*. 2017).

For both discrete and continuous data, the number of states required to coarse-grain a given sample will be required, but if not provided, a heuristic will be used to calculate the number of system states (Santamaría-Bonfil *et al*. 2017).

Reported values – some examples

Values of Differential *E*, *S* and *C* between 0.00 and 0.83, 0.17 and 1.00, and 0.00 and 0.99, respectively, are reported for various real-world datasets in Santamaría-Bonfil *et al*. (2016).

The use of plots

Plots of *E*, *S*, *C* and *H* against connectivity (*k*) in Random Boolean networks are shown in Gershenson & Fernández (2012), repeated in Fernández *et al*. (2014). Such plots could be used to explore how *E*, *S*, *C* and *H* vary with scale: 'Measuring emergence at multiple scales at once with an "emergence profile"

can give more insight about the dynamics of a system' (Gershenson & Fernández 2012).

SYMBOLIC DYNAMICS (SymDyn)

Continuous data will need to be transformed ('discretised' or 'coarse-grained' in time, or 'quantised' in amplitude) in some way before SymDyn methods can be used, whereas SymDyn may sometimes be appropriate for data that is already discrete.

Data preparation for SymDyn

In time:

- **Decimation** (compression or downsampling. In this method, a data string is reduced by a constant decimation factor (e.g. 10, retaining only 1/10 of the original data). This approach has been used for long datasets, such as EEG.

- **Coarse-graining**. For a given time series, multiple coarse-grained time series are constructed by averaging the data points within non-overlapping windows of increasing length, τ (**Figure 3**), i.e. two points at 'scale two', three points at 'scale three', and so on. In multiscale coarse-graining, there will in fact be *two* such series of averages at scale two (or $\tau = 2$), one starting at the first point in the data series, and one at the second. At scale three (or $\tau = 3$), there will be *three* such series, starting at the first, second and third points, respectively; and so on for higher values of τ, as illustrated by Azami and Escudero (2016a). For scale 1, the coarse-grained time series is simply the original time series (Costa *et al.* n.d.). If N is the number of data points in the original series, the length of each resulting coarse-grained time series is N/τ.

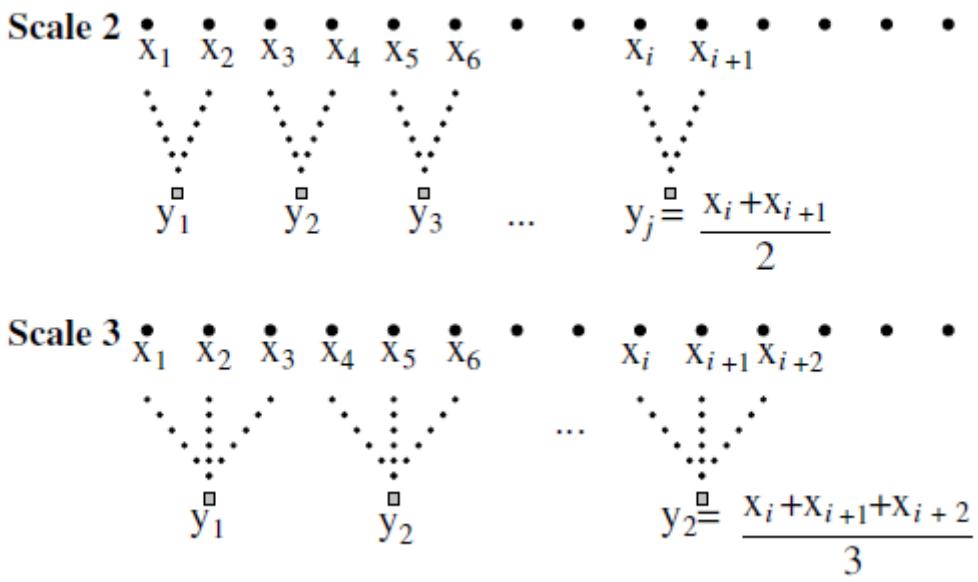

Figure 3. Schematic illustration of average coarse-graining for scales 2 & 3 (from Costa *et al.* n.d.).

The description above is for the original coarse-graining method based on averaging data point values. It is also possible to carry out coarse-graining based on their variance (Costa & Goldberger 2015) or standard deviation (Azami & Escudero 2017c; Costa & Goldberger n.d.).

More complex 'adaptive segmentation' approaches have also been proposed (e.g. Azami *et al*. 2015), but they are beyond the scope of this GUI.

In amplitude:

- **Equal intervals**. The range of data values (from minimum to maximum) is divided (quantised, partitioned) into a set of equal intervals or 'bins', ζ ('zeta'), often 4 or 6. Optimally, this method requires prior Z-score normalisation[40] (Porta *et al*. 2001).

- **Mean-based symbolisation**. Four symbols are defined relative to the mean, according to the following rules:

  0: mean < $X_i \leq (1 + \alpha)$ * mean

[40] Such 'normalisation to unit variance' is particularly important when comparing data recorded in different situations or for different conditions (Xiong *et al.* 2017).

1: $(1 + \alpha) * \text{mean} < X_i \leq \infty$

2: $(1 - \alpha) * \text{mean} < X_i \leq \text{mean}$

3: $0 < X_i \leq (1 - \alpha) * \text{mean}$

This method entails setting a threshold parameter α (Voss *et al.* 1996). Z-score normalisation is not required.

Unlike Equal intervals SymDyn, Mean-based symbolisation results in four *non*-equidistant levels of quantisation (Keshavan *et al.* 2004).

A simpler, binary alternative is to convert the original time series into absolute differences, or $|x - \bar{x}|$, with '1' allocated to all values of the absolute differences greater than a certain threshold and '0' to other values (Aziz & Arif 2006).

- **Binary Change Δ**. In this method without parameters, successive differences between data points are defined as follows:

  0: $(X_i - X_{i-1}) < 0$

  1: $(X_i - X_{i-1}) \geq 0$

- **Binary Change |Δ|**. This method requires setting of a threshold parameter τ:

  0: $|(X_i - X_{i-1})| < \tau$

  1: $|(X_i - X_{i-1})| \geq \tau$

In general, all these methods may result in imprecise estimations of any entropy (or other) measure, as some important information in the original time series may be lost (Azami & Escudero 2016a). Coarse-graining, in particular, may also involve downsampling (Makarava *et al*. 2014; Faes *et al*. 2019b).

Calculating SymDyn

Once coarse-graining has been carried out, different SymDyn measures can be calculated, as follows:

SymDyn Equal intervals[41]

[1] Taking the output from **Equal Intervals** coarse-graining (i.e. the sequence of partition numbers), then [2] group successive symbols in that output into 'words' of length *k* (where *k* is usually 3). [3] Count the occurrence of the different resulting 'words' (e.g. 113, 552, 142, etc.), then [4] count the numbers of resulting words with the *same structure* (Porta *et al.* 2001):

0V	No variation (e.g. {0 0 0} or {4 4 4}
1V	One variation (e.g. {4 0 0} or {4 4 1}
2LV	Two like variations, so all three symbols form an ascending or descending ramp (e.g. {1 3 4} or {5 4 1}
2UV	Two unlike variations, with the symbols forming a peak or valley (e.g. {3 5 3} or {4 1 3}.

In addition, the following may be calculated:

[5] *N* forbidden words [number of word types that occur with a probability less than 0.001, or less than 0.01 or 0.005 or 0.0005 (Paternoster *et al.* 2013)]

[6] *N* 02 [percentage of words consisting only of symbols "0" and "2"]

[7] *N* 13 [percentage of words consisting only of symbols "1" and "3"] (Henriques *et al*. 2020).

Researchers using this method found that the rate of occurrence of stable patterns in 24-hour HRV recordings (0V%) reflected sympathetic modulation,[42] 1V% reflecting sympathetic *and* parasympathetic modulation, 2LV% reflects sympathetic and parasympathetic modulation but with vagal predominance and 2UV% reflecting vagal modulation exclusively (Porta 2007a; Moura-Tonello *et al.* 2014). Similar results were obtained for short-term HRV as well (Guzzetti *et al.* 2005). This was discussed earlier by Porta *et al.* (2001), who went on to write that 0V% and 2UV% 'might represent a valid

[41] The 3-symbol method developed by Porta's group is sometimes called the Max-min Method, the method of Voss and colleagues the σ-Method, and the two-value method the Binary Δ-coding Method (Cysarz *et al.* 2013b).

[42] In line with other findings by Porta *et al.* (2017) that vagal withdrawal and sympathetic activation decrease the complexity of cardiac control.

alternative to linear spectral indexes for assessment of the cardiac autonomic modulation from short-term heart period variability' (Porta *et al.* 2007b), particularly as the symbolic dynamics method does not require predefined frequency bands, unlike the HRV frequency-domain LF/HF ratio (Tobaldini *et al.* 2009). The 0V/2V ratio has been proposed as a nonlinear equivalent to the LF/HF ratio, which is supposedly indicative of sympatho-vagal balance (Reulecke *et al.* 2015), although this interpretation of the HRV frequency-domain measure is by no means universally accepted (Billman 2013). However, in rats, 1V% was found in one study to be a better index of sympathetic modulation than 0V% (Silva *et al.* 2017), while in humans 1V% was associated with parasympathetic modulation in another report (Cysarz *et al.* 2015a), so clearly HRV SymDyn may not, after all, provide unequivocal answers to questions about autonomic modulation. This has not deterred researchers from using Porta's method with respiration and EEG data as well (Immanuel *et al.* 2014).

Of course, detailed information is lost with this SymDyn method, and outliers (ectopic beats and noise) will influence symbol strings (Tobaldini *et al.* 2009; Voss *et al.* 2009). On the other hand, such coarse-graining (partitioning of data space) results in large-scale features being captured, while lower-amplitude noise will be reduced (Stepien *et al.* 2007; cf. Finn *et al.* 2003).

The number of forbidden words in RRI data increases as complexity decreases, and vice versa (Palazzolo *et al.* 1998); it may increase during general anaesthesia (Huhle *et al.* 2012). Forbidden words have also been defined for other probabilities, such as 0.01, 0.005 or 0.0005 (Paternoster *et al.* 2013).

SymDyn Mean-based

[1] Taking the output from **Mean-based symbolisation** (i.e. the sequence of values 0, 1, 2, 3), steps [2] to [7] are repeated as for Equal intervals SymDyn.

Porta and Voss, proponents of the two main approaches in symbolic dynamics, collaborated in one paper in which both methods were better able to differentiate between healthy individuals and those with ischaemic dilated cardiomyopathy than time- and frequency-domain HRV measures (Valencia *et al.* 2015).

A useful illustration comparing the Equal intervals and Mean-based SymDyn methods may be found in Cysarz *et al.* 2015.[43]

SymDyn Binary Change

[1] Taking the output from Binary Change Δ **OR** |Δ| (i.e. the sequence of values 0, 1), then repeat steps [2] to [3] as for Equal intervals SymDyn. For [4], classification is as:

0V No variations between three successive symbols, i.e. all three symbols are equal ('000' or '111')

1V One variation (or transition) between three successive symbols, i.e. two symbols are equal ('001', '100', '110' and '011')

2V Two variations (or transitions) between successive symbols ('101' and '010').

[5] Compute probability of six consecutive 0's and of six consecutive 1's.

For RRi data, the regularity or irregularity of such Binary Change Δ patterns as assessed using ApEn may change with age and maturation (Cysarz *et al.* 2013a), with regular binary patterns reflecting sympathetic modulation and irregular binary patterns reflecting parasympathetic modulation (Cysarz *et al.* 2007, 2012). These patterns have been interpreted in terms of the rhythmic patterns in African music (Betterman *et al.* 1999).

A similar binary approach has been used for EEG data, with '1' for when the signal *amplitude* is increasing and '0' for when it is decreasing (Stepien *et al.* 2007; Burrello *et al.* 2020). Other binary SymDyn methods have also been used with EEG data (Liu *et al.* 2005).

Coarse-graining of various types is used in computing multiscale versions of many entropy measures.

Data requirements

For RRi data, 300 samples are usually considered a minimum when using the nonlinear methods of SymDyn (e.g. Guzzetti *et al.* 2005; Rebelo *et al.* 2011). Recordings of around 800 beats have been used, for example (Schulz *et al.* 2010), as well as longer recordings of 30 minutes or 24 hours (i.e. up to around 86,000 data points) (Voss *et al.* 1998), although such long recordings are also sometimes divided into approximately

[43] This is available online at https://www.academia.edu/.

5-minute windows (Valencia *et al.* 2015). However, in one animal study, samples of only 150-200 beats were used (Tobaldini *et al.* 2009), and around 250 beats were used in other studies by Porta's group (Porta *et al.* 2007b; Cysarz *et al.* 2015b).

Datasets of around 800, 1,800, 7,500 or as many as 23,000 data points have been used in EEG SymDyn studies (Paternoster *et al.* 2013; Tupaika *et al.* 2010; Immanuel *et al.* 2014; Keshavan *et al.* 2004).

For ECG data, a minimum sampling rate of 500 Hz has been recommended for binary pattern analysis (Cysarz *et al.* 2012). In one study on respiration, datasets of 400 samples (breaths) were used (Caminal *et al.* 2004).

Nonstationarity of data may not be an issue (Porta *et al.* 2015b), but outliers will strongly affect analysis using Equal intervals SymDyn and somewhat affect results using Mean-based SymDyn (Cysarz *et al.* 2018). Although it has been stated that 'One motivation for studying symbolic nonlinear time series analysis is that it offers robustness to noise' (Finn *et al.* 2003), noise has also been stated to influence symbol strings (Voss *et al.* 2009).

Parameter setting

Equal intervals SymDyn

Bin number ζ

ζ is often set at 4 or 6.

Word length k

k is usually set at 3.

Probability p

Sequences of length *k* occurring with a probability $p < 0.01$, 0.005 or a smaller pre-set value are considered as 'forbidden words'.

Mean-based SymDyn

Word length k

k is usually set at 3.

Threshold parameter α

Changes of α between 0.05 and 0.1 do not greatly affect results; both values have been used in HRV studies (Cysarz *et al.* 2015a; Henriques *et al.* 2020), with $\alpha = 0.1$ generally useful for RRi data (Voss *et al.* 1996). α has been set as 0.5 in respiration variability

research (Caminal *et al.* 2004), and as 0.05 (Tupaika *et al.* 2010) or {0.01, 0.025, 0.05, 0.0625, 0.075, 0.0875, 0.1, 0.125} for EEG (Paternoster *et al.* 2013).

Binary Change SymDyn

Threshold parameter τ

τ is commonly set to 10 ms in HRV studies) (Cysarz *et al.* 2015; Henriques *et al.* 2020).

Expected values – some examples

Equal intervals SymDyn

Output will be in the form of (3) Numbers of different words, and/or (4) Numbers of words with the same structure (i.e. 0V, 1V, etc.).

Mean-based SymDyn

Output as for Equal intervals SymDyn, with (5) *N* forbidden words, (6) *N* 02, (7) *N* 13 in addition. *N* 02 may be a measure for intermittently decreased HRV (Voss *et al.* 1998).

Binary Change SymDyn

Output as above for steps (3) and (4), together with (5) probabilities of six consecutive 0's and of six consecutive 1's.

The use of plots

A paper on entropy in gait signals (Yu *et al.* 2017) includes plots of a measure based on normalised corrected SE, 'multivariate multiscale symbolic entropy' (MmSymEn), against scale factor. Of more general interest are the examples of the various symbolisation methods, the thresholds used to partition RRi data and the resulting symbolic series illustrated in Cysarz *et al.* (2018).

ENTROPIES

Shannon and Generalised Entropies

Shannon Entropy (SE)

SE is the precursor of all entropies that estimate amount or frequency of information, providing a simple measure of uncertainty, 'average missing information' (Lesne 2011) or complexity of pattern distribution (Porta *et al.* 2001). However, in itself SE only considers the relative frequency of events in a signal, rather than their order (Ferenets *et al.* 2006), and not their long-range interactions (Liang *et al.* 2015). Thus, SE cannot be used to compare distributions that have different levels of scale; furthermore, it cannot be used to compare parts of distributions to the whole (Rajaram *et al.* 2017). In terms of pattern distribution, if the dynamics of two series are characterised by different patterns which have identical sample frequencies, their SE is equal (Porta *et al.* 2001).

SE has been used with many data types, from EEG and ECG RRi to hydrology and questionnaire responses. However, despite its simplicity, its application to continuous data is not necessarily straightforward and the data will need to be transformed or 'discretised' in some way and may also need to be normalised before SE is computed.

Following Grassberger (1988), Aziz and Arif (2006) derived a 'normalised corrected' version of SE for use in SymDyn. In addition to word sequence length L (similar in this context to embedding dimension) and quantisation level ζ, only the total number of words and the number of occurring words among the possible words are required to calculate it. Other methods directly derived from SE, originally applied to RRi data, are 'entropy of entropy', a measure of complexity (Hsu *et al.* 2017) and 'average entropy', a measure of disorder (Hsu *et al.* 2019;). These have also been used with centre of pressure (movement) data (Wei *et al.* 2019). See below, under 'Further developments from Shannon Entropy'.

Data requirements

SE is not strictly speaking applicable to continuous data, which will therefore need to be transformed or 'discretised' in some way. In fMRI research, for instance, the colour palette was simplified/segmented in one study (Akdeniz 2017). For stride interval data, SE has been applied to patterns of 'words' or 'motifs' of a given length in a

symbol sequence using the simplified binary method of mean-based symbolisation (Aziz & Arif 2006), a method claimed to be more robust for short EEG data series than mSE (Hussain *et al.* 2017). Another approach is to normalise EEG amplitude relative to its RMS value before computing SE from the histogram of the signal (Yoon *et al.* 2011). This permits comparison between results from different studies (Vanluchene *et al.* 2004).

SE – both normalised and not – has often been applied to discretely binned (histogram) amplitudes in EEG research (Inouye *et al.* 1991; Ferenets *et al.* 2006; Sabeti *et al.* 2009; Molina *et al.* 2014).[44] SE has been used with EEG sub-band data obtained from different wavelet methods (Sharmila *et al.* 2018; Dash & Kolekar 2020).

SE requires stationarity of data (Sabeti *et al.* 2009). Epoch length and amplitude resolution (in EEG data) are both likely to affect SE values (Bruhn *et al.* 2001), as may certain types of noise (in data series generally) (Ma *et al.* 2019), particularly for sequences of ≤ 200 data points (Balasubramanian *et al.* 2015). In general, if binning or some form of windowing are used on data before an entropy measure is applied, the actual length of the data sample may have less effect on the values that result than the number and width of the bins/windows themselves.

Parameter setting

Bin number (quantisation level) ζ

For RRi, the Equal intervals method with $\zeta = 6$ is often used (e.g. Porta *et al.* 2007a; Moura-Tonello *et al.* 2014).

Word (sequence) length k [45]

Using the Equal intervals method, patterns (words) containing between two and four symbols were found likely to be most informative (Porta *et al.* 2007a). Using three symbols (e.g. {1 2 3}, {0 4 5}, etc.), the shape and distribution of these patterns could then be calculated with SE (Moura-Tonello *et al.* 2014).

Expected values – some examples

EMG: erector spinae muscles – 2.8 (low back pain) vs 1.2 (healthy participants) (N = 20) (Sung *et al.* 2007)

EEG: In contrast to FD_H and ApEn, SE may decrease with deepening sedation (Ferenets *et al.* 2006).

[44] An alternative to using linearly spaced bins in a histogram is to use Parzen windowing (Greco *et al.* 2008), although this may be more computationally costly as well as difficult to understand for those who are unfamiliar with the method. Useful illustrations of the two methods can be found under 'Kernel density estimation' in Wikipedia.

[45] Equivalent to embedding dimension in this implementation of SE.

The use of plots

In CEPS, it is possible in the Test Parameters mode to check the effects on SE of varying the bin number ζ or word length k.

Rényi Entropy (RE)

Rather than a single entropy, Rényi entropies form a family, a generalisation of SE.[46] Like TE (see below), RE requires an exponent for its computation. Here we call this q, although it is often referred to as α. When $q = 1$, RE = SE (Maszczyk & Duch 2008).

RE has been used with EEG, RRi and respiration data, for example, but has rarely been used in clinical trials as such. However, with variation of q, RE becomes a multiscale measure (Cornforth *et al.* 2015), and RE has been used in algorithms for a number of other entropies, such as multiscale permutation Rényi entropy (Yin *et al.* 2018) or Rényi DistEn (Shi *et al.* 2019).

Data requirements

Like RE, SE is not strictly speaking applicable to continuous data. As for SE, when applied to EEG or other continuous data, the PSD (histogram representing the distribution of power as a function of frequency) or Parzen window methods may be used (Greco *et al.* 2008; Tonoyan *et al.* 2017). For RRi data, RE has been estimated on previously partitioned data, as for SE (Valencia *et al.* 2015).

RE does not require long data series or stationarity of data (Gonzalez Andino *et al.* 2000; Torres *et al.* 2008).

Parameter setting

Order q

The exponent q (often known as α) has sometimes been described as the 'order' or 'entropic index' of RE. When q is varied, this can provide a 'multiscale' version of RE (cf. mSE, below); as q increases, the RE measures become more sensitive to data values occurring at higher probability and less to those occurring at lower probability (Cornforth *et al.* 2015). q of between -0.1 and 2.0 were found useful (of values tested in the range -1.5 to 5.0) for distinguishing between different tissue samples in one pathology study (Maszczyk & Duch 2008), although q is usually considered only as

[46] Further theoretical generalisations, some bringing together both SE and TE, have also been investigated (Amigó *et al.* 2018; Gao & Deng 2020; Masi 2005).

positive and ≠ 1 (Rényi 1961). For q = 2, RE becomes what has been called 'quadratic entropy' (Lake 2006), 'correlation entropy' (K_2) (Bollt *et al.* 2009). or sometimes 'collision entropy' (Bosyk *et al.* 2012); a multiscale version of this also exists (Tonoyan *et al.* 2017). q = 2 has been used in EEG studies (Mammone & Morabito 2008; Mammone *et al.* 2009), as well as q = 3 (Gonzalez Andino *et al.* 2000). Both values were used in one study (Bhagat *et al.* 2009), as well as the ranges {0.1, 0.2, 0.3, 0.4, 0.5, 0.6, 0.7, 0.8, 0.9, 1.5, 2, 2.5, 3} (Paternoster *et al.* 2013) or {0.1, 0.15, 0.2}. For RRi data, RE was estimated in one study for q = 0.1, 0.15, 0.20, 0.25, 2, 4 and 6 (Valencia *et al.* 2015). In another study, on diaphragmatic muscle movement, values of q from 0.001 and 100 were tested, with $q \approx 0.1$ providing best results (Torres *et al.* 2008).

Expected values – some examples

Usable reference values of RE are rarely reported in clinical studies.

The use of plots

In CEPS, it is possible in the Test Parameters mode to check the effects on SE of varying q, with an interesting (and expected) discontinuity at q = 1.

Tsallis Entropy (TE)

Tsallis entropy is a generalised 'non-additive' or 'non-extensive' entropy (unlike SE and RE, which are additive/extensive). As for RE, the algorithm for TE includes the exponent q, which for TS is termed a 'non-extensivity measure' or 'entropic index'; q in itself has itself sometimes (Rajković 2004) – but not always (Ojo *et al.* 2019) – been interpreted as a measure of complexity.

TE may be more stable than RE (Abe 2002) and is more able to describe systems with long-range interactions than SE or RE (Bezerianos *et al.* 2003). For earthquakes, $q < 1$ indicates the presence of shorter-range spatial correlations (a 'sub-extensive' or 'sub-additive' system), while $q > 1$ characterises their longer-range temporal correlations (Abe & Suzuki 2003), i.e. a 'super-extensive' or 'super-additive' system (Ojo *et al.* 2019; Sharma *et al.* 2020). As is the case with RE, for q = 1, TE = SE. 'Calculating the entropic index q is in general an open topic; q can only be determined in very particular problems' (Ramírez-Reyes *et al.* 2016).

Tsallis entropy is less commonly used than RE in medical applications but has been claimed as more accurate in detecting clinical disorders than traditional EEG measures, including SE (Sneddon 2007).

Data requirements

As with SE and RE, the PSD (histogram) method has been used to quantise continuous EEG data (Al-nuaimi *et al.* 2015), indicating that TE is more suited to discrete than continuous data. Otherwise, information on data requirements for TE was difficult to locate in the literature.

Parameter setting

Entropic index q

As Zhang *et al.* wrote in a study on EEG (Zhang *et al.* 2010): 'Although the parameter q plays an important role in the result of TE computation, there has been no established method to optimize its value'. In their EEG study, 'empirically determined' values of q were therefore used (0.5, 1, 3, and 5). $q = 0.5$ and $q = 5$ have been used in other EEG research (Al-nuaimi *et al.* 2015; Capurro *et al.* 1999), and also $q = 2$ (Sharma *et al.* 2020). In other examples, q values of between 0.9 and 5.0 were found useful in distinguishing between different tissue samples in one pathology study (Maszczyk & Duch 2008), and $2.5 \leq q \leq 3.5$ in a study on gene regulatory networks (Martins Lopes *et al.* 2011).

Expected values – some examples

TE increases monotonically with q (Tsallis 1988). Results are sometimes presented as normalised values (Martin *et al.* 2000; Al-nuaimi *et al.* 2015).

The use of plots

In CEPS, it is possible to check the effects on TE of varying q in the Test Parameters mode.

Diffusion Entropy (DnEn or DE)

DnEn, like TE, is closer to thermodynamics than to information theory, but like many entropy methods, is based on SE, although it may less commonly be based on TE (Scafetta *et al.* 2001). The purpose of the DnEn algorithm is to efficiently establish the possible existence of scaling, whether normal or anomalous, without altering the data by any method of

detrending. Unlike DFA, which uses non-overlapping windows, the DnEn method uses overlapping windows (Grigolini *et al.* 2002). In DnEn, the scaling parameter or exponent is known as δ, which is lower, for example, in the RRi data of those with heart failure (around 0.71) than in healthy individuals (around 0.82), suggesting a reduction in longterm memory ('memory beyond memory') in the former (Allegrini *et al.* 2002). In another application, DnEn was used to uncover the intrinsic fractal dynamics of spontaneous stride interval, whatever the speed of walking (Cai *et al.* 2007). DnEn has also been used in EEG research, where it revealed, for example, short-time scaling broken by a strong periodic component (such as alpha waves), whereas the crossover between two scaling regions seen in DFA did not originate from the underlying dynamics of the EEG but was more likely an artefact of the algorithm used (Ignaccolo *et al.* 2010).

As suggested by the phrase 'memory beyond memory', DnEn is appropriate for longer series data, as in the 2002 study by Allegrini *et al.* (20 hours of RRi, or around 72,000 data points), the 2007 study by Cai *et al.* on human gait (around 2,770 to 3,600 steps taken in one hour), or the 2010 study on EEG by Ignaccolo *et al.* (32,000 data points), as well as another 2010 EEG study by Allegrini *et al.* (150,000 data points, although separated into much shorter segments). For very short time series (~ 100 data points), 'balanced estimation of diffusion entropy' (BEDE), a variant of DnEn, has been proposed; this gives almost the same results as DnEn for longer series (3,000 to 4,000 data points) (Zhang *et al.* 2012). Further adaptation by the same Chinese researchers are the 'correlation-dependent balanced estimation of diffusion entropy' (cBEDE) (Pan *et al.* 2014) and 'factorial moment based diffusion entropy' (FMDE) (Yang *et al.* 2017).

Unlike methods of assessing variance, such as the SD, Hurst exponent or DFA, the method of DnEn results in a correct scaling exponent even for data that is not normally distributed (Scafetta *et al.* 2002); Scafetta *et al.* therefore recommend joint use of DnEn and techniques of analysis based on variance to assess when 'strange kinetics' and long-term memory effects force a complex system to depart from ordinary random behaviour.

The measure

Diffusion Entropy Analysis (DEA) is based upon the direct evaluation of the Shannon entropy of the diffusion process. DE is among the most conceptually

challenging of the measures described in this *Primer*. It should thus be used with care, and only after reading some of the associated literature.

Data requirements

The purpose of DEA is to establish the possible existence of a scaling, either normal or anomalous, in the most efficient way as possible without altering the data with any form of detrending (Scafetta 2& Grigolini 2002).

Whereas BEDE can evaluate scale-invariance in very short time series ($\sim 10^2$ points) 'with considerable precision' (Zhang *et al*. 2012), more data will be required for correct estimation of DE (3000-4000 points). As stated by Grigolini *et al*. (2002), 'the DE method can be used as a reliable way to detect scaling only in the long-time limit'. However, results using DE and BEDE may be similar (Pan *et al*. 2014).

Binarisation has been used prior to DEA, for instance in the analysis of teen birth data (Scafetta *et al*. 2001). Another approachhas been to use ordinary differencing, using time series increments obtained from EEG data, for example (Ignaccolo *et al*. 2010b).

DEA has been applied to nonstationary data, such as the EEG, and the method does not require any a priori hypothesis on the nature of the dynamics of the signal, such as the separation of signal, trend and noise required by the DFA algorithm (Ignaccolo *et al*. 2010a).

Parameter settings

Bin size (DEL(t),ε, Q or s) is simply selected as a predetermined fraction of the standard deviation of the initial series, {Zk(t)}. If the bin width was fixed, the number of points falling in some bins could become very low with the passage of time) (Ignaccolo *et al*. 2010a; Zhang *et al*. 2012). : 'Generally, a selection of eps = 2 is proper' (Yang *et al*. 2017).

Reported values – some examples

Vales between about 1.3 and 10.0 are shown in Grigolini *et al*. 2001.

The use of plots

Diffusion entropy increases linearly on a log-linear plot, with the slope equal to the scaling exponent [delta] (Ignaccolo *et al*. 2010a; cf. Zhang *et al*. 2012).

Ignaccolo *et al*. (2010a) also show interesting plots of DnEn v the standard deviation of DFA residuals for EEG data, and of EEG increments v different values of the stability time t_s.

Further developments from Shannon Entropy

Entropy of Entropy (EoE)

EoE was proposed by Hsu *et al*. (2017), combining a variant of mSE (based on SE rather than SampEn) and a measure called 'superinformation' (SI). SI, or 'randomness of randomness', was developed as an alternative to SE for differentiating between coding and non-coding sections of deoxyribonucleic acid (DNA). SI was found to be accurate for this classification task, particularly for short DNA sequences (Bose & Chouhan 2011).

EoE uses SE both to characterise the information state of a system within a given time window, and to characterise how such states change with scale – hence the name 'entropy of entropy'. Its originators describe it as a measure of complexity, and SE as a measure of disorder. Classification accuracy was greater than that of mSE.

Data requirements

EoE was designed to be used with short data sets of 70–500 heartbeat intervals. Classification accuracy may be greater for longer data.

EoE may not be very robust to noise, and perhaps for that reason was not found useful in differentiating between EEG from healthy individuals and those with Alzheimer's disease, for instance. EoE may also be sensitive to sampling rate, but it is not known how nonstationarity will affect this measure (Chang Francis Hsu, Personal communication, November 14, 2020).

Parameter setting

RRi minimum, x_{min}

In their 2017 study of 500 RRi data, Hsu *et al.* found $x_{min} = \text{RRi}_{\text{min}} = 0.3$.
For body sway speed, Wei *et al.* set $v_{min} = 0$ mm/s (for all study participants).

RRi maximum, x_{max}

In their 2017 study of 500 RRi data, Hsu *et al.* found $x_{max} = \text{RRi}_{\text{max}} = 1.6$.

For body sway speed v, Wei *et al.* set v_{max} = 300 mm/s (for all study participants).

Bin size, or number of 'slices' in RRi range, s_1

In their 2017 study of 500 RRi data, Hsu *et al.* set s_1 = 55, but noted that results are robust for a wide range of s_1 between 30 and 70.
In their body sway study, Wei *et al.* set s_1 = 300.

Scale factor τ

In their 2017 study of 500 RRi data, Hsu *et al.* used τ from 1 to 10, but noted that results are robust for a wide range of τ.
In their body sway study, Wei *et al.* set τ = 5.

Expected values – some examples

In their 2017 study of RRi data (N = 105), Hsu *et al.* found EoE = 0.41 in congestive heart failure (CHF) and atrial fibrillation (AF) patients, but 1.40 in healthy controls.

The use of plots

Plots of EoE against τ are included in Hsu *et al.* (2017), showing consistently greater values for EoE from scale 3 to scale 10 for healthy individuals when compared to those with atrial fibrillation or congestive heart failure. Plots of EoE against SE of the original time series are also included, showing that maximal EoE (complexity) occurs between extreme order (low SE, CHF) and extreme disorder (high SE, AF).

Average Entropy (AE)

AE was proposed by Hsu *et al*. (2019) as a measure of disorder in RRi data. Noting that SE measures the average uncertainty of the probability distribution of all discrete values in a time series and SampEn the sequential irregularity (randomness) of the series, they proposed AE to reflect both probability and randomness. It is defined as the average of the local SE values for sequences of length N / τ, where N is the length of the original time series and τ corresponds to scale factor. AE was found to classify differences between CHF, AF and healthy RRi data better than SE, mSE (scales 1 to 5) or DistEn. Hsu *et al.* (2020) found that AE is similar for RRi in healthy individuals and for $1/f^{\alpha}$ noise when $\alpha \sim 1.5$, but that AE for RRi in those with AF was more similar to AE for 'pink' noise (i.e. $1/f^{\alpha}$ noise when $\alpha = 1.0$).

For the three conditions (CHF, AF and healthy), AE increased with increasing α, whereas maximum EoE occurred for $\alpha \sim 1.5$.

Data requirements

AE has been used with both short (500) and long (10,000) RRi data sets (Hsu *et al.* 2019), as well as with body sway speed data (Wei *et al.* 2019).

AE may not be very robust to noise, and perhaps for that reason was not found useful in differentiating between EEG from healthy individuals and those with Alzheimer's disease, for instance. AE may also be sensitive to sampling rate, but it is not known how nonstationarity will affect this measure (Chang Francis Hsu, Personal communication, November 14, 2020).

Parameter setting

RRi minimum, x_{min}

As for EoE, in their 2019 study of RRi data, Hsu *et al.* set $x_{min} = 0.3$.
For body sway speed, Wei *et al.* set $v_{min} = 0$ mm/s (for all study participants).

RRi maximum, x_{max}

As for EoE, in their 2019 study of RRi data, Hsu *et al.* set $x_{max} = 1.6$.
For body sway speed, Wei *et al.* set $v_{max} = 300$ mm/s (for all study participants).

Number of 'slices' in RRi range, s_1

As for EoE, in their 2019 study of RRi data, Hsu *et al.* set $s_1 = 55$, but noted that results are robust for a wider range, 30-70.
In their body sway study, Wei *et al.* set $s_1 = 300$.

Scale factor τ

In their 2019 study of RRi data, Hsu *et al.* used τ from 1 to 100.
In their body sway study, Wei *et al.* set $\tau = 5$.

Expected values – some examples

In their 2017 study of RRi data ($N = 105$), Hsu *et al.* found EoE = 0.41 in congestive heart failure and atrial fibrillation patients, but 1.40 in healthy controls.

In a further study on postural stability (Wei *et al.* 2019), lower AE was associated with greater stability as assessed using centre of pressure data.

The use of plots

Plots of AE against τ (from 0 to 100) are included in Hsu *et al.* (2019), showing values for health individuals consistently between those for atrial fibrillation (higher) and congestive heart failure (lower), whereas this was not the case for mSE (τ from 0 to 20). Plots of EoE against AE show maximal EoE (complexity) between extreme order (low SE, CHF) and extreme disorder (high SE, AF). A similar curve was evident in the study on postural stability.

Tone-Entropy (T-E)

T-E was introduced as a method of HRV analysis by Oida *et al.* in 1997. It provides two indices, 'Tone' and 'Entropy', based on sympathetically-mediated acceleration of heart rate (HR) during inspiration and vagally-mediated slowing of HR during expiration. 'Tone' is considered to represent balance between acceleration and inhibitor mediators, 'Entropy' the total activity of both mediators. Decreasing RR intervals (acceleration) are taken as positive, increasing RR intervals (deceleration) as negative. Tone is simply the average of the percentage index (PI) of successive differences in the RR interval in a recording, where PI is defined as:

$$PI(n) = [RR(n) - RR(n + 1)] \times 100 / RR(n).$$

Tone is thus positive for acceleration, and negative for deceleration, with lower tone (i.e. more negative) values in healthy individuals at rest indicating that vagal activity predominates. For multi-lag or multiscale T-E (mT-E), early lags of around 1-5 beats all predominantly reflect parasympathetic influence (Karmakar *et al.* 2013). Including higher lags in analysis (m = 7 to 10) may permit demonstration of sympathetic effects more than focusing on lower lags (1-6), and more than conventional HRV measures (Khandoker *et al.* 2017).

SE is used as the entropy measure, based on the probability distribution of PI(n) values but excluding P(n) = 0 (as neither acceleration nor deceleration). SE was used instead of simple standard deviation because RR interval data was not normally distributed.

mT-E has been used not just in analysis of RRi data, but also of photoplethysmography (PPG) peak-to-peak (systolic) and trough-to-trough (diastolic) intervals, PTT and even pulse wave amplitude and velocity (Khandoker *et al.* 2017).

Data requirements

Two-minute recordings (overlapping) were used in the original study by Oida *et al.*, five-minute recordings in a later study on diabetic neuropathy by a different group (Karino *et al.* 2009), 10-minute recordings in later studies by Oida's group (Amano *et al.* 2005, 2006), and 20-minute data by Khandoker *et al.* (2010). Thus, time series of around 100 to 1,200 RR intervals are appropriate for this method. 1,000 RR intervals were used by Jelinek *et al.* (2013). However, the method is considered to be relatively independent of data acquisition time length (Amaro *et al.* 2006).

T-E is also considered to be robust against non-stationarity and respiratory influence (Jelinek *et al*. 2013) or noise (Karino *et al.* 2009).

Parameter setting

Lag *m*

mT-E, with $m = 2$ or 3, was better able to differentiate between those with and without cardiac autonomic neuropathy than T-E (i.e. with $m = 1$).

Expected values – some examples

For foetal HRV, values of Tone between -0.07 and 0.08 were at different lags have been reported, with Entropy between 1.80 and 3.14 (Khandoker *et al.* 2015). Neonatal mT-E values are also available, with increased Tone and reduced Entropy during stressful interventions (Šapina *et al.* 2018). Values of mT-E at different scales are shown for PPG peak-to-peak (systolic) and trough-to-trough (diastolic) intervals, PTT, pulse wave velocity and amplitude in depressives with and without suicidal ideation and controls in the 2017 study by Khanoker *et al.* (2017).

The use of plots

Plots of Tone and Entropy against lag are shown in a study of post-myocardial infarction patients by Karmaker *et al.* (2012), and also, together with plots of Tone against Entropy, in a study of foetal HRV by Khandoker *et al.* (2015), as well as in a study comparing real and synthetic RRi data by Karmakar *et al.* (2013).

Entropy of Difference (EoD_m)

EoD_m, or entropy of difference of order m, was created by physicist Pasquale Nardone in around 2010 for use with HRV data (Pasqual Nardone, Personal communication, November 26, 2020). Although superficially similar to the more 'classical' T-E, in that it offers binary analysis of increases and decreases in data (Nardone 2014), EoD_m is closer to PE in that its estimation depends on data partitioning and selection of an embedding dimension, m. Although EoD_m is more economical to compute than PE, it is virtually unknown by most entropy researchers. It is based simply on the SE of strings ('m-tuples') of increases ('+') and decreases ('-') in the series of differences, $y_i = x_{i+1} - x_i$, derived from the original time series.

Data requirements

This information will be provided when EoD_m has been used more.

Parameter setting

m Embedding dimension

s Shift

Default values are 4 and 1, respectively, but as there is very little research on this approach, a range of values may need to be explored, using the 'Test and Plot' facility in CEPS.

Expected values – some examples

This information will be provided when EoD_m has been used more.

The use of plots

Plots should be used to test the effects of varying parameter settings.

Kullback-Leibler Divergence (KLD_m)[47]

"Shannon entropy and Kullback-Leibler divergence (also known as information divergence or relative entropy) are perhaps the two most fundamental quantities in information theory and its applications" (van Erven & Harremoës 2007)

The Kullback-Leibler Divergence (KLD) is a widely used method for measuring the 'distance' between two distributions, although in general the distribution of the KLD itself is unknown (Belov & Armstrong 2011). It can also be considered as a measure of the inefficiency of assuming that a distribution is q when the true distribution is p (Popescu *et al.* 2016). It is closely related to SE and is a measure of information (Kullback & Leibler 1951). Indeed, Mutual Information (MI) is a special case of the KLD (Belov & Armstrong 2011). A 'single-sample' KLD method has been proposed for signalling the pre-disease state of complex diseases (Zhong *et al.* 2020). In CEPS, the KLD has been implemented using the embedding dimension m to estimate the difference between the time series and random data using the probability distributions of EoD_m. In other words, $KLD_m(p \mid q)$ measures the loss of information when a random distribution q_m is used to predict a distribution p_m. Increasing embedding dimension m introduces more bits of information in the signal and the behaviour of KLD_m versus m shows how the data diverges from a random distribution (Nardone 2014), although in fact any noise ($1/f^{\alpha}$) signal may also be used as a comparator to give the same result. However, if the comparator signal q_m has a constant distribution, KLD_m will not provide useful results (Pasquale Nardone, Personal communications, 8 & 16 December 2020).

Data requirements

The KLD can be used with discrete or continuous data (Belov & Armstrong 2011)

Parameter setting

The KLD method implemented in CEPS requires the same two parameters as EoD_m:

m Embedding dimension

[47] This section and the previous one were written in consultation with Pasquale Nardone.

s Shift

Default values are 4 and 1, respectively, but as there is very little research on this approach, a range of values may need to be explored, using the 'Test and Plot' facility in CEPS.

Expected values – some examples

The KLD is always non-negative and equals zero only if two distributions are identical (Belov & Armstrong 2011).

The use of plots

Plots should be used to test the effects of varying parameter settings.

Extropy (Ex)

"Together, in their joint assessment of the information inhering in a system of probabilities, entropy and extropy identify what many people think of as *yin* and *yang*, and what artists commonly refer to as positive and negative space"

(Lad *et al*. 2015)

Extropy[48] was proposed as the 'complementary dual' of Shannon entropy by Frank Lad, Giuseppe Sanfilippo and Gianna Agrò in 2015. Very simply, if X is a discrete random variable, with possible outcomes $x_1,\ldots, x_n$, occurring with probability $P(x_1),\ldots,P(x_n)$, or $p_1,\ldots,, p_n$, then the Shannon entropy of X, $H(X)$, is defined by:

$$\mathrm{H}(X) = -\sum_{i=1}^{n} \mathrm{P}(x_i) \log \mathrm{P}(x_i)$$

and the Extropy of X, or $J(X)$, is defined by:

$$-\sum_{i=1}^{N} (1 - p_i) \log(1 - p_i).$$

[48] Not to be confused with thermodynamic negentropy (Miller 2014), negative ekaentropy (Martinas & Frankowicz 2000), 'the preference for the higher-energy, more complex ways of maintaining homoeostasis [48] Not to be confused with thermodynamic negentropy (Miller 2014), negative ekaentropy (Martinas & Frankowicz 2000), 'the preference for the higher-energy, more complex ways of maintaining homoeostasis over the lower-energy, less complex ones' (Ellis 2008), a definition of extropy related to autopoiesis (Gershenson 2015), or even with what has been termed 'extropianism' (More 2003).

Extropy is defined using natural logarithms, rather than to the base 2. For $N = 2$, $H(X) = J(X)$.

Like Shannon entropy, extropy is interpreted as a measure of the amount of uncertainty represented by the distribution for X (Lad *et al*. 2015). In their original paper, Lad *et al*. included a number of interesting results on the relationships between entropy and extropy for discrete variables, as well as between differential entropy and differential extropy, the corresponding measures for continuous variables, and between relative entropy (or Kullback–Leibler divergence) and relative extropy. They went on to explore the latter in a subsequent publication (Lad *et al*. 2018).

In CEPS, assisted by Giuseppe Sanfilippo, we have only implemented the first version of extropy, for discrete variables. Negextropy (Lad *et al*. 2015) and cross-extropy (Lad & Sanfilippo 2018) are not considered. Extropy and cross-extropy have been used in a deep learning method for automatic speech recognition (Becerra *et al*. 2018). Extropy has also been used as a feature, along with a number of entropies, in deep learning classification of ECG signals (Śmigiel *et al*. 2021a, 2021b). Most other studies on informational extropy may be fascinating mathematically but will seem somewhat abstruse to most users of CEPS.

Other forms of extropy include negative cumulative extropy (Tahmasebi & Toomaj 2020), residual extropy (Qiu & Jia 2018), cumulative residual extropy (Jahanshahi *et al*. 2020) and past extropy (Jose & Abdul Sathar 2021; Kamari & Buono 2021), as well as weighted extropy and weighted residual and past extropies (Balakrishnan *et al*. 2020), interval extropy and weighted interval extropy (Buono *et al*. 2021). Other variants are Deng extropy (Buono & Longobardi 2020) and fractional Deng extropy (Kazemi *et al*. 2021), Tsallis extropy (Balakrishnan *et al*. 2022), with values between 0 and 1 (1 being the maximum value, for uniformly distributed variables), and possibly Rényi extropy (Batra & Taneja 2020?).

Ordinal Entropies

Permutation Entropy (PE)

"Permutation entropy quantifies the diversity of possible orderings of the values a random or deterministic system can take, as Shannon entropy quantifies the diversity of values"

(Amigó *et al.* 2005)

Permutation entropy (PE) is based on computing the SE of the relative frequency of all the ordinal patterns found in a time series (Cuesta-Frau 2019a). It is proving increasingly popular in biomedical research (Zanin *et al.* 2012; Zunino & Kulp 2017; Cuesta-Frau 2019b). Advantages of PE include simplicity and low computational cost (Li *et al.* 2007; Azami *et al.* 2017b[49]), as well as being relatively robust to window length, sampling frequency and noise; its creators therefore considered it useful 'when there are huge data sets and no time for preprocessing and fine–tuning of parameters' (Bandt & Pompe 2002). However, PE may not be precise if data contains many tied values (Zunino *et al.* 2017), although this may not significantly impact results when using PE for classification of signals (Cuesta-Frau *et al.* 2018b). For longer samples ApEn may be less sensitive to noise (Li *et al.* 2008a),[50] although more computationally demanding (Nicolaou & Georgiou 2012). Furthermore, PE parameter selection remains an issue (carefully reviewed by Riedl *et al.* 2013).

Data requirements

As for SE, RE and TE, continuous data is partitioned, values being replaced with a symbol sequence before PE can be computed (Bandt & Pompe 2002). A simple illustration of this process for EEG data can be found in Olofsen *et al.* 2008.[51]

Data is sometimes normalised (e.g. with zero mean and variance of 1) before computing PE (Cuesta-Frau 2019b).

PE does not require stationarity (Kreuzer *et al.* 2014) or linearity of data (Azami & Escudero 2016b), although detrending may affect results (Shi *et al.* 2017). Also, as the method is based on the ordinal relation between the amplitude of neighbouring values of a given data sequence (Zunino & Kulp 2017), it does require 'inherent temporal ordering in the data' (Javier Escudero, Personal communication, July 7, 2018).

[49] While SampEn has a computation cost of order N^2, that of PE is only of order N.
[50] A 'robust' version of PE has thus been proposed for very noisy data (Keller *et al.* 2014).
[51] These authors also include MATLAB code for a 'composite PE index' in their paper.

PE tends to increase with data length (at least for RRi samples) when $m \geq 4$ (Udhayakumar *et al.* 2016), but this may only be true for short data (Cuesta-Frau *et al.* 2019). PE has been used with small samples of 50 data points (Udhayakumar *et al.* 2016b), as well as large samples of 10,000 points (Zunino *et al.* 2017). Requirements from theory are that N (the number of data points) should be $\geq m!$ ('m factorial', or the product 1 x 2 x 3 x … (m-1) x m), where m is the embedding or permutation dimension or 'order' (Rosso *et al.* 2007), or $N > 5m!$ (Amigó *et al.* 2008; Riedl 2013). However, more recent research has shown that even very short time series can be robustly classified based using PE; as a rule of thumb, 'ground truth' values for PE can be considered as those for which increasing data length further produces variations in PE that are < 2% (Cuesta-Frau *et al.* 2019).

Sampling frequency (and down-sampling in particular) may affect τ, and so results (Popov *et al.* 2013).

PE has been used for EEG sub-band data (Zhu *et al.* 2019).

Parameter setting

Order m

Order m is sometimes referred to using n rather than m, and sometimes as Embedding (or permutation) dimension rather than order, which can be a little confusing. For PE, there is no difference between 'order' and 'dimension' (Bandt & Pompe 2002). For most systems, $3 < m < 8$ will be appropriate (Bandt & Pompe 2002; Riedl *et al.* 2013), and even simply selecting $m = 5$ may be adequate (Myers & Khasawneh 2020). m= 4 has been suggested for EEG data (Nicolaou *et al.* 2012; Azami & Escudero 2015), although for RRi data PE is less dependent on data length when $m < 4$ and becomes less stable and efficient when m = 5 (Udhayakumar *et al.* 2016b). $m = 3$ has also been used for EEG data (Nicolaou *et al.* 2012), and $m = 6$ for longer EEG datasets (Li *et al.* 2008).

However, there is a trade-off between lower values of m, which provide more stable results for PE, and higher values (up to $m = 9$, for instance), which provide better classification performance, but are only possible for long data samples – e.g. 40,000 samples for $m = 9$ in EMG data; in general, PE values seem to reach a reasonable stability with 100 samples for $m = 3$, with 500 samples for m = 4, and with 1,000 samples for $m = 5$ (Cuesta-Frau *et al.* 2019).

High values of m in PE and its derivative measures may require more computation power than may be available in a PC (Cuestra-Frau *et al.* 2018c).

Time delay τ

Because PE uses 'neighbouring values' in a dataset, $\tau = 1$ is often appropriate, and so chosen in EEG research (Nicolaou *et al.* 2012); however, higher values have also been suggested, although they reduce the amount of data available for analysis (Azami & Escudero 2016b) and increase the values of PE (Keller *et al.* 2014). Furthermore, the classification performance of PE for EEG data may drop for higher values of τ (Cuesta-Frau *et al.* 2018b).

Selection of τ will also depend on what sort of system is being investigated (Riedl *et al.* 2013).

Expected values – some examples

PE will be at least 0 and at most ln(m!) (Azami & Escudero 2016a).

Using RRi data from emergency care physicians ($N = 13$), PE before and after an alarm situation was ~ 8.5, rising to ~ 10.9 during primary care time (Schneider *et al.* 2017).

In EEG research, signals with a more widely spread spectrum or containing higher frequencies are more likely to display larger PE values than those with power more concentrated at specific (or lower) frequencies (Nicolaou *et al.* 2012).

The use of plots

Plots of PE against sample length are shown in Cuesta-Frau *et al.* (2019). In CEPS, a multiscale version of PE is implemented (Ouyang *et al.* 2013) and can be plotted against time lag in Test mode.

Amplitude-Aware Permutation Entropy (AAPE)

AAPE was developed by Azami and Escudero (2016b) to overcome two main shortcomings of PE, namely (1) that mean value of *amplitudes* and differences between neighbouring samples are not considered in the symbolisation process, so that {1,3,2} and {11,13,12} are given the same ordinal pattern '021', for example, and (2) that a problem of equal amplitude values remains unsolved. AAPE has been described as 'Probably, the most ambitious method to address PE weaknesses' (Cuesta-Frau 2019a). It thus revealed underlying complexity in underwater acoustic signals better than PE itself in one study (Li *et al.* 2018). A 'time-delayed' version of AAPE, also known as Delayed Permutation Entropy (DPE), now exists (Martínez-Rodrigo *et al.* 2019).

Data requirements

AAPE has been used for 700-sample EEG data (Azami and Escudero 2016). 1,000 data points were used for research using an improved multiscale version of AAPE in rotating machinery fault detection (Chen *et al.* 2019a, 2019b), and 2,000 data points in a study on underwater acoustic signals (Li *et al.* 2018). AAPE has been used on various datasets of around 500, 900 or 5,000 data points (Cuesta-Frau 2019a). Computation time for AAPE is only slightly higher than for PE itself (Azami and Escudero 2016).

Parameter setting

Order (Embedding dimension) m

Order m is sometimes referred to using d rather than m, and sometimes as Embedding (or permutation) dimension rather than order, as for PE. $m = 6$ was used in an EEG study of DPA by Martínez-Rodrigo *et al.* (2019), and $d = 5$ in a study of underwater acoustic signals (Li *et al.* 2018); $m = 4$, 6, 8 and 9 were used in a study on various datasets by David Cuesta-Frau (2019a).

Time delay l or t (τ)

Azami and Escudero (2016b) recommended $l = 1$, because the effect of taking $l > 1$ may be equivalent to down-sampling without considering the frequency characteristics of the signal. However, for spike detection, they suggested that values of $l > 1$ may be useful. A very interesting time-delayed version of AAPE, 'delayed permutation entropy' (DPE), using values of l (τ) from 1 to 10, was introduced by Martínez-Rodrigo *et al.* (2019).

Adjusting coefficient A

This should be in the range [0,1]. In general, $A = 0.5$, but if *changes* in amplitude are more important than average amplitude *values*, then A could be set at much lower than 0.5. Spike detection was found to be accurate whether $A = 0.1$, 0.2 or 0.5 in the original study by Azami and Escudero. Martínez-Rodrigo *et al.* used A (which they call K) = 0.5, as did Li *et al.* in their study of underwater acoustic signals (2018).

Expected values – some examples

No values could be found in the published literature.

The use of plots

Plots of multiscale AAPE (mAAPE) against scale are shown in Chen *et al.* (2019a), and of Improved mAAPE (ImAAPE) against scale in Chen *et al.* (2019b).

Improved Multiscale Permutation Entropy (ImPE)

The term 'Improved Multiscale Permutation Entropy' (ImPE) can refer to two different measures, one from Edinburgh (Azami & Escudero 2016a), the other from Seoul (Choi 2017). Here we follow Azami and Escudero's description of the first of these, which they introduced to reduce variability of entropy when measured over long temporal scales, leading to more reliable and stable results. As described above and used for other measures such as mSE, a 'coarse-graining' process is used. ImPE is calculated as the average of the PE values for all the derived time series, from $\tau = 2$ to τ_{max}.

Data requirements

ImPE can be used with discrete or continuous data (the latter will require partitioning). See below for possible limitations on sample length if using high values of d or τ.

Parameter setting

Order (Embedding dimension) m

Order m is sometimes referred to using d rather than m, and sometimes as Embedding (or permutation) dimension rather than order, just as for PE.

Again, as for PE, there is a relationship between the number of data points N and m, but here this relationship is given by $(m + 1)! \leq N/\tau$, which limits the values of m that can be used to give valid results (Azami & Escudero 2016a). As m becomes larger, ImPE will become more computationally demanding. Azami and Escudero noted that ImPE was more stable (performed better) for $m = 3$ or 4 than for $m = 2$.

For EEG data, Azami and Escudero used m =2, 3 or 4. For ECG data, Shi *et al.* (2020) computed ImPE from the first four 'intrinsic mode functions' derived from 'ensemble empirical mode decomposition' rather than the series of RR intervals. They used m = 3.

Time delay τ

For EEG data, Azami and Escudero used τ from 1 to 30. For ECG data, Shi *et al.* (2020) used τ from 2 to 6.

Expected values – some examples

In the application of ImPE to EEG data by Azami and Escudero (2016a), the measure reached a plateau of around 3 when $\tau \approx 12$ in healthy people but plateauing at >3 and at lower values of τ in epileptic patients.

The use of plots

Plots of mPE and ImPE against scale for various synthetic and EEG data are included in Azami & Escudero (2016a).

Multiscale Permutation Min-Entropy (mPM-E)

Permutation min-entropy (PM-E) is the Rényi permutation entropy in the limit as the order $q \rightarrow \infty$ (Zunino *et al.* 2015). It retains the main advantages of PE, such as its simplicity, low computational cost and robustness to noise (Martínez-Rodrigo *et al.* 2019). The multiscale version of PM-E, based on coarse-graining (see above), involves analysing the behaviour of PM-E as a function of the embedding delay (scale factor) τ for a chosen value of embedding dimension m.

Data requirements

mPM-E does not require stationarity or linearity of data. Continuous data will need to be partitioned into ordinal patterns, as with other variants of PE. Zunino has suggested that for EEG data it might instructive be compare results in the full frequency range against those obtained for the filtered bands tool (Luciano Zunino, Personal communication, Sept 21, 2010).

The multiscale generalisation of PM-E was introduced to consider the effect of different sampling frequencies. By checking the behaviour of PM-E as a function of the lag τ, the different temporal scales of the underlying process are considered. Thus, through multiscale implementation, the effect that different sampling rates have on the quantifier analysis can be tested. Downsampling time series will have a strong effect on the analysis with this ordinal tool (Luciano Zunino, Personal communication, Sept 21, 2010).

300-400 RR intervals were used in one HRV study; the 6 (= 3 * 2 * 1, or 3!) ordinal patterns derived from the original RRi data and used as the basis for their analysis are shown in that paper (Xia *et al.* 2018). As it is fast to estimate, mPM-E is especially suitable for long datasets; longer datasets will be required for larger values of m and τ (Luciano Zunino, Personal communication, Sept 21, 2010).

MPM-E is very robust to spurious and missing data (Luciano Zunino, Personal communication, Sept 21, 2010).

Parameter setting

Order (Embedding dimension) m

m for EEG or ECG RRi data: $3 \leq m \leq 6$ (Zunino *et al.* 2015); Xia *et al.* (2018) used $m = 3$ and $m = 4$.

Time delay τ

EEG data: $\tau = 1$ or 5.

ECG RRi data: $\tau \in [5, 25]$[52] or $\tau > 70$ (Zunino *et al.* 2015); $\tau \in [1, 10]$ were used by Xia *et al.* (2018).

Expected values – some examples

As for PE, PM-E will be at least 0 and at most ln(*m*!); for RRi data, PM-E was maximal for $\tau > 5$ in one study (Xia *et al.* 2018).

In addition to PM-E itself, Martínez-Rodrigo *et al.* (2019) in their study on distress recognition also derived slopes between values of PM-E at $\tau = 1$ and $\tau = 2$, 4, 6 and 8 for EEG data, with greater slope values indicating larger entropy increases at higher scales. They also investigated the areas under the multiscale curves, from $\tau = 1$ to $\tau = 2$, $\tau = 1$ to 4, and so forth, just as had been done earlier for mSE and the Complexity index (Costa *et al.* 2005a). They noted that greater distress was associated with lower PM-E, and that differences between a distressed and calm state were much less at higher scales/delays.

The use of plots

Plots of PME against time delay (scale or lag) τ are included in Zunino *et al.* (2015), Martínez-Rodrigo *et al.* (2019) and Olivares and Zunino (2020).

[52] i.e. τ in the range between 5 and 25.

Composite_PE_Index (CPEI)

The composite PE index (CPEI) was developed by Olofsen *et al*. (2008) for use with EEG data, as the sum of two simple permutation entropies (PEs) – one with lag (τ) = 1, the other with τ = 1 – but taking into account a threshold below which most of the 'signal' was thought to consist of noise.

Olofsen *et al*. only included short 'motifs' (ordinal patterns) of order or dimension *m* = 3. Thus, for the two PEs taken together, there were six motifs. However, if the difference between any two of the points in the motif was less than a certain threshold, then the motif was counted as a seventh category ('tied'). For the EEG data they were analysing, they set this threshold at 0.5 mV, or about 1% of the inter-quartile range of the data. This particular choice was, however, not explained. MATLAB code for the CPEI was provided in the paper, which – together with CPEI's robustness to low-frequency noise (e.g., eyeblink) and the need to use only short data segments in its computation (e.g., 30 seconds of EEG sampled at 100 or 128 Hz) – may have contributed to its popularity in subsequent studies.[53]

CPEI reliably tracked anaesthetic-related EEG changes, decreasing (as did PE itself) with increasing anaesthetic concentration, and performed well when compared to standard EEG measures for depth of anaesthesia such as the bispectral index and 'response entropy', and better than spectral entropy and ApEn (Olofsen *et al*. 2008).

Using the same parameters as in the original paper by Olofsen *et al*., some of the same authors (Lopour *et al*. 2011) found that CPEI decreases as sleep depth increases, as might be expected. They went on to use CPEI in a machine learning study on sleep state (Dadok *et al*. 2014), but without reporting actual values for the measure. In another paper from around the same time (Liang *et al*. 2013) but using *m* = 6 rather than *m* = 3, they noted that CPEI did not perform as well as another measure they proposed for analysing EEG dynamics during general anaesthesia, permutation auto-mutual information (PAMI). Since then, although mentioning CPEI in a systematic comparison of 12 measures for monitoring depth of anaesthesia and detecting burst suppression (Liang *et al*. 2015), they do not appear to have used either CPEI or PAMI in their own research.

[53] There were 46 'hits' for "Composite permutation entropy index" in Google Scholar on 14 April 2022.

Nonetheless, CPEI can be found in feature lists in a number of machine learning studies, dissertations and book chapters, albeit without providing further informative results for the index (e.g., Mumtaz *et al*. 2013; Kimiskidis *et al*. 2015; Kafashan 2016; Nishad & Upadhyay 2020).

In 2014, a group of Portuguese researchers developed a software tool using CPEI for automatic EEG analysis of depth of anaesthesia in animals, concluding that their approach could potentially be used for analysis of other biomedical signals in real-time (Correia *et al*. 2014). CPEI was used in another animal study comparing the effects of different sedatives on the EEG and gastrointestinal tract motility; the authors explicitly stated that the threshold was adjusted to 1% of the interquartile range of the EEG data, rather than 0.5 mV (Li *et al*. 2021). This is in contrast to a number of papers, which appear to accept the original apparently arbitrary 0.5 mV threshold uncritically.

CPEI (alongside Hjorth complexity) has also been used in analysis of the EEG in gamers, again using the same parameters for CPEI: both measures were higher in the eyes open condition than when eyes were closed and were also higher in 3-dimensional than 2-dimensional game play. In this study, the EEG electrodes were grouped by brain region (frontal, central, temporal, parietal and occipital), but how values were aggregated was not stipulated (Khairuddin *et al*. 2013). CPEI has also been a feature in machine learning studies on EEG during IQ test conditions, using the same parameters (ties < 0.5 as noise threshold). Results in these studies were not provided for CPEI itself (Ahmad *et al*. 2015; Amin *et al*. 2016), although results in a more recent study (Amin *et al*. 2020) indicate that CPEI performed better as a feature than ApEn and SampEn, but less well than simple band power, Hjorth complexity or (unnamed) fractal dimension.

CPEI has also been used in machine learning EMG studies (Xiao *et al*. 2020, 2022; Karnam *et al*. 2021), and was reported by Xiao *et al*. (2020) as providing better classification accuracy than PE, SampEn or Fuzzy entropy. However, resulting values of CPEI were not themselves reported, and the equation used to calculate CPEI in the 2020 study differs from that provided in the original 2008 paper. No justification was provided for this change. An erroneous (but different) equation for CPEI was also used in a study on the effects of transcutaneous electroacupuncture (TEAS, or TAES) on the EEG (Yan *et al*. 2020), in which

sedation (assessed using the bispectral index) was accompanied by a reduction in alpha band power and frontal CPEI, but an increase in delta band power.

From the literature, it would seem that more research is required on the effects of using different methods of threshold selection.

Conditional Entropies

Essentially, these measure the conditional probability that two time series vectors that are close to each other for m points will remain close at the next point, $m + 1$. Values will be lower for more regular signals (Richman & Moorman 2000), when a pattern of length L is more likely to be predicted by a pattern of length $L - 1$ (Porta *et al.* 1998).

Conditional Entropy (CE)

Shannon first defined the term 'Conditional entropy' for any two chance events, x and y, not necessarily independent. For any value of x, there will be a conditional probability that y has a particular value. The conditional entropy of y is then defined as the average of the entropy of y for each value of x, weighted according to the probability of getting that particular x (Shannon 1948). In the formulation by Porta *et al.* (1998), CE is obtained as the variation of SE with respect to L, the pattern length or embedding dimension of the reconstructed phase space. In other words, CE quantifies the variation of information necessary to specify a new state in a phase space with dimension increased by one:

If $H(x_L)$ stands for the SE of series x when length = L, and $H(x_{L-1})$ stands for the SE of series x when length = L-1, then CE, the likelihood of obtaining the pattern of length L given the occurrence of the pattern of length (L−1) is given by:

$$CE(L) = H(x_L) - H(x_{L-1}).$$

For short data series, CE decreases to zero as a function of L, regardless of the type of the underlying dynamics (Guzzetti *et al.* 2000). CE derived from photoplethysmography pulse-to-pulse intervals (PPi, rather than RRi) may lead to estimates of pulse regularity that are lower than the regularity of HRV (Pernice *et al.* 2019a).

In addition to the original formulation of CE by Porta *et al.*, a generalised version of CE based on RE rather than SE has also been proposed (Valencia *et al.* 2013), as well as other modifications, such as conditional PE (Unakafov & Keller 2014), model-free 'K-nearest-neighbour' (knn) CE (Porta *et al.* 2013) and a faster, model-based 'linear Gaussian approximation' method of computing CE from RRi and PPi data (Porta *et al.* 2017; Pernice *et al.* 2019b; Valente *et al.* 2017). The linear and knn methods, along with the more commonly used 'kernel-based' CE measures such as ApEn and SampEn, are discussed, together with their application to different types of data, in an important, if technical, paper published by Xiong *et al.* (2017).

CE has been used with many data types, from RRi and PPi to hypnograms (Kirsch *et al.* 2012), the EEG (Diniz *et al.* 2016) and gait analysis (Ren *et al.* 2016).

Corrected Conditional Entropy (CCE)

CCE was designed for use with short data sequences, for which CE itself is not particularly meaningful, dealing with the so-called 'curse of dimensionality' (poor performance of CE for short data as dimension *m* is increased) (Porta *et al.* 2018). CCE is the sum of CE and a corrective term, also dependent on SE and *L*, like CE itself (Porta *et al.* 1998). CCE provides a measure of the complexity of the dynamic relation between patterns that follow each other in a series (Zamunér *et al.* 2013). Its minimum value quantifies regularity (the more regular the process, the smaller the CCE minimum), and is sometimes taken as an 'index of complexity' (Pagani *et al.* 2001) or 'complexity index' (Tobaldini *et al.* 2008), not to be confused with the Complexity index calculated for multiscale entropies such as mSE (Costa *et al.* 2008). CCE can be obtained without defining pattern length (*L*, embedding dimension of the reconstructed phase space) and may be measured in 'nats', when natural logarithms are used to calculate CE (Guzzetti *et al.* 2000), or 'normalised units' from 1 (full predictability) to 0 (complete unpredictability) (Pagani *et al.* 2001).[54] CCE has been used frequently in HRV and related studies, but may be less sensitive to the effects of age than some other HRV complexity indices (Porta *et al.* 2014). CE-based methods have also

[54] Alberto Porta co-authored this paper. Confusingly, in a later study which he also co-authored; the opposite is stated: CCE as a function of *L* 'decreases to zero in case of fully predictable signals' (Tobaldini *et al.* 2008).

been claimed by Alberto Porta, perhaps their main protagonist, to be less susceptible to broad-band noise than PE-based methods (Porta *et al.* 2015a).

Data requirements for CE and CCE

CE and CCE require discrete data (Kirsch *et al.* 2012). Data must first be normalised (Valente *et al.* 2017; Xiong *et al.* 2017), with zero mean and unit variance, and is then coarse-grained (i.e. quantised or partitioned) (Faes *et al.* 2012).

For HRV, samples are usually 300 beats long (e.g. Diniz *et al.* 2016; Pernice *et al.* 2019), and it has been suggested that data should be detrended before computing CE (Valente *et al.* 2017; Xiong *et al.* 2017), although others have found that prior detrending may reduce the usefulness of CE (Shi *et al.* 2017).

CE has been used on bandpass-filtered EEG data (Wu *et al.* 2007), and values will depend on sampling rate (Graham *et al.* 2013).

Nonstationarity of data may strongly affect some forms of CE (Xiong *et al.* 2017).

Parameter setting

Pattern length (Embedding dimension) L

For RRi data, $L_{max} = 10$ has been used (Faes *et al*. 2012).

Bin number (quantisation level) ζ

Faes *et al.* used $\zeta = 6$ for their RRi data (2012, 2013), following Porta *et al.* (1998).

Expected values – some examples

CCE (measured in 'nats' when natural logarithms are used to calculate CE) was of the order of 0.8 in both patients and controls in one study of RRi in chronic heart failure (Guzzetti *et al.* 2000). Those who are physically active may show higher CCE (around 0.8) than those who are not (around 0.7) (Rebelo *et al.* 2011); this is also the case in paraplegics (Zamunér *et al.* 2013).

The use of plots

Plots of CE as a function of word length are included in Karamanos *et al.* (2005), and of CCE against *L* (termed *k* by the authors) in *Faes et al.* (2012).

Approximate Entropy (ApEn)

"Since ApEn values for a given system can vary significantly with different *m* and *r* values, we do not view ApEn as an absolute measure. The power of ApEn is its ability to compare systems" (Pincus *et al.* 1991b)

Twenty years ago, D_2 was the most popular nonlinear measure used in EEG analysis (Hornero *et al.* 1999); now that position is held by ApEn. As a conditional entropy, ApEn quantifies the similarity probability of patterns of length *m* and *m*+1 in series data (Cuesta-Frau *et al.* 2017), in other words the regularity of the signal. Simply, ApEn represents the entropy computed at each data (time) point and then averaged (Furutani *et al.* 2020). Lower values of ApEn reflect more regular time series, while higher values are associated with greater complexity (Costa *et al.* 2002). To circumvent bias in the method due to 'self-matching' (ties) in the data, a 'corrected' version of ApEn (cApEn) has been introduced (Porta *et al.* 2007c, 2013), and its creators have continued to use this for assessment of knee extensor torque, for example (Fiogbé *et al.* 2018).

Although, for HRV data, the same researchers now consider ApEn to be outmoded (Porta *et al.* 2019), ApEn has been found more useful than SampEn in analysis of body temperature (Cuesta-Frau *et al.* 2009[55]), particularly in combination with PE (Cuesta-Frau *et al.* 2018a).

Data requirements

Stationarity is required,[56] so that detrending prior to use should be considered (Shi *et al.* 2017). According to its creators, ApEn is relatively robust to noise and outliers, provided the threshold parameter *r* is chosen as sufficiently large; for $m = 2$, data will need to comprise at least 100 (i.e. 10^m) points, but preferably at least 900 (or 30^m) (Pincus & Goldberger 1994); however, even for EEG data sampled at 400 Hz, 5 s of data did not give reliable results, whereas 20 s did (Ferenets *et al.* 2006).

ApEn in HRV increases with data length for values of *m* from 2 to 5 (Udhayakumar *et al.* 2016b). However, as data length increases, it becomes more likely to drift away from stationarity; the number of self-matches, and so bias, will also increase (Yentes *et*

[55] 'Our results indicate that ApEn can not be discarded as a regularity metric since in a few cases it might outperform SampEn'.
[56] So-called 'instantaneous point-process ApEn' may circumvent this requirement, and similarly for SampEn (Valenza *et al.* 2014).

al. 2013). Yentes *et al.* suggest that ApEn (and SampEn) may stabilise at around 2,000 data points for some data types. For EEG data, ApEn has been reported as more stable for longer samples (Feng *et al.* 2002).

Although Pincus *et al.* (1991b) originally reported that ApEn is 'very stable to infrequent, large outliers or numeric artifacts', others have found ApEn sensitive to outliers (Lake *et al.* 2002), such as spikes or ectopic beats in RRi data (Molina-Picó *et al.* 2011, 2013). ApEn may also not be robust to sampling rate, if low (García-González *et al.* 2009), increasing for some data types as sampling rate decreases (Rose *et al.* 2009; Rhea *et al.* 2011). Indeed, there may be a nonlinear (inverted U) association between ApEn and sampling rate, with differing optimum downsampling frequencies for different conditions (Rose *et al*. 2009). ApEn is thus likely to be sensitive to noise, both in EEG data (Cuesta-Frau *et al.* 2017) and postural control data, for which ApEn increased with noise (Rhea *et al.* 2011).

ApEn has been used with in HRV sub-band data (Li *et al.* 2015c), as well as in EEG sub-band data obtained with the discrete wavelet transform method (Sharmila *et al.* 2018).[57]

High-pass filtering of EEG data may have a strong effect on ApEn results (Lee *et al.* 2013).

Parameter setting

"No consensus has been established to properly select the parameters needed to calculate both ApEn and SampEn"

(Yentes *et al*. 2013)

Pattern length (Embedding dimension) m

m, or the length of the data segment being compared (Yentes *et al.* 2013), is most commonly selected as 2 (Henriques *et al.* 2020) or sometimes 3 (Liang *et al.* 2015; Cuesta-Frau 2019b) and is rarely > 4 (Lu *et al.* 2008), although values as high as 10 have been used in HRV research (Acharya *et al.* 2011). For EEG data, increasing *m* does not improve how ApEn discriminates between levels of sedation, and for short data segments, ApEn may vary with *m* (Ferenets *et al.* 2006). If *m* is high, although this may allow more detailed reconstruction of the dynamic process, it will be difficult to find data series long enough to analyse (Azami *et al.* 2019). Choosing *m*=2 will permit comparison with other studies, and with *m*=2 the use of a larger *r* value may limit the amount of bias associated with the calculation of ApEn; however, it may be advisable to test different values of *m* rather than simply selecting *m*=2 (Yentes *et al.* 2013). The FNN/AFN methods can be used to estimate *m*.

Tolerance (similarity threshold) r

[57] Cross-ApEn has also been computed for sub-band EEG data by some researchers (Ruiz-Gómez *et al.* 2018).

Pincus *et al.* (1991b) originally stipulated that r should be 'at least three times an estimated mean noise amplitude', so this parameter is usually defined with reference to the standard deviation (SD) of the data. Pincus and Goldberger originally recommended using a value of *r* between 0.1*SD and 0.2*SD (Pincus & Goldberger 1994). In HRV data, values of *r* between (0.1 * SDNN and 0.9 * SDNN) will maximise ApEn (Melillo *et al.* 2011), but to test all values will be time-consuming (Azami *et al.* 2019). Nonetheless, Yentes *et al.* (2013) recommended testing a range of *r* values (and reporting results) before selecting a particular value for a whole study. In one study on body temperature, values of *r* between 0.1 and 0.25 were tested, in steps of 0.05 (Cuesta-Frau *et al.* 2018a).

If two sets of data are analysed using different values of *m* and *r*, the relative regularity of the two sets may also differ, so that results may not be consistent (Richman & Moorman 2000). ApEn is more sensitive to the choice of *r* than of *m* (Lu *et al.* 2008) and can even exhibit a 'flip–flop' response, with the entropy values of two signals being compared swapping order, depending on *r* (Bošković *et al.* 2011).

Time delay τ

For uncorrelated signals, Rhea *et al.* (2011) suggest selecting $\tau = 1$, and for data with long-range correlations, $\tau = 15$.[58] The AMI method can be used to estimate τ.

Expected values – some examples

ApEn is nonegative (Pincus *et al.* 1991b).

ECG: normal breathing 0.5, apnoea/hypopnea 0.8 (*N* = 39, Acharya *et al*. 2011).

RRi: ~1.8 in normal sinus rhythm, smaller in cardiac pathology (*N* = 300, Acharya *et al.* 2004); ~0.9 in static exercise, 1.0 in dynamic exercise (*N* = 23, Weippert *et al.* 2013).

The use of plots

Plots of ApEn against data length are illustrated in Karmakar *et al.* (2015).

Sample Entropy (SampEn)

SampEn was developed to eliminate the bias implicit in ApEn as a result of including self-matching (tied points) and is largely independent of record length as well as more economical to compute than ApEn (Richman & Moorman 2000). Like ApEn, SampEn measures the probability of subsequences in a dataset being close at two lengths *m* and *m*+1,

[58] Not all implementations of ApEn require setting a time delay parameter.

within a tolerance of *r* (Cuesta-Frau *et al.* 2017). SampEn then represents the average of each probability before computing entropy (Furutani *et al.* 2020). A reduction in SampEn indicates increased regularity, the presence of spikes, or both (Lake *et al.* 2002). However, as for ApEn, changes in irregularity may not necessarily indicate changes in complexity (Costa *et al.* 2005a). SampEn and ApEn have been found to change in opposite directions in some HRV studies (Steffert & Mayor 2014; Shi *et al.* 2017), whereas cApEn results showed a strong positive correlation with those from SampEn in others (Shi *et al.* 2017).

Variants of the original SampEn method by Richman and Moorman include 'local' SampEn (LSampEn), which Porta and his colleagues (2019) found may be more sensitive to sympathetic activation in HRV than conventional SampEn. LSampEn represents entropy after averaging probability distribution but does not yet appear to have been used by research groups not linked to Porta's own (Faes *et al.* 2019a), although it is cited by Japanese researchers as background to their own measure of 'expanded SampEn', which they define as the 'time evolution of complexity without performing averaging over time' (Furutani *et al.* 2020).

Another variant is 'fixed' SampEn (fSampEn), i.e. using fixed values of tolerance parameter *r* (in the range of 0.1 to 1 times the *global* standard deviation of the original signal) for overlapping moving windows, rather than values normalised by the *local* standard deviation of the window analysed, as is usual when computing SampEn. Both window size (*N*) and percentage window overlap (%) are user-defined. The method computes SampEn for every overlap (step), applying a linear interpolation between the calculated values to obtain another data series the same length as the original. Results can be summarised in a single value in the usual way (mean and standard deviation, or median and IQR), and are more affected by *N* than by %. fSampEn 'tracks' both complexity and amplitude variations of a signal. Quantifying amplitude variations using fSampEn is currently under investigation (Estrada *et al*. 2017).

This method has been used to characterise respiratory electromyographic (EMGdi) and mechanomyographic (MMG) signals (Sarlabous *et al.* 2014, 2019; Lozano-García *et al.*

2018) and is reasonably robust to 'impulsive' noise, such as heartbeat (Estrada *et al.* 2017). Data should be tested before final analysis to ensure elected parameters are optimal.[59]

Other SampEn variants include an optimised, faster version (Martínez-Cagigal 2020), and fast 'lightweight' and 'bucket-assisted' algorithms (Manis *et al.* 2018). Bhavsar *et al.* (2018), for example, compared three methods of data reduction to check their effects on SampEn computation time and accuracy for EEG data sampled at 250 Hz. Using windows of different lengths, from 0.06 to 4 s long, they noted that computing SampEn for the signal averaged by window produced values closest to those obtained using the conventional method of estimating SampEn when using windows of 1 s duration. Although the results using this signal averaging method were rather different, the trends found were similar to those obtained with the standard approach.

Data requirements

SampEn may produce biased results for very small data series ($n \approx 10$) (Richman & Moorman 2000) and was found to give invalid results in one HRV study for a series of 50 data points (Li *et al.* 2015a), although it is thought to be less dependent on sample length than ApEn (Costa *et al.* 2002) and is more reliable for short datasets than ApEn (Yentes *et al.* 2013). Mariani *et al.* (2015) consider that SampEn is largely independent of time series length if > 750 samples. However, this may depend on the value of m selected: SampEn of RRi data decreases with data length (Udhayakumar *et al.* 2016b). A minimum of $N = 200$ has been suggested (Yentes *et al.* 2013), and for EEG data Cuesta-Frau *et al.* (2017) recommend $N = 1{,}000$ in order to keeping the computational burden relatively low (cf. Azami & Escudero 2018).

Moreover, for temporally correlated data, SampEn may depend on sampling rate (Liao & Jan 2014). SampEn (and fSampEn) were also found to depend on sampling rate in EMGdi research (Estrada *et al.* 2017). However, in one study of downsampled HRV data, the mean error in resulting SampEn was < 10% (Mesin 2017).

Filtering may affect SampEn of EMG data (Diab *et al.* 2015); filtering, detrending or differencing may affect SampEn in postural movement data as well (Lubetzky *et al.* 2018). However, missing data points do not greatly alter SampEn estimates for clinical HR data (Lake *et al.* 2002), although ectopic beats in RRi data did affect results in a more recent study (Molina-Picó *et al.* 2013), and outliers may affect values (Voss *et al.* 2009). Low frequency drift or slow, genera trends may lead to increased SampEn (Gow *et al.* 2015). However, SampEn may be less affected by sampling rate than ApEn (Rhea *et al.* 2011).

[59] This section was written in consultation with Luis Estrada Petrocelli and Abel Torres Cebrián.

SampEn is reasonably robust to noise, provided the signal-to-noise ratio is not too high (Ramdani *et al.* 2009), although – like ApEn – it does appear sensitive to noise in EEG data (Cuesta-Frau *et al.* 2017) and movement data (Rhea *et al.* 2011). It is more robust to data loss than ApEn (Cirugeda-Roldán *et al.* 2011). Like ApEn, SampEn requires stationarity of data (Tsai *et al.* 2012). Detrending prior to use should thus be considered (Shi *et al.* 2017).

SampEn has been used on continuous as well as discrete data, with the former more susceptible to sampling rate and m (and both affected by changes in r). The authors of that finding recommend not using continuous data to achieve long enough series data to obtain accurate results, even though SampEn is now more often used on continuous data than when it was originally introduced. They point out that higher sampling rates will depress the resulting values of SampEn (McCamley *et al.* 2018).

Data for SampEn estimation is sometimes normalised (e.g. with zero mean and variance of 1) (Cuesta-Frau 2019b).

Since at least 2004, SampEn has been estimated for band-filtered EEG data (Tong *et al.*2004; Cui *et al.* 2020), as well as for wavelet-decomposed EEG bands (Shamila *et al.* 2018; Zhang *et al.* 2018; Li *et al.* 2019; Zhao *e al.* 2019; Du *et al.* 2020).[60]

Parameter setting

Pattern length (Embedding dimension) m

m = 3 was used in one study of neonatal HR (Lake *et al.* 2002); m of > 4 gave invalid results in one HRV study (Li *et al.* 2015a), and in another HRV study this was the case in some situations even for m = 3 (Udhayakumar *et al.* 2016b). The FNN/AFN methods can be used to estimate m.

For fSampEn and EMGdi, m = 1 (Sarlabous *et al*. 2014; Estrada *et al.* 2016) or m = 2 (Estrada *et al.* 2017; Lozano-García *et al.* 2019).

Tolerance (similarity threshold) r

r = 0.2 was used in one study of neonatal HR (Lake *et al.* 2002); values of 0.05 or less gave invalid results in one HRV study (Li *et al.* 2015a). r = 0.2 and r = 0.5 have both been used in respiration research (Vlemincx *et al*. 2013; Dunn & Kenny 2017).

SampEn is less liable to the 'flip-flop' effect than ApEn or FE (Bošković *et al.* 2011).

For fSampEn and EMGdi, r = 0.3 (Sarlabous *et al*. 2014; Estrada *et al.* 2015), or from 0.1 to 0.64 when m = 1, and from 0.13 to 0.45 when m = 2 (Estrada *et al.* 2017). For other

[60] Cross-SampEn has also been computed for sub-band EEG data by some researchers (Ruiz-Gómez *et al.* 2018).

respiratory EMG and mechanomyography (MMG) data, other r values may be appropriate (Lozano-García *et al.* 2019).

For SampEn, some authors have used r * MAD (median absolute deviation) rather than r * SD (Govindan *et al.* 2007).

Time delay τ

τ = 1 was used in the original paper by Richman and Moorman (2000). The AMI method can be used to estimate τ if required by the algorithm.

For fSampEn, additional parameters are required:

Window Length (N)

N = 200 data points as default (agreed in discussion with Luis Estrada and Abel Torres).

For fSampEn, window length of 0.5 s maximised performance (Lozano-García *et al.* 2019).

Percentage Overlap (%)

% = 95% overlap as default (agreed in discussion with Luis Estrada and Abel Torres).

Expected values – some examples

SampEn may be relatively consistent for conditions where ApEn is not (Richman & Moorman 2000).

SampEn ~1.2 in static exercise, 1.4 in dynamic exercise (N = 23, Weippert *et al.* 2013).

The use of plots

Plots of SampEn against data length are illustrated in Karmakar *et al.* (2015).

More variants of ApEn and SampEn

ApEn and SampEn and their variants are the most frequently used entropies (Mayor *et al*. 2021). As they are conditional entropies, with a computation cost of order N^2, they are slower than PE (computation cost O(N)) but faster than FE (O(N^3)), and many entropists

have amended the original algorithms for the two measures in an attempt to make them faster.[61]

A fast algorithm for ApEn was published, for example, by Hong *et al*. as early as 1998, and has been adapted for SampEn by other Chinese researchers since (e.g., Wang XP *et al*. 2016, Wang YF *et al*. 2016). In 2007, Manis and Nikolopoulos published two new algorithms for APEn, one using a 'box-assisted' algorithm based on one for correlation dimension (Grassberger 1990), the other a 'bucket-assisted' algorithm (bApEn), the latter being faster than the basic and the box-assisted algorithms. The following year, Manis presented results for both a heart rate (RR interval) signal (>88,000 data points), as well as ECG (> 65,000 points) and EEG (> 81,000 points) data using the basic algorithm, together with an 'improved' basic algorithm and bApEn (Manis 2008). Computation times for bApEn decreased slightly with increasing window size (m) for all three signals, while increasing for a random signal, whereas they increased very clearly with threshold distance (r) for the signals as well as the random data.

Manis *et al*. also developed an amended and improved bucket-assisted algorithm for SampEn, with computation cost O(log N), together with a second, 'lightweight', algorithm with O(N log$N$). They noted that both showed better computation times than an improved version of the k-d tree algorithm (Bentley 1975). In a useful Table, they summarised how the lightweight version provided better execution times for specific values of m and r, and for smaller values of N. They concluded that the two methods are complementary, and that the method to be used had to be selected appropriately (Manis *et al*. 2018).

Again, using the k-d tree (or x-Sort) algorithm, Pan *et al*. managed to increase computation speed for multiscale SampEn (mSE) by 10-70 times compared to that of the 'conventional brute force' method for RR interval, ECG or EEG data of length N = 80,000 points. Their method outperformed the bucket-assisted method (Pan *et al*. 2011a). They went on to develop a sliding k-d tree method which was even faster, even for data as short as 500 data points, although for 300 data points the 'brute force' method was quicker. For a typical

[61] Interestingly, although fast PE algorithms can be located using Google Scholar (e.g., Piek et al. 2019; Unakafova & Keller 2013), there appear to be no studies for 'fast FE'.

value of pattern length $m = 2$, time complexity for this new method was reduced to $O(N^{3/2})$ (Pan *et al*. 2011b).

In 2012, Song *et al*. developed an 'optimised' version of SampEn for use with EEG data. Although time complexity was still $O(N^2)$, calculation time was still greatly reduced, especially for longer data (e.g., 4096 points). An even faster 'norm component matrix' algorithm for calculating ApEn, SampEn and D2, suited to parallel computing, was published the same year; the authors also demonstrated that the two entropies, especially SampEn, can be considered as 'building blocks' for D2 (Żurek *et al*. 2012a). In collaboration with Paolo Castiglioni, the same authors produced 3-dimensional plots of SampEn vs m and Log r (Żurek *et al*. 2012b, 2014).

More recent fast algorithms include a 'vectors with dissimilarity' (VDS) method for computing ApEn and SampEn in ECG, EMG and ECG signals (Lu *et al*. 2017). Values of the VDS and original SampEn measures were identical, but computation time was around 80% less for the VDS method, and similarly for ApEn. Code was written in MATLAB.[62] Other, faster algorithms for ApEn and SampEn have been written in both R and C by Tomčala, although without any reference to work by Manis (2019, 2021).[63] These new algorithms were claimed to be up to 500 times faster in real world time series than the original versions, being faster in C than in R. However, computation cost was still of order N^2 (Liu *et al*. 2022). Another method is the 'assisted sliding box' algorithm (SBOX), whose computation time depends on signal length N, pattern length m and distance r. SBOX is approximately 4.2 times faster than the box-assisted algorithm, outperforming the standard SampEn algorithm for $N \geq 100$ and the k-d tree and sliding k-d tree methods as well for $N \geq 1000$, with speedup > 20 for $N > 8000$ (Wang *et al*. 2021).[64]

'OpenCLSampEn', a fast algorithm for SampEn based on parallel computing was proposed by Dong *et al*. (2021),[65] and found to perform faster than k-d tree (Pan *et al*. 2011)

[62] Code for the VDS method was made available at https://sites.google.com/site/hitluyu)n/code/acemvds. However, this site dos not currently appear to be accessible without the Lu Yun's permission.
[63] Code for Tomčala's algorithms in both R and C is available at: https://cran.r-project.org/web/packages/TSEntropies/index.html [accessed 18 April 2022].
[64] Code for SBOX, with MATLAB interface, can be found at: https://sites.google.com/view/yhw-personal-homepage [accessed 19 April 2022].
[65] OpenCLSampEn code in R is available on GitHub: https://github.com/dongxinzheng/ParallelSampEn [accessed 18 April 2022].

and Lightweight SampEn (Manis *et al*. 2018), particularly for longer data. 'Speedup' compared to the basic SampEn algorithm was 75 for OpenCLSampEn ($N > 60{,}000$), but < 5 for the *k*-d tree and Lightweight methods. Results were superior for OpenCLSampEn over a wide range of embedding dimensions (m) and tolerances (r). However, for 'short' time series ($N < 5000$ for a PC), OpenCLSampEn provided no particular advantages.

MCSampEn, a 'superfast' Monte-Carlo-based algorithm for SampEn, has been developed by Liu *et al*. (2022).[66] They did not compare computing efficiency for MCSampEn and the algorithms from Manis and his group, although clearly aware of them. For EEG, ECG and ECG RR interval and other real-world data, MCSampEn provided 100-1000 times speedup compared to the *k*-d tree and SBOX algorithms, with satisfactory (if approximate) accuracy, even without employing parallel computing.

Entropy profiling

However, speed is not everything. A team of researchers in Australia aimed to simplify calculation of ApEn and SampEn by eliminating the need for using r as an input parameter in entropy estimations, using a data-driven, non-parametric approach to generate all appropriate r values for a given signal automatically and so eventually generating a complete 'profile' (instead of a single estimate) of entropy values (Udhayakumar 2019).

Using a cumulative histogram method, keeping m fixed (e.g., at 2) but varying r, a number of secondary measures are generated. For ApEn, these are MaxApEn, TotalApEn, AvgApEn, SDApEn (standard deviation of value sin the ApEn profile), KurtApEn and SkewApEn (kurtosis and skewness of the profile), and similarly for SampEn. The various secondary measures may have different applications. AvgApEn, for example, was found to be the most efficient and reliable regularity statistic for arrhythmia detection in ECG RR interval data ($N > 100$) (Udhayakumar *et al*. 2017a), and TotalApEn can differentiate data with length as low as $N = 50$ (Udhayakumar *et al*. 2017b). An advantage of the ApEn secondary measures is that they may be useful for classifying 'short' data ($N \leq 200$), whereas

[66] Codes for a number of *k*-d tree and MCSampEn algorithms are available at: https://github.com/phreer/fast_sampen_impl [accessed 19 April 2022].

ApEn itself cannot distinguish signals of length $N < 400$ (Udhayakumar *et al*. 2017a), possibly because of incorrectness in r selection (Udhayakumar *et al*. 2017b).

TotalSampEn outperformed both SampEn and FE in classification of foetal arrythmias, but only for $N = 1000$ (Keenan *et al*. 2020). However, TotalSampEn and AvgSampEn were found more useful for classification ECG RR interval data than both SampEn and FE (Udhayakumar *et al*. 2018). Data samples of length $N = 50$ to $N = 300$ were used. At $N = 250$ or 300, FE outperformed AvgSampEn. However, at all data lengths, starting from the lowest, TotalSampEn was the only one of the four measures that offered consistently good classification performance (AvgSampEn being more sensitive to noise). Importantly, the cumulative histogram method was considerably faster than the 'traditional' approach (which presumably included FE).[67] In a further study, the same group found that a shortened duration of the ST segment in the ECG, associated with myocardial ischaemia, could be detected from the RR interval data using TotalSampEn, even at $N = 50$. Nonetheless, they concluded that a safe choice for this particular application would require $N = 750$ or 800 (Udhayakumar *et al*. 2019a).

Multiscale entropy profiling has also been applied to RR interval data by the same researchers (Udhayakumar *et al*. 2019b). They noted that maximum scale factor for TotalSampEn was $N/5$, whereas for normalised FE it was only $N/8$. Thus, only 100 data points were required to reach scale 20 (with $m = 2$). However, classification results were more clear-cut for 500 data points. In contrast, for SampEn itself, 20,000 data points would be required.

Cross entropy profiling using TotalSampEn has also been used by these authors to test synchrony between signals and was found to offer an accurate estimation of such pattern synchrony even for $N = 50$ (Udhayakumar *et al*. 2019c).

Karmakar *et al*. have provided a useful summary of their results using entropy profiling with HRV data (Karmakar *et al*. 2020).[68] They point out that 'the right choice of m is

[67] Anecdotally, this has not necessarily been my experience when using CEPS.
[68] MATLAB codes for entropy profiling are available at: https://github.com/radhagayathri/Entropy-Codes [accessed 20 April 2022].

as ambiguous as that of *r* and propose 'eliminating embedding dimension (*m*) from entropy formulations' as their primary future target.

A somewhat similar approach has been taken by Bolea *et al*. (2018), using a measure they call 'multidimensional approximate entropy', $MApEn_{max}$, based on the maximum value of ApEn at each embedding dimension, using the value of *r* that provides this maximum value:

$$MApEn_{max} = \sum_{m=1}^{m=m_{max}} ApEn\left(m, r_{max}\left(m\right)\right)$$

.

The selected range for the tolerance threshold *r* was from 0.01 to 3 times the standard deviation of the time series, with a resolution of 0.01. This method does not require the use of coarse-graining and overcomes the variations in data length that occur for different time scales. $MApEn_{max}$ from RR interval data was greater in older than younger individuals, and (at night) in patients with congestive heart failure than in those who were healthy.

Entropy profiling was also the inspiration for an EEG temporal profiling method using 'dynamic sample entropies' with sliding windows in a machine learning study of emotion recognition (Lu *et al*. 2020). A variant of Refined cross-SampEn based on the cumulative histogram method has also been proposed by Contreras-Reyes and colleagues (Ramírez-Parietti *et al*. 2021; Contreras-Reyes & Brito 2022). Otherwise, the method does not appear to have been greatly used, as yet

Coefficient of Sample Entropy (CosEn) and Quadratic SampEn (QSE)

These are both variants of SampEn, developed for use with RRi data.

CosEn = SampEn - ln(2*r*) - ln(mean RR interval)

QSE = SampEn + ln(2*r*),

where $\ln(x) = \log_e(x)$.

An 'optimised' version of QSE, capable of optimising parameters and also able to deal with non-uniformly sampled or incomplete short time series, also exists (Cirugeda-Roldán *et al.* 2014), but is not considered further here.

Data requirements

Very short RRi recordings – e.g. hourly 12-beat calculations (Lake & Moorman 2011) – may be used with CosEn to distinguish between atrial fibrillation and normal sinus rhythm. QSE has been used for short EEG signals of 1,000 data points (Simons *et al*. 2015).

As both CosEn and QSE are based on SampEn, the same limitations and susceptibilities will apply.

Parameter setting

Pattern length (Embedding dimension) m

For RRi data, m =1 was used originally (Lake & Moorman 2011).

Tolerance (similarity threshold) r

For RRi data, $r \approx 30$ ms was used originally (Lake & Moorman 2011).

As with most entropy measures, 'the nature of the QSE calculation only allows results to be truly comparable with results calculated with the same parameters' (Simons *et al.* 2015).

Expected values – some examples

QSE is generally less than SampEn itself (Cirugeda-Roldán *et al.* 2014).

The use of plots

Plots of QSE against data length (N) are included in Lake (2011) and Simons *et al.* (2015).

Multiscale Entropy (mSE)

Unlike ApEn and SampEn, mSE provides a measure of complexity that is low in both highly regular and very random processes (Escudero *et al.* 2006).

In the mSE method, the original signal is first divided into non-overlapping segments of length τ, the 'scale factor' (**Figure 3** above). Next, the mean (μ) of each segment is estimated to derive so-called 'coarse-grained' signals. Finally, the entropy measure, using

SampEn, is calculated for each coarse-grained sequence (Costa *et al.* 2005). The length of each coarse-grained sequence is τ times shorter than the length of the original signal (Escudero *et al.* 2006), so that if τ is too high, there may not be enough points to ensure an accurate estimation of SampEn (Escudero *et al.* 2015b). Other methods of computing MSE may be based on coarse-graining using variance ($MSE\sigma^2$) (Costa & Goldberger 2015), standard deviation ($MSE\sigma$) or mean absolute deviation (MSE_{MAD}) (Costa & Goldberger n.d.), rather than the mean (V). Three of these versions are implemented in CEPS.

As mentioned above, there are many other multiscale entropies, some based on SampEn and others not, such as multiscale DistEn (Lee & Choi 2018, 2020). Some of these were reviewed by Humeau-Heurtier (2015), but their number and 'lack of mature development' have put off other reviewers (Gow *et al.* 2015). Different approaches to multiscale analysis also exist, such as 'multiscale information storage' and a 'model-based linear multiscale complexity analysis' method, both devised by Porta's group (Faes *et al.* 2013; Porta *et al.* 2018). The latter provides a 'complexity index' (CI)[69] that is not itself derived from entropy but described as providing complementary information when compared to the CI derived from the single-scale CCE approach (Porta *et al.* 2018).

Data requirements

As mSE is based on SampEn, the same limitations and susceptibilities are likely to apply. In particular, it may not be applicable to very short data (100 or 500 points, for example) because the length of the coarse-grained time series decreases with increasing scaling factor τ (Awan *et al.* 2018); some authors have suggested that at least 20,000 RR intervals may be required for accuracy in HRV research (Udhayakumar *et al.* 2019), others that between 14^m and 23^m points be present at the highest MSE scale analysed[70] (Gow *et al.* 2015). On the other hand, mSE may also be computationally demanding for long data (Azami *et al.* 2017b). Variants of mSE such as modified or composite mSE (CmSE) (Wu *et al.* 2013) and short time mSE (smSE) (Chang *et al.* 2014) have been proposed for short data series.

Noise will affect mSE values (Mariani *et al.* 2015), although eyeblink artefacts in EEG data may impact mSE (at multiple time scales) less than SampEn (i.e. mSE at scale 1) (Liu *et al.* 2015).

[69] Not to be confused with the CI developed by Costa *et al.* (See below).

[70] The number of points at the highest scale analysed is given by multiplying sample rate by data length and then dividing by the largest scale, τ_{max} (Gow *et al.* 2015).

Data loss may have considerable impact on mSE at scales > 3 (Cirugeda-Roldán *et al.* 2011).

mSE has been used to analyse complexity in EEG sub-bands (Li CX *et al.* 2016), although not so commonly as SampEn. It is also commonly used in HRV analysis.

Parameter setting

Pattern length (Embedding dimension) m

Costa *et al.* (n.d.) suggest 2 as a default value, and indeed this was the value found to be typically selected in one systematic review of MSE studies in human postural control (Gow *et al.* (2015).

Tolerance (similarity threshold) r

Costa *et al.* (n.d.) suggest 0.15 as a default value. on. The value of *r* should be set for the time series at scale 1 (not coarse grained) (Gow *et al.* 2015). In their systematic review, these authors noted that 0.15 or 0.2 are the usual values of *r*.

Whereas SD (in *r* * SD) is usually calculated for an entire time series, it is also possible to compute it for a fixed window width, stepped across the time series, take the median of the results to calculate a single value of *r* for use at all scales. This method has been called 'windowed-mSE', or WmSE (Gow *et al.* 2015).

Scale factor τ

Costa *et al.* (n.d.) suggest a maximum for τ of 20 as default, but Mariani *et al.* (2015) consider that if epochs contain *n* data points, then analysis can extend to include scale *n*/750. If there are erratic patterns in MSE as scale is increased, such instability may render results unreliable. As a rule-of-thumb, τ_{max}, the last stable scale to include, can be determined by checking for changes of ±0.1 in SampEn between successive scales $\tau_{max} - 1$ and τ_{max}, followed by a change in the opposite direction between τ_{max} and $\tau_{max} + 1$ (Gow *et al.* 2015).

For $\tau = 1$, mSE is identical to SampEn.

Expected values – some examples

Applied to RRi data, mSE at short and long time scales (1-4, 5-10) has been interpreted in terms of predominant vagal or sympathetic control (Silva *et al.* 2016; Matić *et al.* 2020). MSE at scale 5 was found to differentiate best between pulmonary hypertension patients and controls (Tsai *et al.* 2019), as well as between patients undergoing dialysis without prior cardiovascular disease and those with normal renal function (Lin *et al.* 2016).

If the WmSE method is used, values of SampEn will be higher at all scales than those found with the usual method (Gow *et al.* 2015).

The use of plots

Many plots of SampEn against scale can be found in the literature, for instance, in Costa *et al.* (2008), Javorka *et al.* (2008), Xie *et al.* (2008), Yuan *et al.* (2011), McIntosh *et al.* (2014), Lu *et al.* (2015), Tsai *et al.* 2019 and elsewhere, as well as of the related 'Gaussian entropy' against scale in Signorini *et al.* (2006). Plots of SampEn against scale for MSE with different coarse-graining methods (and different values of r) are shown in Costa & Goldberger (n.d.), demonstrating differences with age and health condition.

Complexity Index (CI) and Multiscale Slope (mSlope)

As already noted, there are various possible and very different definitions for a complexity index, CI (e.g. Bhaduri *et al.* 2018). CI was originally defined as the area under the mSE curve plotted against time scale factor (τ), bearing in mind the slope of the curve (Costa *et al.* 2008). In principle, the CI can be estimated for any multiscale method. Some authors have also examined the linear fitted slope of the graph of SampEn of each coarse-grained sequence versus scale, for both small (e.g. $1 \leq \tau \leq 5$) and large (e.g. $6 \leq \tau \leq 12$) time scales (Escudero *et al.* 2006), sometimes described as 'short scale' and 'long scale'; in one HRV study, the latter was subdivided into 'steady ascending' and 'plateau' (Chiu *et al.* 2017). Again, deriving mSlope is possible for other multiscale measures as well, such as DPE and PM-E (Martínez-Rodrigo *et al.* 2019), multiscale fuzzy SampEn (Glowinski *et al.* 2011) or multiscale symbolic entropy (Lin *et al.* 2014). **Figure 4** shows derivation of CI areas and mSlope from one HRV study on vagus nerve stimulation (Liu *et al.* 2018).

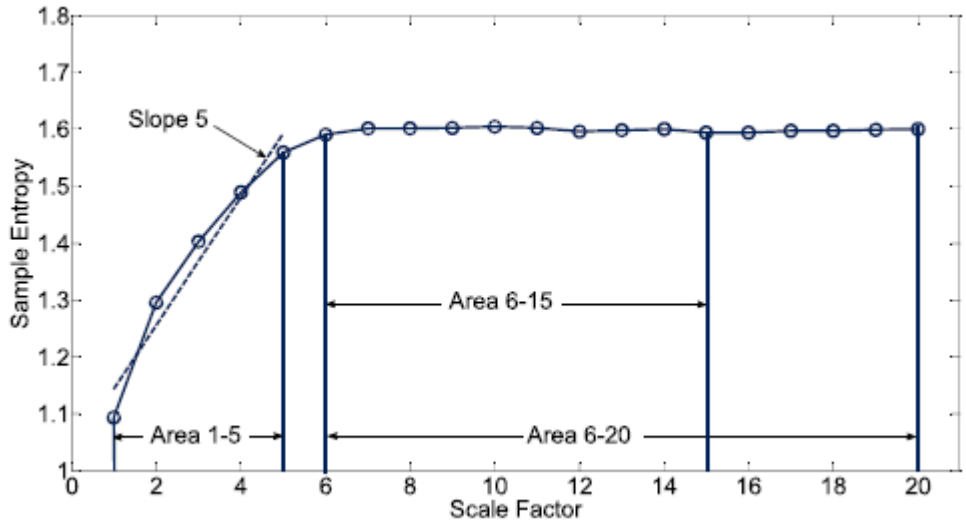

Figure 4. $CI_{1\text{-}5}$, $CI_{6\text{-}15}$, $CI_{6\text{-}20}$ and $mSlope_{1\text{-}5}$ from an HRV study on vagus nerve stimulation. Reproduced without change from Liu *et al.* (2018) under Creative Commons Attribution 4.0 International License (http://creativecommons.org/licenses/by/4.0/.).

Data requirements

As CI (and slope) are derived from mSE or other multiscale measures, the same limitations and susceptibilities are likely to apply. In particular, nonstationarity may be an important issue; Costa *et al.* (2014) used a 'parsing' algorithm to isolate relatively stationary segments from transient marked changes in RRi data (acceleration/deceleration episodes), noting that concatenation of the relatively stationary periods did not bias results. Other methods of detrending may also be appropriate.

mSE and the CI have been used for both EEG and HRV (RR interval) data (e.g. Weng *et al.* 2017; Chen *et al.* 2018), as well as other types of physiological time series data.

Parameter setting

Pattern length (Embedding dimension) m

Costa *et al.* (2014) used $m = 2$ in their study on foetal heart rate dynamics, as recommended for mSE.

Tolerance (similarity threshold) r

Costa *et al.* (2014) used $r = 0.15$ for foetal heart rate dynamics.

Scale factor τ

Costa *et al.* set $\tau_{max} = 6$ in their 2008 study on red blood cell vibration ('flickering') and used τ from 1 to 8 in their 2014 study. In HRV studies on stroke, Taiwanese researchers used τ from 1 to 20 (Chen *et al.* 2015, 2018; Tang *et al.* 2015).

Expected values – some examples

In their 2014 study, Costa *et al.* found that the mean CI_{1-8} (area under the curve from $\tau = 1$ to $\tau = 8$) was significantly lower ($p < 0.004$) for acidaemic (10.16, 9.64 – 10.98) than non-acidaemic foetuses (12.46, 11.25 – 13.34). In the Taiwanese stroke studies, CI_{1-5} was interpreted as representing short-term complexity, CI_{6-20} long-term complexity, and CI_{1-20} as overall complexity. More severe stroke was associated with lower CI_{1-20}; overall values for all stroke types were 5.9 ± 1.7 (CI_{1-5}), 21.0 ± 6.0 (CI_{6-20}) and 26.9 ± 7.4 (CI_{1-20}) (Chen *et al.* 2018). In pulmonary hypertension, CI_5, $mSlope_{1-5}$, CI_{1-5} and CI_{6-20} were all lower than in controls (e.g. $mSlope_{1-5}$ mean values 0.003 vs 0.046). 1/*f* noise will be associated with a high CI, uncorrelated white noise with a comparatively smaller CI (Gow *et al.* 2015).

WmSE yields higher values of CI than MSE (Gow *et al.* 2015).

The use of plots

Plots are generally of SampEn against τ, rather than CI or mSlope against τ. Fitted slopes for short- and long-term lags in mSE of winds near the earth's surface are shown in Nogueira 2017.

Fuzzy Entropy (FE)

FE provides a measure of 'indefiniteness' of a situation or data (Azami *et al.* 2019). Like ApEn and SampEn, FE is a conditional entropy, its value being the negative natural logarithm of the conditional probability that two vectors which are similar for *m* points remain similar for the next *m* + 1 points, but this similarity is now defined in terms of fuzzy set theory (Chen *et al.* 2007). A fuzzy set is a class of objects with a *continuum* of grades of membership, i.e. a membership function which is not equal simply to 0 (not belonging) or 1 (belonging) (Zadeh 1965).

Before using the code implemented in CEPS, it is advisable to read the associated published paper (Azami *et al.* 2019). Using the 'Gaussian' membership function is most economical in terms of processing time – although still slow if compared to DE or PE (Azami *et al.* 2019). The 'Exponential' membership function (mf) is that used in the original paper on FE, 'an ad hoc choice due to its easiness to be understood' (Chen *et al.* 2007), the 'Gaussian'

mf in studies by Li *et al.* (2014) and Ahmed *et al.* (2017), the 'Triangular' mf and 'Trapezoidal' mf in studies by Zhao and Bose (2002) and others, and the 'Bell-shaped' mf in studies by Toprak and Güler (2007), Maturo and Fortuna (2016) and Dutta and Limboo (2017), for example. 'Global' fuzziness is an extension of SampEn, whereas 'local' fuzziness is not (Azami *et al.* 2019).

Chen's original algorithm for FE has also been termed Fuzzy ApEn (fApEn). Fuzzy SampEn (fSampEn, not to be confused with fixed SampEn) was introduced in 2010 by Xie *et al.* (2010) and, independently, by Xiong *et al.* (2010). Both fApEn and fSampEn methods have been used, for example, in EEG studies (Cao *et al.* 2015), for analysing EMG (Xie *et al.* 2010), and in head movement in fMRI research (de Vries *et al.* 2020). Three-dimensional fApEn was used in one hand-tracking study (Fan *et al.* 2019). fApEn has been used in further EEG, EMG and hand grip studies on stroke patients (Sun *et al.* 2017; Ao *et al.* 2013; Zhu *et al.* 2018), for RRI data (Strang *et al.* 2014), and in research on resting state fMRI complexity across the adult life span (Sokunbi *et al.* 2015). fSampEm has been used in analysis of postural control following sedation (Tietäväinen *et al.* 2014) and in Parkinson's disease (Pasluosta *et al.* 2017).

Data requirements

For short data (50-400 points), it is advisable to use the FE Gaussian membership function; for long data (> 500 points), the 'Exponential' membership function (order 4). FE is less affected by data length than ApEn or SampEn (Azami *et al.* 2019), although it tends to be greater for data of 50 or 100 data points than for longer samples (Udhayakumar *et al.* 2016b) and may not be as stable as sometimes claimed (Cuesta-Frau *et al.* 2017).

FE is slightly slower to compute than SampEn (Udhayakumar *et al.* 2016b; Azami *et al.* 2017a), being of the order of N^2 for SampEn (and ApEn), but N^3 for FE. However, FE is more robust to noise and parameter selection than ApEn and SampEn (Cuesta-Frau *et al* 2017). fApEn is less sensitive to sampling rate than SampEn (Kahl *et al.* 2015).

FE is frequently used for EEG (i.e. nonstationary, continuous) data, less frequently with ECG RRi data (nonstationary, discrete).

Detrending prior to using FE should be considered (Shi *et al.* 2017).

Parameter setting

FE is based on SampEn, so basic parameter selection is on similar principles (Liang *et al.* 2015).[71]

Pattern length (Embedding dimension) m

$m > 1$; m = 2 has often been used (Azami *et al.* 2019), and $m = 3$ is recommended by some experienced researchers (Cuesta-Frau *et al.* 2017).

Tolerance (similarity threshold) r

FE is less affected by r than are ApEn or SampEn; $0.1 \leq r \leq 0.5$ were tested (Azami *et al.* 2019). FE is liable to the 'flip-flop' effect, described above for ApEn (Bošković *et al.* 2011).

Time delay d

For oversampled signals, $d > 1$ may be used, but this may result in aliasing, so in general $d = 1$ is recommended (Azami *et al.* 2019).

Fuzzy power (order) n

For the FE Gaussian membership function, $n_g = 2$, and for the Exponential membership function, $n_e = 4$ (or 3).

Fuzziness

Fuzziness may be 'global' or 'local' (with the latter, it is not possible to use $m = 1$).

In general, as for ApEn and SampEn, different scenarios may require different parameter settings, and there is no general consensus on how best to select them. A range could be carefully tested, in order, for example, to assess which parameters provide better separability between groups in a particular study (Cuesta-Frau *et al.* 2017).

Expected values – some examples

In a study of patients with knee cartilage pathology, FE of the vibroarthrographic signal showed a clear reduction when compared to that of healthy knees (mean 0.16 vs 0.24 in men, 0.17 vs 0.23 in women); in contrast, ApEn and SymDyn increased (Wu *et a.* 2016).

Local and global FE appeared to be strongly correlated for 15 samples of detrended RRi data from our own research.

[71] However, the algorithms for FE used here deal with both local and global characteristics of the data sequence, unlike SampEn, which considers only their global characteristics (Azami et al. 2019).

The use of plots

A plot of FE against window (pattern) length can be found in Li *et al.* (2018). Plots of FE against r are shown in the original papers on FE by Chen *et al.* (2007, 2009), and of different estimates of FE against data length N in Azami *et al.* (2019).

Plots of fApEn against r and N for RRI data are included in Li *et al.* 2020), and for EMG data in Ao *et al.* (2013). Plots of fApEn against r, N and d (i.e. τ) for EEG data may be found in Sun *et al.* (2017), and of fApEn and fSampEn against r and noise level in a paper on EEG by Cao *et al.* (2015). Plots of fSampEn against scale for RRi data are shown in von Tscharner & Zandiyeh (2017), and of fApEn against sampling rate in Kahl *et al.* (2105).

Centred and Averaged Fuzzy Entropy (CAFE)

FE, a derivative of SampEn, albeit with a computation cost of order N^3, is less dependent on sample length than SampEn. Nonetheless, the precision of the FE values is less for shorter signals. Both methods depend on use of 'translated' patterns. Greater precision is obtained using the more recent 'centred and averaged FE' (CAFE): the number of samples (m-patterns) used to compute the entropy measure is increased without changing the length of the time series, by centring and/or averaging the patterns. Furthermore, not only translated patterns, but reflected, inverted, and 'glide-reflected' patterns (the four 'isometries') are also considered. CAFE resulted in better classification of foetal heart rate time series than FE, for example (Girault & Humeau-Heurtier 2015; Humeau-Heurtier 2018). However, increasing pattern matching rate without enlarging series length has been criticised as a strategy because of the inherent risk of destroying peculiar features of the dynamic and underestimating actual complexity (Porta *et al*. 2020). The same critics noted that the four isometries may introduce their own irregularities, especially at longer time scales, so should be used with caution (Valencia *et al*. 2019).

In CEPS, CAFE is implemented with parameters for embedding dimension (m), threshold (r), 'membership function power' (p), and the choice of one of the four isometries, as well as centring or non-centring. The membership function power $p = 2$ for the Gaussian function (as for FE), and > 1000 for the 'classical' rectangular function.

Other Entropies

In this section, you will find information on some multiscale entropies introduced between 2016 and 2019 by Hamed Azami and Javier Escudero when they were both at Edinburgh University, together with some other interesting and innovative entropies.

Refined Composite Multiscale Sample Entropy based on standard deviation (RCmSEσ)

RCmSEσ was derived from RCmSE (Wu *et al.* 2014), itself based on mSE, by Azami *et al.* in 2016 (Azami *et al.* 2016c). The 'sigma' (σ) extension indicates that the measure uses coarse-graining based on standard deviation over multiple time scales rather than variance (as in Costa & Goldberger 2015) or local averaging, as in the original formulation for mSE (Costa *et al.* 2002).

Wu's method has been used in studies of HRV (Deschodt-Arsac *et al.* 2020), cardiovascular and respiratory complexity (Reulecke *et al.* 2018), gait (Raffalt *et al.* 2018b), MEG (Escudero *et al.* 2015b), polysomnography (electro-oculogram, EOG) (Kuo & Chen 2020) and even 72-hour blood glucose monitoring (Lai *et al.* 2018), but Azami's does not appear to have been used by other researchers to date, apart from in a study on arrhythmia detection (Hussain *et al.* 2020). It should therefore be used circumspectly.

Data requirements

As RCmSEσ is based on mSE, some of the same limitations and susceptibilities are likely to apply. In particular, it may not be suited to either very short or very long data samples and may not be stable for the former (Azami *et al.* 2017b).

Parameter setting (Azami *et al.* 2017a, 2017b)

Embedding dimension (segment length) $m = 2$

Tolerance $r = 0.15 \times SD$

Time lag $\tau = 1$

Scale factor S (i.e. max τ): In their EEG study, Azami *et al.* (2017b) distinguished slopes of RCmSE for values of τ between 1 and 4 and between 5 and 12.

Expected values – some examples

RCmSEσ classification of Alzheimer's disease from MEG data was most significant for temporal scales 5-7 (Azami *et al.* 2017a), or 5-12 as against 1 to 4 (Azami *et al.* 2017b).

Results with RmSE may be more stable than those with mSE (Azami *et al.* 2017b).

The use of plots

Plots of RCmSE against scale factor are included in Azami *et al.* (2017b).

Refined Composite Multiscale Fuzzy Entropy based on standard deviation (RCmFEσ)

RCmFEσ was developed by Azami and Escudero (2016c) with the hypothesis that it would be more accurate, robust and stable than previous SampEn-based metrics. As with RCmSEσ, it uses coarse-graining based on the standard deviation of the signal. Results have only been published for this measure when used on MEG and EEG data (Azami *et al.* 2017a), and on corneal pulse data (Danielewska *et al.* 2020).[72]

For MEG, RCmFEσ features led to higher classification accuracy than RCmFEμ ones for Alzheimer's disease vs controls; for EEG, the RCmFEσ method achieved significant differences between focal (seizure) and non-focal (non-seizure) signals at all scales factors (1 to 30), whereas the RCmFEμ algorithm yielded significant differences at fewer scale factors (1-20), with better classification accuracy for RCmFEσ (Azami and Escudero 2016c). In the corneal pulse study, statistically significantly differences between groups were found for scales in the 26–43 range, with greatest significance for scale factor 32 (Danielewska *e al.* 2020).

Data requirements

RCmFEσ is suitable for both short (Danielewska *e al.* 2020) and long (Azami *et al.* 2017a) data samples. Normalisation to SD (σ) = 1 and coarse-graining of data are prerequisites.[73]

Parameter setting (Azami *et al.* 2017a; Danielewska *e al.* 2020)

Embedding dimension *m*

[72] RCmFEμ rather than RCmFEσ was used in the latter study.
[73] These are included in the code implemented in CEPS.

m = 2

Threshold r

r = 0.15 x SD (0.05-2 x SD); r was kept constant across temporal scales (Azami *et al.* 2017a).

Fuzzy power FP

FP=2

Time lag τ

τ = 1

Scale factor S

S = 1 to 30 (Azami *et al.* 2017a), or 1 to 50 (Danielewska *e al.* 2020)

Expected values – some examples

No actual values for RCmSEσ could be found in published studies.

The use of plots

Plots of RCmFEσ against scale factor are included in Azami *et al.* (2017a).

Refined Composite Multiscale Dispersion Entropy (RCmDE)

RCmDE was introduced by Azami *et al.* (2017b) to overcome deficiencies in mSE, namely that mSE values may be undefined for short signals, and that mSE is slow to compute for some real-time applications. RCmDE is a development from Dispersion entropy (DE), created by the same research group in 2016 to describe the spread in a set of data (Rostaghi & Azami 2016). DE has advantages over PE in that it can show changes in both signal amplitude and frequency and is also faster to compute (although both have a computation cost of the order of N rather than N^2). DE is also relatively insensitive to noise. RCmDE was almost 20 times faster than RCmSE in one test (Azami *et al.* 2017b).

RCmDE has also been used, by other research groups, for single-channel electro-oculogram (EOG) sleep stage classification (Rahman *et al.* 2018) and in underwater acoustic signal denoising to reveal signal complexity, for which it performed better than mSE or DE itself (Li *et al.* 2019).

Data requirements

RCmDE is stable and reliable for both long and short signals of continuous data, even if noisy. It has been tested on long datasets, so is presumably reasonably robust to nonstationarity (Azami *et al.* 2017b). It does not appear to have been tested on discrete data such as RR intervals.

Parameter setting (Azami *et al.* 2017b; Rahman *et al.* 2018)

Embedding dimension m

$m = 3$

Number of classes to be mapped c

$c = 6$ (although $2 < c < 9$ may lead to similar results)

Time delay d

$d = 1$ (to avoid aliasing)

Scale factor τ

$\tau = 4$ for EOG ($\tau_{max} = 30$ for EEG in the study by Azami *et al*.)

If L = signal length, $c^m < L$ (Azami *et al.* 2017b).

Expected values – some examples

Like RCmFEσ, RCmDE showed larger differences between physiological conditions (e.g. Alzheimer's disease vs controls), and at more scales, than RCmSE.

No actual values for RCmDE could be found in published studies.

The use of plots

Plots of RCmDE against scale factor τ are included in Azami *et al.* (2017b).

As for mSE and other measures, the graph for RCmDE vs τ can sometimes be separated into two parts – an initial steep increase for small τ, followed by a smoother section for larger τ. For EEG in Alzheimer's patients, these two parts were $1 \leq \tau \leq 6$ and $7 \leq \tau \leq 12$ (Azami *et al.* 2017b).

Distribution Entropy (DistEn)

DistEn is a measure of complexity or chaotic behaviour in series data. Based on SE, it has been shown to be more sensitive to differences in HRV data for ageing and heart failure than SampEn and FE, for example (Li *et al.* 2015a; Karmakar *et al.* 2017). The measure is based on state-space reconstruction and the empirical probability density function (ePDF) of distances among vectors formed from a given signal in the state space (Li *et al.* 2015a). DistEn may correlate more strongly with the LE than with SampEn (Karmakar *et al.* 2017). DistEn based on RE rather than SE has also been used in HRV analysis (Shi *et al.* 2019), and a 'modified' form of DistEn in EEG epilepsy detection (Aung & Wongsawat 2020). Multiscale DistEn also exists (Lee & Choi 2018, 2020).

Data requirements

DistEn has been used for both discrete (RRi) and continuous (EEG) data (Li *et al.* 2015a, 2015b). Prior detrending may affect results (Shi *et al.* 2017).

It is stable even for very short data (50 points) and is independent of data variance (Li *et al.* 2015a). Correspondingly, for EEG data, DistEn was able to differentiate between ictal and interictal states consistently, whether for samples of 174, 868 or 4,097 points (Li *et al.* 2015b). DistEn in the EEG has been estimated using single windows from 1 to 23 s long, or by averaging results over overlapping 1-s windows (Li *et al.* 2018).

Sampling rate may affect DistEn, while noise may become an issue if parameters m and τ are not selected carefully (Li *et al.* 2016, Supplementary material).

Parameter setting

Embedding dimension m

$m = 2$, tested from 1 to 10 (Li *et al.* 2015a; cf. Karmakar *et al.* 2015), or 2 to 10 (Li *et al.* 2016). DistEn is minimally affected by the choice of m (Li *et al.* 2015a) but may increase and stabilise for $m \geq 3$ (Udhayakumar *et al.* 2016a). In recent EEG studies, m was determined to be optimal when within the range 2 to 5 (Li *et al.* 2016, 2018).

Bin number M (number of bins used to construct the histogram of state-space distances)

M = 64 (Li *et al.* 2016, 2018) or 512 (Li *et al.* 2015a; Karmakar *et al.* 2015; Shi *et al.* 2017). *M* should be large, fixed and an integral multiple of 2 if SE is defined using the logarithm to the base 2 (Li *et al.* 2015a). DistEn is very stable for almost all values of *M* over a large range (512 to 1024).

Time delay τ

In more recent studies on DistEn in the EEG (e.g. Li *et al.* 2016, 2018), the time delay τ has been re-introduced into the algorithm for estimating its value, whereas it was maintained as $\tau = 1$ in the original DistEn HRV (and EEG) studies. In these more recent EEG studies, τ was determined to be optimal when within the range 8 to 12.

Tolerance r

Tolerance *r* is not used in calculating DistEn, the measure being independent of variance, but was reintroduced in 'modified' DistEn (Aung & Wongsawa 2020).

Expected values – some examples

Theoretical lower and upper limits of DistEn are 0 and $\log_2(M)$, corresponding to a one-peak and fully flat ePDF, respectively (0 and 1, when normalised) (Li *et al.* 2015a). For RRi data, DistEn was around 0.80 in healthy older individuals (ages 68-85), and around 0.88 in healthy younger people (ages 21-34); it was also lower (around 0.61) in heart failure patients than in healthy controls (around 0.79) (Li *et al.* 2015a).

DistEn of the EEG is lower with eyes open than with eyes closed, and greater during an epileptic fit than between fits (Li *et al.* 2015b).

The use of plots

Plots of DistEn against data length for EEG data are illustrated in Karmakar *et al.* (2015) and Udhayakumar *et al.* (2016b), of DistEn against window (pattern) length in Li *et al.* (2018) for EEG data, and of DistEn against *M* in Aung & Wongsawa (2020).

Slope Entropy (SlopeEn)

SlopeEn uses an 'Alphabet' of five symbols (-2, -1, 0, 1 and 2), covering a range of slopes for the segment joining two consecutive samples of the input data. The relative frequency of each pattern found is then mapped into a real value using an approach based

on SE. It outperformed both SampEn and PE in one study (Cuesta-Frau 2019b). Like DE, SlopeEn compensates for the shortcomings of the individual ordinal and conditional types of entropy by combining aspects of both (Cuesta-Frau 2019b).

Data requirements

SlopeEn has been used on EEG, EMG and RRi physiological data. It is reasonably robust with noisy data, and indeed noise may improve accuracy when SlopeEn is used to classify different cases. The measure is also reasonably robust against data length and has been used for short datasets of 50 points, although results are more accurate for longer ones (actual length depending on data type). For EEG data, SlopeEn achieved accuracy already for 1,500 points, whereas ApEn and SampEn did not.

Filtering may affect results if τ is high (Cuesta-Frau 2019b), but the effects of sampling frequency or downsampling are not yet known (David Cuesta-Frau, Personal communication, September 21, 2020).

Parameter setting

Embedding dimension m

m may be set between 3 and 8; for most datasets $m = 6$ appeared to perform well, but values should be tested on different data types. SlopeEn may be more dependent than SampEn or PE on *m* (Cuesta-Frau 2019b).

Horizontal and vertical increments between samples, τ and γ

The horizontal increment between samples (τ) is always 1, while vertical increments are thresholded by a parameter γ, also taken as 1, following Azami & Escudero (2016b), although $\gamma = 2$ may also provide accurate results.

Threshold δ

δ is set very low (but not = 0) to avoid ties (Cuesta-Frau 2019b).[74]

Expected values – some examples

"What really matters to me are relative values, not absolute values" (David Cuesta-Frau, Personal communication, September 21, 2020).

The use of plots

[74] In CEPS, the default value of δ is set at 0.001.

No plots of SlopeEn were found in the literature to date (March 2021).

Bubble Entropy (BE)

"BE is a very recently proposed entropy measure that has not received the attention it deserves yet, but it will surely become an indispensable tool in the field of non–linear dynamics analysis due to the possible improvements over PE it introduces"

(Cuesta-Frau & Vargas 2019)

This entropy, 'almost free of parameters' (Manis *et al.* 2017), is a somewhat controversial addition to the list of conditional entropies, derived ultimately from RE, but also PE, and in some ways complementary to the latter (PE is based on order relations, BE on sorting relations) (Cuesta-Frau & Vargas 2019). It is reported as more stable than PE (Manis *et al.* 2017) and is more robust to spikes in RR interval data than SampEn (Manis & Sassi 2017).[75] When tested for classification performance on a variety of datasets (blood sugar, temperature, EMG, ECG, EEG), PE yielded better accuracy in three, BE in three others, suggesting these two methods could be considered complementary. Although for some datasets, using the two methods together improved results, for others results became blurred (Cuesta-Frau & Vargas 2019).

Data requirements

BE can be used with discrete or continuous data, and varies little with sample length, although standard deviation of the measure is less than ~0.05 only for samples of more than around 1,000 data points. It is not yet known how sampling rate affects BE, particularly for continuous data (Manis *et al.* 2017), although in general methods based on embedding dimension may be affected more than simpler ones (George Manis, Personal communication, September 10, 2020).

BE is more tolerant to spikes in HRV data than SampEn (Manis & Sassi 2017), so is also likely to be more accepting of nonstationarity of data.

Parameter setting

Embedding dimension m

[75] No code for BE has been officially published by its authors to date. Please refer to one of the papers cited (Manis & Sassi 2017; Manis *et al.* 2017), if you use Bubble Entropy.

Dependence on m is low in BE, provided it is reasonably large (e.g., 10), and the need for r is totally eliminated (Manis & Sassi 2017). Furthermore, all samples in a given time series can be considered (i.e. $\tau = 1$), whether the data is discrete (as in HRV) or continuous (Manis *et al.* 2017).

Expected values – some examples

No actual values for BE could be found in published studies.

The use of plots

Plots of BE against m and signal length are included in Manis *et al.* (2017). An interesting plot of the 'BE-PE plane' for a blood glucose dataset, with $m = 8$, is shown in Cuesta-Frau & Vargas (2019).

Phase Entropy (PhEn)[76]

Whereas a Poincaré plot show patterns within a data series, $g[n]$, and so represents its degree of variability, a second-order difference plot (SODP) is based on successive differences within the data series, i.e. $g[n + 1] - g[n]$ and provides a visual summary of rate of variability or degree of compressibility of data in a four-quadrant plot format (**Figure 5**). The top left quadrant of the SODP will show accelerations preceded by decelerations, the bottom right quadrant accelerations followed by decelerations, the top right quadrant consecutive accelerations and the bottom left consecutive decelerations. This method is sometimes known as 'sequential trend analysis' (de Carvalho *et al.* 2002).

[76] This section was written in consultation with Ashish Rohila.

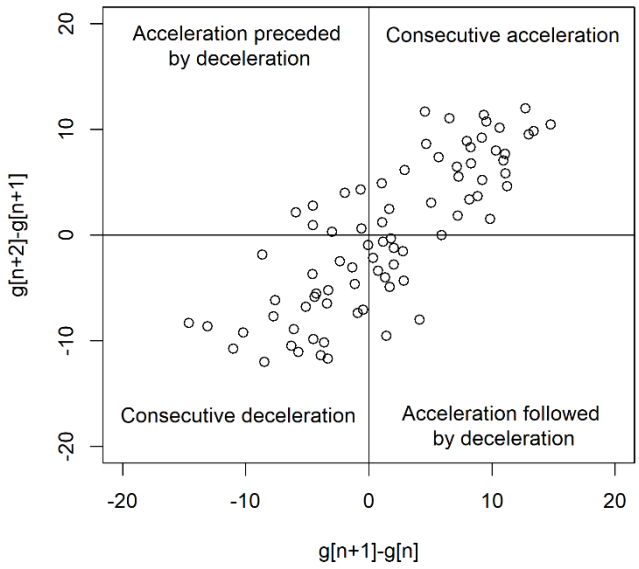

Figure 5. Phase space representation of time series data using a second-order difference plot (based on Rohila and Sharma 2019; redrawn by Tony Steffert).

PhEn then estimates the Shannon entropy (SE) of the weighted distribution in the coarse-grained SODP. Because it is based on rate of variability, PhEn is sensitive to time irreversibility, with higher values of PhEn corresponding to more irreversibility and less compressibility or multiplicity (number of points in the SODP with the same value). PhEn may also demonstrate better discriminating power and stability than some other entropies such as PE and SampEn, and require less computation time than FE, BE and SampEn (Rohila & Sharma 2019).

Data requirements

Preliminary results indicate that PhEn may be used with discrete (e.g. RR interval) or continuous (e.g. 1/*f* noise or EEG) data. For continuous data, sampling rate may affect results. Downsampling will also affect results. However, PhEn would be appropriate to use for EEG in filtered bands, according to its originators (Ashish Rohila, Personal communication, September 9, 2020). To some extent, PhEn is robust to noise in physiological signals. Noise has a little impact on computation of slope angles computation, but much less on the overall PhEn value.

Parameter setting

Coarse-graining parameter k (number of sectors)

k = 16 (tested from 2 to 50)

Time delay τ

Time delay τ has not yet been investigated for its effects on PhEn.

Expected values – some examples

Values of PhEn between approximately 0.1 and 0.9 are shown in Rohila & Sharma (2019).

The use of plots

Second-order difference plots (SODPs) are illustrated in Rohila & Sharma (2019), as well as plots of PhEn against *k* and signal length for both synthetic and real data. Plots are also shown for computation time against signal length for PhEn and several other entropies, and for *t*-test *p*-values against *k* for differentiating between different signals and conditions. Further such plots are provided in Reyes-Lagos *et al.* (2020).

Multiscale PhaseEntropy (mPhEn)

This measure was created by Deepak Panday on the basis of Ashish Rohila's PhEn (Rohila & Sharma 2019). The two measures require the same parameter (the number of sectors, k). To our knowledge, mPhEn has not been used by other authors in physiological research as yet.

Attention Entropy (AttnEn)

AttnEn was developed by Yang Jiawei while at the University of Eastern Finland (Yang 2020) and should not be confused with 'visual attention entropy' (Gu *et al*. 2021) or the entropy of paying attention (e.g., Ghader & Monz 2017). Rather than analysing the frequency of *all* patterns in a time series, AttnEn 'pays attention' only to the frequency distribution of the intervals between *key* observations (peak points, or local maxima and minima in the data), averaging the Shannon entropy for four sets of intervals: max-min, min-max, max-max and min-min. AttnEn requires no parameters to tune, is robust to the time-series length (differentiating between atrial fibrillation, congestive heart failure, young and old even at 100 data points when applied to heart rate time series data), and requires only

linear time to compute, i.e. O(N). It also outperformed 14 other state-of-the-art entropy methods, being faster than all for N = 10,000, faster than all except MSE for N = 1000, and faster than all except spectral entropy for N = 100,000 However, because AttnEn is based on peak points, it is sensitive to noise and outliers (Yang *et al*. 2020).

Cosine Similarity Entropy (CoSiEn)

CoSiEn was developed by Chanwimalueang and Mandic (2017) as an amplitude-independent measure suited to short time series data, using angular rather than Chebyshev distance in its calculation. Values lie within the range -1 to +1 (or 0 to 2 if the cosine distance is modified by subtracting its value from 1). Multiscale CoSiEn results if f coarse graining is carried out prior to calculating CoSiEn itself. Recommended parameters are 0.05 to 2 for tolerance (r), and 2-5 for embedding dimension (m). The authors found CoSiEn useful for classification of 10-minute RR interval data (normal heart rhythm, congestive heart failure, atrial fibrillation), but mCoSiEn was more useful for differentiating between the two pathologies. Unlike MSE and multiscale FE, values of RR interval CoSiEn decreased as scale increased.

A paper on *hierarchical* CoSiEn (HCSE) was published in 2018 by Chen *et al*. for use with passive sonar data and ship-radiated noise. Comparing their Shannon entropy based HCSE method with MSE, they noted that undefined entropy is not likely to occur in HCSE, which is also more suitable for 'short' time series. However, although they found the HCSE method valid even when data-length N = 10, HCSE only provided stable entropy estimation when $N \geq 200$.

Neither CoSiEn nor HCSE appear to have been used except by their creators.

Gridded Distribution Entropy (GDistEn)

Gridded Distribution Entropy (GDistEn) and Gridded Distribution Rate (GDistR), obtained by coarse graining (gridding) the Poincaré plot, were developed by Li Peng and colleagues at Shandong University (Yan 2019). Both GDistR and GDistEn were reduced in older compared to younger healthy individuals, and in cases of coronary artery disease,

whereas differences were not significant for asymmetry indices (Porta's, Guzik's, Slope and Area), which were more sensitive to the position of individual points in the plot.

GDistR and GDistEn do not appear to have been used except by their creators.

Increment entropy (IncrEn)

Increment entropy (IncrEn), a measure of predictability, was created by Liu Xiaofeng and colleagues in Changzhou and Xi'an (2016). Each 'increment' (difference) is mapped onto a word of two letters, one corresponding to its sign (+, -, 0) and the other to its magnitude (dependent on resolution R). As with PE, order (embedding dimension) m also has to be defined. IncrEn of order m is the Shannon entropy of the resulting words and is able to detect abrupt energetic (sign) or structural (magnitude) changes in data, for which there are no particular prerequisites. In contrast, Liu *et al*. consider that PE and SampEn can capture only structural changes. They found that IncrEn is robust to noise, useful even for $N = 100$. and that IncrEn of the EEG is more sensitive to seizure onset than SampEn. In a subsequent study, they used IncrEn as a feature in machine learning, and noted that EEG complexity was lower in epileptics than in healthy volunteers, being lower still during seizure; IncrEn was also lower with eyes closed than with eyes open (Liu *et al*. 2017).

The same authors created a multiscale version of IncrEn ('MIE') and found that it outperformed both MSE and RCMDE (both with recommended parameter settings) when differentiating between focal and non-focal EEG, between RR interval data for healthy individuals and those with atrial fibrillation or congestive heart failure, and between oxygen saturation variability of young and old individuals. Computation times were also significantly lower for MIE. MIE results coincided with those expected from the complexity-loss theory of ageing and disease (Wang *et al*. 2022).

Another group of Chinese researchers developed their own multivariate multiscale increment entropy for analysis of pipeline flow patterns (Wang & Jin 2020). This does not appear to have been used by others and is not referenced in the later MIE paper by Liu's group. Otherwise, IncrEn only appears to have been used by an Iranian group, as an HRV feature in a machine learning study on predicting sudden cardiac death, the other features

being derived from RQA; their paper includes an interesting plot of IncrEn against RQA Laminarity, although the latter was far more useful as a 5-minute predictor than IncrEn iself (Khazaei *et al*. 2018). Quite a number of other authors cite the original paper on IncrEn, but without actually using it themselves.

Liu and colleagues initially recommended that m be 2, 3, 4 or 5, and $R \leq 4$ (for R = 0, IncrEn can be considered a variant of PE). By default, in the entropy equation, logarithms to the base 2 are used, but other bases can be used. In a subsequent study on EEG and RR interval data (Liu *et al*. 2018), they noted that IncrEn is sensitive to changes in m, R and N for short datasets ($N \leq 500$), reaching stability for $N = 1000$ (with $m = 2$ and $R = 2$). They recommended that N should be no less than 100, and for $N = 100$, that $2 \leq m \leq 6$ and $2 \leq R \leq 8$ (bur for clear classification, $2 \leq m \leq 4$ and $2 \leq R \leq 4$).

Entropies for time-frequency domain analysis

Most of the nonlinear measures in CEPS listed so far are appropriate for time series data. Two further methods are now considered, suited to frequency – or 'time-frequency' – data.

Spectral Entropy (SpEn)

SpEn, in contrast to the nonlinear measures of complexity and entropy included so far, is a linear (Li *et al.* 2008b) frequency – or 'time-frequency' (Liang *et al.* 2015) – method, used primarily in EEG research, and usually based on SE, as Shannon SpEn (SSE). For their work with MEG, Roberto Hornero's group at the University of Valladolid also derived versions of SpEn based on Rényi and Tsallis entropies (RSE and TSE) (Poza *et al.* 2007; Bruña *et a.* 2010). SSE has also been used with RRi data (Thuraisingham 2016). Multiscale versions of SSE exist and have been used with HRV data (Humeau-Heurtier *et al.* 2016).

As Pincus *et al*. observed thirty years ago, a wider, more broadband spectrum (i.e. with greater 'spectral reserve') corresponds to greater values of ApEn (Pincus *et al.* 1991b). SpEn describes the degree of skewness in a frequency distribution (Liang *et al.* 2015): a more uniform (i.e. flatter) spectral distribution results in greater SpEn, whereas narrower spectral

peaks are assessed as less complex (Mao *et al.* 2018). Contributions from any particular frequency range can be explicitly separated (Liang *et al.* 2015).

SpEn may be derived from time series data by first 'symbolising' the data, as outlined above under SE. The more usual strategy, and the one to be implemented in CEPS, is to subject the time series (rather than symbolised) data to a Fourier or other transform.[77] The resulting PSD (whether from FFT or other, more sophisticated methods) is then normalised with respect to the total power, yielding a 'probability density function; (PDF) (Rezek & Roberts 1998). SpEn is then computed from this, using SE, RE or TE (Poza *et al.* 2008; Thuraisingham 2016). There is also scope for computing SpEn using other appropriate entropies – perhaps PE, FE, SlopeEn or BE.

Data requirements

SpEn can be used with very short samples, such as 40 beats in the ECG (Thuraisingham 2016) but increases with sample/window length used (Anier *et al.* 2004). Sampling frequency is crucial: a higher sampling rate will increase SpEn estimates; temporal smoothing, in contrast, will decrease SpEn (Rezek & Roberts 1998). SpEn may be relatively insensitive to high frequency components in filtered bands (Ferenets *et al.* 2006). The method to be implemented here, based on FFT rather than a more sophisticated method, requires time series data that is both approximately stationary and linear.

If your time-series data has already been transformed so that it is in time-frequency format and the different frequency components are known, then SE, RE or TE can be used directly on the transformed data.

Parameter setting

Order q

For RSE and TSE, *q* was set as 3.5 and 2, respectively, in one MEG study (Bruña *et al.* 2010).

Expected values – some examples

[77] Simply using the FFT may not be appropriate for nonstationary or rapidly changing signals; a kernel-based method may be more suitable (Giannakakis et al. 2009). Wavelet, multitaper or Hilbert-Huang time/frequency decomposition methods can be used instead of FFT or one of its derivatives. Hilbert-Huang spectral entropy removes the requirements for stationarity and linearity, for example (Huang *et al.* 1998; Humeau-Heurtier *et al.* 2016). Hilbert–Huang spectral entropy exhibited greater resistance to noise in the EEG signal than the usual Fourier-based time–frequency balanced SpEn (Li *et al.* 2008b).

SpEn of the EEG may not show good reproducibility (Van Albada *et al.* 2007).

The use of plots

No particularly useful plots were found in a random selection of studies.

Differential Entropy (DiffEn)[78]

As already mentioned, SE is not really appropriate for continuous data, for which Differential entropy was proposed as an equivalent measure. There are several subtypes of differential entropy, for continuous data distributed in different ways (Lazo & Rathie 1978), but it can only be calculated approximately (Papadakis *et al.* 2009). One algorithm for Differential entropy, the 'Gait Evaluation Differential Entropy Method' (GEDEM), used mostly in gait studies, therefore includes a 'quantization factor' δ (Papadakis *et al.* 2009). GEDEM results are invariant to δ, so that unlike many entropy measures, setting a parameter is not required (Tsivgoulis *et al.* 2009).

Another algorithm, used primarily in the analysis of EEG data, does not include the factor δ (Duan *et al.* 2013; Shi *et al.* 2013). However, this second algorithm is only applicable with any accuracy to data that is normally distributed (i.e. with a Gaussian distribution). Shi *et al.* (2013) found that although their EEG data did not in general follow any particular distribution, when bandpass-filtered into 2 Hz bins (≤ 44 Hz), more than 90% of their 2 Hz data segments were in fact normally distributed (tested using a one sample Kolmogorov-Smirnov test). As a result, for Gaussian EEG data in such binned segments, Differential entropy $h_i(X)$ for each bin i becomes simply (as in Lazo & Rathie 1978):

$$h_i(X) = \log(2\pi e\sigma_i^2)/2 \quad , \qquad (1)$$

where σ_i is the standard deviation of the signal X in that bin and π and e are the usual constants.

A number of EEG studies have used this method to estimate Differential entropy, although with broader frequency bands and without mentioning whether data in these

[78] Not to be confused with Diffusion entropy (here abbreviated as DnEn).

bands was in fact properly tested for normality of distribution (Peng *et al.* 2014; Zhuang *et al.* 2017; Chen *et al.* 2019; Liu *et al.* 2020; Zhang *et al.* 2020), both issues which potentially limit the impact of their findings. Other less straightforward definitions and algorithms for Differential entropy can also be found in the EEG literature.

Like SpEn, Differential entropy is low if there is a predominant frequency component, high if there are more frequency components with relatively high power (Tsivgoulis *et al.* 2009). Differential entropy has been computed for EEG data segments of 600 (Zhang *et al.* 2020), 4,000 (Duan *et al.* 2013), 7,680 (Zhuang *et al.* 2017), 12,000 (Liu *et al.* 2020) and 48,000 points (Chen *et al.* 2019).

Maximum Entropy Spectral Analysis (MESA)

Maximum entropy spectral analysis (MESA) is a long-established method of estimating non-obvious periodicities in time-series data, originally developed by Burg in the 1960s (Burg 1967) in response to shortcomings in Fourier analysis, including the constraints imposed by using the Fast Fourier transform (FFT). It is particularly useful in short, noisy time series, as it estimates phase based on the entire signal rather than just one identifiable phase marker (Dowse 2007). A useful review is provided by Dowse (2013), who provided the MATLAB code for use in CEPS.

Other measures planned for future inclusion

Clearly, the universe of complexity and entropy measures has been expanding exponentially in recent years, although whether this expansion will be followed by a contraction as global conditions become more uncertain is itself very unclear.

Given favourable conditions, in CEPS we plan to include a number of other measures not described here, such as local dimension (D_l), persistence ($1/\theta$) and co-recurrence (α) (Carbone *et al*. 2022), Tangle (Moulder *et al*. 2022) and wavelet entropy, WE (Rosso *et al*. 2001).

REFERENCES

Abásolo D, Hornero R, Escudero J *et al*. (2008). A study on the possible usefulness of detrended fluctuation analysis of the electroencephalogram background activity in Alzheimer's disease. IEEE Transactions on Bio-medical Engineering 55(9), 2171-2179.

Abásolo D, Hornero R, Espino P *et al*. (2007). Electroencephalogram background activity characterization with approximate entropy and auto mutual information in Alzheimer's disease patients. Conference Proceedings, IEEE Engineering in Medicine and Biology Society 2007, 6192-6195.

Abásolo D, Hornero R, Gómez C *et al*. (2006). Analysis of EEG background activity in Alzheimer's disease patients with Lempel-Ziv complexity and central tendency measure. Medical Engineering and Physics 28(4), 315-322.

Abdennaji I, Zaied M, Girault JM. (2021). Prediction of protein structural class based on symmetrical recurrence quantification analysis. Computational Biology and Chemistry92:107450.

Abdul Sathar EI, Nair R D. (2021). On dynamic survival extropy. Communications in Statistics-Theory and Methods 50(6), 1295-313.

Abe S, Suzuki N. (2003). Law for the distance between successive earthquakes. Journal of Geophysical Research: Solid Earth 108(B2), 19-1 – 19-4.

Abe S. (2002). Stability of Tsallis entropy and instabilities of Rényi and normalized Tsallis entropies: a basis for q-exponential distributions. Physical Review. E, Statistical, Nonlinear, and Soft Matter Physics 66(4 Pt 2), 046134.

Abney DH, Warlaumont AS, Haussman A *et al*. (2014). Using nonlinear methods to quantify changes in infant limb movements and vocalizations. Frontiers in Psychology 5, 771.

Aboy M, Hornero R, Abásolo D *et al*. (2006). Interpretation of the Lempel-Ziv complexity measure in the context of biomedical signal analysis. IEEE Transactions on Biomedical Engineering 53(11), 2282-2288.

Abrahão FS, Zenil H. (2021). Emergence and algorithmic information dynamics of systems and observers. arXiv preprint arXiv, 2105.14707.

Abubaker HB, Alsafar HS, Jelinek HF *et al*. (2014). Poincaré plot analysis of heart rate variability in diabetic patients in the UAE. 2nd Middle East Conference on Biomedical Engineering, Doha, Qatar, 3 pp.

Accardo A, Affinito M, Carrozzi M *et al*. (1997). Use of the fractal dimension for the analysis of electroencephalographic time series. Biological Cybernetics 77(5), 339-350.

Acharya U R, Chua ECP, Faust O *et al*. (2011). Automated detection of sleep apnea from electrocardiogram signals using nonlinear parameters. Physiological Measurement 32(3), 287-303.

Acharya U R, Kannathal N, Krishnan SM. (2004). Comprehensive analysis of cardiac health using heart rate signals. Physiological Measurement 25(5), 1139-1151.

Adeli H, Ghosh-Dastidar S, Dadmehr N. (2008). A spatio-temporal wavelet-chaos methodology for EEG-based diagnosis of Alzheimer's disease. Neuroscience Letters 444(2), 190-194.

Ahmad RF, Malik AS, Amin HU *et al.* (2015). Nonlinear features-based classification of active and resting states of human brain using EEG. In: IEEE International Conference on Signal and Image Processing Applications (ICSIPA) 2015 Oct 19 (pp. 264-268). IEEE.

Ahmadi B, Amirfattahi R. (2010). Comparison of correlation dimension and fractal dimension in estimating BIS index. Wireless Sensor Network 2(1), 67-73.

Ahmadlou M, Adeli H, Adeli A. (2011). Fractality and a wavelet-chaos-methodology for EEG-based diagnosis of Alzheimer disease. Alzheimer Disease and Associated Disorders 25(1), 85-92.

Ahmadlou M, Adeli H, Adeli A. (2012). Fractality analysis of frontal brain in major depressive disorder. International Journal of Psychophysiology 85(2), 206-11.

Ahmadlou M, Adeli H, Adeli A. (2011). Fractality and a wavelet-chaos-methodology for EEG-based diagnosis of Alzheimer disease. Alzheimer Disease & Associated Disorders 25(1), 85-92.

Ahmed MU, Chanwimalueang T,Thayyil S *et al*. (2017). A multivariate multiscale fuzzy entropy algorithm with application to uterine EMG complexity analysis. Entropy 19(1), 2, 1-18.

Aittokallio T, Gyllenberg M, Hietarinta J *et al*. (1999). Improving the false nearest neighbors method with graphical analysis. Physical Review. E, Statistical Physics, Plasmas, Fluids, and Related Interdisciplinary Topics 60(1), 416-421.

Akar SA, Kara S, Agambayev S, Bilgiç V. (2015). Nonlinear analysis of EEGs of patients with major depression during different emotional states. Computers in Biology and Medicine 67, 49-60.

Akbarian B, Erfanian A. (2018). Automatic seizure detection based on nonlinear dynamical analysis of EEG signals and mutual information. Basic and Clinical Neuroscience 9(1), 227–240.

Akdeniz G. (2017). Complexity analysis of resting-state fMRI in adult patients with attention deficit hyperactivity disorder: brain entropy. Computational Intelligence and Neuroscience 2017, 3091815.

Alberti T, Consolini G, Ditlevsen PD *et al.* (2020). Multiscale measures of phase-space trajectories. Chaos: An Interdisciplinary Journal of Nonlinear Science 30(12), 123116.

Alizadeh Noughabi H, Jarrahiferiz J. (2019). On the estimation of extropy. Journal of Nonparametric Statistics 1(1), 88-99. Taylor & Francis

Al-Labadi L, Berry S. (2022). Bayesian estimation of extropy and goodness of fit tests. Journal of Applied Statistics 49(2), 357-70. Allan DW. (1966). Statistics of atomic frequency standards. Proceedings of the IEEE 54(2), 221-230.

Allegrini P, Grigolini P, Hamilton P *et al*. (2002). Memory beyond memory in heart beating, a sign of a healthy physiological condition. Physical Review. E, Statistical, Nonlinear, and Soft Matter Physics 65(4 Pt 1), 041926.

Allegrini P, Paradisi P, Menicucci D. (2010). Fractal complexity in spontaneous EEG metastable-state transitions: new vistas on integrated neural dynamics. Frontiers in Physiology 1,128, 1-9.

Al-nuaimi AH, Jammeh E, Sun LF *et al*. (2015). Tsallis entropy as a biomarker for detection of Alzheimer's disease. 37th Annual International Conference of the IEEE Engineering in Medicine and Biology Society (EMBC) 2015, 4166-4169.

Alvarez-Ramirez J, Echeverria JC, Meraz M *et al.* (2017)., Rodriguez E. Asymmetric acceleration/deceleration dynamics in heart rate variability. Physica A: Statistical Mechanics and its Applications 479, 213-224. 2017

Alves MA, Garner DM, do Amaral JAT. (2019). The effects of musical auditory stimulation on heart rate autonomic responses to driving: a prospective randomized case-control pilot study. Complementary Therapies in Medicine 46, 158-164.

Amano M, Oida E, Moritani T. (2005). Age-associated alteration of sympatho-vagal balance in a female population assessed through the tone-entropy analysis. European Journal of Applied Physiology 94(5-6), 602-610.

Amano M, Oida E, Moritani T. (2006). A comparative scale of autonomic function with age through the tone-entropy analysis on heart period variation. European Journal of Applied Physiology 98(3), 276-283.

Amato F, Laib M, Guignard F, et al. (2020). Analysis of air pollution time series using complexity-invariant distance and information measures. Physica A: Statistical Mechanics and its Applications 547, 124391.

Amezquita-Sanchez JP, Mammone N, Morabito FC *et al*. (2019). A novel methodology for automated differential diagnosis of mild cognitive impairment and the Alzheimer's disease using EEG signals. Journal of Neuroscience Methods 322, 88-95.

Amigó JM, Balogh SG, Hernández S. (2018). A brief review of generalized entropies. Entropy 20, 813, 1-21.

Amigó JM, Kennel MB, Kocarev L. (2005). The permutation entropy rate equals the metric entropy rate for ergodic information sources and ergodic dynamical systems. Physica D: Nonlinear Phenomena 210(1-2), 77–95.

Amigó JM, Zambrano S, Sanjuán MAF. (2008). Combinatorial detection of determinism in noisy time series. European Physics Letters 83, 60005.

Amin HU, Malik AS, Kamel N *et al.* (2016). A novel approach based on data redundancy for feature extraction of EEG signals. Brain topography 29(2), 207-217.

Amin HU, Ousta F, Yusoff MZ *et al*. (2021). Modulation of cortical activity in response to learning and long-term memory retrieval of 2D verses stereoscopic 3D educational contents: Evidence from an EEG study. Computers in Human Behavior 114, 106526.

Anier A, Lipping T, Melto S *et al*. (2004). Higuchi fractal dimension and spectral entropy as measures of depth of sedation in intensive care unit. Conference Proceedings, IEEE Engineering in Medicine and Biology Society 2006, 526-529.

Antonio AMS, Garner DM, Raimundo RD (2016). Chaotic analysis of heart rate dynamics after an exercise with flexible pole. Medical Express 3(5), M160505.

Ao D, Sun R, Song R. (2013). Comparison of complexity of EMG signals between a normal subject and a patient after stroke – a case study. Annual International Conference of the IEEE Engineering in Medicine and Biology Society 2013, 4965-4968.

Arpaia P, Azzopardi G, Blanc F *et al.* (2021). Machine learning for beam dynamics studies at the CERN Large Hadron Collider. Nuclear Instruments and Methods in Physics Research, Section A: Accelerators, Spectrometers, Detectors and Associated Equipment 985, 164652.

Artan NS. (2016). EEG analysis via multiscale Lempel-Ziv complexity for seizure detection. Annual International Conference of the IEEE Engineering in Medicine and Biology Society 2016, 4535-4538.

Arunachalam SP, Kapa S, Mulpuru SK *et al*. (2017). Rotor pivot point identification using recurrence period density entropy. 54th Annual Rocky Mountain Bioengineering Symposium, RMBS 2017 and 54th International ISA Biomedical Sciences Instrumentation Symposium 2017, n.p.

Aschero G, Gizdulich P. (2010). Denoising of surface EMG with a modified Wiener filtering approach. Journal of Electromyography and Kinesioliology 20(2), 366-373.

Aung ST, Wongsawat Y. (2020). Modified-distribution entropy as the features for the detection of epileptic seizures. Frontiers in Physiology 11, 607, 1-10.

Avramidis K, Zlatintsi A, Garoufis C *et al*. (2021). Multiscale Fractal Analysis on EEG Signals for Music-Induced Emotion Recognition. In: 29th European Signal Processing Conference (EUSIPCO) 2021 Aug 23 (pp. 1316-1320). IEEE.

Awan I, Aziz W, Shah IH *et al*. (2018). Studying the dynamics of interbeat interval time series of healthy and congestive heart failure subjects using scale based symbolic entropy analysis. PLoS One 13(5), e0196823.

Azami H, Escudero J. (2015). Matlab codes for "Improved Multiscale Permutation Entropy for Biomedical Signal Analysis: Interpretation and Application to Electroencephalogram Recordings". University of Edinburgh, School of Engineering, Institute for Digital Communications (https://doi.org/10.7488/ds/273) [Retrieved August 9, 2020].

Azami H, Escudero J. (2016a). Improved multiscale permutation entropy for biomedical signal analysis: interpretation and application to electroencephalogram recordings. Biomedical Signal Processing and Control 23, 28-41.

Azami H, Escudero J. (2016b). Amplitude-aware permutation entropy: illustration in spike detection and signal segmentation. Computer Methods and Programs in Biomedicine 128, 40-51.

Azami H, Escudero J. (2016c). Matlab codes for "Refined Multiscale Fuzzy Entropy based on Standard Deviation for Biomedical Signal Analysis". University of Edinburgh, School of Engineering, Institute for Digital Communications (https://doi.org/10.7488/ds/1477) [Retrieved August 10, 2020].

Azami H, Escudero J. (2017c). Refined composite multivariate generalized multiscale fuzzy entropy: a tool for complexity analysis of multichannel signals. Physica A: Statistical Mechanics and its Applications 465, 261-276.

Azami H, Escudero J. (2018). Amplitude- and fluctuation-based dispersion entropy. Entropy 20, 210.

Azami H, Fernández A, Escudero J. (2017a). Refined multiscale fuzzy entropy based on standard deviation for biomedical signal analysis. Medical and Biological Engineering and Computing 55(11), 2037–2052.

Azami H, Hassanpour H, Escudero J *et al*. (2015). An intelligent approach for variable size segmentation of non-stationary signals. Journal of Advanced Research 6(5), 687-698.

Azami H, Li P, Arnold SE *et al*. (2019). Fuzzy entropy metrics for the analysis of biomedical signals: assessment and comparison. IEEE Access 7, 04833–104847.

Azami H, Rostaghi M, Abásolo D. *et al*. (2017b). Refined composite multiscale dispersion entropy and its application to biomedical signals. IEEE Transactions on Biomedical Engineering 64(12), 2872-2879.

Azami H, Rostaghi M, Fernandez A *et al*. (2016a). Dispersion entropy for the analysis of resting-state MEG regularity in Alzheimer's disease. Conference Proceedings, IEEE Engineering in Medicine and Biology Society 2016, 6417-6420.

Aziz W, Arif M. (2006). Complexity analysis of stride interval time series by threshold dependent symbolic entropy. European Journal of Applied Physiology 98(1), 30-40.

Babloyantz A, Destexhe A. (1988). Is the normal heart a periodic oscillator? Biological Cybernetics 58(3), 203-211.

Bahari F, Janghorbani A. (2013). EEG-based emotion recognition using recurrence plot analysis and *k* nearest neighbor classifier. In: 20th Iranian Conference on Biomedical Engineering (ICBME) 2013 Dec 18 (pp. 228-233). IEEE.

Bai Y, Li XL, Liang ZH. (2019). Nonlinear neural dynamics. In: EEG Signal Processing and Feature Extraction 2019 (pp. 215-240). Springer, Singapore.

Bai Y, Liang ZH, Li XL *et al*.. Permutation Lempel–Ziv complexity measure of electroencephalogram in GABAergic anaesthetics. Physiological Measurement. 36(12), 2483.

Bai Y, Liang ZH, Li XL. (2015). A permutation Lempel-Ziv complexity measure for EEG analysis. Biomedical Signal Processing and Control 19, 102-14.

Balakrishnan N, Buono F, Longobardi M. (2022). On Tsallis extropy with an application to pattern recognition. Statistics & Probability Letters 180, 109241.

Balakrishnan N, Buono F, Longobardi M. (2020). On weighted extropies. Communications in Statistics-Theory and Methods. 1-31. ArXiv:2008.07826v1.

Balasubramanian K, Nagaraj N. (2016). Aging and cardiovascular complexity: effect of the length of RR tachograms. PeerJ 4, e2755.

Balasubramanian K, Nair S, Nagaraj N. (2015). Classification of periodic, chaotic and random sequences using approximate entropy and Lempel–Ziv complexity measures. Pramana – Journal of Physics 84(3), 365–372.

Bandt C, Pompe B. (2002). Permutation entropy: a natural complexity measure for time series. Physical Review Letters 88(17), 174102, 1-5.

Bandt C, Pompe B. (2012) Permutation entropy: a natural complexity measure for time series. Physical Review Letters 88(17), 174102.

Bandt C, Shiha F. (2007). Order patterns in time series. Journal of Time Series Analysis 28(5), 646–665.

Bansal S, Gupta N. (2020). Weighted extropies and past extropy of order statistics and k-record values. Communications in Statistics-Theory and Methods 1-24. https://doi.org/10.1080/03610926.2020.1853773.

Baranger M. (2000). Complexity, chaos, and entropy. Cambridge, MA: New England Complex Systems Institute. (https://necsi.edu/chaos-complexity-and-entropy) [Retrieved July 26, 2020].

Başar E, Güntekin B. (2007). A breakthrough in neuroscience needs a "Nebulous Cartesian System". Oscillations, quantum dynamics and chaos in the brain and vegetative system. International Journal of Psychophysiology 64(1), 108-122.

Batista GE, Keogh EJ, Tataw OM *et al*. (2014).. CID: an efficient complexity-invariant distance for time series. Data Mining and Knowledge Discovery 28(3), 634-69.

Batista GE, Wang X, Keogh EJ. (2011). A complexity-invariant distance measure for time series. In: Proceedings of the 2011 SIAM international conference on data mining 2011 Apr 28 (pp. 699-710). Society for Industrial and Applied Mathematics.

Batra L, Taneja HC. (2020). Evaluating volatile stock markets using information theoretic measures. Physica A: Statistical Mechanics and its Applications 537, 122711. Elsevier

Batra L, Taneja HC. Renyi extropy: A generalization of information extropy. Delhi Technological University, India (Unpublished?).

Bauer A, Kantelhardt JW, Barthel P *et al.* (2006). Deceleration capacity of heart rate as a predictor of mortality after myocardial infarction: cohort study. The Lancet 367(9523), 1674-1681.

Baumert M, Baier V, Haueisen J *et al*. (2004). Forecasting of life threatening arrhythmias using the compression entropy of heart rate. Methods of Information in Medicine 43(2), 202-206.

Bawa P, Kadyan V, Mantri A *et al.* (2021). Optimal Fractal Feature Selection and Estimation for Speech Recognition Under Mismatched Conditions. In: Deep Learning Approaches for Spoken and Natural Language Processing 2021 (pp. 41-53). Springer, Cham. Eds: Virender Kadyan, Amitoj Singh, Mohit Mittal, Laith Abualigah]

Becerra A, de la Rosa JI, González E *et al*. (2018). Training deep neural networks with non-uniform frame-level cost function for automatic speech recognition. Multimedia Tools and Applications 77(20), 27231-27267.

Becker K, Schneider G, Eder M *et al*. (2010). Anaesthesia monitoring by recurrence quantification analysis of EEG data. PLoS One 5(1), e8876.

Bein B. (2006). Entropy. Best Practice and Research. Clinical Anaesthesiology 20(1), 101-109.

Belov DI, Armstrong RD. (2011). Distributions of the Kullback–Leibler divergence with applications. British Journal of Mathematical and Statistical Psychology (2011), 64(2), 291–309.

Bentley JL. (1975). Multidimensional binary search trees used for associative searching. Communications of the ACM (Association for Computing Machionery) 18(9), 509-517.

Bernaola-Galván PA, Gómez-Extremera M, Romance AR, *et al*. (2017). Correlations in magnitude series to assess nonlinearities: application to multifractal models and heartbeat fluctuations, Physical Review. E, Statistical, Nonlinear, and Soft Matter Physics 96 (3-1), 032218, 1-11.

Bettermann H, Amponsah D, Cysarz D *et al*. (1999). Musical rhythms in heart period dynamics: a cross-cultural and interdisciplinary approach to cardiac rhythms. American Journal of Physiology 277(5), H1762-1770.

Bezerianos A, Tong S, Thakor N. (2003). Time-dependent entropy estimation of EEG rhythm changes following brain ischemia. Annals of Biomedical Engineering 31(2), 221-232.

Bhaduri A, Nowakowski TJ, Pollen AA. (2018). Identification of cell types in a mouse brain single-cell atlas using low sampling coverage. BMC Biology 16(1), 113.

Bhagat M, Bhushan C, Saha G *et al*. (2009). Investigating neuromagnetic brain responses against chromatic flickering stimuli by wavelet entropies. PLoS One 4(9), e7173.

Bhavsar B,-, Helian N, Sun Y *et al*. (2018). Efficient methods for calculating sample entropy in time series data analysis. Procedia Computer Science 145, 97–104.

Billman GE. (2013). The LF/HF ratio does not accurately measure cardiac sympatho-vagal balance. Frontiers in Physiology 4, 26

Billois R, Porée F, Beuchée A *et al.* (2012). Interest of RR deceleration for diagnosis of late onset sepsis. In: Computing in Cardiology 2012 Sep 9 (pp. 633-636). IEEE.

Blanc J, Ponchon P, D Laude D *et al*. (1999). Blood pressure variability in established L-NAME hypertension in rats. Journal of Hypertension 17(11), 1527-1534.

Bodduluri S, Puliyakote ASK, Gerard SE *et al*. (2018). Airway fractal dimension predicts respiratory morbidity and mortality in COPD. Journal of Clinical Investigation 128(12), 5374-5382.

Bogaert C, Beckers F, Ramaekers D *et al*. (2001). Analysis of heart rate variability with correlation dimension method in a normal population and in heart transplant patients. Autonomic Neuroscience 90(1-2), 142-147.

Bolaños JD, Vallverdu M, Caminal P. (2016). Assessment of sedation-analgesia by means of Poincaré analysis of the electroencephalogram. Conference Proceedings of the IEEE Engineering in Medicine and Biology Society 2016, 6425-6428.

Bolea J, Bailón R, Pueyo E. (2018). On the standardization of approximate entropy: multidimensional approximate entropy index evaluated on short-term HRV time series. Complexity. 2018 Jan 1;2018.

Bollt EM, Skufca JD, McGregor SJ. (2009). Control entropy: a complexity measure for nonstationary signals. Mathematical Biosciences and Engineering 6(1), 1-25.

Boonyakitanont P, Lek-Uthai A, Chomtho K *et al.* (2020). A review of feature extraction and performance evaluation in epileptic seizure detection using EEG. Biomedical Signal Processing and Control 57, 101702.

Boostani R, Sadatnezhad K, Sabeti M. (2009). An efficient classifier to diagnose of schizophrenia based on the EEG signals. Expert Systems with Applications 36(3), 6492-6499.

Borg F. (2001). Nonlinear Time Series Analysis. Chydenius Institute. Kokkola. (http://www.netti.fi/~borgbros/nonlin/review1.pdf) [Retrieved August 6, 2020].

Borges JB, Ramos HS, Mini RA *et al.* (2019). Learning and distinguishing time series dynamics via ordinal patterns transition graphs. Applied Mathematics and Computation 362, 124554.

Boruah AN, Biswas SK, Bandyonadhyay S *et al* (2020). An expert system for identification of key factors of Parkinson's disease: B-TDS-PD. In: IEEE India Council International Subsections Conference (INDISCON) 2020 Oct 3 (pp. 37-42).

Bose R, Chouhan S. (2011). Alternate measure of information useful for DNA sequences. Physical Review. E, Statistical, Nonlinear, and Soft Matter Physics 83(5 Pt 1), 051918, 1-6.

Bošković A, T. Lončar-Turukalo T, Japundžić-Žigon N *et al*. (2011). The flip-flop effect in entropy estimation. IEEE International Symposium on Intelligent Systems and Informatics (SISY 2011), Subotica, Serbia, 9, 227-230.

Bosyk GM, Portesi M, Plastino A. (2012). Collision entropy and optimal uncertainty. Physical Review A, 85(1), 012108, 1-7.

Bottaro M, Abid NUH, El-Azizi I *et al*. (2020). Skin temperature variability is an independent predictor of survival in patients with cirrhosis. Physiological Reports 8(12), e14452.

Brennan M, Palaniswami M, Kamen P. (2001). Do existing measures of Poincaré plot geometry reflect nonlinear features of heart rate variability? IEEE Transactions on Bio-medical Engineering 48(11), 1342-1347.

Brindle RC, Ginty AT, Phillips AC *et al*. (2016) Heart rate complexity: A novel approach to assessing cardiac stress reactivity. Psychophysiology 53(4), 465-472.

Bruhn J, Lehmann LE, Röpcke H *et al*. (2001). Shannon entropy applied to the measurement of the electroencephalographic effects of desflurane. Anesthesiology 95(1), 30-35.

Bruña R, Poza J, Gómez C *et al*. (2010). Analysis of spontaneous MEG activity in mild cognitive impairment using spectral entropies and disequilibrium measures. Conference Proceedings of the IEEE Engineering in Medicine and Biology Society 2010, 6296-6299.

Bryce RM, Sprague KB. (2012). Revisiting detrended fluctuation analysis. Scientific Reports 2, 315.

Buono F, Kamari O, Longobardi M. (2021). Interval extropy and weighted interval extropy. Ricerche di Matematica. 2021 Dec 2, 1-6.

Buono F, Longobardi M. (2020). A dual measure of uncertainty: The Deng extropy. Entropy 22(5), 582.

Burg JP. (1967). Maximum entropy spectral analysis. Proceedings, 37th Annual International Meeting, Society of Exploration Geophysics. Oklahoma City, OK, Oct 31, 1967.

Burns T, Rajan R. (2019). A mathematical approach to correlating objective spectro-temporal features of non-linguistic sounds with their subjective perceptions in humans. Frontiers in Neuroscience 13, 794,1-14.

Burrello A, Schindler K, Benini L *et al*. (2020). Hyperdimensional computing with local binary patterns: one-shot learning of seizure onset and identification of ictogenic brain regions using short-time iEEG recordings. IEEE Transactions on Biomedical Engineering 67(2), 601-613.

Busha BF. (2010). The effect of wavelet-based filtering and data set length on the fractal scaling of cardiorespiratory variability. Conference Proceedings of the IEEE Engineering in Medicine and Biology Society 2010, 4546-4549.

Byun S, Kim AY, Jang EH *et al*. (2019). Entropy analysis of heart rate variability and its application to recognize major depressive disorder: A pilot study. Technology and Health Care 27(S1), 407-424.

Cai SM, Zhou PL, Yang HJ. *Et al*. (2007). Diffusion entropy analysis on the stride interval fluctuation of human gait. Physica A: Statistical Mechanics and its Applications 375(2), 687-692.

Cai ZJ, Sun J. (2009). Convergence of C0 complexity. International Journal of Bifurcation and Chaos. 19(3), 977-992.

Calderón-Juárez M, González-Gómez GH *et al*. (2022). Recurrence quantitative analysis of wavelet-based surrogate data for nonlinearity testing in heart rate variability. Frontiers in Physiology 23,1-17.

Caminal P, Mateu J, Vallverdú M *et al*. (2004). Estimating respiratory pattern variability by symbolic dynamics. Methods Information in Medicine 43(1), 22-25.

Campbell DK. (1987). Nonlinear science – from paradigms to practicalities. Los Alamos Science (15), 218-262.

Cao LY, Soofi AS. (1999). Nonlinear deterministic forecasting of daily dollar exchange rates. International Journal of Forecasting 15(4), 421–430.

Cao LY. (1997). Practical method for determining the minimum embedding dimension of a scalar time series. Physica D: Nonlinear Phenomena 110(1-2), 43-50.

Cao Y, Cai ZJ, Shen EH *et al*.(2007). Quantitative analysis of brain optical images with 2D C0 complexity measure. Journal of neuroscience methods. 159(1), 181-6.

Cao YZ, Cai LH, Wang J *et al*. (2015). Characterization of complexity in the electroencephalograph activity of Alzheimer's disease based on fuzzy entropy. Chaos 25(8), 083116, 1-12.

Capurro A, Diambra L, Lorenzo D *et al*. (1999). Human brain dynamics: the analysis of EEG signals with Tsallis information measure. Physica A: Statistical Mechanics and its Applications 265(1-2), 235-254.

Carbone F, Alberti T, Faranda D *et al*. (2022). Local dimensionality and inverse persistence analysis of atmospheric turbulence in the stable boundary layer. Physical Review E. hal-03879836.

Caronni A, Gervasoni E, Ferrarin M *et al*. (2020). Local dynamic stability of gait in people with early multiple sclerosis and no-to-mild neurological impairment. IEEE Transactions on Neural Systems and Rehabilitation Engineering 28(6), 1389-1396.

Carpena P, Gómez-Extremera M, Carretero-Campos C *et al*. (2017). Spurious results of fluctuation analysis techniques in magnitude and sign correlations. Entropy 19(6), 261.

Carvajal R, Wessel N, Vallverdú M *et al*. (2005). Correlation dimension analysis of heart rate variability in patients with dilated cardiomyopathy. Computer Methods and Programs in Biomedicine 78(2), 133-140.

Carvalho P, Gilt P, Henriques J *et al*. (2005). Low complexity algorithm for heart sound segmentation using the variance fractal dimension. In IEEE International Workshop on Intelligent Signal Processing, 2005. 2005 Sep 1 (pp. 194-199).

Castiglioni P, Di Rienzo M, Parati G *et al.* (2011). Fractal dimension of mean arterial pressure and heart-rate time series from ambulatory blood pressure monitoring devices. In: Computing in Cardiology 2011 Sep 18 (pp. 593-596). IEEE.

Castiglioni P, Faini A, (2019). A fast DFA algorithm for multifractal multiscale analysis of physiological time series. Frontiers in Physiology 10, 115, 1-18.

Castiglioni P, Faini A, Lombardi C *et al.* (2014c). Characterization of apnea events in sleep breathing disorder by local assessment of the fractal dimension of heart rate. In: 2014 8th Conference of the European Study Group on Cardiovascular Oscillations (ESGCO) 2014 May 25 (pp. 107-108). IEEE.

Castiglioni P, Faini A, Parati G *et al.* 2014b). Fractal analysis of cardiorespiratory signals for sleep stage classification. In: 2014 8th Conference of the European Study Group on Cardiovascular Oscillations (ESGCO) 2014 May 25 (pp. 83-84). IEEE.

Castiglioni P, Lazzeroni D, Brambilla V *et al*. (2017). Multifractal multiscale DFA of cardiovascular time series: differences in complex dynamics of systolic blood pressure, diastolic blood pressure and heart rate. Annual International Conference of the IEEE Engineering in Medicine and Biology Society 2017, 3477-3480.

Castiglioni P, Merati G, Faini A. (2014a). Assessing the convolutedness of multivariate physiological time series. In: 2014 36th Annual International Conference of the IEEE Engineering in Medicine and Biology Society 2014 Aug 26 (pp. 6024-6027). IEEE

Castiglioni P, Merati G, Gianfranco ParatiG *et al*. (2019). Decomposing the complexity of heart-rate variability by the multifractal-multiscale approach to detrended fluctuation analysis: an application to low-level spinal cord injury. Physiological Measurement 40(8), 084003.

Castiglioni P. (2010). What is wrong in Katz's method? Comments on: "A note on fractal dimensions of biomedical waveforms". Computers in Biology and Medicine 40(11-12), 950-952.

Castiglioni P, Piskorski J, Kośmider M,*et al.* (2013). Assessing sample entropy of physiological signals by the norm component matrix algorithm: Application on muscular signals during isometric contraction. In: 35th Annual International Conference of the IEEE Engineering in Medicine and Biology Society (EMBC) (pp. 5053-5056).

Cerquera A, Vollebregt MA, Arns M. (2018). Nonlinear recurrent dynamics and long-term nonstationarities in EEG alpha cortical activity: implications for choosing adequate segment length in nonlinear EEG analyses. Clinical EEG and Neuroscience 49(2), 71-78.

Cerrada M, Macancela J-C, Cabrera D *et al*. (2020). Reciprocating compressor multi-fault classification using symbolic dynamics and complex correlation measure. Applied Sciences 10(7), 2512, 1-21.

Chang YC, Wu HT, Chen HR *et al*. (2014). Application of a modified entropy computational method in assessing the complexity of pulse wave velocity signals in healthy and diabetic subjects. Entropy 16(7), 4032–4043.

Chanwimalueang T, Mandic DP. (2017. Cosine similarity entropy: self-correlation-based complexity analysis of dynamical systems. Entropy 19(12), 652.

Chelidze D. (2017). Reliable estimation of minimum embedding dimension through statistical analysis of nearest neighbors. Journal of Computational and Nonlinear Dynamics 12(5), 051024.

Chen C-H, Huang P-W, Tang S-C *et al*. (2015). Complexity of heart rate variability can predict stroke-in-evolution in acute ischemic stroke patients. Scientific Reports 5, 17552, 1-5.

Chen C-H, Tang S-C, Lee D-Y *et al*. (2018). Impact of supratentorial cerebral hemorrhage on the complexity of heart rate variability in acute stroke. Scientific Reports 8(1), 11473.

Chen DW, Han N, Chen JJ *et al*. (2017). Novel algorithm for measuring the complexity of electroencephalographic signals in emotion recognition. Journal of Medical Imaging and Health Informatics 7(1), 203-10.

Chen DW, Miao R, Yang WQ. (2019). A feature extraction method based on differential entropy and linear discriminant analysis for emotion recognition. Sensors 19(7), 1631.

Chen F, Gu FJ, Xu JH *et al.* (1998). A new measurement of complexity for studying EEG mutual information. Shengwu Wuli Xuebao 14(3), 508-12.

Chen F, Xu JH, Gu FJ *et al*. (2000). Dynamic process of information transmission complexity in human brains. Biological cybernetics 83(4), 355-66.

Chen LL, Zou JZ, Zhang J. (2012). Dynamic feature extraction of epileptic EEG using recurrence quantification analysis. Proceedings of the 10th World Congress on Intelligent Control and Automation, Beijing, China, 10, 5019-5022.

Chen WT, Wang ZZ, Xie HB *et al*. (2007). Characterization of surface EMG signal based on fuzzy entropy. IEEE Transactions on Neural Systems and Rehabilitation Engineering 15(2), 266-272.

Chen WT, Zhuang J, Yu WX *et al*. (2009). Measuring complexity using FuzzyEn, ApEn, and SampEn. Medical Engineering and Physics 31(1), 61-68.

Chen Y, Yang H. (2012). Multiscale recurrence analysis of long-term nonlinear and nonstationary time series Chaos, Solitons and Fractals 45(7), 978–987.

Chen YS, Zhang TB, Zhao WJ *et al*. (2019a). Fault diagnosis of rolling bearing using multiscale amplitude-aware permutation entropy and random forest. Algorithms 12(9), 184, 1-17.

Chen YS, Zhang TB, Zhao WJ *et al*. (2019b). Rotating machinery fault diagnosis based on improved multiscale amplitude-aware permutation entropy and multiclass relevance vector machine. Sensors 19(20), 4542, 1-26.

Chen Z, Li Y, Liang H *et al*. (2018). Hierarchical cosine similarity entropy for feature extraction of ship-radiated noise. Entropy 20(6), 425.

Chiang JY, Huang JW, Lin LY. (2016). Detrended fluctuation analysis of heart rate dynamics is an important prognostic factor in patients with end-stage renal disease receiving peritoneal dialysis. PLoS One 11(2), e0147282.

Chipperfield AJ, Thanaj M, Scorletti E *et al*. (2019). Multi-domain analysis of microvascular flow motion dynamics in NAFLD. Microcirculation 26(5), e12538.

Chiu HC, Ma HP, Lin C *et al*. (2017). Serial heart rhythm complexity changes in patients with anterior wall ST segment elevation myocardial infarction. Scientific Reports 7, 43507, 1-12.

Chladekova L, Czippelova B, Turianikova Z *et al.* (2012). Multiscale time irreversibility of heart rate and blood pressure variability during orthostasis. Physiological measurement 33(10), 1747. 2012

Choi Y-S. (2017). Improved multiscale permutation entropy measure for analysis of brain waves. International Journal of Fuzzy Logic and Intelligent Systems 17(3), 194-201.

Ciccone AB, Siedlik JA, Jill M Wecht JM *et al*. (2017). Reminder: RMSSD and SD1 are identical heart rate variability metrics. Muscle and Nerve 56(4), 674-678.

Cirugeda-Roldán EM, Cuesta-Frau D, Miró-Martínez P *et al*. (2014). A new algorithm for quadratic sample entropy optimization for very short biomedical signals: application to blood pressure records. Computer Methods and Programs in Biomedicine 114(3), 231-239.

Cirugeda-Roldán EM, Molina-Picó A, Cuesta-Frau D *et al*. (2011). Characterization of entropy measures against data loss: application to EEG records. Conference Proceedings of the IEEE Engineering in Medicine and Biology Society 2011, 6110-6113.

Cirugeda-Roldán EM, Molina-Picó A, Cuesta-Frau D *et al*. (2012). Comparative study between Sample Entropy and Detrended Fluctuation Analysis performance on EEG records under data loss. Conference Proceedings of the IEEE Engineering in Medicine and Biology Society 2012, 4233-4236.

Coelho AL, Lima CA. (2014). Assessing fractal dimension methods as feature extractors for EMG signal classification. Engineering Applications of Artificial Intelligence 36, 81-98.

Contreras-Reyes JE, Brito A. (2022). Refined Cross-sample Entropy based on Freedman-Diaconis Rule: Application to Foreign Exchange Time Series. Journal of Applied and Computational Mechanics 8(3 (In Progress)), 1005-13.

Cornforth D, Jelinek HF, Tarvainen M. (2015). A comparison of nonlinear measures for the detection of cardiac autonomic neuropathy from heart rate variability. Entropy 17(3), 1425-1440.

Correia R, Gabriel J, Brás S *et al.* (2014). Development of new research software for real-time raw electroencephalogram analysis. In: IEEE International Symposium on Medical Measurements and Applications (MeMeA) 2014 Jun 11 (pp. 1-5).

Costa M, Ghiran I, Peng C-K *et al*. (2008). Complex dynamics of human red blood cell flickering: alterations with in vivo aging. Physical Review. E. Statistical, Nonlinear, and Soft Matter Physics 78(2 Pt 1), 02090,.1-4.

Costa M, Goldberger AL, Peng C-K. (2002). Multiscale entropy analysis of complex physiologic time series. Physical Review Letters 89(6), 068102.

Costa M, Goldberger AL, Peng C-K. (2005a). Multiscale entropy analysis of biological signals. Physical Review E 71, 021906.

Costa M, Goldberger AL, Peng C-K. (2005b). Broken asymmetry of the human heartbeat: loss of time irreversibility in aging and disease. Physical Review Letters 95(19), 198102.

Costa M, Goldberger AL, Peng C-K. (n.d.). Multiscale entropy analysis (MSE). Physionet (https://archive.physionet.org/physiotools/mse/tutorial/) [Retrieved September 27, 2020].

Costa M, Goldberger AL. (2015). Generalized multiscale entropy analysis: application to quantifying the complex volatility of human heartbeat time series. Entropy 17(3), 1197-1203.

Costa M, Goldberger AL. (n.d.). Generalized multiscale entropy (GMSE) analysis: quantifying the structure of time series' volatility. Physionet

(http://physionet.cps.unizar.es/physiotools/gmse/tutorial/tutorial.pdf) [Retrieved November 14, 2020].

Costa MD, Schnettler WT, Amorim-Costa C *et al*. (2014). Complexity-loss in fetal heart rate dynamics during labor as a potential biomarker of acidemia. Early Human Development 90(1), 67-71.

Cover TM, Thomas JA. (1991). Entropy, relative entropy and mutual information (Ch. 2). In: Elements of Information Theory, NY: John Wiley & Sons, 12-49. (http://www.cs.columbia.edu/~vh/courses/LexicalSemantics/Association/Cover%26Thomas-Ch2.pdf) [Retrieved September 12, 2020].

Crevecoeur F, Bollens B, Detrembleur C *et al*. (2010). Towards a "gold-standard" approach to address the presence of long-range auto-correlation in physiological time series. Journal of Neuroscience Methods 192(1), 163–172.

Crutchfield JP, Young K. Inferring statistical complexity. (1989). Physical Review Letters 63(2), 105.

Cuesta D, Varela M, P Miró P *et al*. (2007). Predicting survival in critical patients by use of body temperature regularity measurement based on approximate entropy. Medical and Biological Engineering and Computing 45(7), 671-678.

Cuesta-Frau D, Miró-Martínez P, Núñez J *et al*. (2017). Noisy EEG signals classification based on entropy metrics. Performance assessment using first and second generation statistics. Computers in Biology and Medicine 87, 141-151.

Cuesta-Frau D, Miró-Martínez P, Oltra-Crespo S *et al*. (2009). Measuring body temperature time series regularity using approximate entropy and sample entropy. Conference Proceedings of the IEEE Engineering in Medicine and Biology Society 2009, 3461-3464.

Cuesta-Frau D, Miró-Martínez P, Oltra-Crespo S *et al*. (2018a). Model selection for body temperature signal classification using both amplitude and ordinality-based entropy measures. Entropy 20, 853.

Cuesta-Frau D, Miró-Martínez P, Oltra-Crespo S *et al*. (2018c). Classification of glucose records from patients at diabetes risk using a combined permutation entropy algorithm. Computer Methods and Programs in Biomedicine 165, 197-204.

Cuesta-Frau D, Murillo-Escobar JP, Orrego DA *et al*. (2019). Embedded dimension and time series length. practical influence on permutation entropy and its applications. Entropy 21(4), 385.

Cuesta-Frau D, Varela-Entrecanales M, Molina-Picó A *et al*. (2018b). Patterns with equal values in permutation entropy: do they really matter for biosignal classification? Complexity 2018, 1324696, 1-15.

Cuesta-Frau D, Vargas B. (2019). Permutation entropy and bubble entropy: possible interactions and synergies between order and sorting relations. Mathematical Biosciences and Engineering 17(2), 1637-1658.

Cuesta-Frau D. (2019a). Permutation entropy: influence of amplitude information on time series classification performance. Mathematical Biosciences and Engineering 16(6), 6842-6857

Cuesta-Frau D. (2019b). Slope entropy: a new time series complexity estimator based on both symbolic patterns and amplitude information. Entropy 21, 1167, 1-22.

Cui Y-J, Chu W-B, Peng Yang P *et al*. (2020). [Effects of total sleep deprivation on attention network conflict and sample entropy analysis of EEG]. Zhongguo Ying Yong Sheng Li Xue Za Zhi 36(2), 111-114.

Cysarz D, Edelhäuser F, Javorka M *et al*. (2015b). A percentile-based coarse graining approach is helpful in symbolizing heart rate variability during graded head-up tilt. Annual International Conference of the IEEE Engineering in Medicine and Biology Society 2015, 286-289.

Cysarz D, Edelhäuser F, Javorka M *et al*. (2018). On the relevance of symbolizing heart rate variability by means of a percentile-based coarse graining approach. Physiological Measurement 39(10), 105010.

Cysarz D, Lange S, Matthiessen PF *et al*. (2007). Regular heartbeat dynamics are associated with cardiac health. American Journal of Physiology. Regulatory, Integrative and Comparative Physiology 292(1), R368-R372.

Cysarz D, Linhard M, Edelhäuser F *et al*. (2013a). Symbolic patterns of heart rate dynamics reflect cardiac autonomic changes during childhood and adolescence. Autonomic Neuroscience 178(1-2), 37-43.

Cysarz D, Porta A, Montano N *et al*. (2013b). Different approaches of symbolic dynamics to quantify heart rate complexity. Annual International Conference of the IEEE Engineering in Medicine and Biology Society 2013, 5041-5044.

Cysarz D, Van Leeuwen P, Edelhäuser F *et al*. (2012). Binary symbolic dynamics classifies heart rate variability patterns linked to autonomic modulations. Computers in Biology and Medicine 42(3), 313-318.

Cysarz D, Van Leeuwen P, F Edelhäuser F *et al*. (2015a). Symbolic transformations of heart rate variability preserve information about cardiac autonomic control. Physiological Measurement 36(4), 643-657.

Czippelova B, Chladekova L, Uhrikova Z *et al*. Time irreversibility of heart rate oscillations in newborns–Does it reflect system nonlinearity?. Biomedical Signal Processing and Control 19, 85-88.

Czippelova B, Chladekova L, Uhrikova Z *et al*. 2014), Is the time irreversibility of heart rate present even in newborns? In: 8th Conference of the European Study Group on Cardiovascular Oscillations (ESGCO) 2014 May 25 (pp. 15-16). IEEE. 2014

D'Alessandro G, Politi A. (1990). Hierarchical approach to complexity with applications to dynamical systems. Physical Review Letters 64(14), 1609-1612.

Dabiré H, Mestivier D, Jarnet J *et al*. (1998). Quantification of sympathetic and parasympathetic tones by nonlinear indexes in normotensive rats. American Journal of Physiology 275(4), H1290-H1297.

Dadok VM, Kirsch HE, Sleigh JW et al. (2014)). A probabilistic framework for a physiological representation of dynamically evolving sleep state. Journal of computational neuroscience 37(1), 105-24.

Dai YM, He JY, Wu Y *et al.* (2019). Generalized entropy plane based on permutation entropy and distribution entropy analysis for complex time series. Physica A: Statistical Mechanics and its Applications 520, 217-31.

Dames KK, Lopes AJ, De Melo PL. (2014). Airflow pattern complexity during resting breathing in patients with COPD: effect of airway obstruction. Respiratory Physiology & Neurobiology. 192, 39-47.

Danielewska ME, Placek MM, Kicińska AK *et al*. (2020). Using the entropy of the corneal pulse signal to distinguish healthy eyes from eyes affected by primary open-angle glaucoma. Physiological Measurement 41(5), 055011, 1-9.

Dash DP, H Kolekar M. (2020). Hidden Markov model based epileptic seizure detection using tunable Q wavelet transform. Journal of Biomedical Research 34(3), 170-179.

de Carvalho JLA, da Rocha AF, de Oliveira Nascimento FA *et al*. (2002). Development of a Matlab software for analysis of heart rate variability. 6th International Conference on Signal Processing (ICSP), 1488-1491.

De Maria B, Dalla Vecchia LA, Maestri R *et al.* (2021). Lack of association between heart period variability asymmetry and respiratory sinus arrhythmia in healthy and chronic heart failure individuals. PloS One 16(2), e0247145. 2021

De Maria B, Dalla Vecchia LA, Parati M *et al*. (2020). Do Respiratory Sinus Arrhythmia and Respiratory Phase Durations Impact Heart Rate Variability Asymmetry in Healthy Subjects? In: 11th Conference of the European Study Group on Cardiovascular Oscillations (ESGCO) 2020 Jul 15 (pp. 1-2). IEEE.

de Vries CF, Staff RT, Gordon D Waiter GD *et al*. (2020). Motion during acquisition is associated with fMRI brain entropy. IEEE Journal of Biomedical and Health Informatics 24(2), 586-593.

Dehkordi P, Garde A, Karlen W *et al*. (2016). Evaluation of cardiac modulation in children in response to apnea/hypopnea using the Phone Oximeter(™). Physiological Measurement 37(2), 187-202.

Deschodt-Arsac V, Blons,E, Gilfriche P. (2020). Entropy in heart rate dynamics reflects how HRV-biofeedback training improves neurovisceral complexity during stress-cognition interactions. Entropy 22(3), 317, 1-13.

Deshmukh V, Bradley E, Garland J *et al*. (2020). Using curvature to select the time lag for delay reconstruction. Chaos 30(6), 063143.

Destexhe A, Sepulchre JA, Babloyantz A. (1988). A comparative study of the experimental quantification of deterministic chaos. Physics Letters A 132(2-3), 101-106.

Dhanka B, Vijayvargiya A, Kumar R *et al.* (2020). A Comparative Assessment of Machine Learning Techniques for Epilepsy Detection using EEG Signal. In IEEE 7th Uttar Pradesh Section International Conference on Electrical, Electronics and Computer Engineering (UPCON) 2020 Nov 27 (pp. 1-6).

Diab A, Falou O, Hassan M *et al*. (2015). Effect of filtering on the classification rate of nonlinear analysis methods applied to uterine EMG signals. Conference Proceedings of the IEEE Engineering in Medicine and Biology Society 2015, 4182-5.

Diaz JM, Mateos DM, Boyallian C. (2017). Complexity-Entropy maps as a tool for the characterization of the clinical electrophysiological evolution of patients under pharmacological treatment with psychotropic drugs. Entropy 19(10), 540.

Diniz RC, Fontenele AMM, Carmo LHAD *et al*. (2016). Quantitative methods in electroencephalography to access therapeutic response. Biomedicine and Pharmacotherapy 81, 182-191.

Dowse HB. (2007). Statistical analysis of biological rhythm data. In: Rosato E. (Ed.). Circadian Rhythms: Methods and protocols. Totowa, NJ: Humana Press, 29-45.

Dowse HB. (2013). Maximum entropy spectral analysis for circadian rhythms: theory, history and practice. Journal of Circadian Rhythms 11(1), 1-9.

Doyle OM, Temko A, Marnane W *et al*. (2010). Heart rate based automatic seizure detection in the newborn. Medical Engineering and Physics 32(8), 829-839.

Du X, Li JH, Dongsheng Xiong DS *et al*. (2020). [Research on electroencephalogram specifics in patients with schizophrenia under cognitive load]. Sheng Wu Yi Xue Gong Cheng Xue Za Zhi 37(1), 45-53.

Duan R-N, Zhu J-Y, Lu B-L. (2013). Differential entropy feature for EEG-based emotion classification. Proceedings of the 2013 6th International IEEE EMBS Conference on Neural Engineering, NER 2013, San Diego, CA NJ, USA. pp. 81–84.

Dubuc B. (1988). On estimating fractal dimension. MSc thesis, Faculty of Graduate Studies and Research, Université de Montréal.

Duckrow RB, Tcheng TK. (2007).Daily variation in an intracranial EEG feature in humans detected by a responsive neurostimulator system. Epilepsia 48(8), 1614-1620.

Dunn L, Kenny J. (2017). A software platform for statistical evaluation of patient respiratory patterns in radiation therapy. Physica Medica 42, 135-140.

Dutta P, Limboo B. (2017). Bell-shaped fuzzy soft sets and their application in medical diagnosis. Fuzzy Information and Engineering 9, 67-91.

Eckmann J-P, Oliffson Kamphorst S, Ruelle D *et al*. (1986). Liapunov exponents from time series. Physical Review A 34(6), 4971-4979.

Eckmann J-P, Oliffson Kamphorst S, Ruelle D. (1987). Recurrence plots of dynamical systems. Europhysics Letters 4(9), 973–977.

Eckmann JP, Ruelle D. (1992). Fundamental limitations for estimating dimensions and Lyapunov exponents in dynamical systems. Physica D: Nonlinear Phenomena. Physica D: Nonlinear Phenomena 56(2-3), 185-187.

Eguiraun H, López-de-Ipiña K, Martinez I. (2014). Application of entropy and fractal dimension analyses to the pattern recognition of contaminated fish responses in aquaculture. Entropy 16(11), 6133-6151.

Ehlers CL, Havstad J, D Prichard D *et al*. (1998). Low doses of ethanol reduce evidence for nonlinear structure in brain activity. Journal of Neuroscience 18(18), 7474-7486.

Elert G. (1998-2016). Measuring chaos: Lyapunov-1. The Chaos Hypertextbook: Mathematics in the age of the computer. (https://hypertextbook.com/chaos/lyapunov-1/) [Retrieved August 3, 2020].

Ellis R. (2008). Non-consummatory Motivations: Extropy and "Life wish" in the Self-organization of Emotion. Theoria et Historia Scientiarum 8(2), 9-48.

Engin M. (2007). Spectral and wavelet based assessment of congestive heart failure patients. Computers in Biology and Medicine 37(6), 820–828

Eroğlu G, Gürkan M, Teber S *et al*. (2020). Changes in EEG complexity with neurofeedback and multi-sensory learning in children with dyslexia: a multiscale entropy analysis. Applied Neuropsychology. Child June, 1-12.

Escudero J, Abásolo D, Hornero R *et al*. (2006). Analysis of electroencephalograms in Alzheimer's disease patients with multiscale entropy. Physiological Measurement 27(11), 1091-1106.

Escudero J, Acar E, Fernández A *et al*. (2015b). Multiscale entropy analysis of resting-state magnetoencephalogram with tensor factorisations in Alzheimer's disease. Brain Research Bulletin 119(Pt B), 136-144.

Escudero J, Ibañez-Molina A, Iglesias-Parro S *et al*. (2015a). Effect of the average delay and mean connectivity of the Kuramoto model on the complexity of the output electroencephalograms. Annual International Conference of the IEEE Engineering in Medicine and Biology Society 2015, 7873-7876.

Esteller R, Echauz J, Tcheng T *et al*. (2001b). Line length: an efficient feature for seizure onset detection. In: Conference Proceedings of the 23rd Annual International Conference of the IEEE Engineering in Medicine and Biology Society 2001 Oct 25 (Vol. 2, pp. 1707-1710).

Esteller R, Echauz J, Tcheng T. (2004). Comparison of line length feature before and after brain electrical stimulation in epileptic patients. In: 26th Annual International Conference of the IEEE Engineering in Medicine and Biology Society 2004 Sep 1 (Vol. 2, pp. 4710-4713). IEEE.

Esteller R, Echauz JR, Litt B *et al* (2003), inventors; University of Pennsylvania Penn, assignee. Adaptive method and apparatus for forecasting and controlling neurological disturbances under a multi-level control. United States patent US 6,594,524. 2003 Jul 15.

Esteller R, Vachtsevanos G, Echauz J *et al*. (2001a). A comparison of waveform fractal dimension algorithms. IEEE Transactions on Circuits and Systems—I: Fundamental Theory and Applications 48(2), 177-183.

Estrada L, Torres A, Sarlabous L *et al*. (2015). EMG-derived respiration signal using the fixed sample entropy during an inspiratory load protocol. Annual International Conference of the IEEE Engineering in Medicine and Biology Society 2015, 1703-1706.

Estrada L, Torres A, Sarlabous L *et al*. (2016). Improvement in neural respiratory drive estimation from diaphragm electromyographic signals using fixed sample entropy. IEEE Journal of Biomedical Health Informatics 20(2), 476-85.

Estrada L, Torres A, Sarlabous L *et al*. (2017). Influence of parameter selection in fixed sample entropy of surface diaphragm electromyography for estimating respiratory activity. Entropy 19(9), 460, 1-15.

Ezeiza A, López de Ipiña K, Hernández C, Barroso N. (2013). Enhancing the feature extraction process for automatic speech recognition with fractal dimensions. Cognitive Computation 5(4), 545-50.

Fadel PJ, Barman SM, Phillips SW *et al*. (2004b). Fractal fluctuations in human respiration. Journal of Applied Physiology 97(6), 2056-2064.

Fadel PJ, Orer HS, Barman SM *et al*. (2004a). Fractal properties of human muscle sympathetic nerve activity. American Journal of Physiology. Heart and Circulatory Physiology 286(3), H1076-H1087.

Fadlallah B, Chen B, Keil A *et al.* (2013). Weighted-permutation entropy: A complexity measure for time series incorporating amplitude information. Physical Review E 87(2), 022911.

Faes L, Gómez-Extremera M, Pernice R *et al*. (2019a). Comparison of methods for the assessment of nonlinearity in short-term heart rate variability under different physiopathological states. Chaos 29(12), 123114.

Faes L, Nollo G, Porta A. (2012). Non-uniform multivariate embedding to assess the information transfer in cardiovascular and cardiorespiratory variability series. Computers in Biology and Medicine 42(3), 290-297.

Faes L, Nollo G, Porta A. (2013). Mechanisms of causal interaction between short-term RR interval and systolic arterial pressure oscillations during orthostatic challenge. Journal of Applied Physiology 114(12), 1657-1667.

Faes L, Pereira MA, Silva ME *et al*. (2019b). Multiscale information storage of linear long-range correlated stochastic processes. Physical Review E 99(3-1), 032115.

Faini A, Parati G, Bilo G *et al.* (2014). Fractal characteristics of blood pressure and heart rate from ambulatory blood pressure monitored over 24 hours. In 8th Conference of the European Study Group on Cardiovascular Oscillations (ESGCO) 2014 May 25 (pp. 73-74).

Falconer KJ. (1985). The Geometry of Fractal Sets. Cambridge: Cambridge University Press.

Fan MY, Luo J, Li L *et al*. (2019). Kinematic analysis of trajectory dimension-dependent sensorimotor control in arm tracking. IEEE Access 7, 8890-8900.

Fang L, Yang H, Wei H *et al*. (2002). Nonlinear analysis of EEG signals. 45th Midwest Symposium on Circuits and Systems (MWSCAS-2002) 2002, III-288-III-291.

Faure P, Lesne A. (2014). Estimating Kolmogorov entropy from recurrence plots, In: Webber C, Marwan N. (Eds.). Recurrence Quantification Analysis. Berlin: Springer-Verlag, 45-64.

Feldman DP, McTague CS, Crutchfield JP. (2008). The organization of intrinsic computation: Complexity-entropy diagrams and the diversity of natural information processing. Chaos: An Interdisciplinary Journal of Nonlinear Science 18(4), 043106.

Feng Z, Zheng X. (2002). [Effects of sampling parameter variation on the complexity analysis of EEG]. Sheng Wu Yi Xue Gong Cheng Xue Za Zhi 19(4), 616-620.

Ferenets R, Lipping T, Anier A *et al*. (2006). Comparison of entropy and complexity measures for the assessment of depth of sedation. IEEE Transactions on Biomedical Engineering 53(6), 1067-1077.

Fernández A, Gómez C, Hornero R *et al*. (2013). Complexity and schizophrenia. Progress in Neuro-psychopharmacology and Biological Psychiatry 45, 267-276.

Fernández N, Aguilar J, Piña-García CA *et al.* (2017). Complexity of lakes in a latitudinal gradient. Ecological Complexity 31, 1-20.

Fernández N, Aguilar JO, Terán O. (2010. Conceptual modeling of emergent processes in dynamics complex systems. In: 9th WSEAS international conference on computational intelligence, man-machine systems and cybernetics (CIMMACS'10) 2010 Dec 14 (pp. 75-82).

Figueiredo R, Pereira R, Pinto Neto O. (2018). Nonlinear analysis is the most suitable method to detect changes in heart autonomic control after exercise of different durations. Computers in Biology and Medicine 97, 83-88.

Finn JM, Goettee JD, Toroczkai Z *et al*. (2003). Estimation of entropies and dimensions by nonlinear symbolic time series analysis. Chaos 13(2), 444-56.

Finotello F, Scarpa F, Zanon M. (2015), EEG signal features extraction based on fractal dimension. In2015 37th Annual International Conference of the IEEE Engineering in Medicine and Biology Society (EMBC) 2015 Aug 25 (pp. 4154-4157).

Fiogbé E, Vassimon-Barroso V, Catai AM *et al*. (2018). Complexity of knee extensor torque: effect of aging and contraction intensity. Journal of Strength and Conditioning Research 2018 Oct 4.

Fiskum C, Andersen TG, Bornas X. *et al*. (2018). Non-linear heart rate variability as a discriminator of internalizing psychopathology and negative affect in children with internalizing problems and healthy controls. Frontiers in Physiology 9, 561.

Fraga SF, Mondragón JR. (2017). Comparison of Higuchi, Katz and multiresolution box-counting fractal dimension algorithms for EEG waveform signals based on event-related potentials. Revista EIA/English version 14(27),73-83. doi: 10.24050/reia.v14i27.864.

Frank J, Seifert G, Schroeder R *et al*.. (2020). Yoga in school sports improves functioning of autonomic nervous system in young adults: A non-randomized controlled pilot study. PLoS One 15(4), e0231299. 2020

Fraser AM, Swinney HL. (1986). Independent coordinates for strange attractors from mutual information. Physical Review. A, General Physics 33(2), 1134-1140.

Fredkin DR, Rice JA. (1995). Method of false nearest neighbors: A cautionary note. Physical Review. E, Statistical Physics, Plasmas, Fluids, and Related Interdisciplinary Topics 51(4), 2950-2954.

Friedrich R. (2021). Complexity and Entropy in Legal Language. Frontiers in Physics 9, 279.

Fuentes N, Garcia A, Guevara R (2021). . Complexity of brain dynamics as a correlate of consciousness in anaesthetized monkeys. bioRxiv. 2021 Jan 1. https://doi.org/10.1101/2021.08.17.456627.

Furutani N, Nariya Y, Takahashi T *et al*. (2020). Neural decoding of multi-modal imagery behavior focusing on temporal complexity. Frontiers in Psychiatry 11, 746.

Fuss FK. (2013). A robust algorithm for optimisation and customisation of fractal dimensions of time series modified by nonlinearly scaling their time derivatives: mathematical theory and practical applications. Computational and Mathematical Methods in Medicine 2013, 178476, 1-19. doi: 10.1155/2013/178476.

Gao XZ, Deng Y. (2020). The pseudo-Pascal triangle of maximum Deng entropy. International Journal of Computers, Communications and Control 15(1), 1006, 1-10.

García-González MA, Fernández-Chimeno M, Ramos-Castro J. (2009) Errors in the estimation of approximate entropy and other recurrence-plot-derived indices due to the finite resolution of RR time series. IEEE Transactions on Bio-medical Engineering 56(2), 345-351.

Garner DM, Marques Vanderlei F, Marques Vanderlei LZ. (2018). Complex measurements of heart rate variability in obese youths: distinguishing autonomic dysfunction. Journal of Human Growth and Development 28(3), 298-306.

Garner DM, Vanderlei LC. (2018). Complex measurements of heart rate variability in obese youths: distinguishing autonomic dysfunction. Journal of Human Growth and Development 28(3), 298-306.

Geng YH, Xing YY, Zhang X *et al.* (2017). Complexity analysis of EEG under magnetic stimulation on acupoint of Guangming (GB37). In2017 39th Annual International Conference of the IEEE Engineering in Medicine and Biology Society (EMBC) 2017 Jul 11 (pp. 2316-2319).

Gershenson C, Fernández N. (2012). Complexity and information: Measuring emergence, self-organization, and homeostasis at multiple scales. Complexity 18(2), 29-44.

Gershenson C, Heylighen F. (2003). When can we call a system self-organizing? In European Conference on Artificial Life 2003 Sep 14 (pp. 606-614). Springer, Berlin, Heidelberg.

Gershenson C. (2012). The world as evolving information. In Unifying themes in complex systems VII 2012 (pp. 100-115). Springer, Berlin, Heidelberg.Ghader H, Monz C. (2017). What does attention in neural machine translation pay attention to?. arXiv preprint arXiv, 1710.03348. 2017 Oct 9.

Ghanbari M, Kinsner W. (2018 Extracting features from both the input and the output of a convolutional neural network to detect distributed denial of service attacks. In: IEEE 17th International Conference on Cognitive Informatics & Cognitive Computing (ICCI* CC) 2018 Jul 16 (pp. 138-144).

Ghanbari M. (2021. Adaptive machine learning and signal processing detection schemes for DDoS attacks. PhD Thesis, Department of Electrical and Computer Engineering, University of Manitoba, Winnipeg.

Giannakakis GA, Tsiaparas NN, Papageorgiou C *et al*. (2009). Spectral entropy of dyslexic ERP signal by means of adaptive optimal kernel. 16th International Conference on Digital Signal Processing (DSP 2009), n.p.

Gierałtowski J, Żebrowski JJ, Baranowski R. (2012). Multiscale multifractal analysis of heart rate variability recordings with a large number of occurrences of arrhythmia. Physical Review. E, Statistical, Nonlinear, and Soft Matter Physics 85(2 Pt 1), 021915.

Girault JM, Humeau-Heurtier A. (2018). Centered and averaged fuzzy entropy to improve fuzzy entropy precision. Entropy 20(4), 287.

Girault JM. (205). Recurrence and symmetry of time series: Application to transition detection. Chaos, Solitons & Fractals ;77, 11-28.

Giuliani A, Piccirillo G, Marigliano V *et al*. (1998). A nonlinear explanation of aging-induced changes in heartbeat dynamics. American Journal of Physiology 275(4), H1455-H1461.

Gleick J. (1988). Chaos. London: William Heinemann.

Glowinski D, Mancini M, Rukavishnikova N *et al*. (2011). Analysis of dominance in small music ensemble. Proceedings of the second workshop on Affective Interaction in Natural Environments, ACM AFFINE'11, 4 pp.

Gneiting T, Ševčíková H, Percival DB. (2012). Estimators of fractal dimension: Assessing the roughness of time series and spatial data. Statistical Science 27(2), 247-277.

Gnitecki J, Moussavi Z, Pasterkamp H. (2008). Diagnostic potential in state space parameters of lung sounds. Medical and Biological Engineering and Computing 46(1), 93-99.

Gnitecki J, Moussavi Z. (2005). The fractality of lung sounds: a comparison of three waveform fractal dimension algorithms. Chaos, Solitons & Fractals 26(4), 1065-72.

Goh C, Hamadicharef B, Henderson G, Ifeachor E. (2005). Comparison of fractal dimension algorithms for the computation of EEG biomarkers for dementia. In: 2nd international conference on computational intelligence in medicine and healthcare (CIMED2005) 2005 Jun 29, Lisbon, Portugal, 464-471.

Goldberger AL, Amaral LAN, Hausdorff JM *et al*. (2002). Fractal dynamics in physiology: alterations with disease and aging. Proceedings of the National Academy of Sciences of the USA 99 (Suppl 1), 2466-2472.

Gomes RL, Vanderlei LCM, Garner DM *et al*. (2017). Higuchi fractal analysis of heart rate variability is sensitive during recovery from exercise in physically active men. MedicalExpress 2017(3), M170302, 1-8.

Gómez C, Mediavilla A, Hornero R *et al*. (2009). Use of the Higuchi's fractal dimension for the analysis of MEG recordings from Alzheimer's disease patients. Medical Engineering and Physics 31(3), 306-313.

Gomolka RS, Kampusch S, Kaniusas E *et al*. (2018). Higuchi fractal dimension of heart rate variability during percutaneous auricular vagus nerve stimulation in healthy and diabetic subjects. Frontiers in Physiology 9, 1162.

Gonzalez Andino SL, Grave de Peralta Menendez R, Thut G *et al*. (2000). Measuring the complexity of time series: an application to neurophysiological signals. Human Brain Mapping 11(1), 46-57.

González C, Jensen EW, Pedro L Gambús PL *et al*. (2018). Poincaré plot analysis of cerebral blood flow signals: Feature extraction and classification methods for apnea detection. PLoS One 13(12), e0208642.

Goshvarpour A, Goshvarpour A. (2021). Asymmetry of lagged Poincare plot in heart rate signals during meditation. Journal of Traditional and Complementary Medicine 11(1), 16-21. 2021

Govindan RB, Wilson JD, Eswaran H *et al*. (2007). Revisiting sample entropy analysis. Physica A 376, 158–164.

Gow BJ, Peng C-K, Wayne PM *et al*. (2015). Multiscale entropy analysis of center-of-pressure dynamics in human postural control: methodological considerations. Entropy 17(12), 7926-7947.

Graff G, Graff B, Kaczkowska A. *et al.* (2013). Ordinal pattern statistics for the assessment of heart rate variability. The European Physical Journal Special Topics 222(2), 525-534. 2013

Graham MJ, Drake AJ, Djorgovski SG *et al*. (2013). Using conditional entropy to identify periodicity. Monthly Notices of the Royal Astronomical Society 434, 269-2635.

Grassberger P, Procaccia I. (1983a). Measuring the strangeness of strange attractors. Physica D: Nonlinear Phenomena 9(1-2), 189-208.

Grassberger P, Procaccia I. (1983b). Characterization of strange attractors. Physical Review Letters 50(5), 346–349.

Grassberger P. (1988). FINITE sample corrections to entropy and dimension estimates. Physics Letters A 128(6-7), 369-373.

Grassberger P. (1990). An optimized box-assisted algorithm for fractal dimensions. Physics letters A 148(1-2), 63-68.

Greco A, Gallitto G, D'Alessandro M *e al.* (2021). Increased Entropic Brain Dynamics during DeepDream-Induced Altered Perceptual Phenomenology. Entropy 23(7), 839.

Greco A, Mammone N, Morabito FC *et al*. (2008). Kurtosis, Renyi's entropy and independent component scalp maps for the automatic artifact rejection from EEG data. International Journal of Biomedical and Biological Engineering 2(9), 344-348.

Green A. (2012). Computationally Characterizing Schizophrenia. Thesis submitted in conformity with the requirements for the degree of Master's of Applied Science, Graduate Department of Electrical and Computer Engineering, University of Toronto.

Grigolini P, Leddon D, Scafetta N. (2002). Diffusion entropy and waiting time statistics of hard-x-ray solar flares. Physical Review. E. Statistical, Nonlinear, and Soft Matter Physics 65(4 Pt 2A), 046203.

Grigolini P, Palatella L, Raffaelli G. (2001). Asymmetric anomalous diffusion: an efficient way to detect memory in time series. Fractals 9(4), 439–449.

Gu FJ, Meng X, Shen EH, Cai ZJ. (2003). Can we measure consciousness with EEG complexities? International Journal of Bifurcation and Chaos 13(03), 733-42.

Gu Z, Jin C, Chang D, Zhang L. (2021). Predicting webpage aesthetics with heatmap entropy. Behaviour & Information Technology 40(7), 676-690.

Guo L, Rivero D, Dorado J *et al.* (2010). Automatic epileptic seizure detection in EEGs based on line length feature and artificial neural networks. Journal of Neuroscience Methods 191(1), 101-109.

Gupta A, Singh P, Karlekar M. (2018). A novel signal modeling approach for classification of seizure and seizure-free EEG signals. IEEE Transactions on Neural Systems and Rehabilitation Engineering 26(5), 925-935.

Gutiérrez-de Pablo V, Gómez C, Poza J *et al*. (2020). Relationship between the presence of the ApoE ε4 allele and EEG complexity along the Alzheimer's disease continuum. Sensors 20(14), 3849.

Guzik P, Piskorski J, Awan K *et al.* (2013). Obstructive sleep apnea and heart rate asymmetry microstructure during sleep. Clinical Autonomic Research 23(2), 91-100. 2013b

Guzik P, Piskorski J, Barthel P *et al.* (2012). Heart rate deceleration runs for postinfarction risk prediction. Journal of Electrocardiology 45(1), 70-76. 2011a

Guzik P, Piskorski J, Contreras P *et al.* (2010b). Asymmetrical properties of heart rate variability in type 1 diabetes. Clinical Autonomic Research. 2010 Aug;20(4), 255-257.

Guzik P, Piskorski J, Ellert J *et al.* (2014). Asymmetry of haemodynamic variability in healthy people. In: 8th Conference of the European Study Group on Cardiovascular Oscillations (ESGCO) 2014 May 25 (pp. 129-130). IEEE.

Guzik P, Piskorski J, Krauze T. *et al.* (2010a). Asymmetric features of short-term blood pressure variability. Hypertension Research. 2010 Nov;33(11), 1199-1205.

Guzik P, Piskorski J, Krauze T *et al.* (2006a). Heart rate asymmetry by Poincaré plots of RR intervals. Biomed Tech 2006; 51, 272–275.

Guzik P, Piskorski J. (2020). Asymmetric properties of heart rate microstructure. Journal of Medical Science. 89(2), 121-131. 2020

Guzik P, Zuchowski B, Blaszyk K *et al.* (2013a) Asymmetry of the variability of heart rate and conduction time between atria and ventricles. Circulation Journal 77(12), 2904-2911.

Guzzetti S, Borroni E, Garbelli PE *et al*. (2005). Symbolic dynamics of heart rate variability: a probe to investigate cardiac autonomic modulation. Circulation 112(4), 465-470.

Guzzetti S, Mezzetti S, Magatelli R *et al*. (2000). Linear and non-linear 24 h heart rate variability in chronic heart failure. Autonomic Neuroscience 86(1-2), 114-119.

Hadjidimitriou S, Zacharakis A, Doulgeris P *et al.* (2010). Sensorimotor cortical response during motion reflecting audiovisual stimulation: evidence from fractal EEG analysis. Medical & Biological Engineering & Computing 48(6), 561-572.

Hagerman I, Berglund M, M Lorin M *et al*. (1996). Chaos-related deterministic regulation of heart rate variability in time- and frequency domains: effects of autonomic blockade and exercise. Cardiovascular Research 31(3), 410-418.

Han B, Wang S, Zhu Q *et al.* (2020). Intelligent fault diagnosis of rotating machinery using hierarchical Lempel-Ziv complexity 2020 Jan;10(12), 4221.

Hausdorff F. (1919). Dimension und äußeres Maß. Mathematische Annalen 79(1-2), 157–179.

Hayashi K, Mukai N, Sawa T. (2015). Poincaré analysis of the electroencephalogram during sevoflurane anesthesia. Clinical Neurophysiology 126(2), 404-411.

He J, Erfani S, Wijewickrema S, O'Leary S *et al.* (2020). Segmented Pairwise Distance for Time Series with Large Discontinuities. In: International Joint Conference on Neural Networks (IJCNN) 2020 Jul 19 (pp. 1-8). IEEE.

He SB, Li CB, Sun KH *et al*. (2018). Multivariate multiscale complexity analysis of self-reproducing chaotic systems. Entropy 20(8), 556.

Hegger R, Kantz H, Schreiber T. (2000). TISEAN 2.1. Nonlinear Time Series Analysis. (https://www.pks.mpg.de/~tisean/TISEAN_2.1/index.html) [Retrieved October 25, 2020].

Hegger R, Kantz H, Schreiber T. *et al*. (2007). TISEAN 3.0.1. Nonlinear Time Series Analysis. (https://www.pks.mpg.de/~tisean/Tisean_3.0.1/index.html) [Retrieved October 25, 2020].

Hegger R, Kantz H. (1999). Improved false nearest neighbor method to detect determinism in time series data. Physical Review. E, Statistical Physics, Plasmas, Fluids, and Related Interdisciplinary Topics 60(4 Pt B), 4970-4973.

Hejjel L. (2014). Heart rate variability and heart rate asymmetry analysis: does the inspiration/expiration ratio matter? Journal of Applied Physiology 116(6), 709. 2014

Hekmatmanesh A, Mikaeili M, Sadeghniiat-Haghighi K *et al.* (2017). Sleep spindle detection and prediction using a mixture of time series and chaotic features. Advances in Electrical and Electronic Engineering 15(3),435-447.

Henderson G, Ifeachor E, Hudson N *et al.* (2006). Development and assessment of methods for detecting dementia using the human electroencephalogram. IEEE Transactions on Biomedical Engineering. 2006 Jul 17;53(8), 1557-1568.

Henderson GT, Ifeachor EC, Wimalaratna HS *et al.* (2000). Prospects for routine detection of dementia using the fractal dimension of the human electroencephalogram. IEE Proceedings-Science, Measurement and Technology. 2000 Nov;147(6), 321-326.

Henderson GT. (2004). Early Detection of Dementia Using the Human Electroencephalogram. PhD Thesis, School of Computing, Communication and Electronics, Faculty of Technology, University of Plymouth.

Henriques T, Ribeiro M, Teixeira A. (2020). Nonlinear methods most applied to heart-rate time series: a review. Entropy 22, 309.

Henriques TS, Mariani S, Burykin A *et al*. (2016). Multiscale Poincaré plots for visualizing the structure of heartbeat time series. BMC Medical Informatics and Decision Making 16, 17.

Heylighen F, Cilliers P, Gershenson C. (2006). Complexity and philosophy. arXiv preprint cs/0604072. 2006 Apr 19.

Higuchi T. (1988). Approach to an irregular time-series on the basis of the fractal theory. Physica D 31(2), 277–283.Hjorth B. (1970). EEG analysis based on time domain properties. Electroencephalography and Clinical Neurophysiology 29(3), 306-310.

Hjorth B. (1973). The physical significance of time domain descriptors in EEG analysis. Electroencephalography and Clinical Neurophysiology 34(3), 321-325.

Höll M, Kantz H, Zhou Y. (2016). Detrended fluctuation analysis and the difference between external drifts and intrinsic diffusionlike nonstationarity. Physical Review E 94(4-1), 042201.

Hong B, Yang FS, Tang QY *et al.* (1998). Approximate entropy and its preliminary application in the field of EEG and cognition. In: Proceedings of the 20th Annual International Conference of the IEEE Engineering in Medicine and Biology Society. Vol. 20 Biomedical Engineering Towards the Year 2000 and Beyond (Cat. No. 98CH36286) 1998 Nov 1 (Vol. 4, pp. 2091-2094).

Hopkins P, Outram N, Lofgren N *et al.* (2006). A comparative study of fetal heart rate variability analysis techniques. In: International Conference of the IEEE Engineering in Medicine and Biology Society 2006 Jan 1 (pp. 1784-1787).

Hornero R, Espino P, Alonso A *et al*. (1999). Estimating complexity from EEG background activity of epileptic patients. IEEE Engineering in Medicine and Biology Magazine 18(6), 73-79.

Houle MS, Billman GE. (1999) Low-frequency component of the heart rate variability spectrum: a poor marker of sympathetic activity. American Journal of Physiology-Heart and Circulatory Physiology 276(1), H215-H223.]

Hsu CF, Hsu L, Chi S. (2020). Complexity and disorder of 1/ f α noises. Entropy 22, 1127, 1-10.

Hsu CF, Lin PY, Chao HH *et al*. (2019). Average entropy: measurement of disorder for cardiac RR interval signals. Physica A: Statistical Mechanics and its Applications 529, 121533, 1-10.

Hsu CF, Wei SY, Huang HP *et al*. (2017). Entropy of entropy: measurement of dynamical complexity for biological systems. 19(10), 550, 1-12.

Hu G, Wang KJ, Liu LL. (2021). Detection Line spectrum of ship radiated noise based on a new 3D chaotic system. Sensors;21(5), 1610.

Hu K, Ivanov PC, Chen Z *et al*. (2001). Effect of trends on detrended fluctuation analysis. Physical Review. E, Statistical Physics, Plasmas, Fluids, and Related Interdisciplinary Topics 64, 011114-1–011114-19.

Huang NE, Shen Z, Long SR *et al*. (1998). The empirical mode decomposition and the Hilbert spectrum for nonlinear and non-stationary time series analysis. Proceedings of the Royal Society of London. A 454, 903–995

Huhle R, Burghardt M, S Zaunseder S *et al*. (2012). Effects of awareness and nociception on heart rate variability during general anaesthesia. Physiological Measurement 33(2), 207-217.

Humairani A, Atmojo BS, Wijayanto I *et al.* (2020). Fractal based feature extraction method for epileptic seizure detection in long-term EEG recording. In: 2nd International Conference on Science & Technology (2020 2nd ICoST), Journal of Physics: Conference Series 2021 Mar 1 (Vol. 1844, No. 1, 012019, 1-10).

Humeau A, Stefanovska A, Abraham P. (2005). Lyapunov exponents of laser Doppler flowmetry signals in healthy and type 1 diabetic subjects. Annals of Biomedical Engineering 33(11), 1574-1581.

Humeau-Heurtier A, Wu C-W, Wu S-D *et al*. (2016). Refined multiscale Hilbert-Huang spectral entropy and its application to central and peripheral cardiovascular data. IEEE Transactions on Biomedical Engineering 63(11), 2405-2415.

Humeau-Heurtier A. (2015). The multiscale entropy algorithm and its variants: a review. Entropy 17, 3110-3123.

Humeau-Heurtier A. (2018). Evaluation of systems' irregularity and complexity: Sample entropy, its derivatives, and their applications across scales and disciplines. Entropy 20(10), 794.

Hurst HE. (1965). Long-Term Storage: An experimental study. London: Constable.

Hussain L, Aziz W, Alowibdi JS *et al*. (2017). Symbolic time series analysis of electroencephalographic (EEG) epileptic seizure and brain dynamics with eye-open and eye-closed subjects during resting states. Journal of Physiological Anthropology 36(1), 21.

Hussain L, Aziz W, Sharjil Saeed S *et al*. (2018). Arrhythmia detection by extracting hybrid features based on refined Fuzzy entropy (FuzEn) approach and employing machine learning techniques. Waves in Random and Complex Media 30(4), 656-686.

Iardukhina I, Dimitriev D, Remizova N *et al.* (2019). Nonlinear dynamics of heart rate variability during paced breathing: Recurrence quantification analysis of heart rate. FASEB Journal 33(S1), 531-521. 2019

Ibáñez-Molina AJ, Iglesias-Parro S, Soriano MF *et al*. (2015). Multiscale Lempel-Ziv complexity for EEG measures. Clinical Neurophysiology 126(3), 541-548.

Ibáñez-Molina AJ, Lozano V, Soriano MF *et al*. (2018). EEG multiscale complexity in schizophrenia during picture naming. Front Physiology 9, 1213.

Ignaccolo M, Latka M, Jernajczyk W *et al*. (2010a). Dynamics of electroencephalogram entropy and pitfalls of scaling detection. Physical Review. E. Statistical, Nonlinear, and Soft Matter Physics 81(3 Pt 1), 031909,1-9.

Ignaccolo M, Latka M, Jernajczyk W *et al*. (2010b). The dynamics of EEG entropy. Journal of Biological Physics 36(2), 185-196.

Immanuel SA, Kohler M, Kabir MM *et al*. (2014). Symbolic dynamics of respiratory cycle related sleep EEG in children with sleep disordered breathing. Annual International Conference of the IEEE Engineering in Medicine and Biology Society 2014, 6016-6019.

Inouye T, Shinosaki K, Sakamoto H *et al*. (1991). Quantification of EEG irregularity by use of the entropy of the power spectrum. Electroencephalography and Clinical Neurophysiology 79(3), 204-210.

Iwanski JS, Bradley E. (1998). Recurrence plots of experimental data: to embed or not to embed? Chaos 8(4), 861.

Jacob JE, Gopakumar K. (2018). Automated diagnosis of encephalopathy using fractal dimensions of EEG sub-bands. In: IEEE Recent Advances in Intelligent Computational Systems (RAICS) 2018 Dec 6 (pp. 94-97).

Jahanshahi SM, Zarei H, Khammar AH. (2020). On cumulative residual extropy. Probability in the Engineering and Informational Sciences 34(4), 605-25.

Janoušek O, Francisco S, Ronzhina M *et al*. (2013). In-vivo and ex-vivo HRV discrimination by Complex Correlation Measure. Proceedings of the 40th IEEE Annual Computers in Cardiology Conference (CinC 2013), Piscataway, NJ, 441-443.

Jauregui M, Zunino L, Lenzi EK *et al.* (2018). Characterization of time series via Rényi complexity–entropy curves. Physica A: Statistical Mechanics and its Applications 498, 74-85.

Javorka M, Trunkvalterova Z, Tonhajzerova I *et al*. (2008). Short-term heart rate complexity is reduced in patients with type 1 diabetes mellitus. Clinical Neurophysiology 119(5), 1071-1081.

Jeffery K, Pollack R, Cavelli C. (2019). On the statistical mechanics of life: Schrödinger revisited. Entropy 21, 1211.

Jelinek HF, August KG, Imam MH *et al*. (2011). Heart rate asymmetry and emotional response to robot-assist task challenges in post-stroke patients. Computing in Cardiology 38, 521-524.

Jelinek HF, August KG, Imam MH *et al.* (2011). Heart rate asymmetry and emotional response to robot-assist task challenges in post-stroke patients. In: Computing in Cardiology 38, 521-524. IEEE.

Jelinek HF, Khandoker AH, Quintana DS *et al*. (2011a). Complex correlation measure as a sensitive indicator of risk for sudden cardiac death in patients with depression. Proceedings of the 38th IEEE Annual Computers in Cardiology Conference (CinC 2011), Piscataway, NJ, 809−812.

Jelinek HF, Md Imam H, Al-Aubaidy H *et al*. (2013). Association of cardiovascular risk using non-linear heart rate variability measures with the Framingham risk score in a rural population. Frontiers in Physiology 4(186), 1-8.

Jeong J, Kim DJ, Kim SY. (2001). Effect of total sleep deprivation on the dimensional complexity of the waking EEG. Sleep 24(2), 197-202.

Jernajczyk W, Sobańska A, Marczak M *et al*. (2006). The influence of acute progressive hypoxia on bioelectrical activity of the brain. Journal of Physiology and Pharmacology 57 Suppl 4, 165-174.

Jevtic N, Nilsen W, Stinea P, Schweitzer JS. (2011). Using average mutual information to preview the power spectrum and to guide nonlinear noise reduction. Chaotic Modeling and Simulation 1, 187-197.

Jiang J, Chen X, Zhang C *et al.* (2017). Heart rate acceleration runs and deceleration runs in patients with obstructive sleep apnea syndrome. Sleep and Breathing 21(2), 443-451. 2017

Jin Y, Chen C, Cao ZX *et al*. (2017). Entropy change of biological dynamics in COPD. International Journal of Chronic Obstructive Pulmonary Disease 12, 2997-3005.

Jose J, Abdul Sathar EI. (2021). An ordered approach on cumulative extropy measures for information analysis. Communications in Statistics-Theory and Methods. 2021 May 11, 1-21.

Jose J, Abdul Sathar EI. (2021). Extropy for past life based on classical records. Journal of the Indian Society for Probability and Statistics. 2021 Jun;22(1), 27-46.

Jose J, Sathar EA. (2019). Residual extropy of k-record values. Statistics & Probability Letters. 146, 1-6. Elsevier

Kaczmarek LD, Behnke M, Enko J *et al.* (2019). Effects of emotions on heart rate asymmetry. Psychophysiology 56(4), e13318.

Kafashan MM. (2016). Understanding the Role of Dynamics in Brain Networks: Methods, Theory and Application. PhD Thesis, Washington University, St. Louis, MO.

Kahl L, Eger M, Hofmann UG. (2015). Effects of sampling rate on automated fatigue recognition in surface EMG signals. Current Directions in Biomedical Engineering 1(1), 80-84.

Kalauzi A, Bojić T, Rakić L. (2009). Extracting complexity waveforms from one-dimensional signals. Nonlinear Biomedical Physics 3(1), 8.

Kalauzi A, Bojić T, Rakić L. (2009). Extracting complexity waveforms from one-dimensional signals. Nonlinear biomedical physics. 3(1), 1-11.

Kalev K, Bachmann M, Orgo L *et al*. (2015). Lempel-Ziv and multiscale Lempel-Ziv complexity in depression. International Conference of the IEEE Engineering in Medicine & Biology Society 2015, 4158-4161.

Kamari O, Buono F. (2021). On extropy of past lifetime distribution. Ricerche di Matematica. 70(2), 505-515.

Kamath C. (2013). A classification system to discriminate epileptic patients using multi-valued coarse-graining Lempel–Ziv complexity. International Journal of Biomedical Engineering and Technology 11(1), 96-106.

Kamizawa T, Hara T, Ohya M. (2014). On relations among the entropic chaos degree, the Kolmogorov-Sinai entropy and the Lyapunov exponent. Journal of Mathematical Physics 55, 032702.

Kannathal N, Puthusserypady SK, Min LC. (2004). Complex dynamics of epileptic EEG. International Conference of the IEEE Engineering in Medicine & Biology Society 2006, 604-607.

Kantelhardt JW, Zschiegner SA, Koscielny-Bunde E *et al*. (2002). Multifractal detrended fluctuation analysis of nonstationary time series. Physica A: Statistical Mechanics and its Applications 316(1–4), 87-114.

Karamanos K, Peratzakis A, Kapiris P *et al*. (2005). Extracting preseismic electromagnetic signatures in terms of symbolic dynamics. Nonlinear Processes in Geophysics 12(6), 835-848.

Karino K, Nabika T, Nishiki M *et al*. (2009). Evaluation of diabetic neuropathy using the tone-entropy analysis, a noninvasive method to estimate the autonomic nervous function. Biomedical Research 30(1), 1-6.

Karmakar C, Jelinek HF, Khandoker A *et al*. (2012). Identifying increased risk of post-infarct people with diabetes using multi-lag tone-entropy analysis. Annual International Conference of the IEEE Engineering in Medicine and Biology Society 34, 25-28.

Karmakar C, Jelinek HF, Khandoker A *et al*. (2015). Multi-lag HRV analysis discriminates disease progression of post-infarct people with no diabetes versus diabetes. Annual

International Conference of the IEEE Engineering in Medicine and Biology Society 2015, 2367-2370.

Karmakar C, Khandoker A, Kimura Y *et al.* (2014b). Investigating foetal heart rate asymmetry. In: 2014 36th Annual International Conference of the IEEE Engineering in Medicine and Biology Society 2014 Aug 26 (pp. 2261-2264).

Karmakar C, Khandoker A, Palaniswami M. (2013). Multi-scale tone entropy in differentiating physiologic and synthetic RR time series. 35th Annual International Conference of the IEEE Engineering in Medicine and Biology Society 2013, Osaka, 6135-6138.

Karmakar C, Khandoker A, Palaniswami M. (2012a). Analysis of slope based heart rate asymmetry using Poincaré plots. In: 2012 Computing in Cardiology 2012 Sep 9 (pp. 949-952). IEEE.

Karmakar C, Khandoker A, Palaniswami M. (2010). Heart rate asymmetry in altered parasympathetic nervous system activity. In: 2010 Computing in Cardiology 2010 Sep 26, 37, 601-604. IEEE.

Karmakar C, Khandoker A, Palaniswami M. (2012b).Investigating the changes in heart rate asymmetry (HRA) with perturbation of parasympathetic nervous system. Australasian Physical & Engineering Sciences in Medicine 35(4), 465-474.

Karmakar C, Khandoker A, Tulppo M *et al*. (2012). Dynamics of heart rate changes following moderate and high volume exercise training. Proceedings of the 39th IEEE Annual Computing in Cardiology Conference (CinC 2012), Piscataway, NJ, 953-956.

Karmakar C, Kimura Y, Palaniswami M *et al.* (2015). Analysis of fetal heart rate asymmetry before and after 35 weeks of gestation. Biomedical Signal Processing and Control 21, 43-48. 2015b

Karmakar C, Udhayakumar R, Palaniswami M. (2020). Entropy profiling: A reduced-parametric measure of Kolmogorov-Sinai entropy from short-term HRV signal. Entropy 22(12), 1396.

Karmakar C, Udhayakumar RK, Li P *et al*. (2017). Stability, consistency and performance of distribution entropy in analysing short length heart rate variability (HRV) signal. Frontiers in Physiology 8, 720.

Karmakar C, Udhayakumar RK, Palaniswami M. (2015). Distribution Entropy (DistEn): A complexity measure to detect arrhythmia from short length RR interval time series. International Conference of the IEEE Engineering in Medicine & Biology Society 2015, 5207-5210.

Karmakar CK, Jelinek HF, Warner P *et alk*. (2014a). Effect of gender and diabetes on major depressive disorder using heart rate asymmetry. In: 2014 36th Annual International Conference of the IEEE Engineering in Medicine and Biology Society 2014 Aug 26 (pp. 6679-6682).

Karmakar CK, Khandoker AH, Gubbi J *et al*. (2009a). Complex Correlation Measure: a novel descriptor for Poincaré plot. BioMedical Engineering OnLine 8(17), 1-12.

Karmakar CK, Khandoker AH, Gubbi J *et al*. (2009b). Novel feature for quantifying temporal variability of Poincaré plot: a case study. Proceedings of the 36th IEEE Annual Computers in Cardiology Conference (CinC 2009), Piscataway, NJ, 53-56.

Karmakar CK, Khandoker AH, Gubbi J *et al.* (2009). Defining asymmetry in heart rate variability signals using a Poincaré plot. Physiological measurement 30(11), 1227. 2009a

Karmakar CK, Khandoker AH, Gubbi J *et al.* (2009b). Modified Ehlers' index for improved detection of heart rate asymmetry in Poincaré plot. In: 2009 36th Annual Computers in Cardiology Conference (CinC) 2009 Sep 13 (pp. 169-172). IEEE.

Karmakar CK, Khandoker AH, Jelinek HF *et al*. (2013). Risk stratification of cardiac autonomic neuropathy based on multi-lag tone-entropy. Medical and Biological Engineering and Computing 51(5), 537-546.

Karmakar CK, Khandoker AH, Palaniswami M. (2015a). Phase asymmetry of heart rate variability signal. Physiological measurement. 2015 Jan 14;36(2), 303-314. Slope I

Karnam NK, Turlapaty AC, Dubey SR *et al.* (2021). Classification of sEMG signals of hand gestures based on energy features. Biomedical Signal Processing and Control 70, 102948.

Karthikeyan R, Mcdonald AD, Mehta R. (2022).Stress Detection during motor activity: comparing neurophysiological indices in older adults. IEEE Transactions on Affective Computing (01), 1-15. 2022

Katebi SD, Sabeti M. (2012). Complexity measure as a feature to classify schizophrenic and healthy participants. In: 14th International Conference on Computer Modelling and Simulation 2012 Mar 28 (pp. 377-382). IEEE.

Kattumannil SK, Sreedevi EP. (2022). Non-parametric estimation of cumulative (residual) extropy. Statistics & Probability Letters 185, 109434.

Katz MJ. (1988). Fractals and the analysis of waveforms. Computers in Biology and Medicine 18(3), 145-56.

Kazemi MR, Tahmasebi S, Buono F *et al.* (2021). Fractional Deng entropy and extropy and some applications. Entropy 23(5), 623.

Keenan E, Udhayakumar RK, Karmakar CK *et al.* (2020). Entropy profiling for detection of fetal arrhythmias in short length fetal heart rate recordings. In: 42nd Annual International Conference of the IEEE Engineering in Medicine & Biology Society (EMBC) (pp. 621-624). .

Keller K, Sinn M. (2010). Kolmogorov-Sinai entropy from the ordinal viewpoint. Physica D 239(12), 997–1000.

Keller K, Unakafov AM, Unakafova VA. (2014). Ordinal patterns, entropy, and EEG. Entropy 16(12), 6212-6239.

Kello CT, Dalla Bella S, Médé B *et al*. (2017). Hierarchical temporal structure in music, speech and animal vocalizations: jazz is like a conversation, humpbacks sing like hermit thrushes. Journal of the Royal Society, Interface 14(135), 20170231.

Kello CT. (2013). Critical branching neural networks. Psychological Review 120(1), 230–254.

Kennel MB, Brown R, Abarbanel HD. (1992). Determining embedding dimension for phase-space reconstruction using a geometrical construction. Physical Review. A, Atomic, Molecular, and Optical Physics 45(6), 3403-3411.

Keshavan MS, Cashmere JD, Miewald J *et al*. (2004). Decreased nonlinear complexity and chaos during sleep in first episode schizophrenia: a preliminary report. Schizophrenia Research 71(2-3), 263-272.

Kesić S, Spasić SZ. (2016). Application of Higuchi's fractal dimension from basic to clinical neurophysiology: a review. Computer Methods and Programs in Biomedicine 133, 55-70.

Kesić S, Spasić SZ. (2016). Application of Higuchi's fractal dimension from basic to clinical neurophysiology: a review. Computer Methods and Programs in Biomedicine. 133, 55-70.

Khairuddin HR, Malik AS, Mumtaz W *et al.* (2013). Analysis of EEG signals regularity in adults during video game play in 2D and 3D. In: 35th Annual International Conference of the IEEE Engineering in Medicine and Biology Society (EMBC) 2013 Jul 3 (pp. 2064-2067).

Khandoker A, Karmakar C, Kimura Y *et al*. (2015). Tone entropy analysis of foetal heart rate variability. Entropy 17, 1042-1053.

Khandoker AH, Jelinek HF, Moritani T *et al*. (2010). Association of cardiac autonomic neuropathy with alteration of sympatho-vagal balance through heart rate variability analysis. Medical Engineering and Physics 32(2), 161-167.

Khandoker AH, Luthra V, Abouallaban Y *et al*. (2017). Suicidal ideation is associated with altered variability of fingertip photo-plethysmogram signal in depressed patients. Frontiers in Physiology 8, 501, 1-17.

Khazaei M, Raeisi K, Goshvarpour A *et al.* (2018). Early detection of sudden cardiac death using nonlinear analysis of heart rate variability. Biocybernetics and Biomedical Engineering 38(4), 931-940.

Khoa TQD, Ha VQ, Toi VV. (2012). Higuchi fractal properties of onset epilepsy electroencephalogram. Computational and Mathematical Methods in Medicine 2012, 461426.

Kim KK, Kim JS, Lim YG *et al*. (2011). Effect of missing RR-interval data on nonlinear heart rate variability analysis. Computer Methods and Programs in Biomedicine 106(3), 210-218.

Kimiskidis VK, Koutlis C, Tsimpiris A *et al.* (2015). Transcranial magnetic stimulation combined with EEG reveals covert states of elevated excitability in the human epileptic brain. International Journal of Neural Systems 25(05), 1550018.

Kinsner W. (2008). A unified approach to fractal dimensions. Journal of Information Technology Research (JITR) 1(4), 62-85.

Kirsch MR, Monahan K, Weng J *et al*. (2012). Entropy-based measures for quantifying sleep-stage transition dynamics: relationship to sleep fragmentation and daytime sleepiness. IEEE Transactions on Biomedical Engineering 59(3), 787-796.

Klintworth A, Ajtay Z, Paljunite A *et al.* (2012). Heart rate asymmetry follows the inspiration/expiration ratio in healthy volunteers. Physiological Measurement 33(10), 1717-1731. 2012

Klonowski W, Olejarczyk E, Stepien E. (2014). 'Epileptic seizures' in economic organism. Physica A: Statistical Mechanics and its Applications 342(3-4), 701–707.

Kobayashi M, Musha T. (1982). 1/f fluctuation of heartbeat period. IEEE Transactions on Biomedical Engineering 29(6), 456-457.

Kolmogorov AN. (1965). Three approaches to the quantitative definition of information. Problemy Peredachi Informatsii [Problems of Information Transmission] 1(1), 3-11.

Komalasari R, Rizal A, Suratman FY. (2020). Classification of Normal and Murmur Hearts Sound using the Fractal Method. International Journal 9(5), 8178-8183.

Kong ZB, Wang XD, Shen SR *et al.* (2020). Risk prediction for arrhythmias by heart rate deceleration runs in patients with chronic obstructive pulmonary disease. International Journal of Chronic Obstructive Pulmonary Disease. 2020;15, 585-593.

Koolen N, Jansen K, Vervisch J *et al.* (2013). Automatic burst detection based on line length in the premature EEG. In: BIOSIGNALS 2013-Proceedings of the International Conference on Bio-inspired Systems and Signal Processing (pp. 105-111). SciTePress.

Kotimäki V, Räsänen E, Hennig H *et al*. (2013). Fractal dynamics in chaotic quantum transport. Physical Review. E, Statistical, Nonlinear, and Soft Matter Physics 88(2), 022913.

Kovatchev BP, Farhy LS, Cao H *et al.* (2003). Sample asymmetry analysis of heart rate characteristics with application to neonatal sepsis and systemic inflammatory response syndrome. Pediatric Research 54(6), 892-898. 2003

Kraemer KH, Donner RV, Heitzig J *et al.* (2018). Recurrence threshold selection for obtaining robust recurrence characteristics in different embedding dimensions. Chaos: An Interdisciplinary Journal of Nonlinear Science 8(8), 085720.

Krakovská A, Mezeiová K, BudáIová H. (2015). Use of false nearest neighbours for selecting variables and embedding parameters for state space reconstruction. Journal of Complex Systems 2015, 932750, 1-12.

Kramarić K, Šapina M, Garcin M *et al.* (2019). Heart rate asymmetry as a new marker for neonatal stress. Biomedical Signal Processing and Control 47, 219-223.

Kreuzer M, Kochs EF, Schneider G. *et al*. (2014). Non-stationarity of EEG during wakefulness and anaesthesia: advantages of EEG permutation entropy monitoring. Journal of Clinical Monitoring and Computing 28(6), 573-580.

Kroupi E, Vesin JM, Ebrahimi T. (2015). Subject-independent odor pleasantness classification using brain and peripheral signals. IEEE Transactions on Affective Computing 7(4), 422-34.

Kroupi E, Yazdani A, Ebrahimi T. (2011). EEG correlates of different emotional states elicited during watching music videos. In: International Conference on Affective Computing and Intelligent Interaction 2011 Oct 9 (pp. 457-466). Springer, Berlin, Heidelberg.

Kullback S, Leibler RA. (1951). On information and sufficiency. Annals of Mathematical Statistics 22(1), 79–86.

Kumar A, Liu N, Zhi Xiong Koh ZX *et al*. (2019). Development of a heart rate variability and complexity model in predicting the need for life-saving interventions amongst trauma patients. Burns and Trauma 7, 12.

Kuo C-E, Chen G-T. (2020). A short-time insomnia detection system based on sleep EOG with RCMSE analysis. IEEE Access 8, 69763-69773.

Lad F, Sanfilippo G, Agro G. (2015). Extropy: Complementary dual of entropy. Statistical Science 30(1), 40-58.

Lad F, Sanfilippo G, Agrò G. (2018). The duality of entropy/extropy, and completion of the Kullback information complex. Entropy 20(8), 593,1-11.

Lad F, Sanfilippo G. (2018). Scoring alternative forecast distributions: completing the Kullback distance complex. arXiv preprint arXiv, 1806.11178. 2018 Jun 28.

Lai YY, Zhang ZB, Li PY *et al*. (2018). Investigation of glucose fluctuations by approaches of multi-scale analysis. Medical and Biological Engineering and Computing 56(3), 505-514.

Lake DE, Moorman JR. (2011). Accurate estimation of entropy in very short physiological time series: the problem of atrial fibrillation detection in implanted ventricular devices. American Journal of Physiology. Heart and Circulatory Physiology 300(1), H319-H325.

Lake DE, Richman JS, Griffin MP *et al*. (2002). Sample entropy analysis of neonatal heart rate variability. American Journal of Physiology. Regulatory, Integrative and Comparative Physiology 283(3), R789-R797.

Lake DE. (2006). Renyi entropy measures of heart rate Gaussianity. IEEE Transactions on Biomedical Engineering 53(1), 21-27.

Lake DE. (2011). Improved entropy rate estimation in physiological data. 33rd Annual International Conference of the IEEE Engineering in Medicine & Biology Society, Boston, MA, 1463-1466.

Lamanna J, Malgaroli A, Cerutti S *et al*. (2012). Detection of fractal behavior in temporal series of synaptic quantal release events: a feasibility study. Computational Intelligence and Neuroscience 2012, 704673.

Lau ZJ, Pham T, Annabel SH *et al.* (2021). brain entropy, fractal dimensions and predictability: a review of complexity measures for EEG in healthy and neuropsychiatric populations. PsyArXiv. September 13 2021, 1-22. doi:10.31234/osf.io/f8k3x.

Lazo AV, Rathie P. (1978). On the entropy of continuous probability distributions. IEEE Transactions on Information Theory 24(1), 120-122.

Lebiecka K, Zuchowicz U, Wozniak-Kwasniewska A *et al*. (2018). Complexity analysis of EEG data in persons with depression subjected to transcranial magnetic stimulation. Frontiers in Physiology 9, 1385.

Ledesma-Ramírez CI, Bojorges-Valdez E, Yanez-Suarez O *et al.* (2020). Recurrence Analysis of EEG Power and HRV Time Series for Asynchronous BCI Control. In: González Díaz CA, Chapa González C, Laciar Leber E. *et al*. (Eds). VIII Latin American Conference on Biomedical Engineering and XLII National Conference on Biomedical Engineering. CLAIB 2019. IFMBE Proceedings, vol 75. Springer, Cham. https://doi.org/10.1007/978-3-030-30648-9_27

Lee D-Y, Choi Y-S. (2018). Multiscale distribution entropy analysis of short-term heart rate variability. Entropy 20(12), 952, 1-15.

Lee D-Y, Choi Y-S. (2020). Multiscale distribution entropy analysis of heart rate variability using differential inter-beat intervals. IEEE Access 8, 48761-48773.

Lee GMH, Fattinger S, Anne-Laure Mouthon A-L *et al*. (2013). Electroencephalogram approximate entropy influenced by both age and sleep. Frontiers in Neuroinformatics 7, 33.

Lee SH, Choo JS, Im WY *et al*. (2008). Nonlinear analysis of electroencephalogram in schizophrenia patients with persistent auditory hallucination. Psychiatry Investigation 5(2), 115-120.

Lempel A, Ziv J. (1976). On the complexity of finite sequences. IEEE Transactions on Information Theory IT-22(1), 75-81.

Lerma C, Reyna MA, R. Carvajal R. (2015). Association between abnormal electrocardiogram and less complex heart rate variability estimated by the correlation dimension. Revista Mexicana de Ingeniería Biomédica 36(1), 55-64.

Lesne A. (2011). Shannon entropy: a rigorous notion at the crossroads between probability, information theory, dynamical systems and statistical physics. Mathematical Structures in Computer Science 24(3), E240311.

Li CX, Chen YN, Li YJ *et al*. (2016). Complexity analysis of brain activity in attention-deficit/hyperactivity disorder: a multiscale entropy analysis. Brain Research Bulletin 124, 12-20.

Li GH, Guan QR, Yang H. (2019). Noise reduction method of underwater acoustic signals based on CEEMDAN, effort-to-compress complexity, refined composite multiscale dispersion entropy and wavelet threshold denoising. Entropy 21(1), 11, 1-21.

Li GH, Yang ZC, Yang H. (2018). Noise reduction method of underwater acoustic signals based on uniform phase empirical mode decomposition, amplitude-aware permutation entropy, and Pearson correlation coefficient. Entropy 20(12), 918, 1-18.

Li H, Du W, Ivanov K *et al*. (2019). The EEG analysis of actual left/right lateral bending movements in patient of lumbar disc herniation. Conference Proceedings of the IEEE Engineering in Medicine and Biology Society 2019, 4707-4711.

Li M, Vitányi PM. (1990). Kolmogorov complexity and its applications. In: van Leeuwen J. (Ed.) Handbook of Theoretical Computer Science A. Algorithms and complexity (pp. 187-254). Cambridge, MA: MIT Press.

Li P, Ji LZ, Chang Yan C *et al*. (2014). Coupling between short-term heart rate and diastolic period is reduced in heart failure patients as indicated by multivariate entropy analysis. Computing in Cardiology 41, 97-100.

Li P, Karmakar C, Yan C *et al*. (2016). Classification of 5-S epileptic EEG recordings using distribution entropy and sample entropy. Frontiers in Physiology 7, 136.

Li P, Karmakar C, Yearwood J *et al*. (2018). Detection of epileptic seizure based on entropy analysis of short-term EEG. PLoS One 13(3), e0193691.

Li P, Liu CY, Li K *et al*. (2015a). Assessing the complexity of short-term heartbeat interval series by distribution entropy. Medical and Biological Engineering and Computing 53(1), 77-87.

Li P, Yan C, Karmakar C *et al*. (2015b). Distribution entropy analysis of epileptic EEG signals. Conference Proceedings of the IEEE Engineering in Medicine and Biology Society 2015, 4170-4173.

Li R, Wang J. (2017). Symbolic complexity of volatility duration and volatility difference component on voter financial dynamics. Digital Signal Processing 63, 56-71.

Li X, Yu S, Chen H *et al*. (2015c). Cardiovascular autonomic function analysis using approximate entropy from 24-h heart rate variability and its frequency components in patients with type 2 diabetes. Journal of Diabetes Investigation 6(2), 227-235.

Li XL, Cui SY, Voss LJ. (2008a). Using permutation entropy to measure the electroencephalographic effects of sevoflurane. Anesthesiology 109(3), 448-456.

Li XL, Li D, Liang ZH *et al*. (2008b). Analysis of depth of anesthesia with Hilbert-Huang spectral entropy. Clinical Neurophysiology 119(11), 2465-2475.

Li XL, Ouyang GX, Richards DA. (2007). Predictability analysis of absence seizures with permutation entropy. Epilepsy Research 77(1), 70-74.

Li YF, Wu S, Yang QN *et al*. (2020). Application of the variance delay fuzzy approximate entropy for autonomic nervous system fluctuation analysis in obstructive sleep apnea patients. Entropy 22(9), 915, 1-13.

Li YL, Li HR, Wang WG *et al.* (2017). C0 complexity: An alternative complexity measure for degradation status of rolling bearings. In Prognostics and System Health Management Conference (PHM-Harbin) 2017 Jul 9 (pp. 1-8). IEEE.

Li YS, Wang YB, Chang HQ *et al.* (2021). Inhibitory Effects of Dexmedetomidine and Propofol on Gastrointestinal Tract Motility Involving Impaired Enteric Glia Ca2+ Response in Mice. Neurochemical Research 46(6), 1410-1422.

Liang Z, Shao S, Lv Z *et al.* (2020). Constructing a consciousness meter based on the combination of non-linear measurements and genetic algorithm-based support vector machine. IEEE Transactions on Neural Systems and Rehabilitation Engineering 28(2), 399-408.

Liang ZH, Wang YH, Ouyang GX *et al.* (2013). Permutation auto-mutual information of electroencephalogram in anesthesia. Journal of Neural Engineering. 10(2), 026004,1-9.

Liang ZH, Wang YH, Sun X *et al*. (2015). EEG entropy measures in anesthesia. Frontiers in Computational Neuroscience 9, 16.

Liang ZH, Wang YH, Sun X *et al.* (2015). EEG entropy measures in anesthesia. Frontiers in Computational Neuroscience 9, 16,1-17.

Liao FY, Jan Y-K. (2014). Assessing skin blood flow dynamics in older adults using a modified sample entropy approach. Conference Proceedings of the IEEE Engineering in Medicine and Biology Society 2014, 722-725.

Lim TP, Puthusserypady S. (2005). Postprocessing methods for finding the embedding dimension of chaotic time series. Physical Review. E, Statistical, Nonlinear, and Soft Matter Physics 72(2 Pt 2), 027204.

Lima CA, Coelho AL, Madeo RC *et al.* (2016). Classification of electromyography signals using relevance vector machines and fractal dimension. Neural Computing and Applications 27(3), 791-804.

Lin Y-H, Huang H-C, Chang Y-C *et al*. (2014). Multi-scale symbolic entropy analysis provides prognostic prediction in patients receiving extracorporeal life support. Critical Care 18(5), 548, 1-11.

Lin Y-H, Lin C, Ho Y-H *et al*. (2016). Heart rhythm complexity impairment in patients undergoing peritoneal dialysis. Scientific Reports 6, 28202.

Lipsitz LA. (1995). Age-related changes in the "complexity" of cardiovascular dynamics: A potential marker of vulnerability to disease. Chaos 5(1), 102-109.

Lipsitz LA. (2002). Dynamics of stability: the physiologic basis of functional health and frailty. Journal of Gerontology. Series A, Biological Sciences and Medical Sciences 57(3), B115-B125.

Little M, McSharry P, Moroz I *et al.* (2006). Nonlinear, biophysically informed speech pathology detection. In: IEEE International Conference on Acoustics Speech and Signal Processing Proceedings 2006 May 14 (Vol. 2, pp. II-II).

Little M, Mcsharry P, Roberts S *et al.* (2007). Exploiting nonlinear recurrence and fractal scaling properties for voice disorder detection. Nature Precedings. 2007 Jul 9, 1-35.

Liu H-Y, Yang Z, Meng F-G *et al*. (2018). Preoperative heart rate variability as predictors of vagus nerve stimulation outcome in patients with drug-resistant epilepsy. Scientific Reports 8, 3856, 1-11.

Liu J, Xiao F. (2022). Information volume of mass function based on extropy. Soft Computing ;26(5), 2409-18.

Liu JZ, Yang Q, Yao B *et al.* (2005). Linear correlation between fractal dimension of EEG signal and handgrip force. biological Cybernetics 93(2), 131-140.

Liu Q, Chen Y-F, Fan S-Z *et al*. (2015). EEG signals analysis using multiscale entropy for depth of anesthesia monitoring during surgery through artificial neural networks. Computational and Mathematical Methods in Medicine 2015, 232381.

Liu S, Wang X, Zhao L *et al*. (2020). Subject-independent emotion recognition of EEG signals based on dynamic empirical convolutional neural network. IEEE Transactions on Neural Systems and Rehabilitation Engineering 2020, PP.

Liu WF, Jiang Y, Xu YS. (2022). A super fast algorithm for estimating sample entropy. Entropy 24(4), 524,1-25.

Liu X, Zhang C, Ji Z *et al*. (2016). Multiple characteristics analysis of Alzheimer's electroencephalogram by power spectral density and Lempel-Ziv complexity. Cognitive Neurodynamics 10(2), 121-133.

Liu XF, Jiang AM, Xu N *et al.* (2016). Increment entropy as a measure of complexity for time series. Entropy 18(1), 22.

Liu XF, Jiang AM, Xu N. (2017). Automated epileptic seizure detection in EEGs using increment entropy. In: IEEE 30th Canadian conference on electrical and computer engineering (CCECE) 2017 Apr 30 (pp. 1-4).

Liu XF, Wang X, Zhou X *et al.* (2018). Appropriate use of the increment entropy for electrophysiological time series. Computers in Biology and Medicine ;95, 13-23.

Liu Y, Sun LS, Zhu YS *et al*. (2005). Novel method for measuring the complexity of schizophrenic EEG based on symbolic entropy analysis. Conference Proceedings of the IEEE Engineering in Medicine and Biology Society 2006, 37-40.

Long Z, Jing B, Guo R *et al*. (2018). A brainnetome atlas based mild cognitive impairment identification using Hurst exponent. Frontiers in Aging Neuroscience 10, 103.

López-De-Ipiña K, Martinez-de-Lizarduy U, Barroso N *et al*.. (2015b). Automatic analysis of Categorical Verbal Fluency for Mild Cognitive impartment detection: A non-linear language independent approach. In 4th International Work Conference on Bioinspired Intelligence (IWOBI) 2015 Jun 10 (pp. 101-104). IEEE.

López-de-Ipiña K, Martinez-de-Lizarduy U, Calvo PM *et al.* (2018a). Advances on Automatic Speech Analysis for Early Detection of Alzheimer Disease: A Non-linear Multi-task Approach. Curr Alzheimer Res. 2018;15(2), 139-148. doi: 10.2174/1567205014666171120143800. PMID: 29165084.

López-de-Ipiña K, Solé-Casals J, Eguiraun H *et al.* (2015) Feature selection for spontaneous speech analysis to aid in Alzheimer's disease diagnosis: A fractal dimension approach. Computer Speech & Language 30(1), 43-60.

Lopez-de-Ipina K, Solé-Casals J, Faúndez-Zanuy M *et al.* (2018b). Automatic analysis of Archimedes' spiral for characterization of genetic essential tremor based on Shannon's entropy and fractal dimension. Entropy ;20(7), 531.

López-Ruiz R, Mancini HL, Calbet X. (1995). A statistical measure of complexity. Physics letters 209(5-6), 321-6.

Lopour BA, Tasoglu S, Kirsch HE *et al.* (2011). A continuous mapping of sleep states through association of EEG with a mesoscale cortical model. Journal of computational neuroscience 30(2), 471-487.

Lorimer B. (2020). The Improvement of Shewhart-Stable Time Series Processes by Applying Jensen-Shannon Complexity Measures to Characterize Emergent Structure. Doctoral Dissertation, University of Central Florida. https://stars.library.ucf.edu/etd2020/247 [accessed 26 March 2022].

Lowen SB, Cash SS, Poo MM. (1997). Quantal neurotransmitter secretion rate exhibits fractal behavior. Journal of Neuroscience 17(15), 5666–5677.

Lozano-García M, Estrada L, Jané R. (2019). Performance evaluation of fixed sample entropy in myographic signals for inspiratory muscle activity estimation. Entropy 21(2), 183, 1-16.

Lozano-García M, Sarlabous L, Moxham J *et al*. (2018). Surface mechanomyography and electromyography provide non-invasive indices of inspiratory muscle force and activation in healthy subjects. Scientific Reports 8(1), 16921, 1-13.

Lu S, Chen XN, Kanters JK *et al*. (2008). Automatic selection of the threshold value r for approximate entropy. IEEE Transactions on Bio-medical Engineering 55(8), 1966-1972.

Lu W-Y, Chen J-Y, Chang C-F *et al*. (2015). Multiscale entropy of electroencephalogram as a potential predictor for the prognosis of neonatal seizures. PLoS One 10(12), e0144732.

Lu Y, Wang MJ, Peng RC *et al.* (2017). Accelerating the computation of entropy measures by exploiting vectors with dissimilarity. Entropy 19(11), 598.

Lu Y, Wang MJ, Wu WQ *et al.* (2020). Dynamic entropy-based pattern learning to identify emotions from EEG signals across individuals. Measurement 150, 107003.

Lu YL, Jiang DN, Jia XF *et al*. (2008). Predict the neurological recovery under hypothermia after cardiac arrest using C0 complexity measure of EEG signals. In: 30th Annual International Conference of the IEEE Engineering in Medicine and Biology Society 2008 Aug 20 (pp. 2133-2136).

Lubetzky AV, Harel D, Lubetzky E. (2018). On the effects of signal processing on sample entropy for postural control. PLoS One 13(3), e0193460.

Lund V, Laine J, Laitio T *et al*. (2003). Instantaneous beat-to-beat variability reflects vagal tone during hyperbaric hyperoxia. Undersea and Hyperbaric Medicine 30(1), 29-36.

Ma J, Xu Y, Li Y *et al*. (2019). Predicting noise-induced critical transitions in bistable systems. Chaos 29(8), 081102.

MacCallum JK, Olszewski, AE, Zhang Y *et al*. (2011). Effects of low-pass filtering on acoustic analysis of voice. Journal of Voice 25(1), 15-20.

Magagnin V, Bassani T, Bari V *et al*. (2011). Non-stationarities significantly distort short-term spectral, symbolic and entropy heart rate variability indicesterm spectral, symbolic and entropy heart rate variability indices. Physiological Measurement 32(11), 1775-1786.

Makarava N, Menz S, Theves M *et al*. (2014). Quantifying the degree of persistence in random amoeboid motion based on the Hurst exponent of fractional Brownian motion. Physical Review. E, Statistical, Nonlinear, and Soft Matter Physics 90(4), 042703.

Malekzadeh A, Zare A, Yaghoobi M *et al.* (2021). Automatic Diagnosis of Epileptic Seizures in EEG Signals Using Fractal Dimension Features and Convolutional Autoencoder Method. Big Data and Cognitive Computing 5(4), 78,1-31.

Malik N. (2020). Uncovering transitions in paleoclimate time series and the climate driven demise of an ancient civilization. Chaos 30, 083108.

Mammone N, Inuso G, La Foresta F *et al*. (2009). Clustering of entropy topography in epileptic electroencephalography. Communications in Computer and Information Science (11th International Conference on Engineering Applications of Neural Networks, EANN, London), 43, 453-462.

Mammone N, Morabito FC. (2008). Enhanced automatic artifact detection based on independent component analysis and Renyi's entropy. Neural Networks 21(7), 1029-1040.

Mandelbrot BB. (1967). How long is the coast of Britain? Statistical self-similarity and fractional dimension. Science 156(3775), 636–638.

Mandelbrot BB. (1982). The Fractal Geometry of Nature. San Francisco, CA: WH Freeman.

Mandelbrot BB. (1983). The Fractal Geometry of Nature. New York: WH Freeman.

Manis G, Aktaruzzaman M, Sassi R. (2017). Bubble entropy: an entropy almost free of parameters. IEEE Transactions in Biomedical Engineering 64(11), 2711-2718.

Manis G, Aktaruzzaman M, Sassi R. (2018). Low computational cost for sample entropy. Entropy 20, 61.

Manis G, Nikolopoulos S. (2007). Speeding up the computation of approximate entropy. In: Jarm T, Kramar P, Zupanic A (Eds.). 11th Mediterranean Conference on Medical and Biomedical Engineering and Computing 2007 (pp. 785-788). Springer, Berlin, Heidelberg.

Manis G, Sassi R. (2017). Tolerance to spikes: a comparison of sample and bubble entropy. 2017 Computing in Cardiology (CinC) Conference, Rennes, France, 44, 1-4.

Manis G. (2008). Fast computation of approximate entropy. Computer Methods and Programs in Biomedicine. 2008 Jul 1;91(1), 48-54.

Mao XG, Shang P, Wang J *et al.* (2018). Characterizing time series by extended complexity-entropy curves based on Tsallis, Rényi, and power spectral entropy. Chaos: An Interdisciplinary Journal of Nonlinear Science. 28(11), 113106.

Mao XG, Shang PJ, Wang J *et al*. (2018). Characterizing time series by extended complexity-entropy curves based on Tsallis, Rényi, and power spectral entropy. Chaos 28(11), 113106.

Mao XG, Shang PJ, Xu M *et al.* (2020). Measuring time series based on multiscale dispersion Lempel–Ziv complexity and dispersion entropy plane. Chaos, Solitons & Fractals 137, 109868.

Maragos P, Potamianos A. (1999). Fractal dimensions of speech sounds: Computation and application to automatic speech recognition. The Journal of the Acoustical Society of America 105(3), 1925-1932.

Maragos P, Sun FK. (1993). Measuring the fractal dimension of signals: morphological covers and iterative optimization. IEEE Transactions on signal Processing. 1993 Jan;41(1), 108-121.

Mardi Z, Ashtiani SN, Mikaili M. (2011). EEG-based drowsiness detection for safe driving using chaotic features and statistical tests. Journal of Medical Signals and Sensors. 2011 May;1(2), 130-137.

Mariani S, Borges AFT, Henriques T *et al*. (2015). Use of multiscale entropy to facilitate artifact detection in electroencephalographic signals. Conference Proceedings of the IEEE Engineering in Medicine and Biology Society 2015, 7869-7872.

Martin MT, Plastino A, Rosso OA. (2006). Generalized statistical complexity measures: Geometrical and analytical properties. Physica A: Statistical Mechanics and its Applications. 369(2), 439-62.

Martin MT, Plastino AR, Plastino A. (2000). Tsallis-like information measures and the analysis of complex signals. Physica A: Statistical Mechanics and its Applications 275(1–2), 262-271.

Martinas K, Frankowicz M. (2000).Extropy-reformulation of the entropy principle. Periodica Polytechnica Chemical Engineering 44(1), 29-38.

Martinez HE. (2015). Towards intelligent aquaculture. Development of an early Biological Warning System to monitor exposure to contaminants and fish welfare: from artificial vision to systems modelling (Doctoral dissertation, Universidad del País Vasco-Euskal Herriko Unibertsitatea).

Martínez-Cagigal V. (2020). A bearable and vectorized implementation of Sample Entropy (SampEn). MATLAB Central File Exchange. (https://uk.mathworks.com/matlabcentral/fileexchange/69381-sample-entropy) [Retrieved August 9, 2020]

Martínez-Rodrigo A, García-Martínez B, Zunino L *et al*. (2019). Multi-lag analysis of symbolic entropies on EEG recordings for distress recognition. Frontiers in Neuroinformatics 13, 40, 1-15.

Martins Lopes F, de Oliveira EA, Cesar RM Jr, (2011). Inference of gene regulatory networks from time series by Tsallis entropy. BMC Systems Biology 5, 61.

Marwan N, Donges JF, Donner RV *et al.* (2021). Nonlinear time series analysis of palaeoclimate proxy records. Quaternary Science Reviews 274, 107245.

Marwan N, Kurths J, Foerster S. (2015). Analysing spatially extended high-dimensional dynamics by recurrence plots. Physics Letters A 379(10-11), 894-900.

Marwan N, Romano MC, Thiel M *et al*. (2007). Recurrence plots for the analysis of complex systems. Physics Reports 438(5-6), 237 – 329.

Marwan N, Wessel N, Meyerfeldt U *et al*. (2002). Recurrence-plot-based measures of complexity and their application to heart-rate-variability data. Physical Review. E, Statistical, Nonlinear, and Soft Matter Physics 66(2 Pt 2), 026702.

Masi M. (2005). A step beyond Tsallis and Rényi entropies. Physics Letters A 338(3–5), 217-224.

Maszczyk T, Duch W. (2008). Comparison of Shannon, Renyi and Tsallis entropy used in decision trees. 9th International Conference on Artificial Intelligence and Soft Computing (ICAISC 2008), 643-651.

Mateos DM, Gómez-Ramírez J, Rosso OA. (2021).Using time causal quantifiers to characterize sleep stages. Chaos, Solitons & Fractals 146, 110798.

Mateos DM, Zozor S, Olivarez F. (2017). On the analysis of signals in a permutation Lempel-Ziv complexity-permutation Shannon entropy plane. arXiv preprint arXiv, 1707.05164. 2017 Jul 17.

Matić Z, Platiša MM, Kalauzi A *et al*. (2020). Slow 0.1 Hz breathing and body posture induced perturbations of RRI and respiratory signal complexity and cardiorespiratory coupling. Frontiers in Physiology 11, 24.

Maturo F, Fortuna F. (2016). Bell-shaped fuzzy numbers associated with the normal curve. In: Di Battista T, Moreno E, Racugno W. (Eds.). Topics on Methodological and Applied Statistical Inference. Cham, Switzerland, Springer Nature, 131-144.

Mayor D, Panday D, Kandel H *et al*. (2020). CEPS: An Open Access MATLAB Graphical User Interface (GUI) for the Analysis of Complexity and Entropy in Physiological Signals. Entropy 23(3), 321, 1-34; https://doi.org/10.3390/e23030321. Also available at: https://www.mdpi.com/1099-4300/23/3/321.

Mayor D, Steffert T, Panday D. (2019). The effects of transcutaneous electroacupuncture stimulation (TEAS) on heart rate variability (HRV) and nonlinearity (HRNL): Is stimulation frequency or amplitude more important? Poster presentation, AACP Conference, London, 18 May 2019. (https://f1000research.com/posters/8-678) [Retrieved July 28, 2020].[1]

McCamley JD, Denton W, Arnold A *et al*. (2018). On the calculation of sample entropy using continuous and discrete human gait data. Entropy 20(10), 764.

McIntosh AR, Vakorin V, N Kovacevic N *et al*. (2014). Spatiotemporal dependency of age-related changes in brain signal variability. Cerebral Cortex 24(7), 1806-1817.

Mehdizadeh S, Sanjari MA. (2017). Effect of noise and filtering on largest Lyapunov exponent of time series associated with human walking. Journal of Biomechanics 64, 236-239.

Mehdizadeh S. (2018). The largest Lyapunov exponent of gait in young and elderly individuals: A systematic review. Gait and Posture 60, 241-250.

Mehrnam AH, Nasrabadi AM, Ghodousi M *et al*. (2017). A new approach to analyze data from EEG-based concealed face recognition system. International Journal of Psychophysiology 116, 1-8.

Meisel C, Bailey K, Achermann P *et al*. (2017). Decline of long-range temporal correlations in the human brain during sustained wakefulness. Scientific Reports 7(1), 11825.

Mekler A. (2008). Calculation of EEG correlation dimension: large massifs of experimental data. Computer Methods and Programs in Biomedicine 92(1), 154-160.

Melillo P, Bracale M, Pecchia L. (2011). Nonlinear Heart Rate Variability features for real-life stress detection. Case study: students under stress due to university examination. Biomedical Engineering Online 10, 96.

Melis M, Littera R, Cocco E *et al*. (2019). Entropy of human leukocyte antigen and killer-cell immunoglobulin-like receptor systems in immune-mediated disorders: A pilot study on multiple sclerosis. PLoS One 14(12), e0226615.

Mesin L. (2017). Heartbeat monitoring from adaptively down-sampled electrocardiogram. Computers in Biology and Medicine 84, 217-225.

Mestivier D, Dabiré H, Safar M *et al*. (1998). Use of nonlinear methods to assess effects of clonidine on blood pressure in spontaneously hypertensive rats. Journal of Applied Physiology 84(5), 1795-1800.

Mieszkowski D, Kośmider M, Krauze T *et al.* (2016). Asymmetric detrended fluctuation analysis reveals asymmetry in the RR intervals time series. Journal of Applied Mathematics and Computational Mechanics 15(1), 99-106. 2016

Miller I. (2014). On the quantum aspects of brain-mind problem. Scientific GOD Journal 5(3), 201-215.

Moctezuma LA, Molinas M. (2020). Classification of low-density EEG for epileptic seizures by energy and fractal features based on EMD. Journal of Biomedical Research 34(3), 180-190.

Mohamed MS, Abdulrahman AT, Almaspoor Z *et al.* (2021). Ordered variables and their concomitants under extropy via COVID-19 data application. Complexity. 2021 Jul 6;2021.

Moharreri S, Dabanloo NJ, Maghooli K. (2018). Modeling the 2D space of emotions based on the poincare plot of heart rate variability signal. Biocybernetics and Biomedical Engineering 38(4), 794-809. 2018

Moharreri S, Rezaei S, Dabanloo NJ *et al.* (2019). Automatic Emotions Assessment Using Heart Rate Variability Analysis and 2D Regression Models of Emotions. In: Computing in Cardiology (CinC) 2019 Sep 8; 46, 1-4. IEEE.

Mohebbi M, Ghassemian H, Mohammadzadeh Asl B. (2011). Structures of the recurrence plot of heart rate variability signal as a tool for predicting the onset of paroxysmal atrial fibrillation. Journal of Medical Signals and Sensors 1(2), 113–121.

Moisy F. (2022). boxcount (https://www.mathworks.com/matlabcentral/fileexchange/13063-boxcount), MATLAB Central File Exchange. Retrieved April 2, 2022.

Moisy F. 2008. Computing a fractal dimension with Matlab: 1D, 2D and 3D Box-counting. http://www.fast.u-psud.fr/~moisy/ml/boxcount/html/demo.html#2 [accessed 2 April 2022].

Molina V, Bachiller A, Suazo V *et al*. (2014). Noise power associated with decreased task-induced variability of brain electrical activity in schizophrenia. European Archives of Psychiatry and Clinical Neuroscience 266(1), 55-61.

Molina-Picó A, Cuesta-Frau D, Aboy M *et al*. (2011). Comparative study of approximate entropy and sample entropy robustness to spikes. Artificial Intelligence in Medicine 53(2), 97-106.

Molina-Picó A, Cuesta-Frau D, Miró-Martínez P *et al*. (2013). Influence of QRS complex detection errors on entropy algorithms. Application to heart rate variability discrimination. Computer Methods and Programs in Biomedicine 110(1), 2-11.

Moore JM, Walker DM, Yan G. (2020). Mean local autocovariance provides robust and versatile choice of delay for reconstruction using frequently sampled flowlike data. Physical Review. E 101(1-1), 012214.

More M. (2003). Principles of Extropy v 3.11. An evolving framework of values and standards for continuously improving the human condition. http://extropy.org/principles.htm [accessed 12 April 2022].

Morse M, Hedlund G. (1938). Symbolic dynamics. American Journal of Mathematics 60(4), 815–866.

Moulder RG, Daniel KE, Teachman BA *et al.* (2022). Tangle: A metric for quantifying complexity and erratic behavior in short time series. Psychological Methods, 27(1), 82–98. https://doi.org/10.1037/met0000386

Moura-Tonello SC, Takahashi AC, Francisco CO *et al*. (2014). Influence of type 2 diabetes on symbolic analysis and complexity of heart rate variability in men. Diabetology and Metabolic Syndrome 6(1), 13.

Mukherjee S, Palit SK, Banerjee S *et al.* (2015). Can complexity decrease in congestive heart failure?. Physica A: Statistical Mechanics and its Applications 439, 93-102.

Müller W, Jung A, Ahammer H. (2017). Advantages and problems of nonlinear methods applied to analyze physiological time signals: human balance control as an example. Scientific Reports 7(1), 2464.

Mumtaz W, Xia L, Malik AS *et al.* (2013). EEG classification of physiological conditions in 2D/3D environments using neural network. In: 35th Annual International Conference of the IEEE Engineering in Medicine and Biology Society (EMBC) 2013 Jul 3 (pp. 4235-4238).

Murugappan M, Alshuaib WB, Bourisly A *et al*. (2020). Emotion classification in Parkinson's disease EEG using RQA and ELM. 16th IEEE International Colloquium on Signal Processing & its Applications (CSPA 2020), Langkawi, Malaysia, 290-295.

Myers A, Khasawneh FA. (2020). On the automatic parameter selection for permutation entropy. Chaos 30(3), 033130.

Nair A, Kiasaleh K. (2014). Function mapped trajectory estimation for ECG sets. Biomedical Engineering Letters 4(3), 277-84.

Nardone, P. (2014). Entropy of difference. 2014. arXiv.org, Cornell University. (https://arxiv.org/abs/1411.0506v2) [Retrieved December 1, 2020].

Nasario-Junior O, Benchimol-Barbosa PR, Nadal J. (2014).Refining the deceleration capacity index in phase-rectified signal averaging to assess physical conditioning level. Journal of Electrocardiology 47(3), 306-310.

Nascimento GL, Freitas CG, Rosso OA *et al.* (2021). Data Sampling Algorithm Based on Complexity-Entropy Plane for Smart Sensing Applications. IEEE Sensors Journal 21(22), 25831-42.

Nayak SK, Bit A, Dey A *et al*. (2018). A review on the nonlinear dynamical system analysis of electrocardiogram signal. Journal of Healthcare Engineering 2018, 6920420.

Nicolaou J, Georgiou J. (2012). Detection of epileptic electroencephalogram based on permutation entropy and support vector machines. Expert Systems with Applications 39(1), 202–209.

Niknazar M, Mousavi SR, Vahdat BV *et al*. (2013). A new framework based on recurrence quantification analysis for epileptic seizure detection. . IEEE Journal of Biomedical and Health Informatics 17(3), 572-578.

Nishad A, Upadhyay A. (2020). Empirical wavelet transform based classification of surface electromyogram signals for hand movements. In: Bajaj V, Sinha GR (Eds.) Modelling and Analysis of Active Biopotential Signals in Healthcare 1, 9-1 to 9-31.

Nogueira M. (2017). Exploring the link between multiscale entropy and fractal scaling behavior in near-surface wind. PLoS One 12(3), e0173994, 1-19.

Noughabi HA, Jarrahiferiz J. (2020). Extropy of order statistics applied to testing symmetry. Communications in Statistics-Simulation and Computation. 2020 Jan 20, 1-1.

Novák D, Kremen V, Cuesta D *et al.* (2009). Discrimination of endocardial electrogram disorganization using a signal regularity analysis. In: Annual International Conference of the IEEE Engineering in Medicine and Biology Society 2009 Sep 3 (pp. 1812-1815).

Nurujjaman M, Narayanan R, Iyengar AS. (2009). Comparative study of nonlinear properties of EEG signals of normal persons and epileptic patients. Nonlinear Biomedical Physics 3(1), 6.

Oida E, Moritani T, Yamori Y. (1997). Tone-entropy analysis on cardiac recovery after dynamic exercise. Journal of Applied Physiology 82(6), 1794-1801.

Ojo JS, Adelakun AO, Edward OV. (2019). Comparative study on radio refractivity gradient in the troposphere using chaotic quantifiers. Heliyon 5(8), e02083.

Olivares F, Zunino L. (2020). Multiscale dynamics under the lens of permutation entropy. Physica A: Statistical Mechanics and its Applications 559, 125081.

Olofsen E, Sleigh JW, A Dahan A. (2008). Permutation entropy of the electroencephalogram: a measure of anaesthetic drug effect. British Journal of Anaesthesia 101(6), 810-821.

Olofsen, E., Sleigh, J.W. and Dahan, A., 2008. Permutation entropy of the electroencephalogram: a measure of anaesthetic drug effect. British Journal of Anaesthesia, 101(6), pp.810-821.

Ono Y. (2018). Lecture 32. Kolmogorov-Sinai entropy. Introduction to Dynamical Systems. Urbana, IL: University of Illinois. (https://www.yoono.org/Y_OONO_official_site/LectureSlides_510_files/Lect32KSEntropy.pdf) [Retrieved July 31, 2020].

Osmane A, Dimmock AP, Pulkkinen TI. (2019). Jensen-Shannon Complexity and Permutation Entropy Analysis of Geomagnetic Auroral Currents. Journal of Geophysical Research: Space Physics 124(4), 2541-51.

Ouyang GX, Li J, Liu XZ, Li XL. (2013). Dynamic characteristics of absence EEG recordings with multiscale permutation entropy analysis. Epilepsy Research 104(3), 246-252.

Pagani M, Iellamo F, Lucini D *et al*. (2001). Selective impairment of excitatory pressor responses after prolonged simulated microgravity in humans. Autonomic Neuroscience 91(1-2), 85-95.

Palazzolo JA, Estafanous FG, Murray PA. (1998). Entropy measures of heart rate variation in conscious dogs. American Journal of Physiology 274(4), H1099-H1105.

Pan X, Hou L, Stephen M *et al*. (2014). Evaluation of scaling invariance embedded in short time series. PLoS One 9(12), e116128, 1-27.

Pan YH, Lin WY, Wang YH *et al.* (2011a). Computing multiscale entropy with orthogonal range search. Journal of Marine Science and Technology 19(1), 107-113.

Pan YH, Wang YH, Liang SF *et al.* (2011b). Fast computation of sample entropy and approximate entropy in biomedicine. Computer Methods and Programs in Biomedicine 104(3), 382-396. 2011b

Paoletti G, Huber A, Balocchi R *et al.* (2014). Heart rate dynamics in subjects with different hypnotizability. Contemporary Hypnosis & Integrative Therapy 30(2),102-112.

Papadakis NC, Christakis DG, Tzagarakis GN *et al*. (2009). Gait variability measurements in lumbar spinal stenosis patients: part A. Comparison with healthy subjects. Physiological Measurement 30(11), 1171-1186.

Paramanathan P, Uthayakumar R. (2008b). An algorithm for computing the fractal dimension of waveforms. Applied Mathematics and Computation 195(2), 598-603. [2008b]

Paramanathan P, Uthayakumar R. (2008a). Application of fractal theory in analysis of human electroencephalographic signals. Computers in Biology and Medicine. 38(3), 372-8.

Parvaneh S, Dabanloo NJ, Rezaei S *et al.* (2017). Heart rate asymmetry in response to colored light. In: 2017 Computing in Cardiology (CinC) 2017 Sep 24; 44, 1-4. IEEE.

Parvaneh S, Toosizadeh N, Moharreri S. (2015). Impact of mental stress on heart rate asymmetry. In: Computing in Cardiology Conference (CinC) 2015 Sep 6 (pp. 793-796). IEEE. 2015

Pasluosta CF, Steib S, Klamroth S *et al*. (2017). Acute neuromuscular adaptations in the postural control of patients with Parkinson's disease after perturbed walking. Frontiers in Aging Neuroscience 9, 316, 1-8.

Paternoster L, Vallverdú M, Melia U *et al*. (2013). Analysis of epileptic EEG signals in children by symbolic dynamics. Annual International Conference of the IEEE Engineering in Medicine and Biology Society (EMBC) 2013, 4362-4365.

Paul JK, Iype T, Dileep R *et al*. (2019). Characterization of fibromyalgia using sleep EEG signals with nonlinear dynamical features. Computers in Biology and Medicine 111, 103331.

Pavithra M, NiranjanaKrupa B, Sasidharan A *et al.* (2014). Fractal dimension for drowsiness detection in brainwaves. In: International Conference on Contemporary Computing and Informatics (IC3I) 2014 Nov 27 (pp. 757-761). IEEE.

Peng C-K, Buldyrev SV, Havlin S *et al*. (1994). Mosaic organization of DNA nucleotides. Physical Review E 49(2), 1685–1689.

Peng CK, Havlin S, Stanley HE *et al*. (1995). Quantification of scaling exponents and crossover phenomena in nonstationary heartbeat time series. Chaos 5(1), 82-87.

Peng Y, Zhu JY, Zheng WL *et al*. (2014). EEG-based emotion recognition with manifold regularized extreme learning machine. Conference Proceedings of the IEEE Engineering in Medicine and Biology Society 2014, 974-977.

Penzel T, Kantelhardt JW, Grote L *et al*. (2003). Comparison of detrended fluctuation analysis and spectral analysis for heart rate variability in sleep and sleep apnea. IEEE Transactions in Biomedical Engineering 50(10), 1143-1151.

Pernice R, Faes L, Kotiuchyi I *et al*. (2019c). Time, frequency and information domain analysis of short-term heart rate variability before and after focal and generalized seizures in epileptic children. Physiological Measurement 40(7), 074003, 1-12.

Pernice R, Javorka M, Krohova J *et al*. (2019a). Comparison of short-term heart rate variability indexes evaluated through electrocardiographic and continuous blood pressure monitoring. Medical and Biological Engineering and Computing 57(6), 1247-1263.

Pernice R, Javorka M, Krohova J *et al*. (2019b). A validity and reliability study of conditional entropy measures of pulse rate variability. Annual International Conference of the IEEE Engineering in Medicine and Biology Society (EMBC) 2019, 5568-5571.

Pesin YB. (1977). [Characteristic Lyapunov exponents and smooth ergodic theory]. Russian Mathematical Surveys 32(4(196)), 55-112.

Petrosian A. (1995). Kolmogorov complexity of finite sequences and recognition of different preictal EEG patterns. In: Proceedings, Eighth IEEE Symposium on Computer-Based Medical Systems, 212–217.

Phothisonothai M, Nakagawa M. (2008). EEG-based classification of motor imagery tasks using fractal dimension and neural network for brain-computer interface. IEICE TRANSACTIONS on Information and Systems. 2008 Jan 1;91(1), 44-53.

Pham TD. (2016). Fuzzy recurrence plots, Europhysics letters. 116, 1-5. http://dx.doi.org/10.1209/0295-5075/116/50008

Pham TD. (2018). Pattern analysis of computer keystroke time series in healthy control and early-stage Parkinson's disease subjects using fuzzy recurrence and scalable recurrence network features. Journal of Neuroscience Methods. 307, 194-202.

Pham TD. (2022). Identifying critical transitions in major depression with fuzzy recurrence entropy. All Life 15(1), 1086-1100.

Pham TD. (n.d.). Matlab Codes. https://sites.google.com/site/professortuanpham/codes [accessed 9 December 2022].

Piek AB, Stolz I, Keller K. (2019). Algorithmics, possibilities and limits of ordinal pattern-based entropies. Entropy 21(6), 547.

Pincus SM, Gladstone IM, Ehrenkranz RA. (1991b). A regularity statistic for medical data analysis. Journal of Clinical Monitoring 7(4),335-345.

Pincus SM, Goldberger AL. (1994). Physiological time-series analysis: what does regularity quantify? American Journal of Physiology 266(4 Pt 2), H1643-H1656.

Pincus SM. (1991). Approximate entropy as a measure of system complexity. Proceedings of the National Academy of Sciences of the USA 88(6), 2297–2301.

Pincus SM. (1995). Approximate entropy (ApEn) as a complexity measure. Chaos 5(1), 110-117.

Piskorski J, Ellert J, Krauze T *et al.* (2019). Testing heart rate asymmetry in long, nonstationary 24 hour RR-interval time series. Physiological Measurement 40(10), 105001. 2019

Piskorski J, Guzik P, Krauze T *et al.* (2010). Cardiopulmonary resonance at 0.1 Hz demonstrated by averaged Lomb-Scargle periodogram. Central European Journal of Physics 8(3), 386-92.

Piskorski J, Guzik P. (2011). Asymmetric properties of long-term and total heart rate variability. Medical & biological engineering & computing 49(11), 1289-1297.

Piskorski J, Guzik P. (2012). Compensatory properties of heart rate asymmetry. Journal of Electrocardiology 45(3), 220-224. 2012

Piskorski J, Guzik P. (2007). Geometry of the Poincaré plot of RR intervals and its asymmetry in healthy adults. Physiological Measurement 28(3), 287. 2007a

Piskorski J, Guzik P. (2011a). The structure of heart rate asymmetry: deceleration and acceleration runs. Physiological measurement 32(8), 1011-1023. 2011a

Piskorski J, Kosmider M, Mieszkowski D *et al.* (2018). Properties of asymmetric Detrended Fluctuation Analysis in the time series of RR intervals. Physica A: Statistical Mechanics and its Applications 491, 347-360.

Platiša MM, Bojić T, Mazić S *et al.* (2019a). Generalized Poincaré plots analysis of heart period dynamics in different physiological conditions: Trained vs. untrained men. PloS One 14(7), e0219281.

Platiša MM, Bojić T, Pavlović SU *et al.* (2016).. Generalized Poincaré plots - a new method for evaluation of regimes in cardiac neural control in atrial fibrillation and healthy subjects. Frontiers in Neuroscience 10, 38, 1-9. 2016

Platiša MM, Radovanović NN, Kalauzi A *et al.* (2020). Asymmetry of Cardiac Interbeat Intervals in Heart Failure. In: 11th Conference of the European Study Group on Cardiovascular Oscillations (ESGCO) 2020 Jul 15 (pp. 1-2). IEEE.

Platiša MM, Radovanović NN, Kalauzi A *et al.* (2019). Differentiation of heart failure patients by the ratio of the scaling exponents of cardiac interbeat intervals. Frontiers in Physiology 10, 570. 2019b

Polychronaki GE, Ktonas PY, Gatzonis S *et al.* (2010). Comparison of fractal dimension estimation algorithms for epileptic seizure onset detection. Journal of Neural Engineering 7(4), 046007,1-18.

Ponce-Flores M, Frausto-Solís J, Santamaría-Bonfil G *et al.* (2020).. Time series complexities and their relationship to forecasting performance. Entropy 22(1), 89.

Popescu PG, Dragomir SS, Sluşanschi EI *et al*. (2016). Bounds for Kullback-Leibler divergence. Electronic Journal of Differential Equations 2016(237), pp. 1-6.

Popov A, Avilov O, Kanaykin O. (2013). Permutation entropy of EEG signals for different sampling rate and time lag combinations. IEEE Signal Processing Symposium (SPS) 2013, 1–4.

Porta A, Bari V, De Maria B *et al*. (2019). On the relevance of computing a local version of sample entropy in cardiovascular control analysis. IEEE Transactions in Biomedical Engineering 66(3), 623-631.

Porta A, Bari V, Marchi A *et al*. (2015a). Limits of permutation-based entropies in assessing complexity of short heart period variability. Physiological Measurement 36(4), 755-765.

Porta A, Baselli G, Liberati D *et al*. (1998). Measuring regularity by means of a corrected conditional entropy in sympathetic outflow. Biological Cybernetics 78(1), 71-78.

Porta A, Baumert M, Cysarz D *et al*. (2015b). Enhancing dynamical signatures of complex systems through symbolic computation. Philosophical Transactions. Series A, Mathematical, Physical and Engineering Sciences 373(2034), 20140099.

Porta A, Casali KR, Casali AG *et al*. (2008). Temporal asymmetries of short-term heart period variability are linked to autonomic regulation. American Journal of Physiology. Regulatory, Integrative and Comparative Physiology 295(2), R550–R557.

Porta A, Casali KR, Casali AG *et al.* (2008).. Temporal asymmetries of short-term heart period variability are linked to autonomic regulation. American Journal of Physiology-Regulatory, Integrative and Comparative Physiology 295(2), R550-R557.

Porta A, Castiglioni P, Bari V *et al*. (2013). K-nearest-neighbor conditional entropy approach for the assessment of the short-term complexity of cardiovascular control. Physiological Measurement 34(1), 17-33.

Porta A, De Maria B, Bari V *et al*. (2017). Are nonlinear model-free conditional entropy approaches for the assessment of cardiac control complexity superior to the linear model-based one? IEEE Transactions in Biomedical Engineering 64(6), 1287-1296.

Porta A, De Maria B, Cairo B *et al*. (2018). Short-term model-based multiscale complexity analysis of cardiac control provides complementary information to single-scale approaches. Conference Proceedings of the IEEE Engineering in Medicine and Biology Society 2018, 4848-4851.

Porta A, Faes L, Bari V. (2014). Effect of age on complexity and causality of the cardiovascular control: comparison between model-based and model-free approaches. PLoS One 9(2), e89463.

Porta A, Faes L, Masé M *et al*. (2007a). An integrated approach based on uniform quantization for the evaluation of complexity of short-term heart period variability: Application to 24 h Holter recordings in healthy and heart failure humans. Chaos 17(1), 015117.

Porta A, Gnecchi-Ruscone T, Tobaldini E *et al*. (2007c). Progressive decrease of heart period variability entropy-based complexity during graded head-up tilt. Journal of Applied Physiology 103(4), 1143-1149.

Porta A, Guzzetti S, Montano N *et al.* (2006a). Time reversibility in short-term heart period variability. In: Computers in Cardiology. 2006, 33, 77-80.

Porta A, Guzzetti S, N Montano N *et al*. (2001). Entropy, entropy rate, and pattern classification as tools to typify complexity in short heart period variability series. IEEE Transactions in Biomedical Engineering 48(11), 1282-1291.

Porta A, Tobaldini E, Guzzetti S *et al*. (2007b). Assessment of cardiac autonomic modulation during graded head-up tilt by symbolic analysis of heart rate variability. American Journal of Physiology. Heart and Circulatory Physiology 293(1), H702-H708.

Porta A, Valencia JF, Cairo B *et al.* (2020). Are strategies favoring pattern matching a viable way to improve complexity estimation based on sample entropy? Entropy 22(7), 724.

Pourafzal A, Fereidunian A. (2020). A Complex Systems Approach to Feature Extraction for Chaotic Behavior Recognition. In: 6th Iranian Conference on Signal Processing and Intelligent Systems (ICSPIS) 2020 Dec 23 (pp. 1-6). IEEE.

Poza J, Hornero R, Abásolo D *et al*. (2007). Analysis of spontaneous MEG activity in patients with Alzheimer's disease using spectral entropies. Conference Proceedings of the IEEE Engineering in Medicine and Biology Society 2007, 6180-6183.

Pregowska A, Proniewska K, van Dam P *et al*. (2019). Using Lempel-Ziv complexity as effective classification tool of the sleep-related breathing disorders. Computer Methods and Programs in Biomedicine 182, 105052.

Prokopenko M, Boschetti F, Ryan AJ. (2009). An information-theoretic primer on complexity, self-organization, and emergence. Complexity 15(1), 11-28.

Pu JB, Xu HH, Wang YZ *et al*. (2016). Combined nonlinear metrics to evaluate spontaneous EEG recordings from chronic spinal cord injury in a rat model: a pilot study. Cognitive Neurodynamics 10(5), 367-373.

Qi JC, Yang HJ. (2011). Hurst exponents for short time series. Physical Review E 84, 066114, 1-7.

Qiu G, Jia K. (2018. Extropy estimators with applications in testing uniformity. Journal of Nonparametric Statistics 30(1), 182-96.

Qiu G, Jia K. (2018). The residual extropy of order statistics. Statistics & Probability Letters 133, 15-22.

Qiu G, Wang L, Wang X. (2019). On extropy properties of mixed systems. Probability in the Engineering and Informational Sciences 33(3), 471-86.

Qiu G. (2017). The extropy of order statistics and record values. Statistics & Probability Letters 120, 52-60.

Racz FS, Stylianou O, Mukli P *et al*. (2018). Multifractal dynamic functional connectivity in the resting-state brain. Frontiers in Physiology 9, 1704

Radhakrishnan S, Kamarthi S. (2016). Complexity-entropy feature plane for gear fault detection. In: IEEE International Conference on Big Data (Big Data) 2016 Dec 5 (pp. 2057-2061).

Raffalt PC, Alkjær T, Brynjólfsson B *et al*. (2018a). Day-to-day reliability of nonlinear methods to assess walking dynamics. Journal of Biomechanical Engineering 140(12), 124501.

Raffalt PC, Denton W, Yentes JM. (2018b). On the choice of multiscale entropy algorithm for quantification of complexity in gait data. Computers in Biology and Medicine 103, 93-100.

Raffalt PC, Kent JA, Wurdeman SR *et al*. (2019). Selection procedures for the largest Lyapunov exponent in gait biomechanics. Annals of Biomedical Engineering 47(4), 913-923.

Raffalt PC, Senderling B, Stergiou N. (2020). Filtering affects the calculation of the largest Lyapunov exponent. Computers in Biology and Medicine 122, 103786.

Raghavendra BS, Dutt DN. (2009). A note on fractal dimensions of biomedical waveforms. Computers in Biology and Medicine 39(11) 1006-1012.

Raghavendra BS, Dutt DN. (2008). Multiresolution area-based fractal dimension estimation of signals applied to EEG data. In TENCON 2008-2008 IEEE Region 10 Conference 2008 Nov 19 (pp. 1-5).

Raghavendra BS, Dutt ND. (200). Computing fractal dimension of signals using multiresolution box-counting method. International Journal of Information and Mathematical Sciences 6(1), 50-65.

Raghavendra BS, Dutt ND. (2011). Multiscale fractal dimension technique for characterization and analysis of biomedical signals. In: Digital Signal Processing and Signal Processing Education Meeting (DSP/SPE). 2011, 370-34.

Rahman MM, Bhuiyan MIH, Hassan AR. (2018). Sleep stage classification using single-channel EOG. Computers in Biology and Medicine 102, 211-220.Rahmani B, Wong CK, Norouzzadeh P. (2018). Dynamical Hurst analysis identifies EEG channel differences between PTSD and healthy controls. PLoS One 13(7), e0199144.

Rahmawati D, Rizal A, Silalahi DK. (2021). Combination of Coarse-Grained Procedure and Fractal Dimension for Epileptic EEG Classification. IJCCS (Indonesian Journal of Computing and Cybernetics Systems) 15(4), 427-438.

Rajaram R, Castellani B, Wilson AN. (2017). Advancing Shannon entropy for measuring diversity in systems. Complexity 2017, 8715605.

Rajković M. (2004). Entropic nonextensivity as a measure of time series complexity. Physica A: Statistical Mechanics and its Applications 340(1-3), 327 – 333.

Ramdani S, Bouchara F, Lagarde J. (2009). Influence of noise on the sample entropy algorithm. Chaos 19(1), 013123.

Ramírez-Parietti I, Contreras-Reyes JE, Idrovo-Aguirre BJ. (2021). Cross-sample entropy estimation for time series analysis: a nonparametric approach. Nonlinear Dynamics 105(3), 2485-2508.

Ramírez-Reyes A, Hernández-Montoya AR, Herrera-Corral G *et al*. (2016). Determining the entropic index q of Tsallis entropy in images through redundancy. Entropy 18(8), 299; 1-14.

Rampichini S, Vieira TM, Castiglioni P *et al.* (2020). Complexity analysis of surface electromyography for assessing the myoelectric manifestation of muscle fatigue: A review. Entropy 22(5), 529,1-31.

Rani TG, Jayalalitha G, Thiagarajan K. (2016). Size measure relationship for speech recognition. International Journal of Advanced Engineering Technology 7(2), 15-17.

Ranuzzi G, Bari V, De Maria B *et al.* (2017). Stratifying the risk of developing atrial fibrillation after coronary artery bypass graft surgery using heart rate asymmetry indexes. In: Computing in Cardiology (CinC) 2017 Sep 24; 44, 1-4. IEEE. 2017

Rapp PE, Cellucci CJ, Watanabe TAA *et al*. (2005). Quantitative characterization of the complexity of multichannel human EEGs. International Journal of Bifurcation and Chaos 15(5), 1737–1744.

Raqab MZ, Qiu G. (2019). On extropy properties of ranked set sampling. Statistics 53(1), 210-26.

Rebelo AC, Tamburús N, Salviati M *et al*. (2011). Influence of third-generation oral contraceptives on the complexity analysis and symbolic dynamics of heart rate variability. European Journal of Contraception and Reproductive Health Care 16(4), 289-297.

Ren G, Aleed Y, Kinsner W *et al.* (2018). Evaluation of walking ability using variance fractal dimension trajectory. Proceedings of the 5th International Conference of Control, Dynamic Systems, and Robotics (CDSR'18), Niagara Falls, Canada – June 7 – 9, 2018, Paper No. 132, 128-1 to 128-8 DOI: 10.11159/cdsr18.132

Ren P, Zhao WH, Zhao ZY *et al*. (2016). Analysis of gait rhythm fluctuations for neurodegenerative diseases by phase synchronization and conditional entropy. IEEE Transactions on Neural Systems and Rehabilitation Engineering 24(2), 291-299.

Rényi A. (1961). On measures of information and entropy. Proceedings of the fourth Berkeley Symposium on Mathematics, Statistics and Probability 1960, 547–561.

Reulecke S, Charleston-Villalobos S, Voss A *et al*. (2015). Temporal analysis of cardiac autonomic regulation during orthostatic challenge by short-term symbolic dynamics. Conference Proceedings of the IEEE Engineering in Medicine and Biology Society 2015, 2067-2070.

Reulecke S, Charleston-Villalobos S, Voss A *et al*. (2018). Temporal analysis of cardiovascular and respiratory complexity by multiscale entropy based on symbolic dynamics. IEEE Journal of Biomedical and Health Informatics 22(4),1046-1058.

Reyes-Lagos JJ, Pliego-Carrillo AC, Ledesma-Ramírez CI *et al*. (2020). Phase entropy analysis of electrohysterographic data at the third trimester of human pregnancy and active parturition. Entropy 22(8), 798.

Rezek IA, Roberts SJ. (1998). Stochastic complexity measures for physiological signal analysis. IEEE Transactions in Biomedical Engineering 45(9), 1186-1191.

Rhea CK, Kiefer AW, Wright WG *et al*. (2015). Interpretation of postural control may change due to data processing techniques. Gait and Posture 41(2), 731-735.

Rhea CK, Silver TA, Hong SL *et al*. (2011). Noise and complexity in human postural control: interpreting the different estimations of entropy. PLoS One 6(3), e17696.

Ribeiro HV, Zunino L, Mendes RS *et al.* (2012).. Complexity–entropy causality plane: A useful approach for distinguishing songs. Physica A: Statistical Mechanics and its Applications 391(7), 2421-8.

Richman JS, Moorman JR. (2000). Physiological time-series analysis using approximate entropy and sample entropy. American Journal of Physiology. Heart and Circulatory Physiology 278(6), H2039-2049.

Riedl M, Müller A, Wessel N. (2013). Practical considerations of permutation entropy: a tutorial review. European Physical Journal Special Topics 222(2), 249–262.

Rivolta MW, Migliorini M, Aktaruzzaman M *et al*. (2014). Effects of the series length on Lempel-Ziv complexity during sleep. Conference Proceedings of the IEEE Engineering in Medicine and Biology Society 2014, 693-696.

Rohila A, Sharma A. (2019). Phase entropy: a new complexity measure for heart rate variability. Physiological Measurement 40(10), 105006, 1-11.

Rohila A, Sharma A. (2020). Asymmetric spread of heart rate variability. Biomedical Signal Processing and Control 60, 101985, 1-11.

Rohila A, Sharma A. (2020). Asymmetric spread of heart rate variability. Biomedical Signal Processing and Control. 2020 Jul 1;60, 101985. 2020a

Rohila A, Sharma A. (2020). Correlation Between Heart Rate Variability Features. In: 7th International Conference on Signal Processing and Integrated Networks (SPIN) 2020 Feb 27 (pp. 669-674). IEEE.

Rolink J, Kutz M, Fonseca P *et al.* (2015). Recurrence quantification analysis across sleep stages. Biomedical Signal Processing and Control 20, 107-16.

Röschke J, Fell J, Beckmann P. (1995). Nonlinear analysis of sleep EEG in depression: calculation of the largest Lyapunov exponent. European Archives of Psychiatry and Clinical Neuroscience 245(1), 27-35.

Rose MH, Bandholm T, Jensen BR. (2009). Approximate entropy based on attempted steady isometric contractions with the ankle dorsal- and plantarflexors: reliability and optimal sampling frequency. Journal of Neuroscience Methods 177(1), 212-216.

Rosenstein MT, Collins JJ, De Luca CJ. (1993). A practical method for calculating largest Lyapunov exponents from small data sets. Physica D: Nonlinear Phenomena 65(1-2), 117-134.

Rosso OA, Blanco S, Yordanova J *et al.* (2001). Wavelet entropy: a new tool for analysis of short duration brain electrical signals. Journal of neuroscience methods 105(1), 65-75.

Rosso OA, Larrondo HA, Martın MT *et al*. (2007). Distinguishing noise from chaos. Physical Review Letters 99(15), 154102,:1–154102:4.

Rosso OA, Larrondo HA, Martin MT *et al.* (2007). Distinguishing noise from chaos. Physical Review Letters 99(15), 154102.

Rosso OA, Martin MT, Plastino A. (2005). Evidence of self-organization in brain electrical activity using wavelet-based informational tools. Physica A: Statistical Mechanics and its Applications 347, 444-64.

Rostaghi M, Azami H. (2016). Dispersion entropy: a measure for time-series analysis. IEEE Signal Processing Letters 23(5), 610-614.

Rubin D, Fekete T, Mujica-Parodi LR. (2013). Optimizing complexity measures for FMRI data: algorithm, artifact, and sensitivity. PLoS One 8(5), e63448.

Ruiz-Gómez SJ, Gómez C, Poza J *et al*. (2018). Measuring alterations of spontaneous EEG neural coupling in Alzheimer's disease and mild cognitive impairment by means of cross-entropy metrics. Frontiers in Neuroinformatics 12, 76.

Sá PM, Castro HA, Lopes AJ *et al.* (2019). Entropy analysis for the evaluation of respiratory changes due to asbestos exposure and associated smoking. Entropy 21(3), 225,1-17.

Sabeti M, Katebi S, Boostani R. (2009). Entropy and complexity measures for EEG signal classification of schizophrenic and control participants. Artificial Intelligence in Medicine 47(3), 263-274.

Salazar-Varas R, Vazquez RA. (2019). Facing high EEG signals variability during classification using fractal dimension and different cutoff frequencies. Computational Intelligence and Neuroscience 2019, 9174307.

Salazar-Varas R, Vazquez RA. (2019). Facing high EEG signals variability during classification using fractal dimension and different cutoff frequencies. Computational Intelligence and Neuroscience 2019, 9174307, 1-12.

Santamaría-Bonfil G, Fernández N *et al.* (2016). Measuring the complexity of continuous distributions. Entropy 18(3), 72.

Santamaría-Bonfil G, Gershenson C, Fernández N. ()2017. A Package for Measuring emergence, Self-organization, and Complexity Based on Shannon entropy. Frontiers in Robotics and AI ;4, 10.

Šapina M, Karmakar CK, Kramarić K *et al*. (2018). Multi-lag tone-entropy in neonatal stress. Journal of the Royal Society, Interface 15(146), 20180420, 1-8.

Sarbaz Y, Towhidkhah F, Jafari A *et al.* (2012). Do the chaotic features of gait change in Parkinson's disease? Journal of Theoretical Biology 307, 160-167.

Sarlabous L, Estrada L,Cerezo-Hernández A *et al*. (2019). Electromyography-based respiratory onset detection in copd patients on non-invasive mechanical ventilation. Entropy 21(3), 258, 1-15.

Sarlabous L, Torres A, Fiz JA *et al*. (2009). Multistate Lempel-Ziv (MLZ) index interpretation as a measure of amplitude and complexity changes. Conference Proceedings of the IEEE Engineering in Medicine and Biology Society 2009, 4375-4378.

Sarlabous L, Torres A, Fiz JA *et al*. (2014). Evidence towards improved estimation of respiratory muscle effort from diaphragm mechanomyographic signals with cardiac vibration interference using sample entropy with fixed tolerance values. PLoS One 9(2), e88902, 1-9.

Sathar EA, Nair RD. (2021). On dynamic weighted extropy. Journal of Computational and Applied Mathematics 393, 113507.

Satti R, Abid NUH, Bottaro M *et al*. (2019). The application of the extended Poincaré plot in the analysis of physiological variabilities. Frontiers in Physiology 10, 116.

Scafetta N, Grigolini P. (2002). Scaling detection in time series: diffusion entropy analysis. Physical Review. E, Statistical, Nonlinear, and Soft Matter Physics 66(3 Pt 2A), 036130, 1-21.

Scafetta N, Hamilton P, Grigolini P. (2001). The thermodynamics of social processes: the teen birth phenomenon. Fractals 9(2), 193-208.

Schepers HE, van Beek JHGM, Bassingthwaighte JB. (1992). Four methods to estimate the fractal dimension from self-affine signals. IEEE Engineering in Medicine and Biology Magazine 11(2), 57-64.

Schinkel S, Dimigen O, Marwan N. (2008). Selection of recurrence threshold for signal detection. European Physical Journal. Special Topics 164, 45–53.

Schneider F, Martin J, Hapfelmeier A *et al*. (2017). The validity of linear and non-linear heart rate metrics as workload indicators of emergency physicians. PLoS One 12(11), e0188635.

Schneider M, Mustaro PN, Lima CA. (2009). Automatic recognition of epileptic seizure in EEG via support vector machine and dimension fractal. In: International Joint Conference on Neural Networks 2009 Jun 14 (pp. 2841-2845). IEEE.

Schulz S, Koschke M, Bär KJ *et al*. (2010). The altered complexity of cardiovascular regulation in depressed patients. Physiological Measurement 31(3), 303-321.

Sevcik C. (198). A procedure to estimate the fractal dimension of waveforms. Complexity International 5, 1-19. arXiv preprint arXiv:1003.5266. 2010 Mar 27.

Shabani H, Mikaili M, Noori TRMS. (2016). Assessment of recurrence quantification analysis (RQA) of EEG for development of a novel drowsiness detection system. Biomedical Engineering Letters 6(3), 196-204.

Shannon CE. (1948). A mathematical theory of communication. Bell System Technical Journal 27(3), 379–423; 27(4), 623–656.

Sharanya B, Murali L, Manigandan T. (2014). Adaptive filtering of EEG and epilepsy detection using recurrence quantification analysis. IEEE International Conference on Advanced Communications, Control and Computing Technologies 2014, 1316-1320.

Sharma N, Kolekar MH, Jha K. (2020). Iterative filtering decomposition based early dementia diagnosis using EEG with cognitive tests. IEEE Transactions on Neural Systems and Rehabilitation Engineering 2020, (accepted for publication).

Sharmila M, Goyal D, Achuth PV *et al*. (2018). An accurate sleep stages classification system using a new class of optimally time-frequency localized three-band wavelet filter bank. Computers in Biology and Medicine 98, 58-75.

Shelhamer M. (1997). On the correlation dimension of optokinetic nystagmus eye movements: computational parameters, filtering, nonstationarity, and surrogate data. Biological Cybernetics 76(4), 237-250.

Shen EH, Cai ZJ, Gu FJ. (205). Mathematical foundation of C0 complexity. Applied Mathematics and Mechanics 26(9), 1083-1090.

Shi B, Wang LL, Yan C *et al.* (2019). Nonlinear heart rate variability biomarkers for gastric cancer severity: A pilot study. Scientific Reports 9(1), 1-9. 2019

Shi B, Zhang YD, Yuan CC *et al*. (2017). Entropy analysis of short-term heartbeat interval time series during regular walking. Entropy 19(10), 568, 1-14.

Shi CT. (2018). Signal pattern recognition based on fractal features and machine learning. Applied Sciences 8(8), 1327, 1-15.

Shi LC, Jiao YY, Lu BL. (2013). Differential entropy feature for EEG-based vigilance estimation. Conference Proceedings of the IEEE Engineering in Medicine and Biology Society 2013, 6627-6630.

Shi MH, He HX, Geng WC *et al*. (2020). Early detection of sudden cardiac death by using ensemble empirical mode decomposition-based entropy and classical linear features from heart rate variability signals. Frontiers in Physiology 11, 118.

Shi MH, Zhan CY, He HX *et al*. (2019). Renyi distribution entropy analysis of short-term heart rate variability signals and its application in coronary artery disease detection. Frontiers in Physiology 10, 809.

Shi P, Zhu YS, Allen J *et al*. (2009). Analysis of pulse rate variability derived from photoplethysmography with the combination of lagged Poincaré plots and spectral characteristics. Medical Engineering and Physics 31(7), 866-871.

Shi QX, Liu A, Chen RY *et al.* (2020). Depression Detection using Resting State Three-channel EEG Signal. arXiv preprint arXiv, 2002.09175. 2020 Feb 21.

Shumbayawonda E, Abásolo D, López-Sanz D *et al.* (2019). Sex differences in the complexity of healthy older adults' magnetoencephalograms. Entropy 21(8), 798.

Siddiqui MK, Morales-Menendez R, Huang X *et al.* (2020). A review of epileptic seizure detection using machine learning classifiers. Brain informatics 7(1), 1-8.

Signorelli CM, Meling D. (2021). Towards new concepts for a biological neuroscience of consciousness. Cognitive Neurodynamics 15(5), 783-804.

Signorini MG, Ferrario M, Marchetti M *et al*. (2006). Nonlinear analysis of heart rate variability signal for the characterization of cardiac heart failure patients. Conference Proceedings of the IEEE Engineering in Medicine and Biology Society 2006, 3431-3434.

Silva LEV, Geraldini RZ, de Oliveira BP *et al*. (2017). Comparison between spectral analysis and symbolic dynamics for heart rate variability analysis in the rat. Scientific Reports 7(1), 8428.

Silva LEV, Lataro RM, Castania JA *et al*. (2016). Multiscale entropy analysis of heart rate variability in heart failure, hypertensive, and sinoaortic-denervated rats: classical and refined approaches. American Journal of Physiology. Regulatory, Integrative and Comparative Physiology 311(1), R150-R156.

Simons S, Abasolo D, Escudero J. (2015). Classification of Alzheimer's disease from quadratic sample entropy of electroencephalogram. Healthcare Technology Letters 2(3), 70-73.

Simons S, Abásolo D. (2017). Distance-based Lempel–Ziv complexity for the analysis of electroencephalograms in patients with Alzheimer's disease. Entropy 19(3), 129.Sinai Y. (2009). Kolmogorov-Sinai entropy. Scholarpedia 4(3), 2034. (http://www.scholarpedia.org/article/Kolmogorov-Sinai_entropy) [Retrieved July 31, 2020].

Skinner JE, Carpeggiani C, Landisman CE *et al*. (1991). Correlation dimension of heartbeat intervals is reduced in conscious pigs by myocardial ischemia. Circulation Research 68(4),966-976.

Śmigiel S, Pałczyński K, Ledziński D. (2021). Deep Learning Techniques in the Classification of ECG Signals Using R-Peak Detection Based on the PTB-XL Dataset. Sensors 21(24), 8174.

Śmigiel S, Pałczyński K, Ledziński D. (2021). ECG signal classification using deep learning techniques based on the PTB-XL dataset. Entropy 23(9), 1121.

Smith Hussain V, Spano ML, Lockhart TE. (2020). Effect of data length on time delay and embedding dimension for calculating the Lyapunov exponent in walking. Journal of the Royal Society, Interface 17(168), 20200311.

Smits FM, Porcaro C, Cottone C *et al*. (2016). Electroencephalographic fractal dimension in healthy ageing and Alzheimer's disease. PLoS One 11(2), e0149587.

Sneddon R. (2007). The Tsallis entropy of natural information. Physica A: Statistical Mechanics and its Applications 386(1), 101-118.

Sokunbi MO, Cameron GG, Ahearn TS *et al*. (2015). Fuzzy approximate entropy analysis of resting state fMRI signal complexity across the adult life span. Medical Engineering and Physics 37(11), 1082-1090.

Soloviev V, Serdiuk O, Semerikov S *et al.* (2020). Recurrence plot-based analysis of financial-economic crashes. CEUR Workshop Proceedings 2020, 21-40.

Song Y, Crowcroft J, Zhang J. *et al.* (2012). Automatic epileptic seizure detection in EEGs based on optimized sample entropy and extreme learning machine. Journal of Neuroscience Methods 210(2), 132-146.

Soundirarajan M, Augustynek M, Krejcar O *et al.* (2021). Evaluation of the correlation between facial muscle and brain activities in auditory stimulation. Fractals 29(01), 2150100.

Spasić S, Kalauzi A, Culić M *et al*. (2005). Estimation of parameter kmax in fractal analysis of rat brain activity. Annals of the New York Academy of Sciences 1048, 427-429.

Stadnitski T. (2012). Measuring fractality. Frontiers in Physiology 3, 127.

Stam CJ, de Bruin EA. (2004). Scale-free dynamics of global functional connectivity in the human brain. Human Brain Mapping 22(2), 97-109.

Stam CJ, Jelles B, Achtereekte HA, *et al*. (1995). Investigation of EEG non-linearity in dementia and Parkinson's disease. Electroencephalography and Clinical Neurophysiology 95(5), 309-317.

Stam CJ, van Woerkom TC, Pritchard WS. (1996). Use of non-linear EEG measures to characterize EEG changes during mental activity. Electroencephalography and Clinical Neurophysiology 99(3), 214-224.

Steffert T, Mayor D. (2014). The fickleness of data: estimating the effects of different aspects of acupuncture treatment on heart rate variability (HRV). Initial findings from three pilot studies. Poster presentation, 16th International Acupuncture Research Symposium, London,

29 March (http://electroacupuncture.qeeg.co.uk/wp-content/uploads/2018/03/HRV-poster-background-ARRC-2014.pdf) [Retrieved September 21, 2020].

Stepien RA, Klonowski W, Androsiuk W. (2007). New symbolic method for studying brain connectivity during sleep onset. International Journal of Bioelectromagnetism 9(4), 260-264.

Strang AJ, Best C, Funke GJ. (2014). Heart rate correlates of mental workload in a large-scale air-combat simulation training exercise. Proceedings of the Human Factors and Ergonomics Society Annual Meeting 58, 2325-2329.

Struzik ZR, Hayano J, Seiichiro Sakata S. *et al*. (2004). 1/f scaling in heart rate requires antagonistic autonomic control. Physical Review. E, Statistical, Nonlinear, and Soft Matter Physics 70(5 Pt 1), 050901.

Sun R, Wong W-W, Wang J *et al*. (2017). Changes in electroencephalography complexity using a brain computer interface-motor observation training in chronic stroke patients: a fuzzy approximate entropy analysis. Frontiers in Human Neuroscience 11, 444, 1-13.

Sung PS, Zurcher U, Kaufman M. (2007). Comparison of spectral and entropic measures for surface electromyography time series: a pilot study. Journal of Rehabilitation Research and Development 44(4), 599-609.

Supriya S, Siuly S, Wang H *et al.* (2020). Automated epilepsy detection techniques from electroencephalogram signals: a review study. Health Information Science and Systems 8(1), 1-5.

Sürücü CE, Güner S, Cüce C *et al.* (2021). The effects of six-week slow, controlled breathing exercises on heart rate variability in physically active, healthy individuals. Pedagogy of Physical Culture and Sports 25(1), 4-9.

Tahmasebi S, Toomaj A. (2020). On negative cumulative extropy with applications. Communications in Statistics-Theory and Methods. 2020 Oct 13, 1-23.

Takahashi T, Cho RY, Murata T *et al*. (2009). Age-related variation in EEG complexity to photic stimulation: a multiscale entropy analysis. Clinical Neurophysiology 120(3), 476–483.

Takens F. (1981). Detecting strange attractors in turbulence. In: Rand DA, Young LS (Eds.). Dynamical Systems and Turbulence. Lecture Notes in Mathematics 898. Berlin: Springer-Verlag, 366–381.

Tamulevičius G, Karbauskaitė R, Dzemyda G. (2019). Speech emotion classification using fractal dimension-based features. Nonlinear Analysis: Modelling and Control 24(5), 679-95.

Tang SC, Jen HI, Lin YH *et al*. (2015). Complexity of heart rate variability predicts outcome in intensive care unit admitted patients with acute stroke. Journal of Neurology, Neurosurgery, and Psychiatry 86(1), 95-100.

Tang Y, Li L, Liu X. (2021). State-of-the-Art Development of Complex Systems and Their Simulation Methods. Complex System Modeling and Simulation 1(4), 271-90.

Tantisatirapong S, Senavongse W, Phothisonothai M. (2010). Fractal dimension-based electroencephalogram analysis of drowsiness patterns. In: ECTI-CON2010: ECTI International Conference on Electrical Engineering/Electronics, Computer, Telecommunications and Information Technology 2010 May 19 (pp. 497-500). IEEE.

Tarvainen MP, Lipponen J, Niskanen J-P *et al*. (2019). Kubios HRV (ver. 3.2) User's Guide. Kuopio: Kubios Oy.

Tavasoli M, Einalou Z, Akhondzadeh R. (2021). Dynamic Analysis of Human Brain in the Pain State by Electroencephalography. Research Square. https://doi.org/10.21203/rs.3.rs-275018/v1.

Teixeira JP, Oliveira C, Lopes C. (2013). Vocal acoustic analysis–jitter, shimmer and HNR parameters. Procedia Technology 9, 1112-22. https://doi.org/10.1016/J.PROTCY.2013.12.124

Terrier P. (2019). Complexity of human walking: the attractor complexity index is sensitive to gait synchronization with visual and auditory cues. PeerJ 7, e7417.

Terrill PI, Wilson SJ, Suresh S *et al*. (2009). Characterising infant inter-breath interval patterns during active and quiet sleep using recurrence plot analysis. Conference Proceedings of the IEEE Engineering in Medicine and Biology Society 2009, 6284-6287.

Tewatia DK, Tolakanahalli RP, Paliwal BR *et al*. (2011). Time series analyses of breathing patterns of lung cancer patients using nonlinear dynamical system theory. Physics in Medicine and Biology 56(7), 2161-2181.

Thai Q. (2020). calc_lz_complexity. MATLAB Central File Exchange (https://www.mathworks.com/matlabcentral/fileexchange/38211-calc_lz_complexity) [Retrieved August 25, 2020].

Thakre TP, Michael L Smith ML. (2006). Loss of lag-response curvilinearity of indices of heart rate variability in congestive heart failure. BMC Cardiovascular Disorders 6, 27.

Thiel M, Romano MC, Read PL *et al*. (2004). Estimation of dynamical invariants without embedding by recurrence plots. Chaos 14, 234-243.

Thuraisingham RA. (2016). Development of an alert system for subjects with paroxysmal atrial fibrillation. Journal of Arrhythmia 32(1), 57-61.

Tietäväinen A, Kuvaldina M, Hæggström E. (2018). Nintendo Wii fit-based sleepiness testing is not impaired by contagious sleepiness. Safety and Health at Work 9(2), 236-238.

Tobaldini E, Montano N, Wei SG *et al*. (2009). Autonomic cardiovascular modulation: symbolic analysis of the effects of central mineralocorticoid receptor antagonist in heart failure rats. IEEE Engineering in Medicine and Biology Magazine 28(6), 79-85

Tobaldini E, Porta A, Bulgheroni M *et al*. (2008). Increased complexity of short-term heart rate variability in hyperthyroid patients during orthostatic challenge. Conference Proceedings of the IEEE Engineering in Medicine and Biology Society 2008, 1988-1991.

Tomčala J. (2019). Acceleration of time series entropy algorithms. Journal of Supercomputing 75(3), 1443-1454.

Tomčala J. (2020). New fast ApEn and sampen entropy algorithms implementation and their application to supercomputer power consumption. Entropy 22(8), 863.

Tong QY, Kong J, Xu JH. (1996). A note on analyzing schizophrenic EEG with complexity measure. Chaos, Solitons & Fractals 7(3), 371-5.

Tong SB, Hong B, Vigderman L *et al*. (2004). Subband EEG complexity after global hypoxic-ischemic brain injury. Conference Proceedings of the IEEE Engineering in Medicine and Biology Society 2006, 562-565.

Tonhajzerova I, Ondrejka I, Chladekova L *et al*. (2012). Heart rate time irreversibility is impaired in adolescent major depression. Progress in Neuro-Psychopharmacology and Biological Psychiatry 39(1), 212-217.

Tonhajzerová I, Ondrejka I, Farsky I *et al*. (2014). Attention deficit/hyperactivity disorder (ADHD) is associated with altered heart rate asymmetry. Physiological Research 63(Suppl 4), S509-S519.

Tonoyan Y, Chanwimalueang T, Mandic DP *et al*. (2017). Discrimination of emotional states from scalp- and intracranial EEG using multiscale Rényi entropy. PLoS One 12(11), e0186916.

Toprak A, Güler I. (2007). Impulse noise reduction in medical images with the use of switch mode fuzzy adaptive median filter. Digital Signal Processing 17, 711–723.

Torres A, Fiz JA, Jane R *et al*. (2008). Rényi entropy and Lempel-Ziv complexity of mechanomyographic recordings of diaphragm muscle as indexes of respiratory effort. Conference Proceedings, IEEE Engineering in Medicine and Biology Society 2008, 2112-2115.

Tosun PD, Abásolo D, Stenson G *et al*. (2017). Characterisation of the effects of sleep deprivation on the electroencephalogram using Permutation Lempel–Ziv Complexity, a non-linear analysis tool. Entropy 19(12), 673.

Tosun PD, Dijk DJ, Winsky-Sommerer R *et al*. (2019). Effects of ageing and sex on complexity in the human sleep EEG: A comparison of three symbolic dynamic analysis methods. Complexity. 2019 Jan 2;2019.

Trimer R, Mendes RG, Costa FSM *et al*. (2014). Is there a chronic sleep stage-dependent linear and nonlinear cardiac autonomic impairment in obstructive sleep apnea? Sleep and Breathing 18(2), 403-409.

Trulla LL, Giuliani A, Zbilut JP *et al*. (1996). Recurrence quantification analysis of the logistic equation with transients. Physics Letters, A 223(4), 255–260.

Tsai C-H, Ma H-P, Lin Y-T *et al*. (2019). Heart rhythm complexity impairment in patients with pulmonary hypertension. Scientific Reports 9(1), 10710, 1-8.

Tsai PH, Lin C, Tsao JH *et al*. (2012). Empirical mode decomposition based detrended sample entropy in electroencephalography for Alzheimer's disease. Journal of Neuroscience Methods 210(2), 230-237.

Tsallis C. (1988). Possible generalization of Boltzmann-Gibbs statistics. Journal of Statistical Physics 52(1–2), 479–487.

Tsivgoulis SD, Papagelopoulos PJ, Efstathopoulos N *et al*. (2009). Accelerometry for evaluation of gait pattern in healthy soccer athletes. Journal of International Medical Research 37(6), 1692-1700.

Tupaika N, Vallverdu M, Jospin M *et al*. (2010). Assessment of the depth of anesthesia based on symbolic dynamics of the EEG. Annual International Conference of the IEEE Engineering in Medicine and Biology Society (EMBC) 2010, 5971-5974.

Udhayakumar RK, Karmakar C, Li P *et al*. (2016a). Influence of embedding dimension on distribution entropy in analyzing heart rate variability. Conference Proceedings, IEEE Engineering in Medicine and Biology Society 2016, 6222-6225.

Udhayakumar RK, Karmakar C, Li P *et al*. (2016b). Effect of embedding dimension on complexity measures in identifying arrhythmia. Conference Proceedings, IEEE Engineering in Medicine and Biology Society 2016, 6230-6233.

Udhayakumar RK, Karmakar C, Palaniswami M (2019). Multiscale entropy profiling to estimate complexity of heart rate dynamics. Physical Review E 100(1-1), 012405.

Udhayakumar RK, Karmakar C, Palaniswami M. (2017). Approximate entropy profile: a novel approach to comprehend irregularity of short-term HRV signal. Nonlinear Dynamics. 88(2), 823-837. 2017b

Udhayakumar RK, Karmakar C, Palaniswami M. (2019c). Cross entropy profiling to test pattern synchrony in short-term signals. In: 2019 41st Annual International Conference of the IEEE Engineering in Medicine and Biology Society (EMBC) 2019 Jul 23 (pp. 737-740).

Udhayakumar RK, Karmakar C, Palaniswami M. (2019a). Entropy profiling to detect ST change in heart rate variability signals. In: 41st Annual International Conference of the IEEE Engineering in Medicine and Biology Society (EMBC) 2019 Jul 23 (pp. 4588-4591).

Udhayakumar RK, Karmakar C, Palaniswami M. (2019b). Multiscale entropy profiling to estimate complexity of heart rate dynamics. Physical Review E 100(1), 012405.

Udhayakumar RK, Karmakar C, Palaniswami M. (2017a). Secondary measures of regularity from an entropy profile in detecting arrhythmia. In:39th Annual International Conference of the IEEE Engineering in Medicine and Biology Society (EMBC) 2017 Jul 11 (pp. 3485-3488).

Udhayakumar RK, Karmakar C, Palaniswami M. (2018). Understanding irregularity characteristics of short-term HRV signals using sample entropy profile. IEEE Transactions on Biomedical Engineering 65(11), 2569-2579.

Udhayakumar RK. (2019). Analysing Irregularity and Complexity in Short-length Heart Rate Variability Signals. PhD Thesis, Department of Electrical and Electronic Engineering, University of Melbourne.

Unakafov AM, Keller K. (2014). Conditional entropy of ordinal patterns. Physica D: Nonlinear Phenomena 269, 94-102.

Unakafova VA, Keller K. (2013). Efficiently measuring complexity on the basis of real-world data. Entropy 15(10), 4392-4415.

Valencia JF, Bolaños JD, Vallverdú M *et al*. (2019). Refined multiscale entropy using fuzzy metrics: Validation and application to nociception assessment 21(7), 706.

Valencia JF, Vallverdú M, Porta A, *et al*. (2013). Ischemic risk stratification by means of multivariate analysis of the heart rate variability. Physiological Measurement 34(3), 325-338.

Valencia JF, Vallverdu M, Rivero I *et al*. (2015). Symbolic dynamics to discriminate healthy and ischaemic dilated cardiomyopathy populations: an application to the variability of heart period and QT interval. Philosophical Transactions. Series A Mathematical, Physical, and Engineering Sciences 373(2034), 20140092.

Valencia M, Artieda J, Alegre M *et al*. (2008). Influence of filters in the detrended fluctuation analysis of digital electroencephalographic data. Journal of Neuroscience Methods 170(2), 310-316.

Valente M, Javorka M, Turianikova Z *et al*. (2017). Cardiovascular and respiratory variability during orthostatic and mental stress: a comparison of entropy estimators. Annual International Conference of the IEEE Engineering in Medicine and Biology Society (EMBC) 2017, 3481-3484.

Valenza G, Citi L, Scilingo EP *et al*. (2014). Inhomogeneous point-process entropy: an instantaneous measure of complexity in discrete systems. Physical Review. E, Statistical, Nonlinear, and Soft Matter Physics 89(5), 052803.

Van Albada SJ, Rennie CJ, Robinson PA. (2007). Variability of model-free and model-based quantitative measures of EEG. Journal of Integrative Neuroscience 6(2), 279-307.

van Cappellen van Walsum A-M, Pijnenburg YAL, Berendse HW *et al*. (2003). A neural complexity measure applied to MEG data in Alzheimer's disease. Clinical Neurophysiology 114(6), 1034-1040.

van Erven T, Harremoës P. (2007). Rényi divergence and Kullback-Leibler divergence. Journal of Latex Class Files 6(1), 1-24.

Vanluchene AL, Vereecke H, Thas O *et al*. (2004). Spectral entropy as an electroencephalographic measure of anesthetic drug effect: a comparison with bispectral index and processed midlatency auditory evoked response. Anesthesiology 101(1), 34-42.

Visnovcova Z, Mestanik M, Javorka M *et al*. (2014). Complexity and time asymmetry of heart rate variability are altered in acute mental stress. Physiological measurement 35(7), 1319-1334. 2014

Vlemincx E, Vigo D, Vansteenwegen D *et al*. (2013). Do not worry, be mindful: effects of induced worry and mindfulness on respiratory variability in a nonanxious population. International Journal of Psychophysiology 87(2), 147-1451.

von Borell E, Langbein J, Després G *et al*. (2007). Heart rate variability as a measure of autonomic regulation of cardiac activity for assessing stress and welfare in farm animals – a review. Physiology and Behavior 92(3), 293-316.

Von Tscharner V, Zandiyeh P. (2017). Multi-scale transitions of fuzzy sample entropy of RR-intervals and their phase-randomized surrogates: a possibility to diagnose congestive heart failure. Biomedical Signal Processing and Control 31, 350-356.

Voss A, Hnatkova K, N Wessel N *et al*. (1998). Multiparametric analysis of heart rate variability used for risk stratification among survivors of acute myocardial infarction. Pacing and Clinical Electrophysiology: PACE 21(1 Pt 2), 186-192.

Voss A, Kurths J, Kleiner HJ *et al*. (1995). Improved analysis of heart rate variability by methods of nonlinear dynamics. Journal of Electrocardiology 28 Suppl, 81-88.

Voss A, 90Kurths J, Kleiner HJ *et al*. (1996). The application of methods of non-linear dynamics for the improved and predictive recognition of patients threatened by sudden cardiac death. Cardiovascular Research 31(3), 419-433.

Voss A, Schulz S, Schroeder R *et al*. (2009). Methods derived from nonlinear dynamics for analysing heart rate variability. Philosophical Transactions. A, Mathematical, Physical and Engineering Sciences 367(1887), 277-296.

Wajnsztejn R, Dias de Carvalho T, Garner DM *et al*. (2016). Higuchi fractal dimension applied to RR intervals in children with Attention Deficit Hyperactivity Disorder. Journal of Human Growth and Development 26(2), 147-153.

Wang DY, Jin ND. (2020). Multivariate multiscale increment entropy: a complexity measure for detecting flow pattern transition in multiphase flows. Nonlinear Dynamics 100(4), 3853-3865.

Wang J. (2021). Complexity behaviors of volatility dynamics for stochastic Potts financial model. Nonlinear Dynamics 05(1), 1097-119.

Wang LM, Schonfeld D. (2009). Mapping equivalence for symbolic sequences: theory and applications. IEEE Transactions on Signal Processing 57(12), 4895-4905.

Wang X, Liu X, Pang W *et al*. (2022). Multiscale increment entropy: An approach for quantifying the physiological complexity of biomedical time series. Information Sciences. 586, 279-293.

Wang XP, Li YY. (2016). Improving classification accuracy of heart sound recordings by wavelet filter and multiple features. In: Computing in Cardiology Conference (CinC) 2016 Sep 11 (pp. 1149-1152). IEEE.

Wang XP, Yan C, Shi B, Liu CC *et al*. (2018). Does the temporal asymmetry of short-term heart rate variability change during regular walking? A pilot study of healthy young subjects. Computational and Mathematical Methods in Medicine 2018, 1-9. 2018

Wang XY, Meng J, Tan GL *et al*. (2010). Research on the relation of EEG signal chaos characteristics with high-level intelligence activity of human brain. Nonlinear Biomedical Physics 4(1), 2.

Wang YF, Li ZC, Feng LC *et al*. (2016). Hardware architecture of lifting-based discrete wavelet transform and sample entropy for epileptic seizure detection. In: 13th IEEE International Conference on Solid-State and Integrated Circuit Technology (ICSICT) 2016 Oct 25 (pp. 1582-1584).

Wang YH, Chen IY, Chiueh H *et al*. (2021). A low-cost implementation of sample entropy in wearable embedded systems: An example of online analysis for sleep EEG. IEEE Transactions on Instrumentation and Measurement 70, 1-2.

Wang YP, Kuo TB, Lai CT *et al*. (2013). Effects of respiratory time ratio on heart rate variability and spontaneous baroreflex sensitivity. Journal of Applied Physiology. 115(11), 1648-1655.

Wang YP, Kuo TB, Lai CT *et al*. (2015). Effects of breathing frequency on the heart rate deceleration capacity and heart rate acceleration capacity. European journal of applied physiology 115(11), 2415-2420. 2015

Wang YP, Kuo TB, Yang CC. (2014). A possible explanation for the effects of respiration on heart rate and blood pressure asymmetry. International Journal of Cardiology 174(3), 805-807. 2014

Warlop T, Detrembleur C, Buxes Lopez M *et al*. (2017). Does Nordic Walking restore the temporal organization of gait variability in Parkinson's disease? Journal of Neuroengineering and Rehabilitation 14(1), 17.

Webber CL Jr, Zbilut JP. (1994). Dynamical assessment of physiological systems and states using recurrence plot strategies. Journal of Applied Physiology 76(2), 965-973.

Webber CL Jr. (2012). Recurrence quantification of fractal structures. Frontiers in Physiology 3, 382.

Weck PJ, Schaffner DA, Brown MR *et al*. (2015). Permutation entropy and statistical complexity analysis of turbulence in laboratory plasmas and the solar wind. Physical Review E 91(2), 023101.

Wei SY, Hsu CF, Lee YJ *et al*. (2019). The static standing postural stability measured by average entropy. Entropy 21(12), 1210.

Weippert M, Behrens K, Rieger A *et al*. (2013). Heart rate variability and blood pressure during dynamic and static exercise at similar heart rate levels. PLoS One 8(12), e83690.

Weng W-C, Chang C-F, Wong LC *et al*. (2017). Altered resting-state EEG complexity in children with Tourette syndrome: a preliminary study. Neuropsychology 31(4), 395-402.

West BJ. (2006). Where Medicine Went Wrong. Rediscovering the path to complexity. Singapore: World Scientific.

West BJ. Fractal physiology and the fractional calculus: a perspective. Frontiers in physiology. 2010 Oct 14;1, 12,1-17.

Weygand JM, Kivelson MG. (2019). Jensen–Shannon Complexity Measurements in Solar Wind Magnetic Field Fluctuations. The Astrophysical Journal 872(1), 59.

Wierzba TH, Cwikalowska-Grudzinska H, Badtke P *et al*. (2019). Effect of Postural Changes on Complexity Measures of Heart Rhythm in Late Adolescents. In: Computing in Cardiology (CinC) 2019 Sep 8; 46, 1-4. IEEE. 2019

Wolf A, Bessoir T. (1991). Diagnosing chaos in the Space Circle. Physica D: Nonlinear Phenomena 50(2), 239-258.

Woo MA, Stevenson WG, D K Moser DK *et al*. (1992). Patterns of beat-to-beat heart rate variability in advanced heart failure. American Heart Journal 123(3), 704-710.

Wu L, Neskovic P. (2007). Feature extraction for EEG classification: representing electrode outputs as a Markov stochastic process. Proceedings of the 2007 European Symposium on Artificial Neural Networks (ESANN), Bruges, 567-572.

Wu SD, Wu CW, Lee KY *et al*. (2013). Modified multiscale entropy for short-term time series analysis. Physica A: Statistical Mechanics and its Applications 392(23), 5865–5873.

Wu SD, Wu CW, Lin SG *et al*. (2013). Time series analysis using composite multiscale entropy Entropy 15(3), 1069-1084.

Wu SD, Wu CW, Lin SG *et al*. (2014). Analysis of complex time series using refined composite multiscale entropy. Physics Letters A 378, 1369–1374.

Wu YF, Chen PN, Xin Luo X *et al*. (2016). Quantification of knee vibroarthrographic signal irregularity associated with patellofemoral joint cartilage pathology based on entropy and envelope amplitude measures. Computer Methods and Programs in Biomedicine 130, 1-12.

Xia YF, Wu D, Gao ZF *et al*. (2018). Association between beat-to-beat blood pressure variability and vascular elasticity in normal young adults during the cold pressor test. Medicine 96(8), e6000, 1-7.

Xiao F, Mu J, Lu J *et al*. (2022). Real-time modeling and feature extraction method of surface electromyography signal for hand movement classification based on oscillatory theory. Journal of Neural Engineering. 2022 Feb 16.

Xiao F, Yang D, Lv Z *et al*. (2020). Classification of hand movements using variational mode decomposition and composite permutation entropy index with surface electromyogram signals. Future Generation Computer Systems 110, 1023-36.

Xie HB, Guo JY, Zheng YP. (2010). Fuzzy approximate entropy analysis of chaotic and natural complex systems: detecting muscle fatigue using electromyography signals. Annals of Biomedical Engineering 38(4), 1483-1496.

Xie HB, He WX, Liu H. (2008). Measuring time series regularity using nonlinear similarity-based sample entropy. Physics Letters A 372(48), 7140-7146.

Xiong G-L, Zhang L, Liu H-S *et al*. (2010). A comparative study on ApEn, SampEn and their fuzzy counterparts in a multiscale framework for feature extraction. Journal of Zhejiang University-SCIENCE A (Applied Physics & Engineering) 11(4), 270-279.

Xiong WT, Faes L, Ivanov PC. (2017). Entropy measures, entropy estimators, and their performance in quantifying complex dynamics: effects of artifacts, nonstationarity, and long-range correlations. Physical Review E 95(6-1), 062114.

Xu JH, Liu Z-R, Liu R. (194). The measures of sequence complexity for EEG studies. Chaos, Solitons & Fractals 4(11), 2111-9.

Yan C, Li P, Ji LZ *et al*. (2017). Area asymmetry of heart rate variability signal. Biomedical Engineering Online 16(1), 1-4. Area I #1

Yan C, Li P, Li Y *et al*. (2021a). Analysis of heart rate asymmetry during sleep stages. In: Tallón-Ballesteros AJ. (Ed.) Proceedings, 11th International Conference on Electronics, Communications and Networks (CECNet) 2021, 731-736. Yan C, Li P, Liu C *et al*. (2019). Novel gridded descriptors of poincaré plot for analyzing heartbeat interval time-series. Computers in Biology and Medicine 109, 280-289.

Yan C, Li P, Yao L *et al*. (2019). Impacts of reference points and reference lines on the slope- and area-based heart rate asymmetry analysis. Measurement. 2019 Apr 1;137, 515-526.

Yan C, Liu C, Yao L *et al*. (2021a). Short-term effect of percutaneous coronary intervention on heart rate variability in patients with coronary artery disease. Entropy. 2021 May;23(5), 540.

Yan F, Song D, Dong Z *et al*. (2020). Alternation of EEG characteristics during transcutaneous acupoint electrical stimulation–induced sedation. Clinical EEG and Neuroscience 53(3):204-214.

Yan R, Zhang C, Spruyt K *et al*. (2019). Multi-modality of polysomnography signals' fusion for automatic sleep scoring. Biomedical Signal Processing and Control 49, 14-23.

Yang J, Xia W, Hu T. (2019). Bounds on extropy with variational distance constraint. Probability in the Engineering and Informational Sciences 33(2), 186-204.

Yang JW. (2020). Outlier Detection Techniques. Dissertations in Forestry and Natural Sciences No 383. University of Eastern Finland, Joensuu, Finland.

Yang Y, Qiu L, Yang TQ *et al*. (2017). Scaling invariance embedded in very short time series: a factorial moment based diffusion entropy approach. Chinese Journal of Physics 55, 2325–2335.

Yentes JM, Hunt N, Schmid KK *et al*. (2013). The appropriate use of approximate entropy and sample entropy with short data sets. Annals of Biomedical Engineering 41(2), 349-365.

Yilmaz A, Unal G. (2020). Multiscale Higuchi's fractal dimension method. Nonlinear Dynamics 101(2), 1441-55.

Yin YH, Sun KH, He SB. (2018). Multiscale permutation Rényi entropy and its application for EEG signals. PLoS One 13(9), e0202558.

Yoon Y-G, Kim T-H, Jeong D-W *et al*. (2011). Monitoring the depth of anesthesia from rat EEG using modified Shannon entropy analysis. Conference Proceedings, IEEE Engineering in Medicine and Biology Society 2011, 4386-4389.

Young K, Schuff N. (2008). Measuring structural complexity in brain images. NeuroImage. 2008 Feb 15;39(4), 1721-30.

Yu J, Cao JY, Wei-Hsin Liao W-H *et al*. (2017). Multivariate multiscale symbolic entropy analysis of human gait signals. Entropy 19(10), 557, 1-10.

Yu Y, He XQ, Zhao ZY *et al*. (2019). Nonlinear analysis of local field potentials and motor cortex EEG in spinocerebellar ataxia 3. Journal of Clinical Neuroscience 59, 298-304.

Yuan H-K, Lin C, P-H Tsai P-H *et al*. (2011). Acute increase of complexity in the neurocardiovascular dynamics following carotid stenting. Acta Neurologica Scandinavica 123(3), 187-192.

Yuan Y, Li Y, Mandic DP. (2008). A comparison analysis of embedding dimensions between normal and epileptic EEG time series. Journal of Physiological Sciences 58(4), 239-247.

Zadeh HG, Haddadnia J, Montazeri A. (2016). A model for diagnosing breast cancerous tissue from thermal images using active contour and Lyapunov exponent. Iranian Journal of Public Health 45(5), 657-669.

Zadeh LA. (1965). Fuzzy sets. Information and Control 8, 338—353.

Zamunér AR, Silva E, Teodori RM *et al*. (2013). Autonomic modulation of heart rate in paraplegic wheelchair basketball players: Linear and nonlinear analysis. Journal of Sports Sciences 31(4), 396-404.

Zanin M, Olivares F. (2021). Ordinal patterns-based methodologies for distinguishing chaos from noise in discrete time series. Communications Physics 4(1), 1-4.

Zanin M, Zunino L, Rosso OA *et al*. (2012) Permutation entropy and its main biomedical and econophysics applications: a review. Entropy 14, 1553-1577.

Zbilut JP, Thomasson N, Charles L. Webber CL. (2002). Recurrence quantification analysis as a tool for nonlinear exploration of nonstationary cardiac signals. Medical Engineering and Physics 24(1), 53-60.

Żebrowski JJ, Kowalik I, Orłowska-Baranowska E *et al*. (2015). On the risk of aortic valve replacement surgery assessed by heart rate variability parameters. Physiological Measurement 36(1), 163-175.

Zhang AH, Yang B, Huang L. (2008). feature extraction of EEG signals using power spectral entropy. International Conference on BioMedical Engineering and Informatics 2008, 435-439.

Zhang DD, Jia X, Ding H *et al*. (2010). Application of Tsallis entropy to EEG: quantifying the presence of burst suppression after asphyxial cardiac arrest in rats. IEEE Transactions in Biomedical Engineering 57(4), 867-874.

Zhang J-H, Han X, Hong-Wei Zhao H-W *et al*. (2018). Personalized prediction model for seizure-free epilepsy with levetiracetam therapy: a retrospective data analysis using support vector machine. British Journal of Clinical Pharmacology 84(11), 2615-2624.

Zhang LJ, Guo TC, Xi B *et al*. (2015). Automatic recognition of cardiac arrhythmias based on the geometric patterns of Poincare plots. Physiological Measurement 36(2), 283-301.

Zhang P, Barad H, Martinez A. (1990). Fractal dimension estimation of fractional Brownian motion. In: IEEE Proceedings on Southeastcon 1990 Apr 1 (pp. 934-939).

Zhang P, Barad HS, Martinez AB. (1989). Applications of fractal modeling to cell image analysis. InProceedings. IEEE Energy and Information Technologies in the Southeast' 1989 Apr 9 (pp. 618-622).

Zhang WQ, Qiu L, Xiao Q *et al*. (2012). Evaluation of scale-invariance in physiological signals by means of balanced estimation of diffusion entropy. Physical Review E 86(5), 056107, 1-8.

Zhang WW, Wang F, Shichao Wu SC *et al*. (2020). Partial directed coherence based graph convolutional neural networks for driving fatigue detection. Review of Scientific Instruments 91(7), 074713.

Zhang Y, Hao J, Zhou C *et al*. (2009). Normalized Lempel-Ziv complexity and its application in bio-sequence analysis. Journal of Mathematical Chemistry 46(4), 1203–1212.

Zhao DC, Wang Y, Wang QQ *et al*. (2019). Comparative analysis of different characteristics of automatic sleep stages. Computer Methods and Programs in Biomedicine 175, 53-72.

Zhao J, Bose BK. (2002). Evaluation of membership functions for fuzzy logic controlled induction motor drive. 28th Annual Conference of the IEEE Industrial Electronics Society 1, 229–234.

Zhong JY, Liu R, Chen P. (2020). Identifying critical state of complex diseases by single-sample Kullback-Leibler divergence. BMC Genomics 21(1), 87, 1-15.

Zhou Q, Deng Y. (2021). Belief eXtropy: Measure uncertainty from negation. Communications in Statistics-Theory and Methods. 2021 Sep 15, 1-23.

Zhou S, Zhang Z, Gu J. (2011). Interpretation of coarse-graining of Lempel-Ziv complexity measure in ECG signal analysis. Conference Proceedings, IEEE Engineering in Medicine and Biology Society 2011, 2716-2719.

Zhou Y, Xie LL, Yu GH *et al*. (2008).. The study of C0 complexity on epileptic absence seizure. In: 7th Asian-Pacific Conference on Medical and Biological Engineering 2008 (pp. 420-425). Springer, Berlin, Heidelberg.

Zhu G-Y, Zhang R-L, Chen Y-C. (2020). Characteristics of globus pallidus internus local field potentials in generalized dystonia patients with TWNK mutation. Clinical Neurophysiology 131(7), 1453-1461.

Zhu L, Cui GC, Jianting Cao JT *et al*. (2019). A hybrid system for distinguishing between brain death and coma using diverse EEG features. Sensors 19(6), 1342.

Zhu PZ, Wu YY, Jingtao Liang JT *et al*. (2018). Characterization of the stroke-induced changes in the variability and complexity of handgrip force. Entropy 20, 377, 1-11.

Zhuang N, Zeng Y, Tong L *et al*. (2017). Emotion recognition from EEG signals using multidimensional information in EMD domain. Biomedical Research International 2017, 8317357.

Ziv J, Lempel A. (1977). A Universal algorithm for sequential data compression. IEEE Transactions on Information Theory IT-23(3), 337-343.

Zlatintsi A, Maragos P. (2012). Multiscale fractal analysis of musical instrument signals with application to recognition. IEEE Transactions on Audio, Speech, and Language Processing. 21(4), 737-48.

Zozor S, Mateos D, Lamberti PW. (2014). Mixing Bandt-Pompe and Lempel-Ziv approaches: another way to analyze the complexity of continuous-state sequences. The European Physical Journal B 87(5), 1-2.

Zozor S, Ravier P, Buttelli O. (2005). On Lempel–Ziv complexity for multidimensional data analysis. Physica A: Statistical Mechanics and its Applications 345(1-2), 285-302.

Zunino L, Kulp CW. (2017). Detecting nonlinearity in short and noisy time series using the permutation entropy. Physics Letters A 381(42), 3627-3635.

Zunino L, Olivares F, Rosso OA. (2015). Permutation min-entropy: An improved quantifier for unveiling subtle temporal correlations. Europhysics Letters 109(1), 10005-p1-10005-p6.

Zunino L, Olivares F, Scholkmann F *et al*. (2017). Permutation entropy based time series analysis: Equalities in the input signal can lead to false conclusions. Physics Letters A 381(22), 1883-1892.

Zunino L, Soriano MC, Rosso OA. (2012). Distinguishing chaotic and stochastic dynamics from time series by using a multiscale symbolic approach. Physical Review E 86(4), 046210.

Żurek S, Castiglioni P, Kośmider M *et al.* (2012b). A characteristic ridge-ledge in entropy surfaces of cardiovascular time series estimated by the Norm Component Matrix algorithm. In: Computing in Cardiology 2012 Sep 9 (pp. 281-284). IEEE. Żurek 2012b

Żurek S, Guzik P, Pawlak S *et al*. (2012a). On the relation between correlation dimension, approximate entropy and sample entropy parameters, and a fast algorithm for their calculation. Physica A: Statistical Mechanics and its Applications 391(24):6601-10.

Żurek S, Piskorski J, Guzik P *et al.* (2014). Day-to-night variations of RR intervals complexity observed in 24-h ECG Holter R. In: 8th Conference of the European Study Group on Cardiovascular Oscillations (ESGCO) 2014 May 25 (pp. 203-204). IEEE.